# FUNCTIONAL NEUROANATOMY OF DYNAMIC VISUO-SPATIAL IMAGERY

DISSERTATION

zur Erlangung des Doktorgrades der Naturwissenschaften

an der Fakultät für Human- und Sozialwissenschaften

der Universität Wien

eingereicht von

Claus Lamm

Wien, im Juni 2001

Gott würfelt nicht (Albert Einstein)

Alia jacta est (Gajus Julius Caesar)

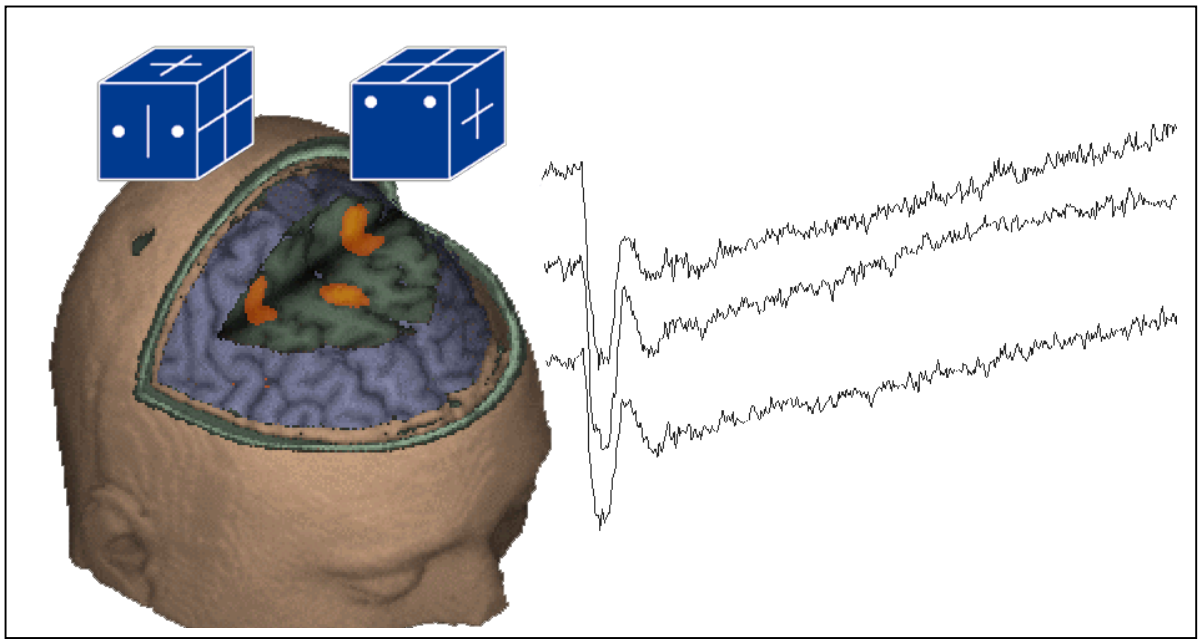

**Summary**

The aim of this thesis was the examination of the neural bases of dynamic visuo-spatial imagery. In addition to the assessment of brain activity during dynamic visuo-spatial imagery using single-trial functional magnetic resonance imaging (fMRI) and slow cortical potentials (SCPs), several methodological issues have been investigated.

The theoretical part of this thesis consists of a selective overview of fMRI and SCPs, and of the advantages of their combination for functional neuroimaging (chapter 2). The methodological and empirical chapters include:

- the presentation of a new, highly accurate and practicable method for the co-registration of MRI- and EEG-data (chapter 3),
- the description of the increase in the accuracy of SCP mapping resulting from the use of individual electrode coordinates and realistic head models (chapter 4),
- the description of regional differences in the consistency of brain activity across several executions of the same task type, as assessed by a new analysis concept based on single-trial fMRI data (chapter 5),
- the demonstration of the involvement of premotor regions in dynamic visuo-spatial imagery, as assessed via a combination of single-trial fMRI and SCPs (chapter 6),
- the description of a combined fMRI-SCP investigation in which earlier findings concerning individual differences in neural efficiency during dynamic imagery could not be replicated (chapter 7).

*an electronic version of this thesis is available at the following addresses:*
*http://mailbox.univie.ac.at/claus.lamm/forschung/publikationen*
*http://www.cogsci.soton.ac.uk*

## Table of Contents

## *1. Introduction and overview*

In the past decade, knowledge about the functional neuroanatomy of human information processing has increased considerably. A significant trigger for this increase in knowledge have been the considerable advances made by the functional neuroimaging techniques which are available to assess functional neuroanatomy.

Functional Magnetic Resonance Imaging (fMRI), for example, did not exist as a non-invasive functional imaging technique before 1990, when Ogawa et al. (1990ab, 1992) and Kwong et al. (1992) described the phenomenon of BOLD contrast (*b*lood *o*xygen *l*evel *d*ependent contrast; see chapter 2.1). Since this initial discovery, fMRI has continuously improved as a method, regarding both its spatial and temporal resolution and the measurement paradigms and analysis concepts which can be used. Today, fMRI seems to be the most frequently used neuroimaging method, which is also indicated by an overview of the recent papers published in journals such as *NeuroImage*, *Human Brain Mapping* or the *Journal of Cognitive Neuroscience*.

After a period of rather little methodological progress (see, e.g., Wikswo et al., 1993), significant methodological and technical advances have also been attained by the more traditional techniques of electroencephalography (EEG) and event-related potentials (ERPs). The spatial accuracy achievable by EEG and ERPs can now be increased considerably due the use of a larger number of recording channels, as well as efforts in the development and implementation of more sophisticated source localization and surface mapping techniques.

As is the case with almost any scientific method, each technique has its specific advantages and disadvantages. fMRI, for instance, provides tomographic measures of processing-related changes in neural activity with excellent spatial detail. On the other hand, neural activity is only assessed indirectly via the hemodynamic response, and the temporal resolution of fMRI is much lower than the one achieved by EEG or ERPs. However, the basic disadvantage of EEG and ERPs is their limited spatial resolution. The intrinsic obstacle in ERP/EEG research is that information about tomographic activity has to be gained via recordings on the surface. The difficulty in finding the generators of surface potentials might be compared to finding the generators of the waves and the wave patterns in the ocean. This results in an "ill-defined" problem, implying a lack of information which is inherent to the method.

To overcome these limitations, the combination and co-registration of neuroimaging methods has been repeatedly recommended (Rugg, 1998; McCarthy, 1999). One rather frequently used approach (see, e.g., Mangun et al., 1998; Opitz et al., 1999; Wang et al., 1999) is the combination of fMRI and ERPs. Using this approach, the major weakness of fMRI, i.e. its limited temporal resolution and the resulting incapability to monitor fast changes in cognitive processing, is balanced out by the sub-second to millisecond temporal resolution of ERPs. In addition, ERPs might also help to decide whether increases in blood flow or blood oxygenation are due to increased activity of excitatory or inhibitory neurons. In return, fMRI provides volumetric measurements of task-related hemodynamic changes with millimeter spatial resolution, and structural MR images of the brain and the skull can be used to compute improved source localizations as well as to visualize inverse solutions in relation to individual cortical anatomy.

Up to about three to four years ago, however, the direct comparability of ERP and fMRI data has been rather limited. This was due to the fact that the hard- and software of most fMRI scanners did not yet allow to use the standard event-related data acquisition mode of ERP research. Most fMRI studies had to present stimuli block-wise, which meant that several stimuli were presented consecutively. Only summed activity over the whole course of such blocks could be assessed. This did not allow a detailed assignment of activities to specific task features as it is possible with ERPs. For instance, activity related to the visual perception of a task or to the response preparation could not be easily separated from the actual cognitive processing. Another problem with this stimulus presentation mode was that a mixture of state- and task-related activity was obtained, resulting in another difference to the type of data acquired with ERPs.

Fortunately, recent technical and methodological developments now allow the use of fMRI data acquisition and stimulus presentation modes which are vastly identical as those used in ERP research. Data are acquired in an event-related manner (i.e. with an individual pre-stimulus and post-stimulus period), and can either be averaged individually to yield event-related images of hemodynamic changes or be analyzed on a single-trial or single-event basis (see chapter 5).

Another problem concerning the comparability of fMRI and ERPs is related to the type of neural processing assessed by the two methods. Common or "classical" ERPs typically consist of a number of components. These components are usually seen as a series of changes in polarity ("ups and downs") of the averaged signal. While earlier, so-called exogeneous components (see, e.g., Rockstroh et al., 1989 for a classification scheme of ERPs), are rather related to neural activity

located in the sensory pathways or in primary sensory cortex (e.g., N100, which designates a component at a latency of about 100 ms post stimulus with negative polarity), the so-called endogeneous components following these initial signal changes seem to reflect processes such as attentional tuning, expectancy or orientation towards the task or the task stimulus (e.g., P300, a positive-going deflection). However, if more complex cognitive information processing is investigated, it seems likely that the genuine cognitive processes required for task solving will not be reflected by these short-latency components (irrespective of whether they are endogeneous or exogeneous). Thus, such components might not be comparable to fMRI signal changes, which - due to the sluggishness of the hemodynamic response - rather seem to reflect the neural activity related to prolonged information processing, than the initial, short-lasting neural response to a task.

Provided that several recording requirements are met (see chapter 2), so-called event-related slow cortical potentials (SCPs) can be observed following the short-latency components. SCPs have been investigated in a variety of cognitive, sensory and motor task paradigms (see, e.g., Bauer, 1998, or Rösler et al., 1997, for recent overviews). They can be described as tonic changes in activity which are obtained at latencies of around 300-500 ms post stimulus whenever prolonged information processing is required. In addition, SCPs usually persist until task completion. Thus, they can be used to monitor neural activity during prolonged information processing. As such, they might not only be more directly comparable to fMRI-derived indices of neural activity, but also have a technical temporal resolution in the sub-seconds range (see also chapter 2.2).

However, up to now, no study has been performed in which SCPs and fMRI were combined to investigate the neural bases of complex cognitive processing. The aim of this thesis was to perform such a study. The functional neuroanatomy of dynamic visuo-spatial imagery was investigated via a combination of fMRI and SCPs. In addition, several methodological aspects which were partly associated with a combination of the two methods were also to be investigated.

All studies were part of a co-operation of the Brain Research Laboratory (BRL) of the Department of Psychology/University of Vienna (Herbert Bauer (head), Ulrich Leodolter), and the AG NMR, Institute for Medical Physics/University of Vienna (Ewald Moser (head), Christian Windischberger).

The main insights derived from these studies are written up in this thesis, which is structured in the following way[1].

In the following theoretical part (*chapter 2*), an overview of the methods employed in this thesis, as well as of the aims, advantages and problems associated with the co-registration and combination of fucntion neuroimaging methods will be provided.

The empirical part is subdivided into five chapters. The first two of them (chapters 3 and 4) deal with methodological issues. *Chapter 3* describes a new method for the co-registration of MR- and EEG data which is based on the head-shape of a subject. In *chapter 4*, the results of a study which assessed the accuracy of SCP mapping using different interpolation algorithms will be presented. *Chapter 5* presents a new approach to analyse single-trial fMRI data. Thus, this chapter has a strong methodological focus, but nevertheless provides some results concerning the functional neuroanatomy of dynamic visuo-spatial imagery. The study presented in *chapter 6* investigated the functional neuroanatomy of dynamic visuo-spatial imagery. The controversially discussed question of whether higher-order motor areas are involved in dynamic visuo-spatial imagery was assessed using a combination of SCPs and fMRI. SCPs and fMRI were also combined in the study described in *chapter 7*. The main intent of this study was a replication and extension of earlier results concerning individual differences in brain activity during visuo-spatial imagery. Finally, a concluding evaluation of the main findings, implications and failures of this thesis, and a brief outlook towards future research will be presented (chapter 8).

[1] The attentive reader will realize that there is some overlap in the description of methods and theory across the chapters. This resulted from the attempt to allow readers to read chapters selectively and independently.

## *2. Overview of the functional neuroimaging methods used in this thesis*

**Abstract**

*In this chapter, a selective overview of the methods used in this thesis will be provided. This overview does not claim to be comprehensive, since only issues which are directly relevant for the methods employed in the empirical chapters will be discussed. In the following subchapter, the technique of functional magnetic resonance imaging (fMRI) will be presented after a brief description of the phenomenon of nuclear magnetic resonance and of magnetic resonance imaging. In chapter 2.2, an overview of electroencephalography will be given which focuses on event-related potentials and particularly on event-related slow cortical potentials (SCPs). Finally, after a summarizing evaluation of the strengths and weaknesses of these two methods, the advantages and problems associated with their combination in a multi-modality imaging approach will be discussed.*

### *2.1 Structural and functional Magnetic Resonance Imaging (MRI/fMRI)*

Functional magnetic resonance imaging (fMRI) is a relatively new technique which entered research about 10 years ago (Ogawa et al., 1990ab, 1992; Kwong et al., 1992; Belliveau et al., 1991). It relies on the long-known phenomenon (James, 1890; Mosso, 1881) that increases in neural activity are accompanied by distinct changes in regional cerebral blood flow (rCBF). Since fMRI relies on the phenomenon of nuclear magnetic resonance (NMR), a selective overview of the basic principles of NMR will be given now.

#### 2.1.1 Nuclear Magnetic Resonance/Magnetic Resonance Imaging (NMR/MRI)

Soon after it became evident that the phenomenon of NMR might be used for clinical imaging, clinicians chose to name the associated technique magnetic resonance imaging (MRI) in order to avoid the negative connotations of the word "nuclear". Although NMR would be the more precise term since it implies that the magnetic properties of the atomic nucleus are assessed and utilized, I will adhere to this convention since the term MRI also describes more directly how the technique is used nowadays (namely to produce images of the human body and brain). However, it should be noted that in the following overview, the term MRI will refer exclusively to imaging using the magnetic properties of the atomic nucleus, and not those of electrons (as in Electron Spin Resonance, ESR).

MRI takes advantage of the angular and the resulting magnetic momentum of atomic nuclei. The nucleus most often assessed in MRI is the hydrogen nucleus. Having angular momentum means that nuclei rotate around their own axis. In their normal state, the orientation of nuclei is randomly distributed, and no magnetic momentum can be observed macroscopically. When placed in a static magnetic field, nuclei align with this external field and precess around its axis (just as a spinning wheel not only rotates around its own axis but also exhibits precession).

The spin can align either in parallel to or opposite to the orientation of the static magnetic field. Spins which are aligned in opposite direction have a higher energy level than spins aligned in parallel. The resulting energy difference can be observed macroscopically as a magnetic momentum or net magnetization in the direction of the static field, which is called $B_0$. Spins precess around $B_0$ at an angular frequency called the Larmor or resonance frequency, which depends linearly on the strength of the external field (the higher the field, the higher the Larmor frequency). If a radio frequency (RF) pulse (an excitation pulse) which is perpendicular to $B_0$ and whose frequency is at or at least near to the Larmor frequency is applied, the spins will absorb energy and transitions between the two ways of alignment and the associated energy states are induced. After the excitation pulse is switched off, the spin system regains its initial equilibrium condition (i.e. magnetization returns to $B_0$), and this process can be picked up by specifically designed MR receiver coils.

The rebound to equilibrium is called relaxation. Relaxation time differs between biological tissues. Thus, it can be used to acquire images of different types of tissue. White matter, for example, shows much faster longitudinal relaxation than grey matter or cerebrospinal fluid (573 ms vs. 991 ms vs. 2063 ms, respectively; measured at 1.5 Tesla, Blüml et al., 1993). It is the sensitivity to different tissues that makes up the basic appeal of MRI, providing a tissue contrast which is far superior to X-ray based brain imaging techniques as computerized tomography.

Two different types of relaxation exist (see Fig. 2-1). Longitudinal relaxation is characterized by the T1 relaxation time. This time is defined as the time required by the system to reach 63 % (1-1/e) of its equilibrium value after a 90° excitation pulse (i.e. a pulse which flips the direction of the magnetization vector from the longitudinal into the transverse plane) has been applied. T1 is also called spin-lattice relaxation since energy is exchanged between the spins and their environment, which is called "the lattice" in dense matter physics. Transverse relaxation is characterized by T2 relaxation time (the time in which the signal decays to 1/e of

the original signal strength). This describes the loss of phase-coherence of the spins, which causes a loss of net magnetization in the x-y plane. This loss of phase-coherence mainly results from an exchange of energy between the spins due to their magnetic interactions, causing continuous changes in precession frequencies. Thus, T2 is also called spin-spin relaxation time. Additional dephasing of the spins is introduced by local inhomogeneities in the external magnetic field, with larger inhomogeneities causing more rapid dephasing and loss of signal. The combination of "instrument-induced" and "true" T2 dephasing results is assessed via T2* relaxation time.

T1 and T2 (T2*) relaxation are occurring simultaneously, but at different rates (in biological tissues, 1/T2 is much higher than 1/T1). Thus, different pulse sequences can be used to produce data which are differentially weighted by the two relaxation parameters. Most functional imaging sequences are designed to obtain T2*-weighted images in order to take advantage of the phenomenon that blood with a lower concentration of deoxy-hemoglobin causes less inhomogeneities than blood with a higher concentration (see below).

Up to now, it would have been more appropriate to use the term NMR instead of MRI, since we would not be able to obtain a structured image with the principles presented so far. Imaging not only requires a static magnetic field and a RF transmitter and receiver coil, but also the application of so-called gradients (see Fig. 2-2 and Fig. 2-3). Gradients consist of coils through which an electric

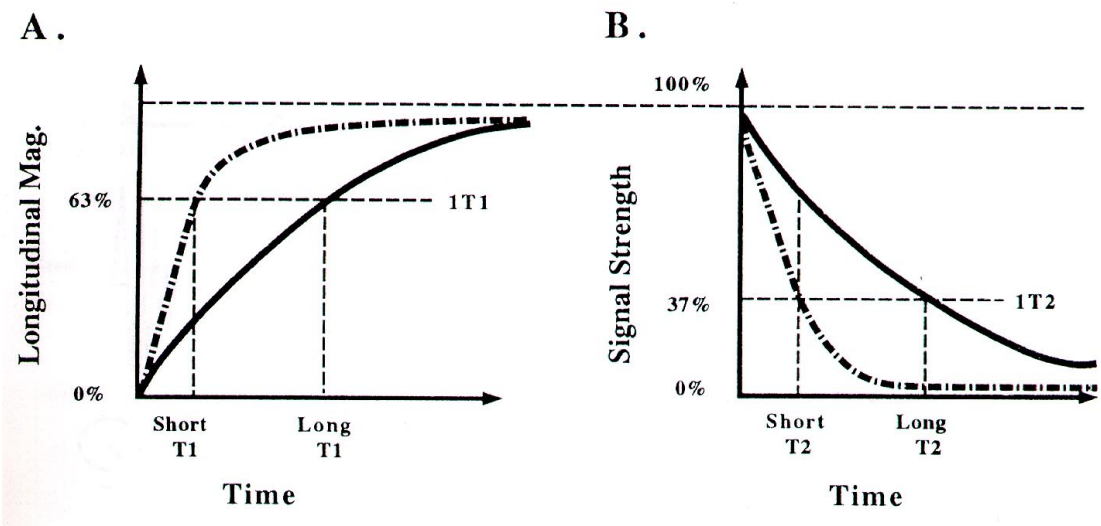


Fig. 2-1: T1 and T2 relaxation curves for two different tissue types (dashed and solid lines). While T1 is defined as the time required to achieve 1-1/e % of the original longitudinal magnetization, T2 is defined as the time in which the signal decreases to 1/e % of its original amplitude (reproduced from Aine, 1995, Fig. 4).

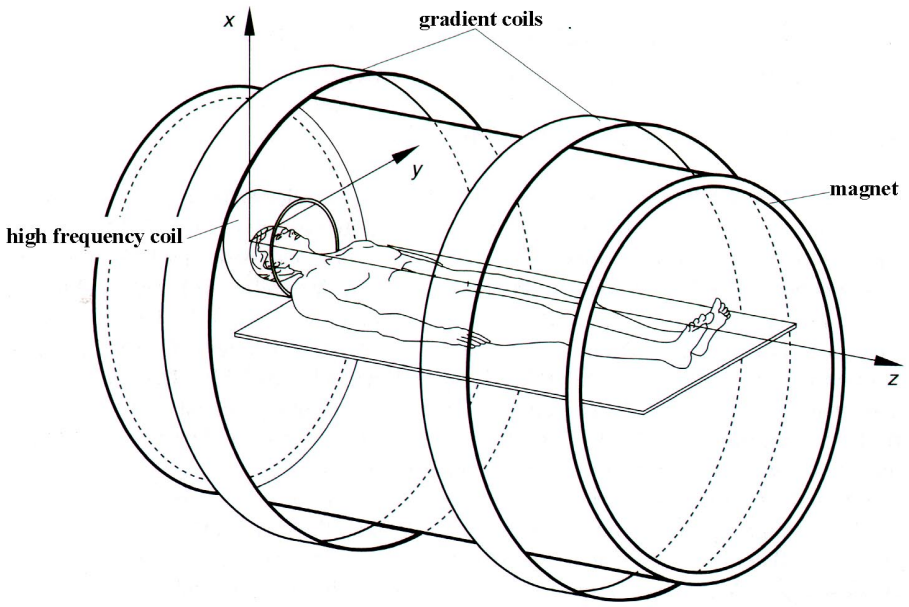


Fig. 2-2: A standard clinical MRI tomograph consists of a magnet which is usually superconductive and produces the main magnetic field ($B_0$), several gradient coils which produce local variations of the main magnetic field, and a high frequency coil (in this case a bird-cage coil for head scanning) for transmission and reception of high frequency radio waves (adapted from Kischka et al., 1997, Fig. 13.10).

current is passed. This results in a magnetic field, which is added to the main static magnetic field $B_0$. Consequently, the effective field strength at a given position within the magnet bore is a function of the main magnetic field and of the imaging gradients switched on and off for imaging. Thus, gradients can be used to define cubes (voxels) of distinct magnetic field strength in the investigated sample. Since a difference in magnetic field strength is associated with a difference in the Larmor frequency of the spins within this voxel, signals of different frequencies can be assigned to these voxels.

Three different gradients are required to encode the three spatial dimensions. They are referred to as the slice selection (z), frequency encoding (x), and phase encoding (y) gradients (see Fig. 2-3). Usually, the first step in imaging is the selection of a slice of the whole volume (hence the name magnetic resonance tomography, since the ancient Greek word "tomos" means slice, or section). This is achieved via application of a gradient along the z-axis. As a result, nuclei will show different precession frequencies as a function of their position along the longitudinal axis of the magnet. Since this also implies that the Larmor frequencies vary, RF pulses can now be applied to selectively excite different slices of the biological probe (the brain, in our case). These RF pulses only contain frequencies near or at the Larmor frequency of the slice which shall be excited.

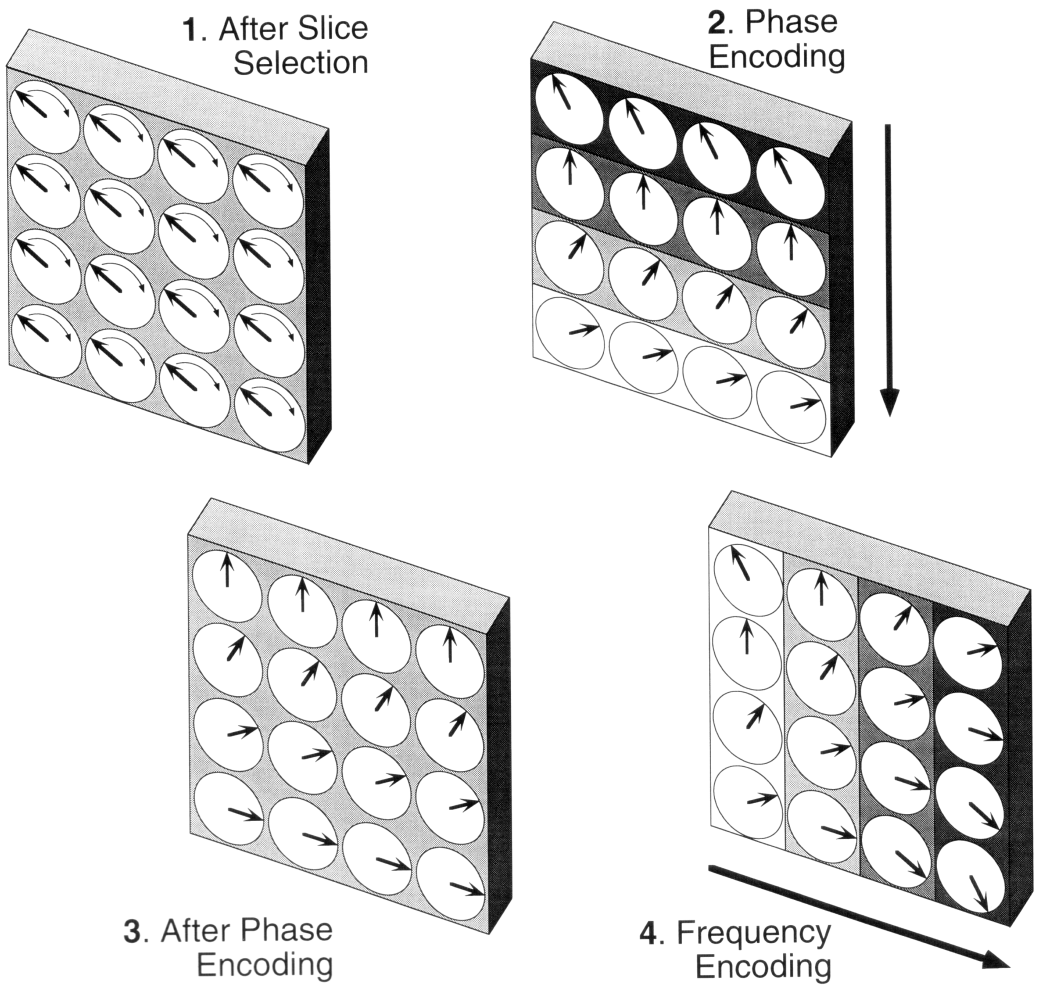


Fig. 2-3: Spin vector orientations related to the application of slice, phase and frequency encoding gradients (reproduced from Cohen, 1996, Fig. 10).

After slice selection, the selected slice has to be additionally subdivided to assess the signal within the slice. This is achieved via a combination of phase and frequency encoding. Phase encoding is achieved via a gradient perpendicular to the slice-selection gradient, which usually is the y-direction. This gradient causes differences in the velocity of precession, which results in a differce in phase between spins along the y-axis. Phase encoding is achieved in several phase encoding steps, which - in echoplanar imaging (EPI; see below) - consist of rapidly repeated blips. With frequency encoding, a gradient is applied in the direction perpendicular to the phase encoding and slice selection direction (usually the x-axis). Since this gradient is switched on during the read-out period (the period when the MR signal is acquired), it is also referred to as the readout gradient, and it produces a distribution of frequencies along the x-axis. Using two-dimensional Fourier

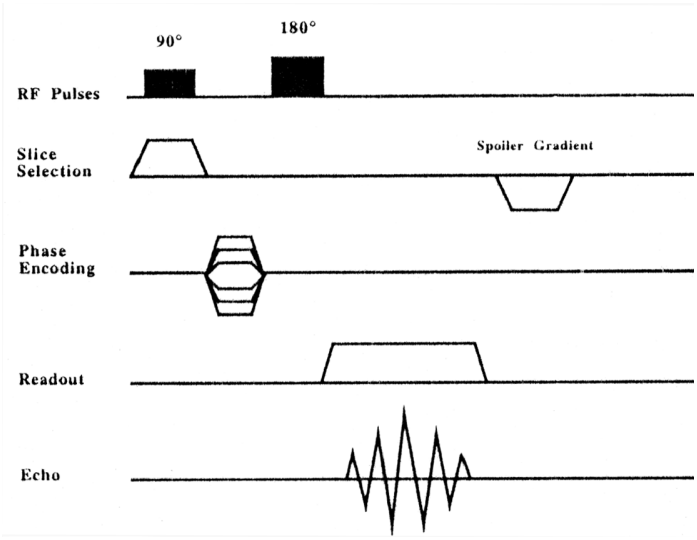


Fig. 2-4: Spin echo (SE) pulse sequence. Note the timing of the three different gradients. While the slice selection gradient is switched on during RF excitation, the readout or frequency encoding gradient is on during signal acquisition (which is, in the case of a SE sequence, during echo acquisition). The shown excitation-inversion-echo sequence has to be repeated from 128 to 256 times in order to achieve phase encoding (see the phase encoding gradient; reproduced from Aine, 1995, Fig. 10).

transformation of the acquired signals, images can be reconstructed whose spatial resolution depends on the resolution of the three gradients and the bandwidth of the slice selection RF pulse. Fig. 2-4 shows a typical pulse sequence used for structural brain imaging.

Summing up, from a layman's perspective, the basic principle of MRI could be simplified as follows: Hydrogen nuclei are placed in an external magnetic field, which "forces" them to align with this field. Radio waves are then used to disturb this alignment for a very short period of time. When the radio waves are switched off, the nuclei return to their initial state. This process is picked up by a special receiver, with the induced voltage in the receiver coil being proportional to the magnetic properties of the tissue containing the nuclei. By using three gradients, the three-dimensional position of the origin of the signals can be determined, and this information can be used to produce an image of the scanned volume. For a physically exact account of MR imaging, the reader is referred to, e.g., Morris, 1987.

### 2.1.2 Functional Magnetic Resonance Imaging (fMRI)

#### *2.1.2.1 Blood oxygen level dependent (BOLD) contrast*

fMRI is based on the principles of NMR plus the phenomenon that increases in neural activity are accompanied by local increases in blood flow and blood oxygenation. As such, fMRI is a truly non-invasive method since it uses the intrinsic contrast agent of blood oxygenation to assess neural activity in the brain. However, the first attempts to use MRI as a functional imaging technique in humans used an extrinsic contrast agent. Belliveau et al. (1991) intravenously in-

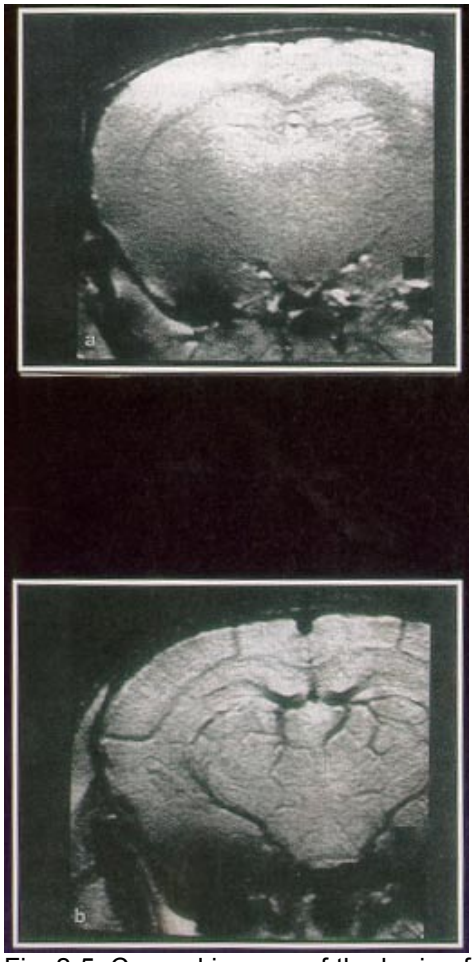

Fig. 2-5: Coronal images of the brain of a rat during inhalation of air with differing oxygen concentration (Ogawa et al. 1990a). Inhalation of air with a higher percentage of oxygen (upper image) resulted in the disappearance of the dark lines in the lower image (adapted from Raichle, 2000, Fig. 18).

jected Gd(DTPA) (gadolinium diethylenetriaminepentacetic acid) and observed an increase in blood volume in the primary visual cortex during photic stimulation.

Although this was one of the first demonstrations of the applicability of MRI as a tool for functional imaging, it did not have many advantages over the then dominantly used invasive imaging technique of positron emission tomography (PET), since Gd(DTPA)-MRI is invasive as well (with DTPA even being a toxic substance). But only one year before Belliveau & colleagues published their results, it had been demonstrated in animal experiments that the intrinsic properties of blood can be used to non-invasively map activity-related hemodynamic changes (Ogawa et al., 1990a). One year later, the usefulness of so-called blood oxygen level dependent contrast (BOLD-contrast) to map human brain activity was presented independently by Ogawa & colleagues and by Kwong & colleagues (1992; ironically in the same issue of the Proceedings of the US National Academy of Science after both groups' papers had been rejected by Nature and Science with the argument that nothing new is presented; Raichle, 2000).

The initial observation that Ogawa and his collaborators made was that varying the percentage of oxygen in the air inhaled by rats changed the brightness of MR images of their brain. When the rat was ventilated with less oxygen, its brain appeared much darker than when the air was highly saturated with oxygen (see Fig. 2-5). This is due to the following phenomenon: Blood consists of liquid plasma and erythrocytes, leukocytes and thrombocytes. Erythrocytes or red blood cells are responsible for the supply of oxygen to metabolically active cells in the human body, and thus also in the brain. This is achieved through the binding of oxygen to hemoglobin, with hemoglobin being composed of globin and heme (the latter gives

blood its red color). The center of heme consists of an iron atom ($Fe^{2+}$) which is capable of binding $O_2$. When an oxygen atom is attached to the iron atom, heme changes its magnetic state from paramagnetic to diamagnetic. The opposite applies when the oxygen atom is taken up by the local environment, that is when hemoglobin is deoxygenated. While de-oxygenated erythrocytes show positive magnetic susceptibility, the surrounding environment is diamagnetic and has negative magnetic susceptibility. This difference in magnetic susceptibility creates a local magnetic field gradient and, consequently, "inhomogeneities" in the magnetic field. Therefore, deoxygenated blood acts as a paramagnetic "contrast agent" which dephases the spins, resulting in faster signal loss and a decreased T2* time.

Now let us consider what happens when neurons become active, e.g. by increasing their firing rate. The oxygen demand of these neurons increases, and the oxygen supply in the environment decreases. This triggers - via several physiological mechanisms (see, e.g., Villringer, 1999) - an increase in arterial blood (containing oxygenated erythrocytes) delivery near the activated area in order to avoid a shortage of oxygen supply. While regional blood flow and blood volume increase considerably (up to ~50%), blood oxygen extraction increases only slightly (as demonstrated by PET studies; Fox et al., 1988; see also Jueptner & Weiler, 1995), resulting in a "paradoxically" higher concentration of oxygenated blood in the activated area (paradoxical because it had previously been expected that the ratio of oxygenated and de-oxigenated blood should become lower due to the increase in oxygen consumption). As a consequence, the blood flowing through the vessels now has a similar magnetic susceptibility as the surrounding tissue, which reduces the strength of the local field gradient in and around the vessels (see Fig. 2-6). This causes less dephasing of the spins and thus a slower drop in signal, which is reflected in a brighter image in a T2*-weighted sequence optimized to detect such changes in local magnetic field inhomogeneities. Thus, most sequences used in fMRI are T2*-weighted and are often referred to as BOLD-weighted sequences. The change in hemodynamic response, which leads to a detectable change in magnetic susceptibility, occurs at a much slower rate than the changes in neuronal activity. This usually results in a several seconds delay in signal strength increase. This delay might show considerable variability between brain regions (see, e.g., Buckner et al., 1998), which seems to result from differences in capillary, neuronal and synaptic density of these regions.

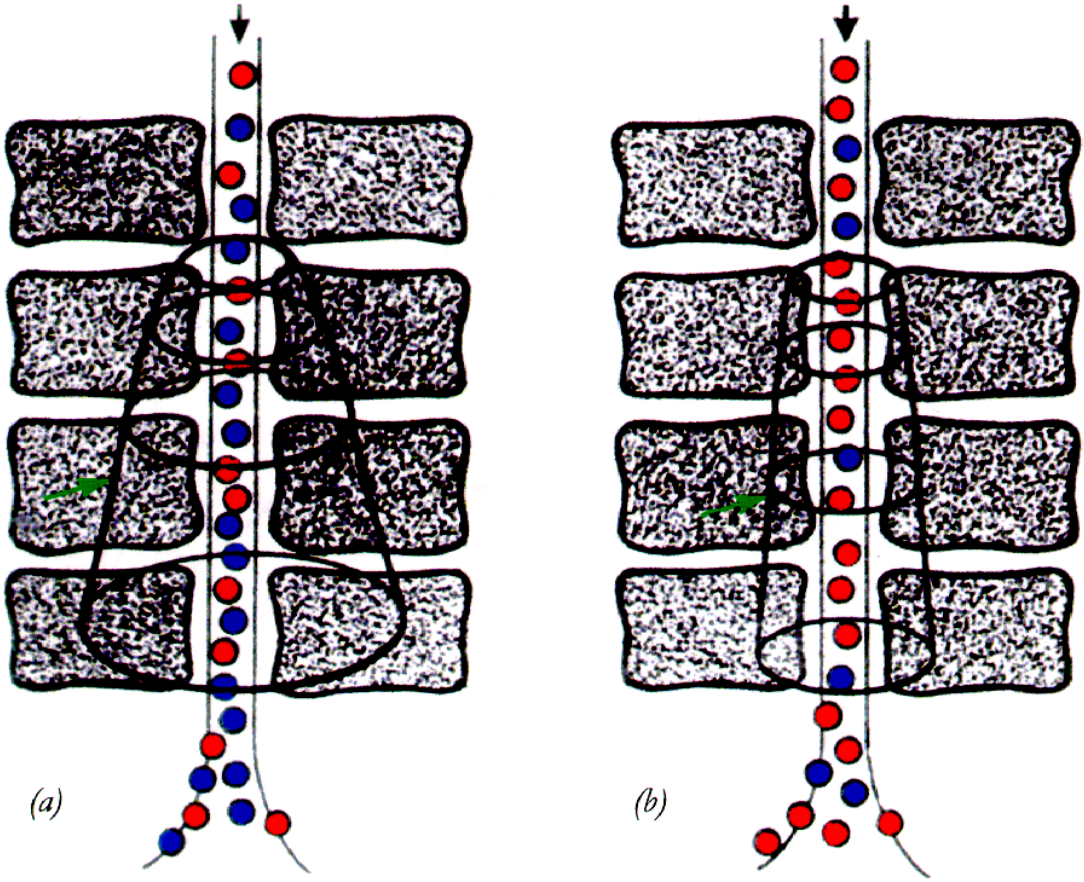


Fig. 2-6: Schematic description of the phemomena underlying BOLD-contrast. (a) Without active neurons, paramagnetic deoxygenated hemoglobin (blue dots) gives rise to local magnetic field gradients (indicated by the cone-like structure). (b) Neural activity leads to an increase in blood flow and a higher amount of diamagnetic oxygenated hemoglobin (red dots). This causes an increased homogeneity of the local magnetic field, and, therefore, slower signal decay/longer T2* times (reproduced from Windischberger, 1998, Fig. 31).

### *2.1.2.2 Imaging sequences used for BOLD-fMRI: echoplanar imaging (EPI)*

Although blood flow changes at a much lower rate than neuronal activity, the tracking of such changes requires fast imaging sequences. The imaging sequence most often or - meanwhile - almost exclusively used in fMRI is called echo planar imaging (EPI). EPI allows the acquisition of an image in far below one second. Although the theoretical basis of EPI was already conceived in 1977 by Mansfield, the technique had to wait until the nineties when improved hard- and software allowed its application.

Cohen (1999, p. 137) impressively demonstrates the temporal advantage of EPI over conventional imaging sequences: "While MRI, as practiced conventionally, builds up the data for an image from a series of discrete signal samples, EPI

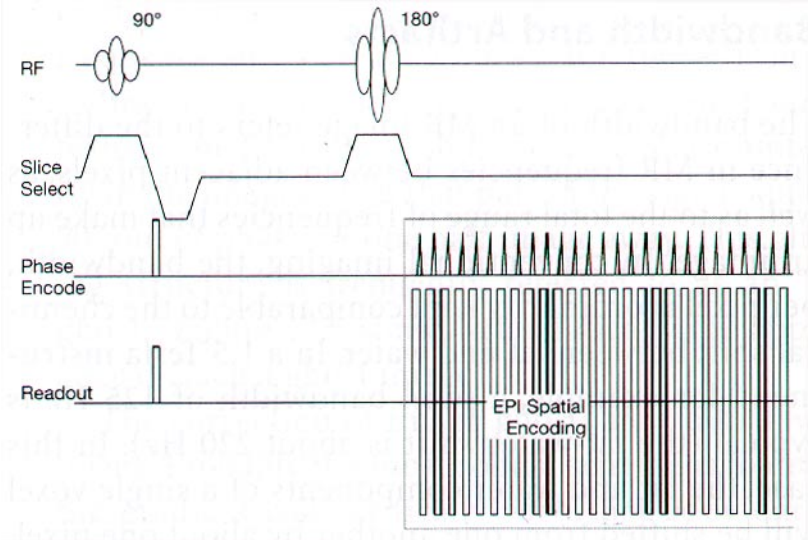


Fig. 2-7: Example for an echo-planar pulse sequence. In contrast to the spin-echo sequence depicted in Fig. 2-4, only a single excitation and inversion pulse has to be applied to acquire an image, since phase encoding is achieved via several short "blips" of the phase encoding gradient. This requires special hardware (ultrafast gradient switching), but results in a significant reduction of acquisition and repetition time (reproduced from Cohen, 1999, Fig. 13.4)

is a method to form a complete image from a single data sample, or a single "shot" (...) For example, a typical T2-weighted imaging series (...) requires that the time between excitation pulses, known as TR, be two to three times longer than (...) T1. The T1 of biological sample is typically on the order of a second or so (...); TR must therefore be 3 sec or more. A more or less typical MR image is formed from 128 repeated samples, so that the imaging time for our canonical T2-weighted scan is about 384 s, or more than 6.5 min. By comparison, the EPI approach collects all of the image data, for an image of the same resolution, in 40-150 ms (depending on hardware and contrast considerations). This reflects a nearly 10,000-fold speed gain".

This fundamental difference between conventional and EP imaging becomes obvious when Fig. 2-4 and Fig. 2-7 are compared. Both sequences are spin-echo sequences (which means that the dephasing signal is rephased using a 180° RF pulse following a 90° excitation pulse, evoking an echo when all spins are in phase again). However, while conventional imaging requires several RF excitations for each phase encoding step, EPI uses short blips in the phase encoding direction to acquire all data with one single shot. This allows the acquisition of multi-slice images of the whole-brain - depending on the in-plane spatial resolution and the slice thickness - in about 1 to 2 seconds.

The application of EPI to functional imaging depends on several (mainly hardware) requirements. High performance gradients with rapid rise times, high peak amplitudes, high accuracy and low eddy currents are required (eddy currents are the main reason for so-called ghost artifacts, which can cause serious problems in EPI). However, the power of the gradients cannot be infinitely expanded since, as the rapid changes in magnetic field produced by high-performance gradients can induce currents in the human body, which might lead to sensory stimulation. Also, the windings of the gradient coils produce considerable noise due to the rapidly changing forces related to the switching of the currents sent through them.

#### *2.1.2.3 Stimulation paradigms in fMRI: event-related and single-trial fMRI*

Data acquisition, data analysis and the mode of stimulus presentation are tightly related in fMRI. As a method which was originally inspired by PET and other similar methods rCBF measurement, stimulus presentation paradigms and data analysis approaches were vastly borrowed from PET in the "early ages" of fMRI. This meant that tasks were presented block-wise, i.e. that several tasks were successively presented, and that the signal acquired during interleaved "off"-blocks or "control"-blocks was subtracted from these "on"-blocks. Although this strategy has several disadvantages (unspecific activity related to the maintenance of attention and effort during a block is mixed with task-specific activity, correctly and incorrectly answered tasks are mixed in the analysis), one important reason for the preference of blocked designs was that even EPI repetition times were generally in the range of several seconds if multi-slice scanning was desired. This was due to limitations of the gradient hardware as well as of the computer hardware (network connections, disk speed etc.) available in the early nineties. Since such long repetition times would have resulted in too small an amount of data points collectable during single task executions, tasks were presented block-wise to obtain a stable and reliable measure of the hemodynamic changes related to task processing.

These hardware limits have now been vastly overcome, and the time required to scan the whole-brain of a subject with multi-slice EPI-fMRI seems to be ever decreasing (in the experiments performed for this thesis, which were started in early 1999, 15 slices were acquired in 1.5 sec; meanwhile, 20 and more slices with even slightly better spatial resolution can be acquired in about the same time with the same scanner due to a faster gradient system and more efficient comput-

ing technology). Thus, it has become more and more common to use a single-trial acquisition scheme.

In single-trial fMRI, stimuli are presented just as in ERP experiments, i.e. trial per trial. Since each trial has its own individual reference or baseline (which is the signal sampled immediately before task presentation), the single-trial acquisition mode minimizes the problem of blocked designs to separate stimulus- or task-from state-related activity. In blocked-designs, a separate or interleaved block with a control task is required. This "control" or "off" block either has to be subtracted or modeled as a covariate from the active "on" block. In order to be sure that differences between blocks are exclusively related to stimulus- or, in the case of cognitive tasks, cognition-related differences, it has to be assumed (apart from the assumption of “pure insertion” which might not always apply to cognitive paradigms; Sidtis et al., 1999) that state-related activity is constant in the control and task block, and that the baseline stability of the MR scanner is sufficient.

Although these assumptions, of course, also hold for single-trial fMRI, the short time interval between “control” (baseline) and task should reduce violations of these assumptions. Instead of fixed inter-stimulus intervals (which might evoke expectancy-related activities in the pre-stimulus baseline), variable interstimulus intervals, or even a subject-paced stimulus presentation mode (subjects decide individually when the next item shall be presented), are possible. The main advantage of the latter is that subjects are allowed to make short breaks between tasks and to call an item only when they feel ready to process it. This is again in contrast to block designs, in which longer breaks between task items are not possible due to the requirement of constant cognitive and neural activity during the whole block epoch. Single-trial acquisition also allows for event-related averaging of the single-trial responses in order to increase the signal-to-noise ratio of measurements. Such averages can either contain all single-trials, or can be sorted post-experimentally to specifically asses certain task-types (e.g., difficult and easy ones) or task-responses (e.g., correct or incorrect ones).

One of the best examples of this strategy is the use of single-trial fMRI data in memory research. In a typical memory experiment, subjects would be presented with items (e.g., words, faces, ...) that had or had not been presented in a previous part of the experiment. Many ERP experiments have revealed that brain responses to, e.g., correctly memorized items (hits) vs. correctly rejected items (correct rejections) are considerably different. Since it is not known before an experiment which items will be answered correctly or not, block designs hardly allowed investigations of such item- or category-specific activity.

Another central advantage of single-trial fMRI is that data acquisition is stimulus- and response-locked. This, in principle, allows a tracking of the interaction between brain regions which are involved in the solving of a complex cognitive task (see Humberstone et al., 1997). For example, brain activity related to the perception and perceptual encoding of a visual stimulus can be separated from activity related to the cognitive operations executed upon the resulting visual representation, and from activity associated with response preparation and response execution. However, due to the presumably rather low temporal resolution or the "sluggishness" of the hemodynamic response, a separation of rapidly changing cognitive processes will still be rather difficult and require sophisticated stimulus presentation protocols and analysis methods (see, e.g., Menon et al., 1998; Kim et al., 1997).

Data acquired in single-trial mode can also be used to perform time-resolved analyses (Richter et al., 1997ab, 2000), which means that the width and the onset of the signal changes in different brain areas are correlated with the processing time of the corresponding task trial. Depending on which aspect of the task a brain region correlates with, it might be inferred whether activity in this region is task-specific or only related to some peripheral, unspecific or constant aspects of task solving, such as response execution.

Summing up, stimulus presentation and data acquisition in single-trial mode has a number of advantages compared to the classical blocked stimulation protocols. However, in order to obtain sufficient data quality, several requirements have to be met (see, e.g., Ugurbil et al., 1999; Thulborn et al., 1999). Chief amongst them is a magnetic field a of sufficient strength to obtain a signal amplitude which is high enough to be detected during single task executions. This is the reason why almost all single-trial studies were performed at a magnetic field strength of 3 Tesla or higher (the most frequently used clinical MR scanners usually "only" provide field strengths of 1.5 Tesla). In addition, high-performance (ultra-fast switching) gradients, excellent homogeneity of the static magnetic field, and high-performance RF coils are mandatory.

#### *2.1.2.4 Analysis of fMRI data*

An enormous amount of data is acquired and stored in a typical fMRI experiment. An EPI-image slice usually consists of 64 x 64 pixels, and if a TR of 1 sec and a trial duration of, say, 10 sec is assumed, 40960 pixel values have to be stored for only one trial and for only one slice. If it is additionally assumed that a

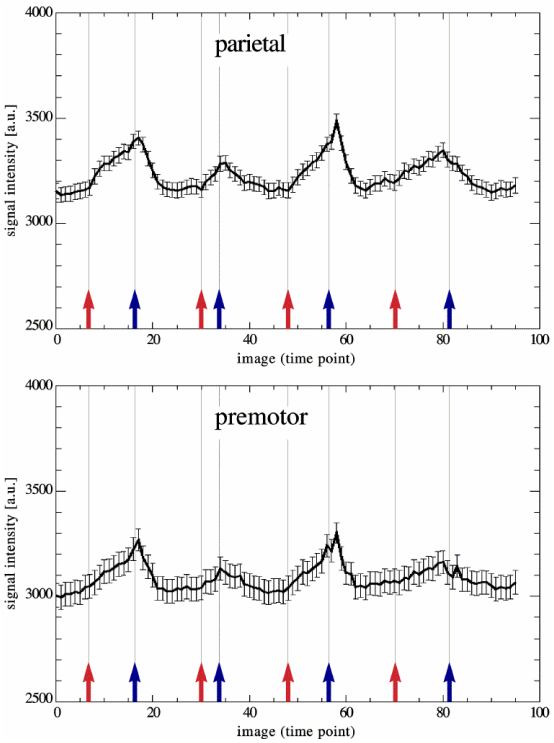


Fig. 2-8: Time course of signal intensity in two different regions of the brain during the solving of a cognitive task (see chapter 6 for details). Task onset and task completion are indicated by red and blue arrows. Note the "ramp-like" time-course of signal intensity.

typical experiment requires about 40 task repetitions, and that 15 or even more slices are acquired, more than 24 millions of individual data values have to be analyzed in order to reveal the task-related brain activity of only one subject.

Although fMRI is an image-oriented technique, it seems evident that image analysis cannot be based on a visual inspection of the spatio-temporal characteristics of these data - a strategy which frequently represents the first analysis step in ERP research. Thus, in fMRI, data have to be massively reduced. Several image processing strategies (see, e.g., Lange et al., 1999, or Lange, 1996, for comprehensive and extensive overviews) exist to extract the relevant information from the vast amounts of data (in fMRI, relevant usually means relevant with respect to functional neuroanatomy, neurological or neuropsychological aspects).

These strategies can be subdivided into paradigm-based and paradigm-free methods. While paradigm-based analysis approaches rely on testing whether and how well data can be fitted with a pre-specified model (e.g., whether a certain time-course is or is not contained in certain pixels), paradigm-free methods do not test existing models or hypotheses, but "look" at the data in an explorative manner. Fuzzy Cluster Analysis (FCA) is one interesting example of the latter type of methods. However, since mainly results obtained with paradigm-based methods will be presented in this thesis, the reader interested in FCA is referred to a number of papers published by the NMR group here in Vienna which specialized on FCA of fMRI data (see, e.g., Moser et al., 1997, 1999; Baumgartner et al., 1997).

One of the first paradigm-based analysis concepts for fMRI was introduced by Bandettini et al. (1993). They suggested that a high correlation of the observed signal time course with a pre-defined reference function should indicate task-related signal changes. As a model for the true hemodynamic response, a boxcar

or trapezoidal reference function was proposed which - depending on the TR - might also be shifted in time to account for the above-mentioned delay in hemodynamic response. It has been demonstrated (Lange, 1996; Klose et al., 1999) that this approach is equivalent to computing t-tests of signals acquired during active ("on") vs. inactive ("off") phases of a trial, an approach which was chosen in this thesis. The correlation analysis approach is easy to implement, does not require high-performance computing devices, and is quite straightforward. Its main assumption concerns the shape of the hemodynamic response. Although a boxcar or trapezoidal reference function might be a rough approximation of this hemodynamic response, Fig. 2-8 shows that the actual signal time-course does not always resemble a boxcar. Another problem with this approach is that a threshold has to be set in order to define when a certain correlation coefficient is believed to indicate significant physiological responses as opposed to random signal fluctuations. This, however, is one of the major "data reduction" tasks all fMRI analysis methods have to overcome.

Although correlation analysis is still used by many groups, it is being replaced more and more by analyses using the statistical parametric mapping software (SPM)[2]. The corresponding MATLAB-coded software is freely available for research purposes (http://www.fil.ion.ucl.ac.uk/spm). SPM was and is continuously developed by the methodology group of the Wellcome Department of Cognitive Neurology/London/UK under the supervision of Karl Friston. Common to all analyses performed with SPM is the use of the General Linear Model (GLM) to assess the variability of data in terms of experimental effects, confounding effects, and residual error. SPM was originally developed for the analysis of rCBF data collected using PET or SPECT, but soon became incorporated by the fMRI community, which also led to the development of an fMRI-specific SPM-module (version SPM99). It is even planned to make SPM a general-purpose analysis tool with which all kinds of brain imaging (including EEG and MEG[3]) data can be analyzed (Stefan Kiebel, personal communication). Since SPM represents a central analysis concept in fMRI research and was also used in the group-analysis of the study

[2] This is also indicated by a survey of the fMRI papers in the year 2000 issues of the journals NeuroImage and Human Brain Mapping (HBM). In 25 % of the HBM fMRI papers, SPM was used. About 50% of the remaining reports used correlation analysis or t-tests. In the journal Neuroimage, a much higher percentage (63%) of SPM-based fMRI analyses was observed. Again, about 50% of the remaining reports used correlation analysis or t-tests.

[3] Indeed, some EEG studies already exist in which SPM-like concepts were used in data analysis (Yoshino et al., 2000).

presented in chapter 7, I will briefly describe the steps involved in the "SPMing" of fMRI data.

#### *2.1.2.4.1 Analysis of fMRI data: Statistical Parametric Mapping (SPM)*

The analysis of fMRI data with SPM requires both patience and time. A number of consecutive and computationally demanding analysis steps have to be accomplished to finally obtain indices of activity at the voxel- and cluster-level (see Fig. 2-9). Following several preprocessing steps (image reconstruction, motion correction, correction of slice timing), data are transformed into a common stereotactic space. This is achieved via normalization of the single-subject data to a template provided by the Montreal Neurological Institute (MNI; see http://www.bic.mni.mcgill.ca).

The main reason for this rather time-consuming and far from trouble-free procedure is to allow for multi-subject comparisons, as well as to obtain a standard framework for reporting results using the three stereotactically defined image coordinates of active voxels (which, however, do not exactly match the coordinates reported by Talairach & Tournoux, 1988; see Brett, 1999).

In SPM99, normalization is fully automatic and is achieved via several affine transformations (rotation, translation, shearing, zooming) which match the original image to the template brain using least-squares optimization. Following normalization, images are spatially smoothed by convolving them with a Gaussian kernel. This is done for several reasons. One of them is to improve the signal-to-noise ratio. According to the matched filter theorem, smoothing data with a filter that matches the signal will increase the signal-to-noise ratio of this signal. In the case of spatial smoothing, however, this would not only require advance knowledge of the size of the active regions/image clusters, but also a similar to identical size of active clusters in different brain regions, which usually does not apply. As a consequence, either several analyses are performed using smoothing with different kernel sizes (which does not only increase computation time, but also the probability of false positives), or a kernel size of about 2-3 times of the voxel size seems to be chosen according to some "tacit" convenience.

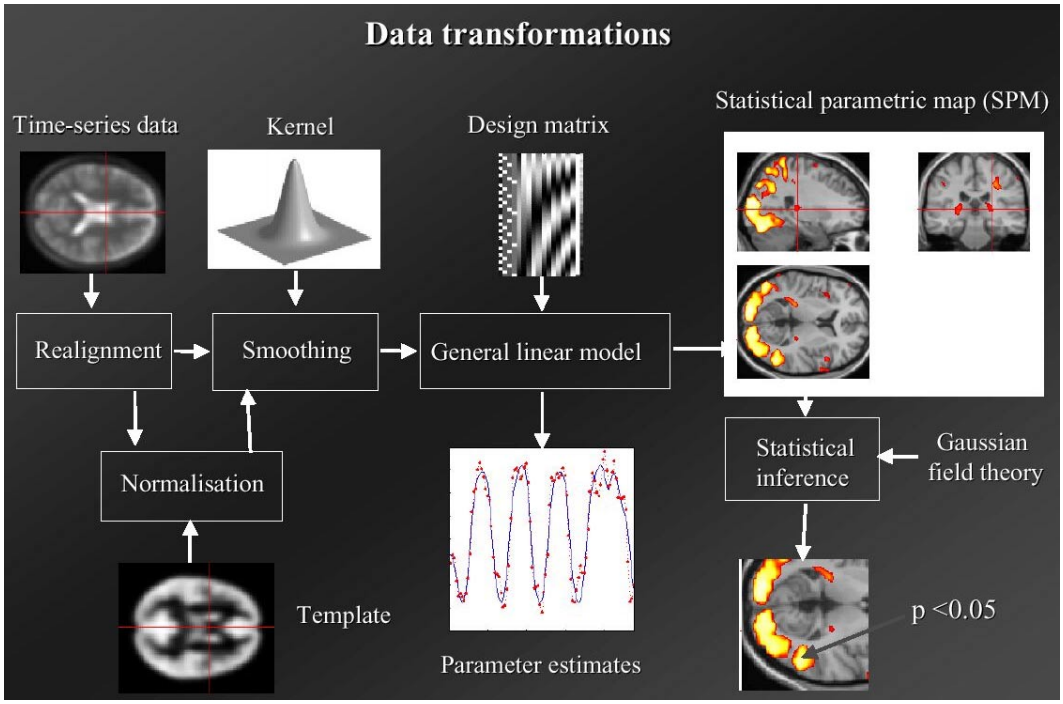


Fig. 2-9: Overview of the processing steps that have to be accomplished when using SPM for data analysis. Following normalization to a template, data are spatially smoothed with a Gaussian kernel. The normalized and smoothed data are then modeled, and statistical maps of parameter estimates are calculated. Statistical significance of these maps can be assessed via the theory of random Gaussian fields (reproduced from http://www.fil.ion.ucl.ac.uk/spm/course/notes00/Ch1slides00.pdf).

Another reason to perform smoothing (and to chose different levels of smoothing) is to account for interindividual differences in both structural and functional neuroanatomy. Depending on the hypothesis, smoothing kernels of up to 20mm full-width-at-half maximum (FWHM), i.e. about 7 times the most common spatial resolution of EPI-fMR images, can be chosen for group analyses (C. Büchel, personal communication). Last, but not least, spatial smoothing with a Gaussian kernel is applied in order to make it more likely that data are distributed according to a normal distribution - which is a central requirement of all kinds of GLM analyses.

Following smoothing, the GLM is used to investigate whether several experimental variables and confounds can be used to predict or model the actually measured data. For example, if a boxcar function determined by the stimulus onset and offset times is used as a predictor, it can be investigated whether and where in the brain it contributes to a better prediction of the data. If the predictor of a certain voxel explains zero of the variance of the signal fluctuations in that voxel, this basically means that there is no task-related signal change in this area. In principle, this is an extended version of using the t-test or correlation analysis ap-

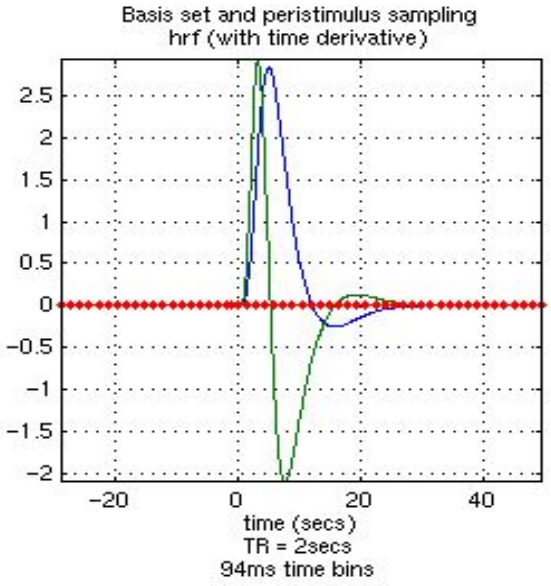


Fig. 2-10: Canonical hemodynamic response function and its temporal derivative used by SPM99 for the modeling of the time-course of fMRI data (figure extracted from the SPM99-software).

proach presented above (since both can be formulated as a special case of the GLM).

However, there are two (optional) important differences in SPM. One is that SPM allows additional modeling of the data with confounds, reducing the residual error in the linear regression. The other, more important difference is that SPM allows the use of different basis or reference functions. These functions can be used to model the time-course of the data with more sophisticated models than represented by a boxcar reference or a t-test (a t-test basically is a box-car reference with value zero in the "off" and value 1 in the "on"-period; see above). The most frequently used basis function is the canonical hemodynamic response function (hrf; see Fig. 2-10). Other approaches, such as the hrf and its temporal derivative, or a fourier set, or a three-gamma-functions basis function, can be chosen to model other time-courses in the data and to yield a more accurate fit of the model to the data. The more time-courses which are potentially contained in the data are modeled, the more accurate the model will be. However, this comes at the cost of losing degrees of freedom for statistical inference, and basis functions such as the fourier function can not be interpreted as straightforwardly as the canonical hrf basis function.

After the explanatory variables (predictors and, if any, confounding effects) and the basis function(s) have been specified, they are entered into the design matrix of the GLM. Each column of the design matrix corresponds to an experimental effect or an effect that is considered to confound the data (including low-pass and high pass-filters). Parameter estimation is then performed using least-squares fitting, resulting in statistical parametric maps based on these parameters (hence the name SPM). These SPMs are thresholded in order to decide whether any of the explanatory variables affects the data in a systematic way. The threshold is defined via critical t- or F-values derived from the t- or F-distribution.

These critical values have a certain probability of being observed given that the null hypothesis is true, which might for example be that the presentation of a visual stimulus has no effect upon blood oxygenation in primary visual cortex. It is here where the problem of multiple comparisons, which is one of the most difficult challenges in the statistical analysis of functional brain images, has to be considered. The core problem is that the probability of obtaining a false positive, i.e. of erroneously rejecting the null hypothesis, exponentially increases with the number of statistical comparisons. As already stated, a typical fMRI image slice is made out of 64 x 64 pixels. If we assume that about 2/3 of these pixels cover the brain, and if we assume a significance threshold of $\alpha \leq .05$ (which implies that we will - on the average - commit a so-called type I error in 5 % of all comparisons), 136.5 of the statistical comparisons in this slice will be significant by chance alone. Put another way, the probability of *not* obtaining any pixel that survives the chosen threshold is $0.05^{2731}$, even if $H_0$ holds for all pixels! Thus, even if no task-related brain activity exists, we will nevertheless observe some pixels surviving the chosen threshold in our images.

Several solutions have been conceived to escape this situation and to maintain the family-wise probability of committing type I errors at the originally chosen $\alpha$-level. One of them is Bonferroni correction, which means that the significance threshold is corrected for the number of comparisons m according to the formula $\alpha(\text{corrected})=1-(1-\alpha)^{1/m}$, with $\alpha$ being the uncorrected level of significance (Bortz, 1993). For example, if we had three tests, the corrected significance threshold would be $\alpha(\text{corrected})\approx 0.017$, so the probability of obtaining a type I error in at least one of these tests would be $P=1-(1-0{,}017)^3\approx .05$. The basic assumption of Bonferroni correction is that the multiple comparisons are independent of each other. If this is not the case, conservative tests result, which means that the probability of type II errors (erroneously maintaining the null hypothesis although the alternative hypothesis is true) is increased. In brain imaging, where neighboring data values show higher correlation than more distant ones (a fact which is, by the way, amplified by the spatial smoothing which "smears" activity from pixels to their neighbors), multiple tests may show substantial dependence of each other.

Thus, another means of p-value correction has been proposed that relies on the theory of random Gaussian fields (see, e.g., Worsley, 1996ab; Friston et al., 1995b). Admitting that this might be an overly simplified statement, the basic approach is to estimate the smoothness or "spatial correlation" in the images. From this value, it is derived how many independent observations can be statistically assessed, and the statistical inference is corrected for this number to maintain the

probability of committing type I errors for all comparisons at the originally chosen $\alpha$-level. In case there is no spatial correlation, i.e. data values are 100% independent, corrected p-values are identical to Bonferroni-corrected ones. In case all observations are entirely dependent, the statistical comparisons will also be entirely dependent, and one single uncorrected test will be sufficient. However, the most common and more complicated case is that data are partially correlated. In this case - without going into too much detail - corrected p-values are calculated as follows: First, the number of resolution elements (resels) of an image is determined, with one resel being a block of pixels of the same size as the FWHM of the smoothness of the image (for instance, with a matrix size of 64 x 64 and a smoothing kernel of 3 x 3 pixels, 64/3 * 64/3, approximately 455 resels are obtained for only one single slice). The number of resels is similar, but not identical to the number of independent observations. Using the number of resels in an image, it is possible to calculate the most likely value of the so-called Euler characteristic (EC). The Euler characteristic is a topological measure based on the number of "peaks" and "holes" in an image (in our case, a statistical map, e.g. a t-map). The more peaks or "blobs" are contained in an SPM (i.e. the more values survived the chosen uncorrected threshold), the higher the EC will be. Taking the chosen uncorrected threshold and the number of resels, the EC is a good approximation of the probability of obtaining blobs surviving this threshold if the image is supposed to conform to a random field, and can thus be used to determine the corrected p-value[4].

After all these steps have been accomplished, a map is computed which contains only pixels which survived the chosen threshold, and which thus are considered to reflect a significant or non-random response. Such a map can be calculated separately for the different explanatory variables by defining so-called t- or F-contrasts. For example, we might test whether activity during stimulus presentation is higher than during the interstimulus-intervals by appropriately weighting the parameters of these predictors in the linear regression equation and by setting the remaining parameters (confounds etc.) to zero. We might also want to know which

[4] Generally, it also seems questionable whether a correction for multiple comparisons is required by all kinds of analyses, especially when inference at the voxel-level is sought. In the latter case, all brain voxels are assessed to test the null hypothesis whether there is no activity in the brain related to the experimental condition(s). Whenever any of these voxels exceeds the pre-defined threshold, it is taken as evidence for the alternative hypothesis. However, such an unspecific hypothesis should only be tested in purely exploratory studies. Usually, the question whether there is activity in the brain is already well-established by former studies. Instead, specific assumptions about the involvement of (a network of) brain regions exist, which is a hypothesis completely different to the one for which the multiple comparisons are corrected for (see also the discussion in chapter 6).

brain areas are more active in a certain task than in another and vice versa (e.g., movements of the left vs. the right finger). The resulting p-value maps and their stereotactic coordinates are usually reported in the literature as the result of a massive data reduction (sometimes from millions of pixels to only one well-defined "blob" of activity).

Inferences can be drawn on three levels, which are the voxel-, cluster, and set-level (Friston et al., 1995a). If inferences at the voxel level are sought, it is tested which voxels have an intensity equal to or higher than a chosen threshold *h*, which gives a test with - generally - high regional specificity but low sensitivity. Inference at cluster level implies assessing the probability of observing a cluster *c* of size *k* or more, defined by a threshold *u* (since in fMRI, cluster level inference is more powerful when a lower threshold is chosen, this threshold is usually lower than the one used for the voxel level inference; see Friston et al., 1995a). This gives a test with generally higher sensitivity, but lower specificity since protection of the risk of committing an error at the voxel level is not given. Finally, inference can be drawn at the set level, which boils down to the probability of obtaining a certain number of clusters or a cluster-set in a given image (more specifically, of obtaining *c* or more clusters with *k* or more voxels, above a threshold *u*). This results in a test which has high specificity but low localizing power/regional specificity. Although Friston et al. (1995a, p. 223) "(...) envisaged that set-level inferences will find a role in making statistical inferences about distributed activations, particularly in fMRI", they are hardly encountered in the results sections of fMRI or PET research reports.

As this very brief and far from comprehensive summary has shown, a number of time-consuming and computationally expensive analysis steps have to be accomplished in order to obtain statistical parametric maps. Also, several assumptions and approximations concerning the distribution of the data have to be made with SPM and its GLM-approach. These assumptions might not always hold, especially when the sample size is low, which is often the case (see also Holmes et al., 1996; Vitouch & Glück, 1997). However, SPM is a research tool widely accepted by the functional neuroimaging community (an acceptance which might partially be related to its free-ware status and the need for a standardized analysis framework), and it is being constantly improved by one of the presumably best-funded and manpower-equipped labs in the world. However, it must be noted that SPM represents only one way amongst many others (see, again, Lange et al., 1999, for an overview) of drawing statistical inferences with fMRI data, and as almost all data analysis approaches for the still very young method of fMRI, it is

work in progress. It should also be noted that the described general approach (scanning the whole search volume for significance) only applies if no definite a-priori hypothesis exists. If, for instance, we had the specific hypothesis that parietal cortex is more active during mental rotation than during reading, we might test this by specifically assessing activity in this brain region using a region-of-interest approach (see also Worsley et al., 1996b).

### *2.2 Electroencephalography (EEG), Event-Related Potentials (ERPs), and Slow Cortical Potentials (SCPs)*

Compared to fMRI, electroencephalography (EEG) is a relatively old technique which was applied in humans for the first time in 1928 by Hans Berger. Some time ago, it appeared that EEG and the associated technique of ERPs would be replaced more and more by the tomographic techniques and even by magnetoencephalography (MEG; Crease, 1991; Wikswo et al., 1993). However, in recent years, a kind of re-launch or re-appreciation of the EEG technique seems to be taking place. This might have been triggered by the insight that the temporal resolution of EEG makes it a technique which can keep pace with the speed of human information processing and the associated fast changes in neural activity. In addition, the main disadvantage of EEG, namely its comparably low spatial resolution, is made up for more and more by technical and methodological advances (such as an ever increasing number of recording channels, improved and more sophisticated source localization and surface mapping techniques, etc.).

Although there are several ways to analyze EEG data (such as spectral analysis, coherence analysis, event-related de-/synchronization), the most common approach is the computation of event-related potentials (ERPs). When topographically recorded, ERPs can be used to map changes in neural activity related to an internal or external event with millisecond resolution (however, see also chapter 2.3). Depending on their latency, morphology and supposed functional significance, ERPs can be subdivided into several components or component classes. For our purposes, the most relevant distinction is between transient phasic responses with an early latency, and sustained tonic responses with rather late onset latencies. These "late components" have been given several labels, such as slow potentials, slow waves, slow potential shifts, slow potential changes, slow brain potentials, steady potentials, DC- or DC-like potentials, DC shifts and many others.

Unfortunately, a clear terminology is still not at hand. Interestingly, many researchers that did not yet have the possibility of working with these "late components" connote with this kind of research that the absolute level of DC-activity (which would be called the steady potential) is measured. This was an approach frequently used in the "early ages" of slow potential research, although some rather rare approaches still exist in which the absolute level of DC-activity is taken as an indicator of brain activity, or, rather, brain activation (e.g., Schmitt et al., 2000; Trimmel et al., 2000).

However, most studies of today (including our own) use the technique of event-related data acquisition and averaging to achieve a sufficient signal-to-noise ratio (with the signal in this case being the slow cortical activity). When event-related averaging is used, the term event-related slow cortical potentials seems to describe most precisely which kind of data was collected and how its was analyzed. Thus, I will also adhere to this terminology, but will use - for the sake of brevity - the abbreviation SCP or SCPs.

### 2.2.1 Event-related Slow Cortical Potentials (SCPs)

SCPs are rather difficult to define on a purely conceptual level. However, they can be characterized based on the morphology of their time-course (which might be described as "ramp-like"; see also Rösler et al., 1997), their onset latency and the EEG recording equipment. The first description of SCP-like components was tightly coupled with two paradigms. These paradigms were designed to elicit either a Bereitschaftspotential (BP; Kornhuber & Deecke, 1964), or a Contingent Negative Variation (CNV; Walter, 1964). In the classical BP-experiment, where subjects have to perform voluntary movements, a movement-preceding increase in negativity could be observed which was thought to reflect neuronal preparation and/or programming of the movement execution. A similar ramp-like increase in negativity of considerable amplitude can be observed in the interstimulus interval of a CNV-paradigm, where subjects have to respond to an imperative stimulus after previous presentation of a warning stimulus.

Thus, both paradigms investigated activity during the anticipation of or the preparation for an event. This led to the hypothesis that such negative variations of the EEG amplitude might be related to the mobilization of resources. This mobilization was thought to be achieved via a lowering of synaptic thresholds and a resulting increase in cortical excitability that would be consumed in the reaction part

of the paradigm, being reflected in a positive signal deflection following the response (see, e.g., Birbaumer et al., 1990; Rockstroh et al., 1989, Elbert, 1993).

However, ramp-like negative amplitude increases have meanwhile been observed in a variety of experiments which did not only require simple response preparation or target detection, but the processing of more or less complex cognitive and sensory tasks (for recent overviews, see Bauer, 1998; Bauer et al., 1998; Rösler et al., 1997). To list only a few newer examples, SCPs were observed during visuo-spatial imagery (e.g., Lamm et al., 1999, 2001; Bajric et al., 1999), numerical reasoning and associated negative emotions (Fretska et al., 1999), affective speech processing (Pihan et al., 1997, 2000), memorization of verbal and spatial material (Rolke et al., 2000), piano playing (Vitouch et al., 1998), and acoustic perception during different states of consciousness (Fitzgerald et al., 2001). Common to all these experiments is that the assessed cognitive or sensory event required prolonged information processing, starting from about 2 sec (Fitzgerald et al., 2001) up to about 25 seconds in the piano-playing study.

Thus, one might conclude that one requisite for SCPs to show up on the scalp surface is prolonged information processing[5]. Fig. 2-11 and Fig. 2-12 exemplify such SCPs recorded in two different experiments. Fig. 2-11 shows SCPs from an experiment in which subjects were presented with simple tones of 2 sec duration. Following an initial transient response with a latency of around 150 msec and a fronto-central peak, a sustained negative potential can be observed with a similar topography, which dissolves within about 200 msec after the stimulus is turned off. The topography and the time-course of this potential make it likely that it reflects ongoing neural activity in auditory cortex related to the prolonged sensory input. Fig. 2-12 shows results from a more "cognitive" experiment. Subjects had to perform a task requiring dynamic visuo-spatial imagery (see Lamm et al., 1999). Again, following initial phasic potentials which now also include a P300-like component, negative-going potential changes can be observed which increase in amplitude during the whole interval of task processing and show a maximum over the occipito-parietal scalp.

[5] This, however, does not exclude that changes in steady potentials (SP) are an omnipresent phenomenon which is also present during shorter stimulus processing times. For instance, it has been shown that the amplitude and latency of P300 depends on the stimulus-preceding SP-level, or that CNV amplitude is diminished depending on the CNV-preceding negativity (see, e.g., Bauer et al., 1993; Gaillard & Näätänen, 1980). However, since it is rather difficult to separate the phasic components from the underlying slow potentials, and since the amplitude of the latter makes up only a small fraction of the former, such SPs are usually ignored or cannot be unambiguously identified in the recordings (especially when an amplifier with a time-constant is used).

Two additional important aspects become evident in a thorough inspection of these two figures. One is that SCPs have a much lower amplitude and a much lower rate of amplitude change at the scalp surface than the "classical" evoked responses (that is also why the adjective "slow" seems to be quite appropriate, although I think it was originally chosen to reflect the slow response in terms of onset latency). For example, despite 5 sec of neural activity and a constant increase in negativity, electrode Pz does not reach an amplitude as high as the one the early phasic components have achieved within several milliseconds. This sometimes makes it quite difficult to separate the slower response from the early transient response, especially if the aim is to determine a discrete onset latency of SCPs (see also the discussion in chapter 2.3 and chapter 6).

The second, more pleasant aspect is that SCPs show processing-specific topographies. While the auditory evoked SCP shows a bilateral fronto-centrally dominated scalp distribution[6], visuo-spatial imagery evoked a parieto-occipital scalp maximum. Since such task-specific topographies have been observed in virtually all studies using SCPs, one might conclude that topographically recorded SCPs can be used as a fairly accurate indicator of cortical activity related to prolonged cognitive, sensory or motor processing (with, however, the same restrictions in the ability to localize as classical ERPs, see Footnote 5). While the early or transient responses, which most ERP research still focuses on, might be useful for the investigation of the effects of stimulus evaluation and of orientation towards a task, SCPs are useful for the investigation of the process of task-solving per se. This makes multi-channel SCP recordings especially attractive for the psychologist or cognitive (neuro-)scientist aiming to gain non-invasive access to the neural bases of human cognition.

#### *2.2.1.1 Measurement of Event-Related Slow Cortical Potentials*

Recording SCPs requires a technology similar to the one used in the recording of "regular" EEG or of short-latency ERPs. However, additional provisions have to be met to avoid slow drifts or other artifact-related changes of the measurement baseline, since such artifacts might easily obscure the low-amplitude SCPs. In the Brain Research Laboratory (Department of Psychology, University of

[6] Köhler et al. (1955) were the first to explain this rather contra-intuitive scalp distribution as an effect of the gyrification and cytoarchitecture of the human auditory cortex. Since the human auditory cortex lies at the upper surface of the temporal lobe, its neurons are oriented radial towards the fronto-central and not towards the temporal scalp region. This results in activity that is picked up in the fronto-central electrodes, rather than in the temporal ones.

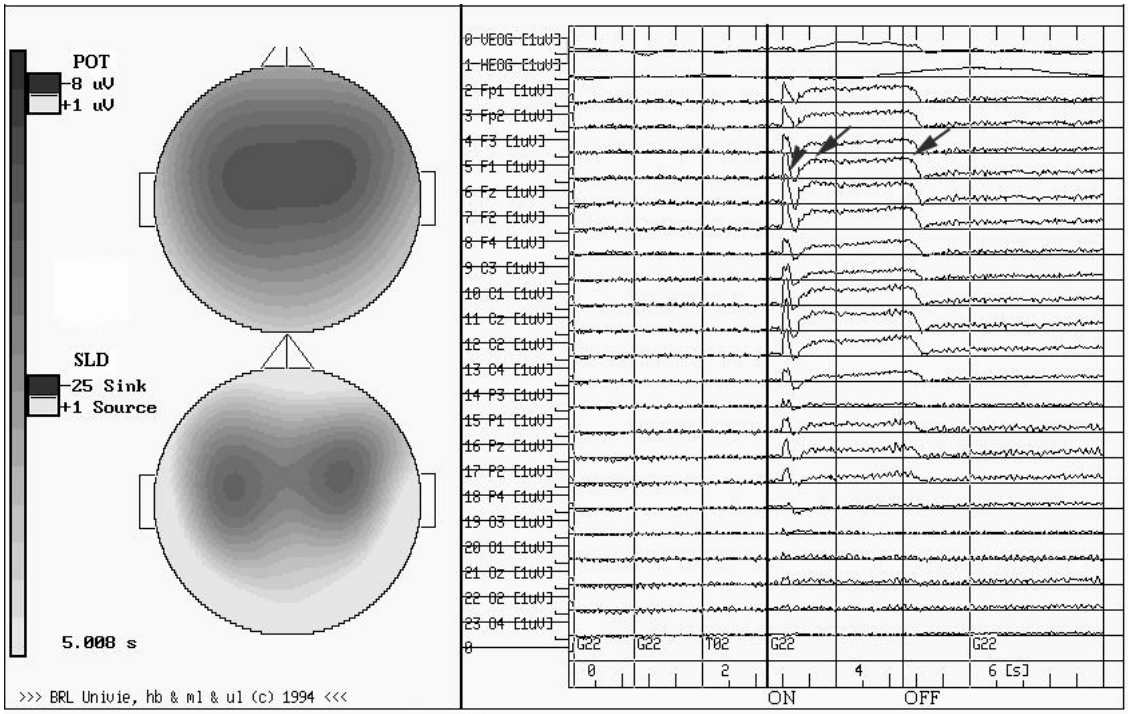


Fig. 2-11: ERPs and SCPs during prolonged acoustic stimulation (presentation of a 800 Hz tone for 2 seconds). Approximately 150 ms after tone presentation (ON), a phasic negative potential is evoked (arrowhead). After ~500 ms, a sustained negative potential develops which persists until the stimulus is switched off (OFF; indicated by two arrows). The left-hand side of the figure shows the SCP and CSD topography of this SCP at a latency of 2 seconds post stimulus onset (adapted from Bauer, 2001, Fig. 1).

Vienna, Austria) which has a long tradition in recording SCPs and steady potential changes, the following standards have proven to provide recordings of excellent quality.

The first indispensable requisite is a DC-amplifier (i.e. an amplifier with a theoretically infinite time-constant) with high-input impedance (> 10 GΩ, based on theoretical considerations; Bauer et al., 1989; Bauer, 1998) and excellent baseline stability (< 5μV/day). Commercial DC-amplifiers are now provided by Neurosan Inc. (Synamps, Neuroscan), albeit with a much lower input impedance (10 MΩ). A high input impedance is mandatory since it allows to keep the currents flowing through the recordings electrodes as low as possible, minimizing the danger of slow polarization in tissue below the recording electrode. Second, skin-scratching (Picton & Hillyard, 1974) is recommended to equalize inter-electrode impedance at a value ≤ 1 kΩ, and to minimize skin potential artifacts. Skin-scratching also allows the electrode-skin interface to be kept stable for a longer period of time compared to other skin-preparation techniques, such as abrasion of the upper layers of the epidermis. Third, non-polarizable electrodes (e.g., Ag/AgCl) have to be used to

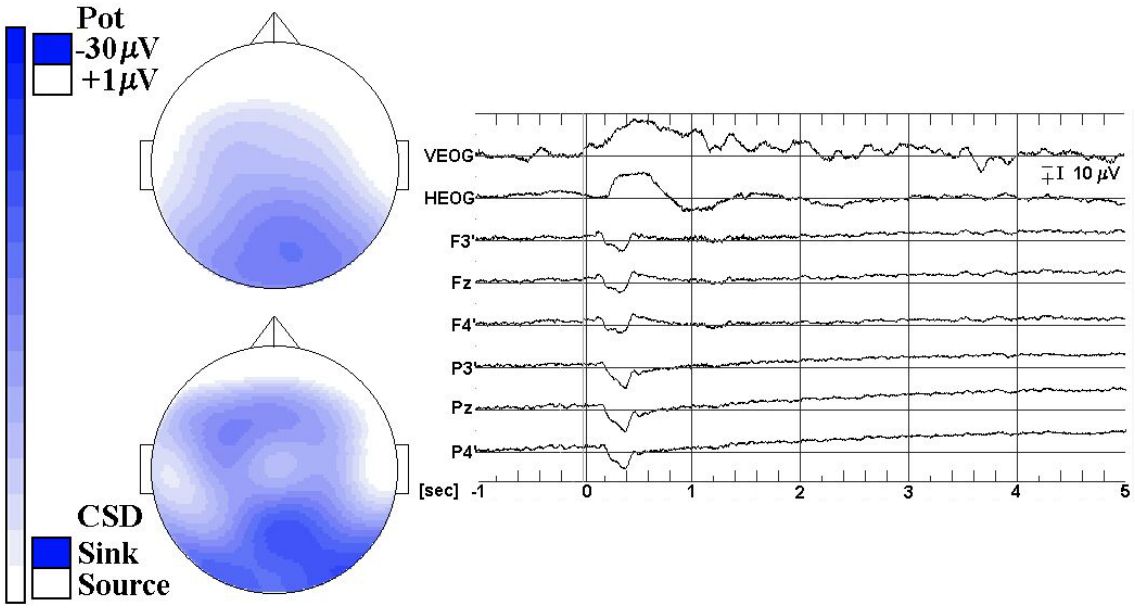


Fig. 2-12: ERPs and SCPs during processing of a dynamic visuo-spatial imagery task. As in Fig. 2-11, phasic ERPs of negative and positive polarity are followed by a slow increase in negativity. On the left side, the topography of activity at a latency of 5 seconds after task presentation is shown. In contrast to Fig. 2-11, this topography shows a maximum over the posterior regions of the scalp, reflecting extended neural processing in the occipital and the parietal cortex (adapted from Lamm et al., 1999, Fig. 2).

avoid polarization at the surface of the electrode, which might result in slow drift artifacts or signal attenuation. Fourth, in order to obtain mechanically independent recordings, and to avoid artifacts resulting from movements of electrodes relative to the skin, electrodes are mounted on electrode sockets glued to the scalp using collodion. An additional provision is to use degassed electrode gel, especially if long-term recordings (> 1h) are performed. Otherwise, macroscopically invisible bubbles contained in the gel might migrate to the electrode surface due to thermal effects and alter the electrode potential, resulting in slow drift artifacts. According to our experience, it is also mandatory to fill electrodes with the gel at least 1/2 hour before their application to allow for the stabilization of the electrode potential. Although this whole procedure results in some extra-time for application (~ 2 1/4 h per subject in this thesis, in which 49 EEG, EOG and reference electrodes have been used), the additional effort is justified by a higher quality of recordings and by a reduced amount of trials which have to be excluded due to artifacts.

#### *2.2.1.2 Analysis of SCPs: visualization and SCP mapping*

The main challenge in EEG and hence also in SCP research is to identify the cortical generators of the surface-recorded activity pattern. Up to about 15

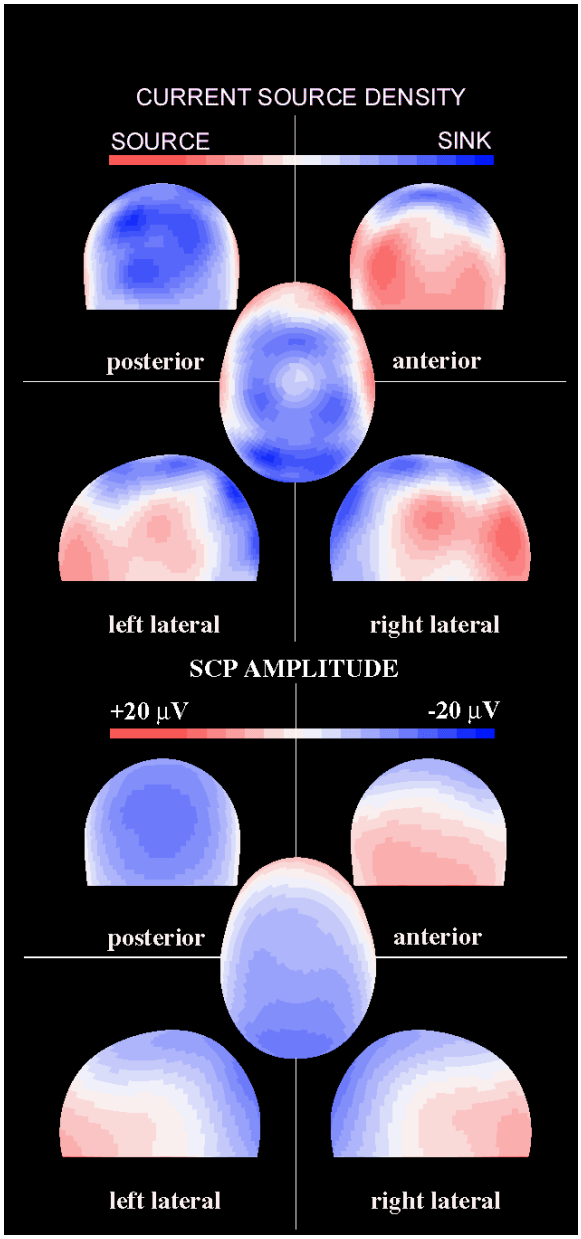


Fig. 2-13: Maps calculated using SCP amplitude and its CSD transform. While the topography based on the SCP amplitude is rather blurred and has low "spatial frequency", the CSD topography depicts several sinks and sources which for instance allow a differentiation of activities over the posterior scalp into parietal and occipital activity.

years ago, ERP and SCP analyses were mainly based on a visual inspection and statistical analysis of wave-form or time-course differences (e.g. to investigate whether neurological or psychiatric patients show increases in the onset latency of certain ERP components compared to normal controls). Questions about the cortical generators of these differences could hardly be asked, since in most studies, only few recording channels were used. In recent years, triggered by faster computing hardware and visualization software and the availability of multichannel amplifiers, several approaches have been developed to relate topographical activity to the underlying cortical anatomy.

The most common of these is the computation of SCP maps. Since the actual surface distribution can be sampled only partially, map computation requires some kind of interpolation algorithm to estimate activity between the electrodes. The main aim of EEG mapping is to provide a more comprehensive and unbiased summary of the spatio-temporal pattern of activity. In addition, the usually rather blurred potential maps can be substantially "sharpened" by calculating scalp Laplacian or scalp current source density (CSD) maps (Fig. 2-13 gives an example of how considerable this effect can be). CSD maps reveal where volume current emerges from the cortex and is passed to the skull and the scalp; thus, they shall provide a more precise estimate of the epicortical surface potential distribution (Nunez, 1989; Nunez et al., 1994;

Srinivasan et al., 1996; Babiloni et al., 1996). An additional advantage is that they are reference free, and that they attenuate low spatial frequencies ('smearing') introduced into the scalp potential distribution due to volume conduction. However, this comes with the disadvantage of a reduced sensitivity to deeper sources.

Independent of whether potential maps or their CSD-transforms are computed, interpolation can either be based on a spherical head model (spherical-spline interpolation; e.g., Perrin et al., 1987, 1989), or a realistic head model (e.g., Babiloni et al., 1996; Gevins et al., 1991). While the spherical approach is easier to implement and requires considerably less computation time, the realistic head model yields more accurate maps (see also chapter 4). When a realistic head model is used, information about the individual head geometry of each subject has to be acquired. Up to now, this information was either gained from structural MRIs (Babiloni et al., 1996, 1997; Gevins et al., 1991), or from a three-dimensional digitization of the head surface (Huppertz et al., 1998; see also chapter 3). Either method requires the measurement of individual electrode coordinates. As chapter 4 will show, this represents yet another attempt to increase accuracy of SCP and EEG mapping, since interpolation errors resulting from the unrealistic assumption that electrode coordinates are constant between subjects are avoided.

In addition to the rather simple and straightforward mapping of surface activity, several more sophisticated source localization algorithms have been developed to solve the so-called inverse problem. Since none of these source localization procedures was used in this thesis[7], I will keep their description very short. The presumably most well-known example is the localization of equivalent dipoles or dipole configurations that explain the surface distribution (see, e.g., Scherg & von Cramon, 1986; Scherg et al., 1993). Dipole solutions have often been criticized as being physiologically unrealistic, and they might indeed be of limited value in the analysis of electrophysiological activity during cognitive tasks which are usually recruiting large and widely distributed networks of brain areas. Also, most of the source localization algorithms require rather specific hypotheses in the form of anatomical constraints, which, unfortunately, do not always exist in the still more exploratory assessment of cognitive processing. However, a good example to overcome these limitations is the proposal of Scherg & Göbel (1998) to use ac-

[7] This has been due to monetary reasons, since source localization software is rather expensive. In addition, as will be shown in detail in chapter 7, EEG data were not acquired simultaneously, but consecutively using two electrode sets. This would presumably affect the accuracy and reliability of source localizations. However, in a follow-up study to this thesis supported by the Jubiläumsfonds der Oesterreichischen Nationalbank, it is currently planned to test the accuracy and plausibility of different source localization algorithms in the analysis of SCP data.

tivity clusters detected via fMRI as constraints for the dipole solutions. Several other source localization approaches, e.g. those pertinent to the general class of minimum-norm based approaches (see, e.g., Pascual-Marqui, 1999, for an overview), try to account for the fact that current sources are extended and mostly non-uniform. The presumably best-known of these algorithms is LORETA (low resolution brain electromagnetic tomography; Pascual-Marqui et al., 1994), whose current version localizes current sources by computing low-resolution ("blurred") tomographic images, with solution space being confined to cortical tissue defined by means of the stereotactic space of Talairach & Tournoux (1988). Yet another innovative approach was introduced with the so-called deblurring technique (see, e.g., Gevins et al., 1991, 1997). By explicitly considering the conductivity of the different compartments of the head (which are derived from MRIs), the surface distribution on the inner surface of the skull is computed in order to reduce the serious distortion of scalp potentials by the high resistance of the skull. Actually, almost all contemporary source localization algorithms now also incorporate the differences in conductivity of the head using either three- or four-shell head models or finite element models.

Finally, it has to be kept in mind that the accuracy of surface mapping and of the source localization algorithms strongly depends on the amount of spatial sampling achieved (being a function of the number of recording channels and the size of the scalp surface of a subject). The higher the sampling, the more accurate the maps and the source localization will be. Using 128 up to 256 channels has been recommended based on the analysis of simulated and real data (see, e.g, Tucker et al., 1993; Srinivasan et al., 1998). However, the application of more electrodes comes at the expense of an increased electrode application time. This especially applies to SCP research where the usage of an electrode cap is not recommended, especially when longer processing epochs shall be investigated (see above). For example, the recent application of 64 SCP electrodes (see http://brl.psy.univie.ac.at/aktuelles/newamplifier.htm) resulted in an application time of ~ 3 h , and the average application time in the experiments performed for this thesis was ~ 2 1/4 h with "only" 42 EEG channels. Also, there are still a lot of studies published in which EEG was recorded from 19 electrodes only. Although there is no doubt that it should be aimed to avoid such low sampling in the future the validity of such studies should not be doubted hastily. It seems more appropriate to ask what kind of research questions want to be answered - and, even more importantly - can be answered with EEG studies. Although recent attempts to turn EEG into a "true" neuroimaging technique have to be acknowledged, it appears

questionable whether a spatial accuracy and validity comparable to tomographic techniques will ever be achieved or at what cost it may be achieved. This is not only related to the spatial sampling issue, but to the more general issue of the inverse problem which cannot be solved without applying numerous constraints and assumptions. Thus, it might be both more cost efficient and realistic to focus on the main advantage of ERPs, which is their temporal resolution, and to add spatial accuracy using other techniques (including whole-head MEG, where the collection of large-array data is much easier). When such a synergistic approach is used, it might be sufficient to achieve rough estimates of the cortical generators (with 1-2 centimeter spatial resolution). Another strategy might be to use "low-resolution" topographies to identify areas of interest in a first step. Depending on the results, a replication study with higher sampling can be performed. In fact, such an approach was partially applied in this thesis, where it was attempted to refine results of earlier studies in which 22 EEG channels had been used (see chapter 7).

#### *2.2.1.3 Analysis of SCPs: statistical inference*

The standard approach of drawing statistical inferences in SCP research is identical to the one recommended for the analysis of ERPs. Although non-parametric approaches have been repeatedly proposed to increase the robustness of inferences (Wassermann et al., 1989; Srebro et al., 1996; Karniski et al., 1994), using parametric analyses is common practice in EEG studies. In most cases, similar to SPM, the general linear model is used to assess whether experimental conditions affect the data in a predictable way. In practice, this means that univariate (ANOVA) or multivariate (MANOVA) repeated measures analyses of variance are computed, and that their main effects and interactions are evaluated (Vasey & Thayer, 1987; O'Brien & Kaiser, 1985). A MANOVA can only be computed when the number of subjects exceeds the number of independent variables, which is rarely the case, especially in high-density studies. In case an ANOVA is calculated, the p-values for effects containing a repeated-measures factor commonly have to be corrected for violations of the so-called sphericity assumption (Vasey & Thayer, 1987). While significant main effects indicate differences in the mean amplitude calculated across all independent variables (usually the electrodes), a condition x electrode interaction indicates scalp topographies which are different between conditions or groups. It is this kind of statistical result EEG-experimenters are usually interested in, since this would signify that different brain regions are active in different conditions or groups.

However, an influential paper by McCarthy & Wood (1985) doubted whether such an interpretation is justified at all. In a simulation study, they showed that a significant condition x electrode interaction might also be caused by a change in source strength without a concomitant change in source location or source orientation. It was therefore suggested that some kind of normalization procedure should be applied prior to all kinds of statistical analyses of topographical data. While this removes differences in the general amplitude level between conditions, the relative strength of activity across electrodes is preserved, and topographical differences due to genuine differences in underlying neural generators would not be affected. On the other hand, Haig et al. (1997; but see also Ruchkin et al., 1999) have argued that the conclusions drawn by McCarthy & Wood were based upon unrealistic assumptions on the nature of ERP data and their neural generators. They exemplify that the type of scaling McCarthy & Wood propose might obscure differences in source configuration and arrive at the conclusion that analyses of both raw and normalized data should be performed and reported in order to avoid such false negatives. This approach seems mandatory because the researcher usually is not only interested to know if source configurations differ between conditions, but also whether there is a change in strength of the same sources (e.g. if differences in task difficulty are investigated).

In addition to testing omnibus effects via ANOVA/MANOVA, a-priori abd post-hoc tests are usually performed in order to assess significant differences at certain factor levels. A-priori hypotheses are commonly tested via linear contrasts. Corrections for violations of the sphericity assumption have to be performed for such contrasts, too. This can be accomplished by using contrast-specific error terms instead of the pooled variance terms (Boik, 1981; Keselman, 1998). It should also be noted that multiple post-hoc tests (such as the Scheffé or Tukey test) are not exact in case of violations of sphericity and should thus not be performed. Thus, post-hoc hypotheses should either be tested via multiple independent linear contrasts or, e.g., the test statistic proposed by Keselman (1982) which is roughly equivalent to computing multiple t-tests. In both cases, a correction for multiple comparisons (Bonferroni or other) is required.

#### *2.2.1.4 Neural generators of SCPs*

The cellular mechanisms giving rise to scalp-recorded SCPs are not substantially different from those generating other kinds of EEG activity. Thus, SCPs are mainly generated by postsynaptic potentials (PSPs) in the apical dendrites of

cortical pyramidal cells (see Fig. 2-14). Such PSPs are triggered by unspecific and specific thalamo-cortical and intracortical axonal inputs (for an overview, see Birbaumer et al., 1990). Based on simultaneous recordings of intracortical and surface potentials, it seems well-established that excitatory PSPs (EPSPs) in the upper cortical layers cause negative SCPs on the surface, and that a reduction in excitatory input, and/or an increase in inhibitory PSP (IPSPs) yields positive SCPs.

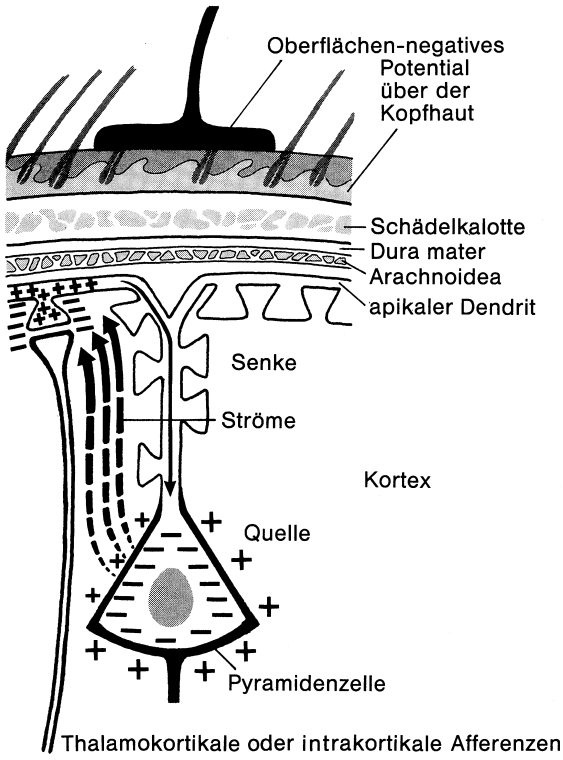


Fig. 2-14: Model of the generation of surface-negative potentials. Thalamocortical or intracortical afferents evoke EPSPs at the apical dendrites, resulting in an extracellular and intracellular flow of ions. The corresponding field potential is picked up by a surface electrode (reproduced from Birbaumer & Schmidt, 1999, Fig. 21-7).

Theoretical considerations and model simulations (see, e.g., Lutzenberger et al., 1987) have shown that the amplitude of surface SCPs is almost exclusively generated by cell assemblies of several thousands of equally oriented cortical neurons with apical dendrites near the recording electrode, and that even very strong subcortical and deeper sources can only contribute to a very small extent to the surface potential. However, even superficial PSPs are only visible on the surface when a considerable number of neurons is active simultaneously (i.e., at least roughly in phase). Also, SCPs maxima are not always located exactly over the area of maximal activity. This results from the massive gyrification of the cerebral cortex, which causes an orientation of neurons (and thus of the resulting orientation of the electrical field) which is not always perpendicular to the curvature of the scalp surface. This is of special importance in studies of the primary motor and somato-sensory cortex (but also of the auditory cortex; see Fig. 2-11, which provides an example of such an effect), where the folding of the cortex along the central fissure might even lead to a surface distribution with an activity maximum ipsilateral and not contralateral to the moving or stimulated body part.

But even if *absolute* localization of activity is difficult and requires precise knowledge of the geometry of the activated neural tissue, *relative* information pro-

vided by SCP topographies acquired in different conditions (e.g., movement of the left vs. the right arm) might help to identify the true generators - since different topographies will reflect a difference in the underlying cortical generators in most cases. Unfortunately, the opposite does not always hold since the inability to reveal a topographical difference might also be due to an insufficient sampling of the surface distribution, or might result from the blurred transmission of potentials to the surface. This caveat has to be kept in mind especially if the investigated sources are not well-separated in space, e.g. in somatotopic mapping.

Long-lasting slow PSPs (s-PSPs; Libet, 1971) and glial cells (Roitbak, 1983) might also play a role in the generation of SCPs. s-PSPs last for several seconds up to minutes and seem to regulate the excitability of neurons. However, according to Birbaumer et al. (1990), the exact electrogenic mechanisms underlying s-PSPs have not yet been established, and it is not yet evident to which type of slow potentials s-PSPs contribute. In my view, it seems that they are rather (co-) responsible for the tonic, long-lasting changes which can be measured via steady potentials and steady potential changes than for the generation of SCPs.

As for glial cells, several arguments speak for an at least indirect involvement in the generation of SCPs (see Roitbak, 1983, and Laming et al., 1998, for extensive reviews). Glial cells are omnipresent in cortical tissue and occupy about 50 % of the cortical volume (Laming, 1998). They act as a local buffer of potassium ($K^+$) that is released to the intersticium by active neurons. When the amount of extra-cellular potassium is high, this triggers glial depolarization. It has been shown that the timecourse of this depolarization is very similar to scalp-recorded SCPs (Caspers et al., 1980; Caspers, 1993). This, however, need not be interpreted in the sense that these cells directly contribute to surface SCPs, since the field gradient evoked by glial depolarization drops steeply with distance. It seems instead to reflect the correlation of prolonged neural activity and the resulting $K^+$-release/uptake by glial cells. On the other hand, the uptake of $K^+$ might - again, indirectly - lead to an amplification of the surface potentials, since positively charged ions are removed from upper and redistributed to lower cortical layers, which "sharpens" the already existent intracellular electrical field that is observed at the surface. Independent of whether glial cells contribute directly or indirectly to scalp SCPs, this contribution should not be considered as an artifact or as evidence that SCPs do not genuinely assess neural activity - since it is in fact the *neural* activity and the resulting $K^+$-release that trigger this additional SCP generator.

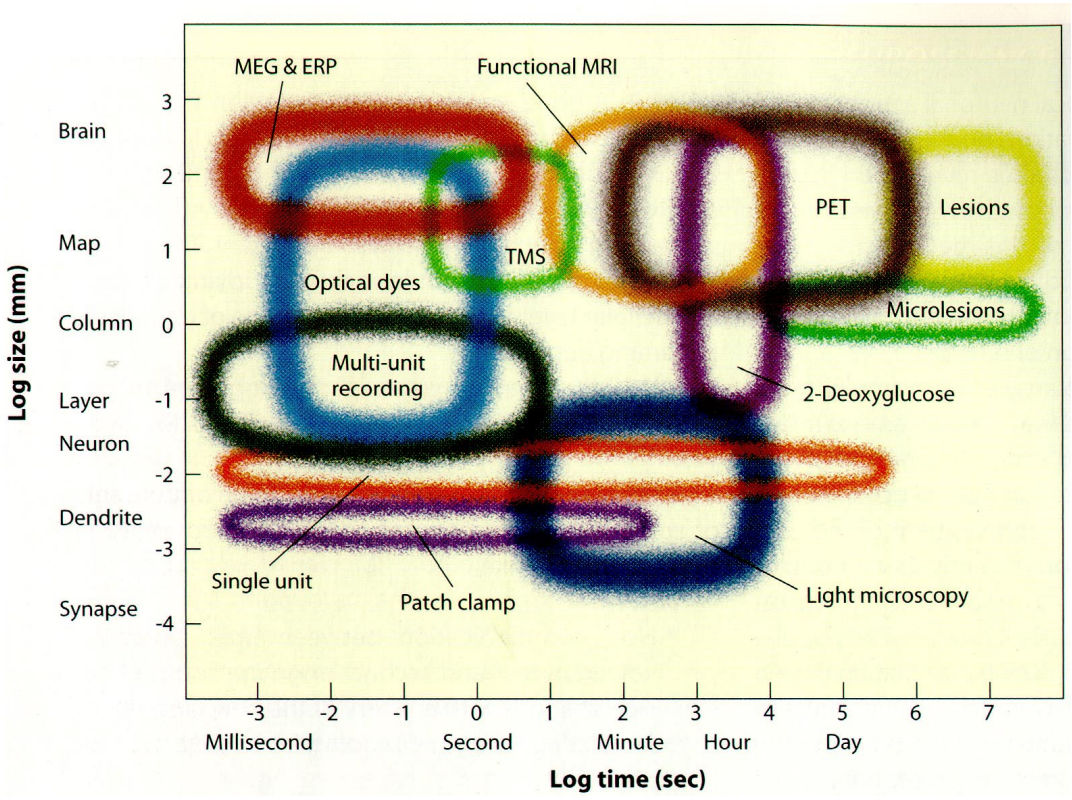


Fig. 2-15: Comparison of the temporal and spatial resolution of most of the currently available methods of investigating brain function (reproduced from Gazzaniga et al., 1998, Fig. 3.40)

### *2.3 Multi-modality neuroimaging*

Fig. 2-15 provides an overview of the temporal and spatial resolution achieved by the methods which are currently available for investigating brain function. This figure perfectly illustrates why Gazzaniga et al. (1998, p. 119) have stated in their Cognitive Neuroscience textbook that "often the convergence of results yielded by different methodologies offers the most complete theories. A single method cannot bring about a complete understanding of the complex processes of cognition that rely on numerous brain structures."

This becomes clearly evident when the temporal and spatial resolution of scalp-recorded electrophysiological (EEG/MEG) and of blood-flow based imaging techniques (PET, SPECT, fMRI) are compared. While the former are generally believed to provide a high temporal and rather coarse spatial resolution, an excellent to good spatial and moderate to poor temporal resolution is assigned to the latter. A combination of these methods should thus provide detailed information not only about the "where", but also about the "when" of brain activity during sen-

sory, motor or cognitive processing. However, Gazzaniga & colleagues' statement does not only apply to synergies with respect to the rather "technical" issue of temporal and spatial resolution.

It is evident that the information provided by the techniques depicted in Fig. 2-15 can be vastly different. Different aspects of cognitive function and underlying brain activity are assessed by different methods. For example, the relatively new technique of TMS (Transcranial Magnetic Stimulation; see, e.g., Pascual-Leone et al., 1999) provokes localized and transient "lesions" in the brain by interrupting neural processing and/or causing neuronal discharges in the stimulated brain tissue. Delivered at different times and to different brain regions, TMS can be used to investigate the effects of such lesions on behavioral parameters as reaction time and/or the correctness of an answer. Whenever effects on these parameters are revealed, it might be concluded that the stimulated region is (at least indirectly) involved in the processing of the investigated task. This represents a completely different approach to brain function than the one pursued with fMRI or ERPs, or, generally, with neuroimaging devices. Here, neural activity evoked by information processing is observed. Thus, one always has to be aware of the correlative nature of neuroimaging data, since it might be - in the worst case - that the region that "lights up" is functionally irrelevant for the function which is investigated (see also Sarter et al., 1996).

To make things even more complicated, the various neuroimaging techniques also provide access to different aspects of neural processing. While, e.g., ERPs directly measure changes in postsynaptic potentials (albeit only of larger, simultaneously active patches of cortical tissue), fMRI or PET assess changes in blood flow which are more or less directly related to changes in the metabolism of neural tissue. Such differences in the measurement substrates should, of course, be considered when comparing results between techniques (see also McCarthy, 1999; Nunez & Silberstein, 2000).

Hence, I will briefly discuss some issues which are relevant for a comparison and combination of fMRI and ERPs (and especially SCPs) in the study of cognitive processing. This will include a) a discussion of the synergies which can be achieved with respect to the temporal and spatial resolution of the two methods, and with respect to the difference(s) in the measurement substrate, and b) a very brief discussion of practical and theoretical problems associated with multimodality imaging, such as the choice of the stimulation paradigm, the coregistration of data, and the interpretability and comparability of results.

### 2.3.1 Combination of fMRI and SCPs: synergies

#### *2.3.1.1 Temporal and spatial resolution*

Clearly, one of the main aims of a combination of fMRI and ERPs/SCPs is to increase the temporal and spatial resolution with which task-related brain activity can be assessed. As already noted, ERPs are usually recommended for their temporal resolution in the milliseconds range, whereas fMRI is praised for its spatial resolution in the millimeter range. On the other hand, ERPs are criticized for their coarse spatial resolution or ability to localize. Similarly, the temporal resolution of fMRI is thought to be rather poor, a statement which is mainly based on the sluggishness of the hemodynamic response. Thus, it is generally believed that a combination of the two methods will reveal the location and timing of cognition-related brain activity. However, some critique or refinement of these statements might be required.

Regarding temporal resolution, it seems debatable whether milliseconds resolution of neural activity is truly provided by ERPs or SCPs, although it is certainly true that electrophysiological signals can be sampled by modern amplifiers in the milliseconds range. From a purely technical point of view, each method can resolve signals (both in space and time) at half its spatial and temporal sampling frequency (according to the Nyquist theorem; see, e.g., Glaser & Ruchkin, 1976). Thus, if we sample the EEG signal at, say, 250 Hz, signal changes as fast as 125 Hz can be monitored without bias. However, this does not imply that the signal one is interested in also changes at such a fast rate. This applies even more to SCPs, since they seem to reflect changes in event-related activity which occur at a much slower rate than the ones of conventional or phasic ERPs. If we inspect, e.g., Fig. 2-11, it becomes evident that the slow potential component of the averaged signal does not appear before about 400-500 ms post stimulus. Nevertheless, the argument discussed below regarding absolute and relative statements certainly applies. An absolute determination of activity onset might not be possible with a resolution higher than 200-300 ms. However, if we are interested in comparing activity between conditions and between regions, differences in onset timing might become visible in the 50-100 ms range.

Similarly, it is only the technical spatial resolution of fMRI that is in the millimeter range. Some of this accuracy is lost during numerous preprocessing steps (such as motion correction and stereotactic normalization, which both require interpolation). In addition, whenever inter-subject averaging or some kind of com-

parison across subjects is required, the technically achieved spatial accuracy is sometimes considerably reduced by spatial smoothing (which is performed to account for interindividual differences in both structural and functional anatomy). Sometimes, smoothing filters as large as 20 mm FWHM are recommended for statistical group comparisons (see chapter 2.1). This definitely blurs the acquired data and does only allow approximate inferences about the involvement of smaller structures (such as, e.g., the thalamus or the amygdalae).

On the other hand, spatial resolution of EEG and temporal resolution of fMRI might be better than widely believed. For example, dipole localization accuracy of 7-8 mm for EEG and 3 mm for MEG has been demonstrated using a human skull phantom (Leahy et al., 1998). Also, single-slice fMR images can be collected within about 50 ms with modern scanners. Although hemodynamic response is usually delayed for several seconds, this does not mean that the relative timing between regions cannot be assessed with a much higher resolution. This was recently demonstrated by Menon & colleagues (Kim et al., 1997; Menon et al., 1998; Menon & Kim, 1999). They demonstrated a separation of hemodynamic responses with a temporal resolution of 50 to 125 ms in averaged, and of 1-2 s in single-trial responses. However, such values could only be achieved when the signal time-course of different brain regions was compared. Within the same region, the upper limit of temporal resolution was approximately 5 s (Kim et al., 1997; however, the TR of this study was 0.87 s, and higher temporal accuracy might have been achieved with a faster repetition rate).

The latter results point towards an important aspect when discussing the temporal and spatial resolution of neuroimaging methods. This aspect is the type of inference we are interested in: do we want to draw absolute inferences, or is a relative inference sufficient? Whenever a relative statement is required, the weaknesses of the two methods might be reduced. As for ERP and SCP studies, differences in topographies revealed with a low spatial sampling might be sufficient to infer that different neural generators are involved in two different sensory, motor or cognitive tasks. Even separation of the scalp topographies of very similar tasks and, accordingly, with very similar and close neural sources (as, e.g., in somatotopic mapping) might be achieved with sufficient reliability. However, the *absolute* determination of the generators of these topographies is usually rather difficult and cannot be achieved without additional, sometimes rather serious constraints which have to be imposed on the source localization algorithm. As for fMRI, the same seems to apply to its temporal resolution. While the sluggishness of the hemodynamic response makes it difficult to separate changes in neural activity within the

same brain region, conclusions about the temporal sequence of activity are still possible when onsets of signal changes across regions are compared (see, e.g., Buckner et al., 1998; Miezin et al., 2000). On the other hand, it should be noted that several studies have shown that the onset of the hemodynamic response can be quite different across different regions of the brain. This might require some caution in equating hemodynamic onset times with the onset of neural activity.

Another aspect that has to be kept in mind is the temporal resolution that is required by a certain study. Certainly, the "temporal resolution" of most cognitive task paradigms is much lower than the one of sensory or motor tasks. In the latter, we might observe changes in neural activity within and across regions far below 100 milliseconds. For example, the preparation and execution of such a "simple" act as a finger movement involves a rapid sequence of activities in the brain which controls this finger movement. This starts with preparatory or programming activity in the premotor region, goes to executive activity in the primary motor cortex, and ends with activity in the somatosensory cortex reflecting the sensation associated with the movement. For both fMRI and EEG, it is especially challenging to separate the latter two processes: While their temporal separation would be difficult for fMRI, their spatial separation would be tricky for EEG due to the vicinity of somatosensory and primary motor cortex.

A different picture arises when we are studying cognitive events, which are usually much more extended in time. For example, the comparison of two objects at angular difference as in the mental rotation paradigm introduced by Shepard & Metzler (1971) usually takes several seconds. Thus, during a longer period of time almost no change in the invoked cognitive functions occurs, and associated neural activity might therefore be resolved even at sampling rates of more than a second. A similar argument applies to the cube comparison task used in this thesis. An initial phase of stimulus evaluation and mental image generation is followed by an extended period (up to 60 seconds!) of cube rotation and cube comparison. In this period, there should not be too much variability in the involved cognitive processing. Therefore, the corresponding brain activity should also be rather constant, and the sampled brain signals should be rather smooth (which is, indeed, shown by several studies, including the ones performed in this thesis).

On the other hand, it has to be considered that the solving of mental rotation tasks does not only require mental rotation. Cognitive processes as object identification, generation of a mental image, matching of the rotated with the reference object, and response execution are also involved. Since these processes require much less time, they are much more difficult to separate in time and might

not be depicted appropriately by the imaging techniques. Also, some of these processes seem to take place in adjacent and overlapping regions and are thus also difficult to separate in space. For instance, it has been shown that solving of mental rotation tasks is accompanied by activity in premotor regions. Parts of premotor and primary motor cortex are also involved in response preparation and execution, and in the control of goal-directed voluntary eye movements. Thus, despite a long tradition in the neuroimaging of mental rotation paradigms, it is still a matter of debate whether or not premotor activity is specifically related to the visuo-spatial operations required by the tasks (see also the discussion in chapter 6)[8].

In general, it should be noted that the technical temporal and spatial resolution of fMRI and ERPs can be substantially improved by choosing "tuned" measurement protocols. For example, if imaging is confined to a single slice only, much higher fMRI sampling rates can be achieved than when whole-head coverage is required (50 ms vs. ~ 1-2 sec). Also, a much better in-plane spatial resolution than the commonly reported 3 x 3 mm with EPI can be achieved when more time is invested to acquire an image. Similarly, the spatial resolution of EEG measurements can be improved when electrodes are densely placed over a certain brain region. Unfortunately, these strategies come at some expense, which is a confinement of results to the pre-experimentally selected brain volume or a reduction in temporal resolution.

[8] One reason for this might be that cognitive events are not as time-locked as "simple" sensory or motor events. This sometimes makes it questionable to average across trials in order to increase the signal-to-noise ratio. Let us assume, for example, that a mental rotation task is solved by carrying out the above mentioned cognitive processes in a sequential manner (object identification → mental image generation → mental rotation of the mental image → matching of the rotated image with the reference object.) Using neuroimaging, we should be able to identify the neural activities associated with these processes. However, their onset and duration is not constant. For instance, mental rotation might not be successful and will therefore be repeated (e.g. because an inappropriate direction of rotation was chosen by the subject). This will result in a jitter of the latency and duration of the cognitive processes. Averaging of such data, therefore, will only give us a rather crude summary of both the spatial and temporal aspects of the neural processing involved in task solving (see also Flexer, 1999.) However, as already discussed above, the advent of single-trial fMRI might provide a solution to this problem. For instance, analysis of the data acquired for this thesis with the exploratory data analysis technique of fuzzy clustering has revealed different signal time courses in parietal, premotor and primary motor cortex (Windischberger et al., 1999). While pixels in parietal and premotor cortex showed an early onset of signal increase persisting until task response, the completely different time-course of pixels in primary motor cortex contralateral to the response-executing hand suggested that this region was not active during task processing itself, but only immediately before response execution. Similarly, it has been shown (Richter et al., 1997, 2000) that the reaction time of a mental rotation task correlated with onset *and* width of parietal and premotor signal changes, while it correlated with only the onset in the contralateral primary motor cortex.

The present chapter should not be misunderstood in the sense that a combination of fMRI and EEG is unnecessary because fMRI can have excellent temporal and because an excellent spatial resolution can be achieved via EEG. It should only become evident that the required temporal and spatial resolution always depends on the task paradigm and the scale of neural events one is interested in. Thus, imaging has to be specifically "tuned" to each new research question. This can either be based on one method alone, or on the combination of two or even more methods. Clearly, there is no method which is superior in all situations, and it should have become evident in this chapter that a more realistic evaluation of the respective weaknesses and strengths of the various techniques will allow for more progress in brain research than the simplistic praise of fMRI for its spatial and of EEG for its temporal resolution (see also Nunez & Silberstein, 2000).

*2.3.1.2 What is measured - neural activity vs. hemodynamic response*

fMRI and ERPs provide different kinds of information about brain activity. Commonly, this is summarized in the statement that fMRI measures only a correlate of neural activity (the hemodynamic response), while ERPs measure neural activity "directly." However, this summary is to simplistic if we want to thoroughly consider the differences and synergies between the two types of measurements. Apart from the fact that the generation of the hemodynamic responses measured by BOLD-fMRI is still not fully understood, ERPs do only measure certain aspects of the various types of "neural activity." In this chapter, I will try to compare in some more detail the types of neural activity assessed by the two methods and discuss the consequences for their comparability and potential con-/divergences.

As discussed in chapter 2.2, only certain aspects of "neural activity" are reflected in ERPs. These are mainly changes in ionic concentration due to input to apical dendrites of pyramidal cells in the upper cortical layers. In order to produce surface-measurable field changes, neurons have to align in a certain way to form an open field. This is one reason why activity of stellate cells is not detectable through scalp measurements (see Nunez & Silberstein, 2000). For a similar reason, neuronal activity in subcortical structures rarely shows up at the surface, since neurons in these structures do have different orientations. The greater distance of subcortical structures or deeper cortical layers to the surface additionally attenuates their amplitude (Lutzenberger et al., 1987). ERPs also show different sensitivity depending on the geometrical orientation of active neural tissue, with

sensitivity being highest for neurons oriented radial to the scalp surface. This is particularly important as most of the cortical surface is considerably folded, with many neurons lying in sulci which might not be oriented exactly normal to the scalp surface. In addition, large pools of neurons have to be active synchronously to produce a measurable surface signal. When activity is not in phase, it might even cancel out and be invisible to the epicranial sensors. Thus, it has to be kept in mind that ERP measurements do not provide a homogeneous sampling of "neural activity", but only a selectively "weighted" image of neural computations. Unsynchronous and deeper activities remain mostly unseen, and the geometrical orientation and the resulting projection of activity to the scalp surface has to be considered in data interpretation. On the other hand, with a few rare exceptions, differences in the timing and the amplitude of surface potential changes between and within brain regions can be used in a quantitative way to assess the amount and onset of neural activity. In addition, there is no requirement that activity is temporally extended in order to be detectable, since ERPs will reflect even very short changes in ionic concentration. Also, increased surface negativity in relation to some baseline can - again with some occasional exceptions - be interpreted as an indicator of increased activity, while positive potentials indicate a reduction of activity and/or an increase in inhibitory activity.

As for fMRI, it is more difficult to provide a definite account of the kind of neural events that lead to a BOLD-response since its neurophysiological and neurovascular mechanisms are yet to be understood comprehensively (see, e.g., Jueptner & Weiler, 1995, and Magistretti & Pellerin, 1999, for some recent models). However, even without such knowledge, it is at least possible to state under which empirical conditions BOLD-contrast responses do or do not occur. fMRI samples brain activity rather homogeneously. Thus, all regions of the brain can be imaged equally well, independent of the type and orientation of their neurons, of whether or not they form an open or closed field, and of the depth of the active structure. One exception to this rule are regions which are prone to susceptibility artifacts, e.g. the anterior parts of the temporal lobe and the orbitofrontal cortex. However, shimming the static magnetic field to these volumes of interest, tailored slice positioning, and multi-shot imaging can be utilized to reduce such artifacts. Since the BOLD-response is triggered by the metabolic demand of neurons, there is also no requirement that neurons are active in phase. On the other hand, it seems that signal amplitude is not as directly related to the amount of neural activity as in ERPs, since blood flow seems to increase in the sense of an all-or-nothing law. Although it has been shown that events as short as 30 ms produced a meas-

urable hemodynamic response, one requirement for a BOLD-response with detectable amplitude might be that neuronal activity extends in time and possibly also in space. Also, due to the already discussed sluggishness of the hemodynamic response, sustained changes in activity are more easily detected than transient or rapid activity changes. Last, but not least, it has to be kept in mind that fMRI signal increases do not unambiguously indicate whether they are related to an increase or a decrease in neural activity, since both the activity of excitatory and inhibitory neurons lead to an increase in metabolic demand.

The present discussion has shown that there a number of reasons for the combination of fMRI and ERPs in addition to the dominantly discussed issue of temporal and spatial accuracy exists. While fMRI provides a precise three-dimensional localization of neural activity, complementing ERPs in the assessment of deeper or subcortical structures, ERPs help to determine whether fMRI signal increases are related to increased excitatory or inhibitory activity, and allow a quantification of signal increases. These differences in the measurement substrate, however, also imply that it should not always be expected that the two methods provide identical to converging results, or show one-to-one correspondence (see also McCarthy, 1999). For example, unsynchronous activity of neurons, or activity of stellate cells only, might result in an increase in blood flow while producing no measurable ERP change. Also, brief changes in cortical activity might go undetected by fMRI while producing a clear change in the surface potential. Nevertheless, although a different, rather provocatively formulated statement was recently presented (Nunez & Silberstein, 2000), such differences in brain maps should rather be an exception to the rule. This should be even more the case when investigating cognitive functions, which are mainly supported by neocortical structures, and which usually require prolonged and synchronous neural processing.

### 2.3.2 Challenges in the combination of neuroimaging methods

As discussed in the previous chapter, the combination of fMRI and ERPs might indeed make sense and provide new and valuable insights into the neural bases of cognitive processing. However, this does not come without additional expenses and challenges. The main expense is, of course, the additional time and money which has to be invested in data acquisition and data analysis. Apart from this rather "secular" problem, one of the main challenges is the choice and set-up of an appropriate stimulation paradigm which evokes robust activity in both fMRI

and ERPs. For instance, it seems inappropriate to use ERPs to investigate subcortical or cerebellar activities, or to use fMRI to image activity associated with very short-lasting and/or rapidly changing neural activities. Apart from these obvious restrictions, the task paradigm used should show no or only negligible practice-related effects, since changes in processing strategy or task proficiency would affect the comparability of results when measurements are performed consecutively (as is the case in most studies)[9]. Also, although combinations of blocked-design fMRI and ERPs are still encountered, such comparisons have serious limitations. Hence, an event-locked presentation mode should also be implemented for the fMRI measurements. Another restriction which is rather unfamiliar to the EEG-researcher is that several subject selection criteria have to be taken into account. Subjects must not be claustrophobic, nor have any metallic implants, and they have to be able to lie still in the scanner for at least an hour. Another, rather logistic problem is the management of measurements. It is mandatory to balance the sequence of measurements across subjects. This should cancel out effects of learning, practice or task familiarity, and the potential change in motivation or familiarity with the investigation encountered from the first to the second measurement session (see also the questionnaire results in chapters 6 and 7). From an analysis point of view, accurate co-registration is required if the results are to be displayed in a joint coordinate system. This issue is discussed in detail in chapter 3. Finally, when co-registering and comparing the results for interpretation, the limitations and strengths of the two methods, and the task designs used for data acquisition, have to be considered in order to fully exhaust the complementary vs. convergent potential of the multi-modality data.

[9] If fMR images and high-resolution ERPs could be acquired simultaneously, tasks need not have this quality. Although several reports demonstrated that EEG of sufficient quality can be recorded within the scanner (e.g., Ives et al., 1993; Goldman et al., 2000), it is evident that both the data quality of fMRI and EEG/ERPs cannot be as good as when data are recorded separately. This results from the considerable number of artifacts the two techniques mutually induce in their measurements. For example, pilot studies performed for this thesis have shown that even the electrode sockets and the electrode gel used for SCP recordings caused considerable artifacts in the MR images.

## 3. Co-registration of EEG and MRI data using matching of spline interpolated and MRI-segmented reconstructions of the scalp surface

**Abstract**

*Accurate co-registration of MRI and EEG data is indispensable for the correct interpretation of EEG maps or source localizations in relation to brain anatomy derived from MRI. In this study, a method for the co-registration of EEG and MRI data is presented. The method consists of an iterative matching of EEG-electrode based reconstructions of the scalp surface to scalp-segmented MRIs. EEG-electrode based surface reconstruction is achieved via spline interpolation of individually digitized 3D-electrode coordinates. In contrast to other approaches, neither fiducial determination nor any additional provisions (such as bite bars, other co-registration devices or head shape digitization) are required, which avoids co-registration errors associated with inaccurate fiducial determination. The accuracy of the method was estimated by calculating the root-mean-square (RMS) deviation of spline interpolated and MRI-segmented surface reconstructions in 20 subjects. In addition, the distance between co-registered and genuine electrode coordinates was assessed via a simulation study, in which surface reconstruction was based on "virtual" electrodes determined on the scalp surface of a high-resolution MRI data set. The mean RMS deviation of surface matches was 2.43 mm, and the maximal distance between any two matched surface points was 5.06 mm. The simulated co-registration revealed a mean deviation of the co-registered to the genuine (i.e., virtual) electrode coordinates of 0.61 mm. This suggests that surface matching using a spline interpolated reconstruction of the scalp surface is a precise and highly practicable method to transform EEG electrode positions to MRI data. All which is required are measurements of the 3D-electrode coordinates of each subject. No extra-time for fiducial or head shape digitization has to be invested, and no specific hard- or software is necessary for the implementation of this method. The highly accurate surface matches also indicate a very good approximation of the scalp surface via spline interpolation. Thus, it is suggested that such individual scalp surface reconstructions can be used for the display of 3D-rendered EEG maps.*

### 3.1 Background

Over the past few years, an increasing number of studies has been performed in which structural and functional magnetic resonance imaging (fMRI/MRI)

and electroencephalography (EEG) were combined. The main intention to invest the extra-costs (both with respect to time and money) associated with this multi-modality imaging approach is to achieve more accurate and complementary insights into neural activity during sensory, motor or cognitive processing. EEG technology has certainly profited from this synergistic approach. For example, the combination of highly detailed anatomical information provided by structural MR imaging with electroencephalographic data triggered the development of more accurate source localization and brain mapping algorithms which take into consideration the differences in conductivity of brain tissue and skull. Even the simple possibility to visualize topographic EEG activity using 3D-rendered views of an individual's head is highly advantageous and desirable - in particular if it is compared to the common strategy to map activity using a two-dimensional schematic representation of the scalp surface. Unfortunately, increases in the localization accuracy of EEG-derived activity measures can be ruined by an imperfect co-registration of EEG to MRI data. Inaccurate transformation of electrode coordinates to the MRI-coordinates will result in considerable error in topographic mapping and seems to be even more problematic when source localization algorithms like equivalent dipole analysis (see, e.g., Scherg & Ebersole, 1993) are applied.

Thus, several approaches have been developed in order to achieve an accurate co-registration of EEG and MRI data. The most frequently used approach relies on matching fiducials determined in the EEG and the MR coordinate systems. Usually, landmarks seemingly easy to determine are taken as fiducials, such as nasion, inion, and pre-auricular points (in MEG, for example, the standard approach implemented by most manufacturers is to use nasion and the two pre-auricular points for co-registration). This, however, requires a highly accurate and reliable determination of fiducials in both coordinate systems. Unfortunately, variability in landmark digitization of several millimeters has been repeatedly reported (Towle et al., 1993; Singh et al., 1997). Particularly when only a small number of fiducials is used for co-registration, such errors might translate in large registration inaccuracies. Other methods, such as matching EEG electrodes or electrode markers visible in the MR images (Gevins et al., 1991, 1994; Lagerlund et al., 1993; Ives et al., 1993), or the use of specifically designed apparatuses (such as dental bite bars, rigid planar or stereotactic devices) to achieve a more precise and reliable identification of fiducials (Singh et al., 1997; Simpson et al., 1995; Barnett et al., 1993), either lack practicability and/or require additional hard- and software.

Recently, a co-registration procedure which used a matching of EEG- and MRI-derived reconstructions of the head or scalp surface has been independently

presented as a more precise and practicable alternative (Brinkmann et al., 1998; Huppertz et al.; 1998; see also Pellizarri et al., 1989, and Wang et al., 1994). EEG-based surface reconstruction was achieved via digitization of 1000-2000 more or less arbitrary points on the scalp surface, with Huppertz et al. (1998) additionally digitizing the region around ears and nose. Surface digitization was performed using a sensor pen digitizer (magnetic or ultrasonic) which was utilized for the scanning of individual electrode positions. The main advantage of this method is that co-registration errors are reduced because more surface points are involved in the matching, and because there is no requirement for precise and reliable landmark or fiducial determination. On the other hand, some extra time (10-20 min) as well as a digitizer with which the head surface can be accurately scanned within reasonable time is required. Such digitizers are now increasingly used in many EEG labs, in particular because determination of individual 3D-electrode coordinates is generally recognized as a requirement to increase the accuracy of topographic maps and of inverse solutions. Thus, it seems realistic to assume that most laboratories involved in topographic EEG and ERP studies will be equipped with such digitizers in the future.

The method which will be presented here is comparable to the one proposed by Huppertz et al. (1998) and Brinkmann et al. (1998) since it is also based on surface matching. However, it is more practical since it saves the cost and time associated with the additional head scanning. In addition, problems with the digitization of the head surface of long-haired subjects as reported by Brinkmann et al. (1998) are also avoided. The method uses a reconstruction of the scalp surface via spline interpolation of the digitized 3D-electrode coordinates and matches this surface to the MRI-segmented scalp surface. The main aim of the present study was to assess the accuracy of co-registration achievable with this method. In addition it was investigated how precisely the individual scalp surface can be reconstructed using this method. Provided a sufficient precision is achieved, it was hypothesized that this would justify the display of EEG maps on 3D-renderings of such interpolated head surfaces. This should considerably increase the interpretability of topographic maps and make the method particularly salient to EEG laboratories having no or only restricted access to MR imaging.

## *3.2 Material and methods*

### 3.2.1 Experimental data

#### *3.2.1.1 Subjects*

The accuracy and practicability of the method was investigated by matching EEG and MRI data of 20 subjects. Only healthy male volunteers with no contraindication for MR scanning, their age ranging from 19 to 28 years, were investigated. MRI scanning and EEG recordings were performed in different departments and on different days.

#### *3.2.1.2 Measurement of individual electrode coordinates*

Measurement of individual electrode coordinates was performed using a 3-dimensional photogrammetric head digitizer (3D-PHD). The inherent measurement error of the 3D-PHD is 0.2 mm, and average test-retest reliability is 0.18 mm (Bauer et al., 2000). The device consists of twelve calibrated, but otherwise unmodified commercially available digital cameras (Olympus Camedia C-400, Olympus Inc., Tokyo/Japan). The cameras which are mounted in a dome to avoid ambient light simultaneously take pictures of light emitting diodes marking electrodes and landmarks such as nasion, inion and preauricular points. In each subject, 40 electrode positions evenly distributed over the scalp surface, two electrodes placed over the mastoids, and nasion, inion and the left and right preauricular point were photographed, and their 3D-coordinates were calculated for each subject using the 3D-PHD software. However, it has to be noted that any other digitizer with comparable measurement accuracy can be used for co-registration.

#### *3.2.1.3 EEG-electrode based reconstruction of the scalp surface*

In order to reconstruct the scalp surface, spline interpolation of the 3D-electrode coordinates was performed using the algorithm published by Perrin et al. (1987). Interpolation was based on the radial distance of the electrode coordinates to the center of the head located at half distance between nasion and inion. For each subject, 1297 points were estimated by spiraling down in 5° steps from the top of the head to the plane defined by nasion, inion and preauricular points. In order to assess the influence of the number of 3D-coordinates used for surface

reconstruction, either the full electrode set or a sub-sample of only 22 electrodes (which were located close to the coordinates of the international 10-20 electrode system; Jasper, 1958) were used for surface interpolation.

*3.2.1.4 MRI scanning and MRI surface reconstruction*

MRIs of the brain and skull were acquired via a gradient-echo sequence with 1 x 1 mm in-plane resolution and a slice thickness of 3 mm (64 contiguous slices), using a 3 Tesla Bruker Medspec (Bruker Inc., Ettlingen/Germany) whole-body magnet. Nasion and left and right preauricular points were marked using MR visible markers. The individual scalp surface was segmented using home-written C programs. Segmentation was achieved by approaching the MR image from its outer edges in order to identify the change from the low-intensity values associated with the air surrounding the head to the hyperintensive grey-scale values associated with the outer surface of the skin. Such a rather simple segmentation approach was chosen since it is fully automatic and neither requires excessive computation time nor special (usually rather expensive) segmentation software. Although this resulted in some segmentation errors around the ears and eyes, these errors were negligible since they were automatically eliminated from the matching by the matching algorithm (see below). 3601 MRI-derived surface points were determined (spiraling down in 3° steps from the top of the head to the nasion-inion-preauricular plane) and used for surface matching. This reduced computation time and the amount of data storage. As a consequence, only the uppermost points of the region around the eyes were included in the scalp reconstruction. This was intended because this region is irrelevant for the display of EEG maps, and because it also could not be accurately reconstructed with the EEG surface interpolation algorithm.

*3.2.1.5 Surface Matching*

Matching of the MRI-based and EEG-electrode based scalp surfaces relied on an iterative point-matching algorithm (Zhang, 1994; see also the documentation at http://www.sop.inria.fr/rapports/sophia/RR-1658.html). This algorithm searches for the nearest points of two 2D- or 3D-objects by an iterative change of three (x, y, z) translation and three (x, y, z) rotation parameters until a certain predefined criterion is achieved. For this study, this criterion was defined as less than 1% change in the translation and rotation vector. Importantly, the matching is robust to

gross errors and outliers (caused by, e.g., artifacts in the MR surface reconstruction, and EEG-MRI differences in surface reconstruction around eyes and ears) since such errors are automatically discarded. This is achieved via an analysis of the statistical distribution of the distances of all matched points (see Zhang, 1994, for details). Since the algorithm was originally developed for motion estimation and motion tracking, it is computationally efficient, does not require any preprocessing of 3D-point data (such as smoothing), but is comparably sensitive to large motion between objects. This, however, was no problem for the present application since the gross motion between objects could be estimated by using nasion and inion as approximate starting points for the matching. However, it has to be noted that likely errors in the determination of these reference points do not have the same effect as when co-registration is exclusively based on fiducials since such errors are eliminated due to the iterative approach which takes all surface points into account. However, the more accurate the starting points are determined, the less iterations and computation time will be required.

*3.2.1.6 Assessment of the accuracy of the surface matching procedure*

The accuracy of the 20 co-registrations was assessed by calculating the Euclidean distance between matched surface points. In order to compare accuracy directly with the one achieved by Huppertz et al. (1998) and Brinkmann et al. (1998), the root mean square (RMS) of these distances was calculated as an indicator for the absolute accuracy achieved by the surface matching. In addition, the standard deviation of these distances and the maximal distance observed for any of the matched surface points were calculated. In order to assess whether the number of iterations or the number of points automatically discarded by the algorithm correlated with these accuracy values, Spearman rank correlations were computed. In addition, it was visually checked whether markers of nasion and preauricular points coincided with the MRI-marker pills. However, since these distances would contain both errors due to unreliable landmark determination and due to to the inexact identification of the rather large markers in the MR images, no quantitative analysis of these distances was performed. As another qualitative check of the accuracy and adequacy of surface matching, an overlay of the two surfaces was computed and visualized.

### 3.2.2 High-resolution MRI test data

In addition to the assessment of matching accuracy in real data, a simulated co-registration was performed. Coordinates of 46 "virtual" electrodes and of nasion, inion and preauricular points were determined on the scalp surface of a high-resolution MRI data set (1x1x1mm, 181 contiguous slices; by courtesy of the Montreal Institute of Neurology, http://www.bic.mni.mcgill.ca/brainweb). These coordinates were then used to reconstruct the "EEG-electrode based" scalp surface via spline interpolation. As in the analysis of the real data, either a full or a reduced electrode montage were used for spline interpolation. The interpolated scalp surface was then matched to the MRI-segmented surface, and the Euclidean distances between the transformed and the genuine (simulated) electrode coordinates were calculated. This additional assessment of co-registration accuracy was mandatory for two main reasons. First, RMS error alone might not provide a quantitative indicator of the (mis-)alignment between two surfaces. For instance (as also discussed by Brinkmann et al., 1998; see also Maurer et al., 1997), the spherical symmetry of head surfaces might allow for considerable rotational misalignment without a concomitant increase in RMS. On the other hand, RMS might overestimate the co-registration error. This particularly applies for surface points around the upper parts of the orbital cavities and around the anterior temporal region, since the higher spatial frequencies in these regions might not be modeled exactly enough by the spline interpolation algorithm. However, it has to be noted that this is irrelevant for the accuracy of the co-registration of electrode to the scalp surface since such points are discarded from the matching procedure. Second, we wanted to obtain an estimate of the accuracy of surface matching under ideal conditions, i.e. without measurement noise originating from the segmented MR images (e.g., 3mm resolution, head movements during scanning), from electrode digitization, or from various other sources (e.g., differences in head shape between MR images and EEG due to geometrical distortions in the MR images), which might result in an a-priori discrepancy of electrode coordinates and the scalp surface.

The simulation approach used here is similar to Brinkmann et al. (1998), who used a phantom (a human skull) to compare transformed to genuine electrode coordinates. The phantom was equipped with MRI-visible electrode markers, and the co-registered electrode coordinates were compared to the position of the MRI-markers. However, this procedure is not only rather laborious, but its accuracy and validity chiefly depends on a precise and reliable determination of the

rather large markers (or, more precisely, the centroids of these markers). The advantage of the simulation approach used in this study is that it is known with the highest achievable precision where the electrodes have been "placed." Hence, these positions can be compared to the transformed coordinates with maximum precision. The only source of error additional to the one inherent to the matching procedure is the precise "placement" of electrodes on the scalp surface. This requires an exact manual determination of the transition between skin and air surrounding the skin.

## *3.3 Results*

### 3.3.1 Experimental data

Fig. 3-1 shows a representative sample of a spline interpolated reconstruction of the scalp surface. Results for the co-registrations are summarized in Table 3-1. Accuracy was higher when the full electrode set was used for surface interpolation, with the RMS of the Euclidean distance between surfaces being 2.43 mm. The maximal distance of any two matched surface points was 3.92 mm, and the standard deviation of the distances was 0.8 mm. A slightly lower accuracy was achieved when the subsample of electrodes was used for surface interpolation. Neither the number of iterations nor the number of discarded points significantly

Table 3-1: Results of the surface matching of EEG- and MR-data. Full Set: surface interpolation using the full electrode set; Subset: surface interpolation using only 22 3D-electrode coordinates; Iterations: number of iterations performed by the algorithm; Discarded: percentage of points automatically discarded by the algorithm; RMS: root mean square of Euclidean distance between matched surface points; MAX: maximal Euclidean distance of any of the matched points; STD: standard deviation of the Euclidean distances between matched points. All values are reported as mean ± standard deviation (range) for the 20 subjects.

| ***METHOD*** | ***ITERATIONS*** | ***DISCARD (%)*** | ***RMS*** | ***MAX*** | ***STD*** |
|---|---|---|---|---|---|
| Full Set | 23.45±11.35 (8-49) | 24±11.7 (11.4-52.35) | 2.43±0.22 (2.15-3.03) | 3.92±0.41 (3.40-5.06) | .80±0.1 (.64-1.06) |
| Subset | 20.75±8.51 (8-37) | 24±10.47 (11.64-50.58) | 2.48±0.17 (2.17-2.76) | 3.99±0.30 (3.42-4.60) | .81±0.08 (.68-.98) |

correlated with any of the three accuracy values (RMS, maximal distance, standard deviation). Also, the number of discarded points did not correlate significantly with the number of iterations. Visual inspection of the overlays of EEG- and MRI-derived surfaces indicated a correct and highly coincident alignment of the two

surfaces, which was not too surprising regarding the low RMS error of the point-matching. The check of the landmarks in the MR images also revealed a high co-incidence between marker points; however, some selective and non-systematic outliers at the preauricular points were observed, reflecting the anticipated lack of reliability in repeated and independent landmark determination.

### 3.3.2 High-resolution MRI test data

Matching based on the full electrode montage resulted in a RMS error of surface matching of 2.40 mm (maximal distance: 3.86 mm, standard deviation of distances: .80 mm). A mean Euclidean distance of genuine to transformed electrode positions of .61 mm (.26 mm standard deviation, maximal distance 1.07 mm) was obtained. When the electrode subset was used, a slightly higher RMS error of 2.43 mm (maximal distance: 3.92 mm, standard deviation of distances: .81 mm), and a mean inter-electrode distance of .56 mm (.24 mm standard deviation, maximal distance 1.03 mm) were observed. Fig. 3-2 shows some of the transformed electrode coordinates drawn on the high-resolution MR data set.

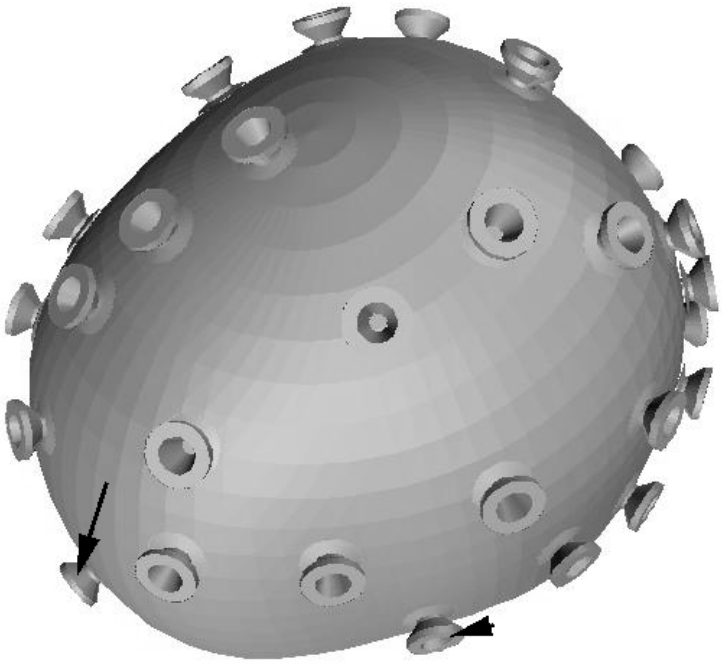

Fig. 3-1: Sample of a scalp surface reconstruction achieved via spline interpolation of 42 individual 3D-electrode coordinates. White objects (electrode sockets) mark the actually measured positions on the scalp surface (arrow: nasion, arrowhead: left preauricular point).

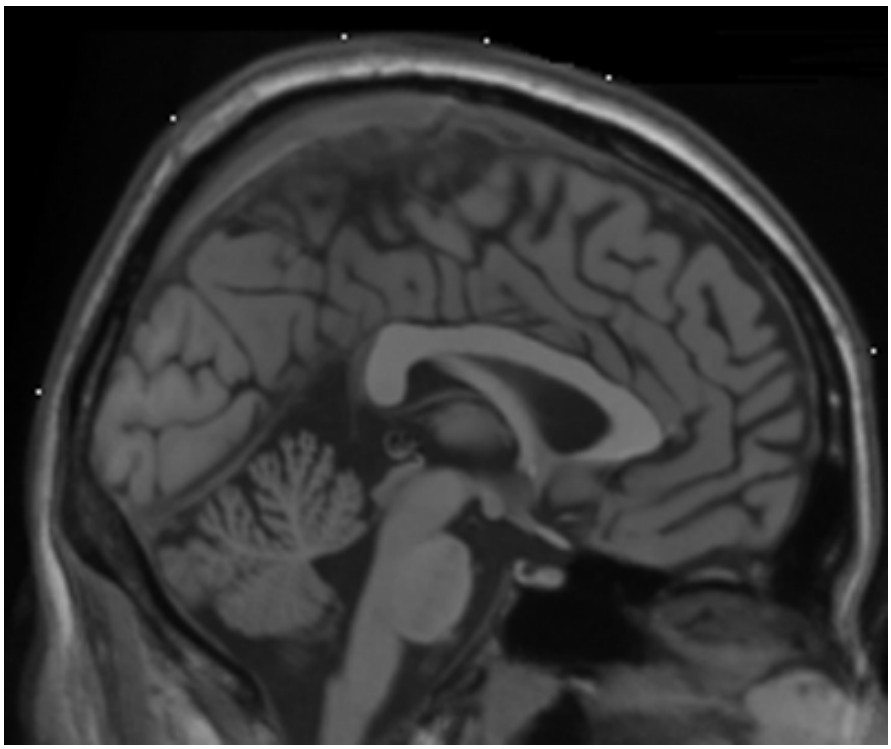

Fig. 3-2: Sagittal view of electrodes (white squares) co-registered to the high-resolution MR data set. Note that all electrodes are clearly located on and not inside the skin surface.

### *3.4 Discussion*

In this study, the accuracy and practicability of surface matching for MRI-EEG co-registration was assessed. The RMS of surface deviations was slightly lower as the ones reported by Brinkmann et al. (1998; 4.16 mm) and Huppertz et al. (1998; 3.4 mm) who had used whole head digitization instead of estimation of the scalp surface via spline interpolation. However, in order to get a more realistic estimate of the electrode *registration* accuracy, errors resulting from inaccuracies in EEG-electrode determination and from EEG- and MRI-derived surface approximation have to be taken into account. Due to the high precision of the 3D-PHD (0.2 mm), errors related to the localization of electrode coordinates are negligible. What has to be considered are possible errors in the reconstruction of the scalp surface by spline interpolation. It was assumed that this error is mainly related to the amount of spatial sampling of the scalp surface. However, as the comparison of the matching based on the full set and the subset of electrodes has shown, even the rather low sampling with only 22 electrodes yielded a sufficiently accurate

surface reconstruction. This might follow from the fact that the scalp surface is rather smooth, with higher spatial frequencies occurring only around the ears and the eyes. These regions, however, were excluded from the matching procedure due to the elimination of outliers implemented in the matching algorithm and due to the clipping of the MR and EEG-reconstruction at the nasion-inion plane.

Another source of errors are geometric distortions in the MR images resulting from inhomogeneities in the main magnetic field. However, phantom measurements revealed that inhomogeneities of the scanner used in this study were rather small (A. Berg, E. Moser, Inst. f. Med. Physics, Univ. of Vienna, personal communication). We also chose to use a simple, fully automatic and fast MRI-segmentation algorithm to extract the scalp surface. This resulted in some surface reconstruction errors around the ears and eyes. Although these errors were eliminated by the iterative point matching algorithm, it seems plausible to assume that a more sophisticated segmentation might yield an even better surface matching and, consequently, a higher co-registration accuracy.

Summing up, the matching of spline interpolated with MRI-derived surfaces suggests a highly accurate co-registration. Even the maximal distance of matched points was still below the diameter of electrodes used in most EEG/ERP studies (8mm for the standard cup Ag/AgCl electrodes used in this study).

This conclusion was clearly corroborated by the simulated co-registration. When most of the just mentioned sources of error were eliminated, a registration accuracy of about .60 mm could be observed. This error is not only an estimate of the accuracy that the surface matching technique may achieve under ideal circumstances. In addition, it also takes into account the potential misestimation of alignment via RMS values alone. As such, the small distance of transformed to genuine electrode coordinates is particularly promising.

The advantages of surface-matching compared to other co-registration methods have been extensively discussed by Huppertz et al. (1998). Surface matching avoids errors resulting from inaccurate fiducial or electrode determination in the EEG and MRI-coordinate system. Also, variations in the registration accuracy for different regions of the scalp (as pointed out by Singh et al., 1997) are reduced since the points which are used for matching are directly lying on the surface which has to be matched. Another advantage is that MRI scanning has to be performed only once per subject since data of multiple EEG/ERP experiments can repeatedly be registered to the same structural MRI. Even retrospective matching is possible. The main drawback of the formerly proposed methods was that additional time (both of the subject and the experimenter) had to be invested

in the digitization of the head surface, and that this digitization seemed to be difficult in subjects with long hair. While Wang et al. (1994) reported that digitization of about 400 points took about one hour, both Brinkmann et al. (1998) and Huppertz et al. (1998) speeded up digitization time considerably to about 10-20 minutes.

The method presented here can be regarded as a simplification of these surface matching methods. Instead of digitization of the head surface, a spline interpolated surface reconstruction was used for the co-registration of the data. Thus, neither any additional provisions (such as special hard- or software), nor head digitization are required. Also, subjects are not bothered by the head digitization procedure. All that is needed are measurements of the 3D-electrode coordinates of each single subject, and a fast and automatic surface matching algorithm. Electrode coordinates can be acquired using sensor pen devices or using photogrammetrically-based digitization (which is now also developed in other labs; Don Tucker, personal communication), or any other approach such as the use of digital calipers (Le et al,, 1998). Since such devices are now increasingly available in many EEG labs, this should not represent a restriction of the presented method.

The encouraging accuracy of the surface approximation by spline interpolation does not only justify the use of this method for co-registration, but has an important implication for EEG and ERP mapping. Provided the only reason for MR scanning is to get a reconstruction of the scalp surface and not its use for source localization or mapping in relation to individual anatomy, the use of spline interpolated surface approximations should be sufficiently accurate for the display of EEG surface maps on a rendered individual realistic scalp surface. This display mode might considerably increase the interpretability of topographic EEG/ERP activity. In addition, it would also avoid the considerable costs associated with MR scanning and allow EEG laboratories not having access to MR imaging to display their EEG maps on individual scalp surfaces.

## *4. Accuracy of event-related slow cortical potential mapping: effects of individual electrode coordinates and realistic head models*

**Abstract**

*Using standard 10-20 electrode coordinates in scalp potential mapping might result in considerable mapping errors due to inaccuracies in electrode positioning. The usage of individually digitized 3D-electrode coordinates was repeatedly recommended for scalp potential mapping. However, the corresponding increase in mapping accuracy was not yet systematically and quantitatively evaluated. In this chapter, results from such an investigation will be described. Accuracy of event-related slow cortical potential (SCP) mapping was assessed using a successive leaving one electrode-out approach. Interpolation error was determined by comparing the interpolated SCP amplitude at the left out electrode with its genuine amplitude. It was investigated whether the usage of individual electrode coordinates for scalp potential mapping results in a reduction in interpolation error compared to the usage of standard electrodes, and whether this effect interacts with the type of head model (spherical vs. realistic) used for interpolation. The results indicated that maps were less accurate when interpolation was based on standard and not on individual electrode coordinates. An even stronger effect was observed for the head model used, with maps calculated with a realistic head model showing considerably less error. Differences in interpolation error of up to 1.78 $\mu V$ were observed for single electrodes. Based on these results, the digitization of individual electrode coordinates and the usage of a realistic head model for scalp potential mapping is clearly recommended.*

### *4.1 Background*

Scalp-recorded event-related potentials (ERPs) provide the unique opportunity to study the rapidly varying brain activity associated with cognitive, sensory and motor processing with appropriate temporal resolution. However, their spatial resolution is thought to be rather restricted. Several approaches have been developed in recent years to overcome this limitation and to turn ERPs more and more into a "true" functional neuroimaging technique. For example, multi-channel ($\geq$ 19 channels) topographical recordings are now standard, and high-density EEG systems which allow simultaneous recordings from 128 to up to 256 EEG channels are increasingly used (see, e.g., Tucker, 1993; Gevins et al., 1999; Babiloni et al., 1997). In order to fully exploit the additional information provided by this improved

sampling of surface activity, sophisticated source localization and brain mapping techniques have been developed, their aim being a more accurate and reliable identification of the cortical sources of ERPs.

Following its introduction about 40 years ago (Jasper, 1958), the international 10-20 system has become the standard approach of electrode application in EEG research. In the original version, nineteen standard electrode positions have been defined. Since then, several supplementary guidelines have been published to allow for a standardized application of additional electrodes (American EEG Society, 1991, 1994). One basic feature of the 10-20 system is that its proportional measurement strategy (which is based on individual measurements of head circumference) allows to accommodate for interindividual differences in head size and head shape, and thus yields electrode locations which are standardized between and within subjects. Thus, the spherical or cartesian coordinates of these electrode locations can be used in the application of source localization algorithms, or in the computation of ERP maps.

However, accuracy of both source localization and surface interpolation critically depends on an accurate and reliable placement of the electrodes onto the 10-20 coordinates. Test-retest measurement errors of up to 7 mm, and between-subject variability of up to 7.7 mm have been reported even when electrodes were applied by an experienced senior registered EEG technologist (Towle et al., 1993). Notably, the amount of placement error was dependent on the position of the electrodes, with more lateral electrodes displaying more error than electrodes placed on the midline. Also, no anatomical landmark could be determined with less than 5 mm of error. Additional within- and across-subject error might result from the experience and reliability of the experimenter, and the length and type of a subject's hair. Thus, an average electrode placement error of about 1 cm seems to be a realistic estimate (see also Kavanagh, 1978; Böcker et al., 1994).

This value is likely to increase with the use of electrode caps. Although the arrangement of electrodes in such caps usually follows the rules of the 10-20 system, the restricted flexibility of the cap fabric and the inability to reposition electrodes separately can result in considerable electrode misplacement. Movements of the subject's head during the experiment might also result in additional electrode displacement.

Individual digitization of the 3-dimensional locations of electrodes has been repeatedly proposed as an alternative to the 10-20 positioning of electrodes (Gevins et al., 1991, 1994; Böcker et al., 1994; Towle et al., 1993; DeMunck et al., 1991). Gevins et al. (1994, p. 102), e.g., stated that "productive application of sig-

nal enhancement techniques also requires that the spatial positions of [...] electrodes be known." Such individual coordinates can be used to compute topographic maps or to determine equivalent dipole solutions with higher accuracy. There are occasional reports which might provide some rough estimates of such an increase in accuracy. Towle et al. (1993), e.g., reported that an occipital equivalent dipole evoked by visual stimulation was displaced by 10 mm when the dipole solution calculated with individual 3D coordinates was compared to the one calculated with standard 10-20 coordinates. Part of this measurement error, however, might be attributable to the spherical model used in the dipole localization algorithm. Also, since only the mean error for four subjects is reported, it cannot be determined whether the amount of dipole localization error correlates with the amount of deviation of the individual from the standard electrode coordinates. The latter was simulated by DeMunck et al. (1991). Their simulations revealed an error in equivalent dipole localization of 4 mm and 10 mm with a simulated electrode placement error of 2.5 mm and 4 mm, respectively.

However, a quantitative and systematic investigation of the effects of using individual electrode coordinates on the accuracy of scalp potential maps has not yet been performed to my knowledge. Thus, the aim of this study was to compare the accuracy of maps calculated with and without individual coordinates. In addition, the effect of using either a spherical or a realistic head model on mapping accuracy was investigated.

## *4.2 Material and methods*

### 4.2.1 Subjects

The EEG data from 25 subjects investigated for the study presented in chapter 7 were analyzed. Due to the subject selection criteria of this experiment, all subjects were male right-handed healthy young volunteers (age range: 19-28 years).

### 4.2.2 EEG recording and analysis

EEG was recorded using a 24-channel DC amplifier with high baseline stability and an input impedance ≥ 100 GΩ. All signals were sampled at 4kHz (125 Hz downsampling for digital storage) and recorded within a frequency range from DC

to 30 Hz. EEG was alternately recorded from two interleaved electrode sets, each containing twenty Ag/AgCl and two mastoid electrodes. Electrodes of both sets were equally distributed across the entire scalp surface. However, sampling was higher (i.e., lower inter-electrode distances) over the parietal and occipital scalp region (see Fig. 4-1). Vertical (electrodes above and below right eye) and horizontal (electrodes on outer canthi) electrooculograms (VEOG, HEOG) were recorded bipolarly in order to control for eye movement artifacts. Electrodes were attached to small plastic adapters individually fixed on the subject's scalp with collodion. Apart from the avoidance of electrode potential disturbance due to head and scalp movements, these adapters provided a uniform and reliable recording area of 4 mm diameter because electrode gel leakage was avoided (see Pellouchoud et al., 1997, for a discussion of the effects of electrolyte leakage on the spatial resolution of EEG measurements) - whcih was of special importance for the present study. The skin at each recording site was slightly scratched using a sterile single-use needle (Picton & Hillyard, 1974) to minimize skin potential artifacts and to keep electrode impedance homogeneous, stable and below 1 kΩ (which was confirmed for each electrode). EEG electrodes were referred to a sterno-vertebral EEG reference (Stephenson & Gibbs, 1951), consisting of a 5 kΩ potentiometer connecting an electrode placed at the 7$^{th}$ cervical vertebra with an electrode placed at the right sterno-clavicular junction. The potentiometer was manually adjusted for each subject to minimize electrocardiographic components in the EEG. 3D coordinates of all EEG electrodes, and of nasion, inion and the two preauricular points were measured using a photogrammetric head digitizer (3D-PHD; Bauer et al., 2000).

During the experiment, subjects were solving tasks requiring dynamic visuo-spatial imagery (see chapters 6 and 7 for a detailed description). Eye movement artifacts were eliminated offline using a linear regression algorithm, and all trials were visually screened to exclude those containing artifacts. Stimulus-onset linked averages of a length of 5 sec post stimulus were computed for each subject with the mean amplitude in the 200 msec epoch preceding task presentation serving as the pre-stimulus baseline. Several mean amplitude values were calculated from the averaged waveforms. These included: pre-stimulus activity (PS; mean amplitude in the interval 1 sec before stimulus presentation); slow cortical potential 1 (SCP1; mean amplitude in the interval from 1 to 2 sec post stimulus); and SCP5 (mean amplitude in the interval from 4 to 5 sec post stimulus). The reason for the computation of these "components" was to assess the impact of SCP amplitude on mapping accuracy. While the amplitude of SCP5 was generally higher than that

of SCP1, PS was a measure of background EEG noise with an expected mean amplitude around zero.

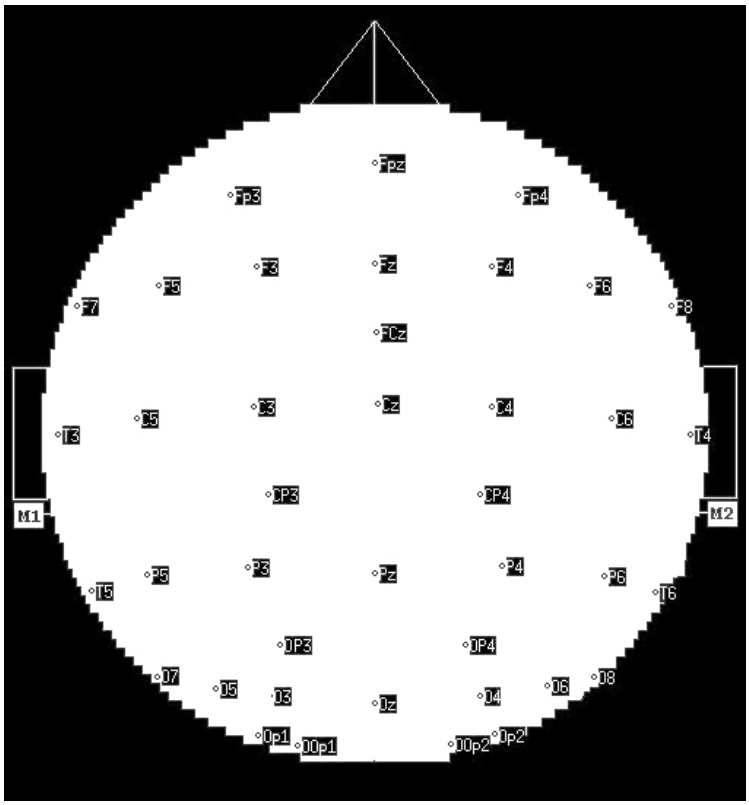


Fig. 4-1: Schematic display of the electrode positions used in this study

### 4.2.3 Mapping and comparison of mapping accuracy

Before maps were computed, the averages of the two data sets were merged by copying them into one file. Thus, all 40 EEG channels were simultaneously used for interpolation. In order to account for small differences in phase between the signals of the two sets, data were low-pass filtered with a 10 Hz filter.

Four different maps were computed for each subject, with two different head models and either utilizing individual or standard (mean) electrode coordinates. The two different head models were a spherical or a realistically shaped head model. While the former was implemented using a spherical-spline interpolation algorithm (Perrin et al., 1989), the latter relied on the 3D- or analytical spline interpolation algorithm published by Babiloni et al. (1996, 1997). The main difference between the two interpolation methods is that the different distances of the electrodes to the center of the head are explicitly considered in the analytical interpolation algorithm, while spherical interpolation assumes that electrodes are

positioned on a sphere (and thus that all electrodes have the same distance to the center of this sphere, which in fact is an unrealistic assumption).

Table 4-1: Standard deviation (in mm) of cartesian coordinates for the electrodes and landmarks used in this study.

| | | | | | |
|---|---|---|---|---|---|
| **Nasion** | 3.361 | **C3** | 9.696 | **OP3** | 13.320 |
| **Fp3** | 9.628 | **Cz** | 10.261 | **OP4** | 11.976 |
| **Fpz** | 8.408 | **C4** | 8.959 | **O7** | 8.822 |
| **Fp4** | 9.808 | **C6** | 8.285 | **O5** | 8.525 |
| **F7** | 7.553 | **T4** | 8.571 | **O3** | 8.043 |
| **F5** | 8.797 | **A2** | 7.282 | **Oz** | 8.739 |
| **F3** | 8.982 | **CP3** | 14.489 | **O4** | 8.477 |
| **Fz** | 9.087 | **CP4** | 12.994 | **O6** | 8.425 |
| **F4** | 8.493 | **T5** | 7.723 | **O8** | 8.892 |
| **F6** | 9.095 | **P5** | 8.362 | **OOp1** | 8.698 |
| **F8** | 8.994 | **P3** | 11.503 | **OOp2** | 8.337 |
| **FCz** | 9.837 | **Pz** | 11.649 | **Op1** | 8.954 |
| **A1** | 7.023 | **P4** | 9.816 | **Inion** | 3.443 |
| **T3** | 8.013 | **P6** | 8.141 | **Op2** | 9.104 |
| **C5** | 8.808 | **T6** | 7.861 | **MEAN STD:** 8.858 | |

Interpolation was either based on the individually digitized cartesian electrode coordinates, or on standard coordinates being defined as the mean cartesian coordinates across all subjects. The variability of these coordinates across subjects is reported in Table 4-1. The mean between-subject variability amounted to about 9 mm, which seems to be quite a realistic estimate of the interelectrode deviations encountered in studies which use a 10-20 application scheme (see the discussion above). In order to compare the accuracy of the four types of maps, a 'leaving one electrode out' procedure was applied, which consisted of the following steps:

1) Temporarily exclude one electrode from interpolation and compute the map with the remaining electrodes
2) Determine the interpolated potential at the coordinates of the electrode which was left out from interpolation
3) Calculate the difference between the interpolated and the genuine potential of the electrode

These steps were performed successively for each electrode. Thus, a value of how much the interpolated value of an electrode deviates from the actually measured amplitude was obtained for each electrode. These deviations were compared between the four mapping approaches. This comparison was based on

absolute and on squared amplitude deviations. As a summarizing statistic, the root mean square (RMS) error of all deviations was calculated. The RMS was calculated according to formula (4-1), with $e_i$ being the estimated interpolated amplitude, $o_i$ being the genuine amplitude value, and $i$ being the electrode ($n$=40).

$$RMS = \sqrt{\frac{1}{n}\sum_{i=1}^{n}(e_i - o_i)^2} \qquad (4\text{-}1)$$

In addition to this assessment of the average accuracy of the maps, repeated measures analyses of variance (ANOVAs) with factors MODEL (k=2, spherical and analytical), COORDINATES (k=2, standard and individual) and LOCATION (k=40, the 40 EEG electrodes) were performed. Post-hoc linear contrasts were also calculated to assess location-specific differences in mapping accuracy. Violations of the sphericity assumption - which were likely to occur due to the repeated measures nature of the data - were considered by using Greenhouse-Geisser correction for the ANOVA results (Greenhouse & Geisser, 1959) and by calculating linear contrasts with specific error variances (Boik, 1981). All statistical analyses were based on *squared* deviations.

## *4.3 Results*

### 4.3.1 RMS error

Table 4-2 shows the RMS values for the four different methods and the three different parameters.

The rank order of RMS values was identical for all three parameters. Maps calculated using a realistic head model and individual electrode coordinates yielded the lowest and maps calculated with a spherical head model and with standard coordinates yielded the highest RMS values. However, these differences were rather small (from two to six percent). Independent of the mapping method, the RMS of SCP5 was more than twice as high as the one for PS.

The effect of the head model was larger than the effect of the coordinates used for interpolation. While the mean difference between RMS error for individual vs. standard coordinates only amounted to ~ 3.7 %, the mean difference for the realistic vs. the spherical head model RMS was ~ 10.57 %. Also, the effect of us-

ing individual electrode coordinates on accuracy was consistently higher when a realistic head model was used.

Table 4-2: Root mean square ± standard deviation for the four different mapping methods and the three different parameters. Note that RMS is lowest for all parameters when maps are calculated with individual coordinates and a realistic head model.

| **Parameter** | **Realistic_Individual** | **Realistic_Standard** | **% difference** |
|---|---|---|---|
| *PS* | 1.30 ± .64 | 1.33 ± .66 | 2.26 |
| *SCP1* | 2.08 ± .98 | 2.21 ± 1.1 | 4.88 |
| *SCP5* | 2.73 ± 1.52 | 2.84 ± 1.57 | 3.87 |
| | **Spherical_Individual** | **Spherical_Standard** | |
| *PS* | 1.47 ± .75 | 1.49 ± .66 | 1.34 |
| *SCP1* | 2.30 ± 1.09 | 2.40 ± 1.25 | 4.17 |
| *SCP5* | 3.03 ± 1.66 | 3.12 ± 1.75 | 2.88 |
| | **% difference** | **% difference** | |
| *PS* | 11.56 | 10.74 | |
| *SCP1* | 9.57 | 7.92 | |
| *SCP5* | 9.90 | 8.97 | |

### 4.3.2 Statistical analyses

Table 4-3 summarizes the results of the repeated measures analyses of variance. In all analyses, the interactions of MODEL x LOCATION and COORDINATES x LOCATION were significant. The main effects of MODEL and of COORDINATES were significant for SCP1 and SCP5, while only the main effect of MODEL was significant for PS. The estimates of effect size ($\eta^2$) indicated a strong effect for the head model and a small, but still significant effect for the COORDINATES factor. However, the interaction of these two factors with the factor LOCATION revealed similar effect sizes.

Fig. 4-2 shows the electrode-specific pattern of deviations. Interestingly, the highest differences between methods were observed for electrodes which were most active during task processing (see, e.g., electrodes Pz, CP1, CP2, C3, C4, OP1 and OP2 in Fig. 4-1; see also chapters 6 and 7 for a detailed description of the SCP topographies during task solving). This was not only the case for the SCP components, but also for the PS value (see Fig. 4-3). The highest difference between the four methods was observed for electrode Pz. For PS, SCP1 and SCP5 this difference amounted to 0.66, 1.37 and 1.78 μV, respectively. In some electrodes (e.g., F3 or Oz), the deviations were almost identical. Also, there was no clear pattern as to whether a more medially placed electrode shows a higher dif-

ference between interpolation methods. For instance, Pz and Fpz showed a large difference between methods, while Oz or Cz did not.

Table 4-3: Results of the three repeated measures analyses of variance. Factor 1=MODEL, Factor 2=COORDINATES, Factor 3=LOCATION; p-values marked with a '*' have been corrected using epsilon-adjustment of degrees of freedom (with epsilon having been calculated according to Greenhouse & Geisser, 1959).

| ***Effect*** | ***df(effect)*** | ***df(error)*** | ***epsilon*** | ***F-value*** | ***p-value*** | ***Eta²*** |
|---|---|---|---|---|---|---|
| *PS* | | | | | | |
| 1 | 1 | 24 | - | 20.33 | <.001 | .46 |
| 2 | 1 | 24 | - | .719 | .405 | .03 |
| 3 | 39 | 936 | .05 | 11.62 | <.001* | .33 |
| 1 x 2 | 1 | 24 | - | .140 | .71 | .01 |
| 1 x 3 | 39 | 936 | .07 | 6.6 | .001* | .22 |
| 2 x 3 | 39 | 936 | .08 | 2.83 | .046* | .11 |
| 1 x 2 x 3 | 39 | 936 | .121 | 1.82 | .119* | .07 |
| *SCP1* | | | | | | |
| 1 | 1 | 24 | - | 14.42 | .001 | .39 |
| 2 | 1 | 24 | - | 4.8 | .037 | .17 |
| 3 | 39 | 936 | .06 | 7.64 | .001* | .24 |
| 1 x 2 | 1 | 24 | - | .34 | .562 | .01 |
| 1 x 3 | 39 | 936 | .09 | 4.23 | .006* | .15 |
| 2 x 3 | 39 | 936 | .06 | 4.81 | .009* | .17 |
| 1 x 2 x 3 | 39 | 936 | .08 | 2.41 | .071* | .09 |
| *SCP5* | | | | | | |
| 1 | 1 | 24 | - | 20.96 | <.001 | .47 |
| 2 | 1 | 24 | - | 4.06 | .034 | .17 |
| 3 | 39 | 936 | .06 | 7.80 | <.001* | .25 |
| 1 x 2 | 1 | 24 | - | .10 | .759 | <.01 |
| 1 x 3 | 39 | 936 | .06 | 4.19 | .013* | .15 |
| 2 x 3 | 39 | 936 | .05 | 2.88 | .065* | .11 |
| 1 x 2 x 3 | 39 | 936 | .06 | 2.00 | .134* | .08 |

Post-hoc linear contrasts were calculated for parameter SCP5 to assess whether electrodes placed over regions with less task-specific activity (Fp3, Fpz, Fp4, F7, F8) showed smaller differences between methods as electrodes placed over task-relevant areas (CP3, CP3, P3, Pz, P4, OP4, OP4). When maps calculated with individual vs. standard coordinates were contrasted (irrespective of the head model), a significant result with F=6.04 and p=.022 was observed. This indicated a higher difference in deviations over the active (i.e., parietal) region. When the two head models were compared (irrespective of the coordinates used), the contrast was also significant with F=6.70 and p=.022. Again, a higher difference over the active (i.e., parietal) scalp region was indicated. Another set of post-hoc

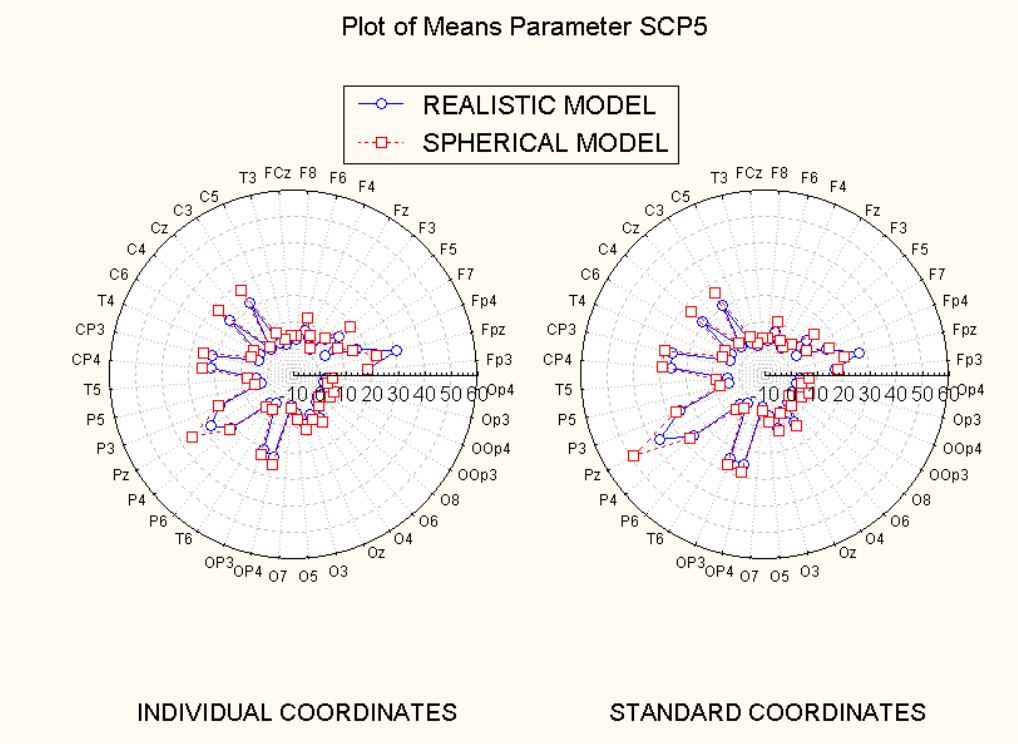


Fig. 4-2: Grand mean squared deviation between interpolated and genuine amplitude values for parameter SCP5. Note that the highest deviations were observed for the parietal, occipital and central electrodes, and that - apart from a few exceptions, e.g. electrode Fpz - deviations were smaller when a realistic head model and individual electrodes were used.

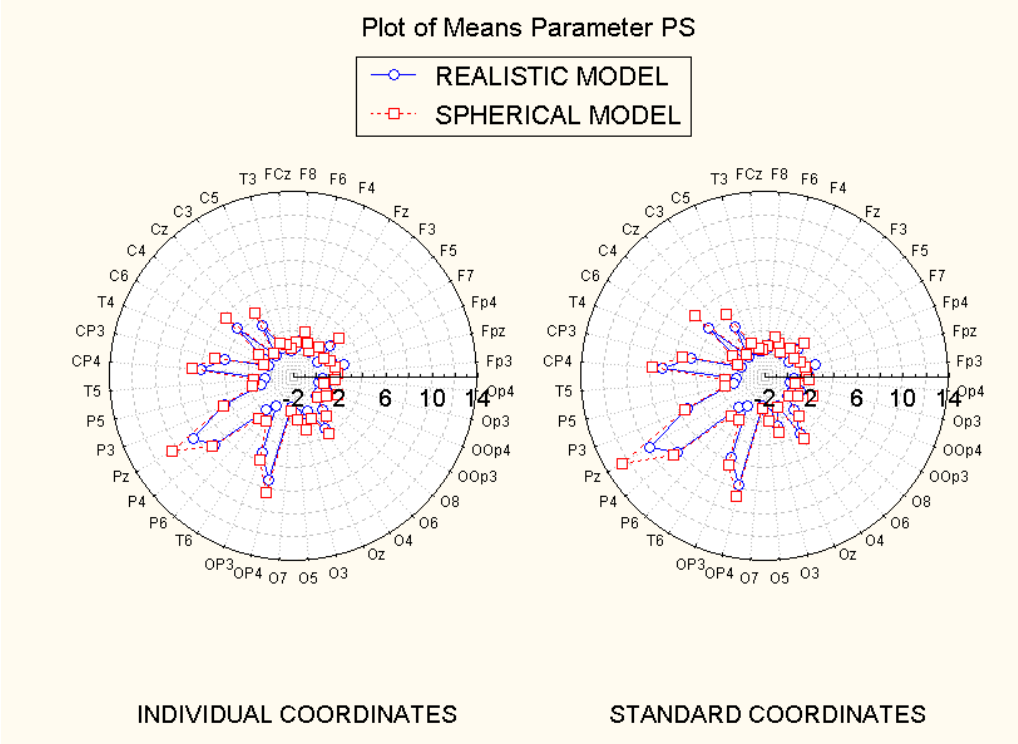


Fig. 4-3: Grand mean squared deviation between interpolated and genuine amplitude values for parameter PS. Note that the pattern of deviations was almost identical to the one observed for parameter SCP5, although deviations were consistently smaller.

contrasts was used to investigate whether the most lateral electrodes (F7, F8, T3, T4, T5, T6, O7, O8) showed less between-method differences than medially placed ones (Fpz, FCz, Fz, Cz, Pz, Oz). No significant results - neither for the coordinates nor for the head model - were observed in this case.

### *4.4 Discussion*

The aim of this study was to assess whether using individual electrode coordinates and a realistic head model affects the accuracy of scalp potential mapping. Generally, the results were consistent with the hypothesis that usage of individual electrode coordinates yields more accurate maps. For all three parameters, maps calculated with individual coordinates showed a smaller RMS of deviations compared to maps calculated with standard coordinates. An even stronger effect was observed for the head model that was used for the interpolation. The realistic head model led to almost 10% decrease in RMS error for parameter SCP5, which is more than twice as high as the 3.7% decrease attributable to the effect of the electrode coordinates. Although the mean differences between methods were generally rather small, between-method differences up to 1.78 µV were also observed (at electrode Pz). Regarding the average SCP amplitude of about 15 µV at this electrode, this represents a substantial effect of the interpolation method.

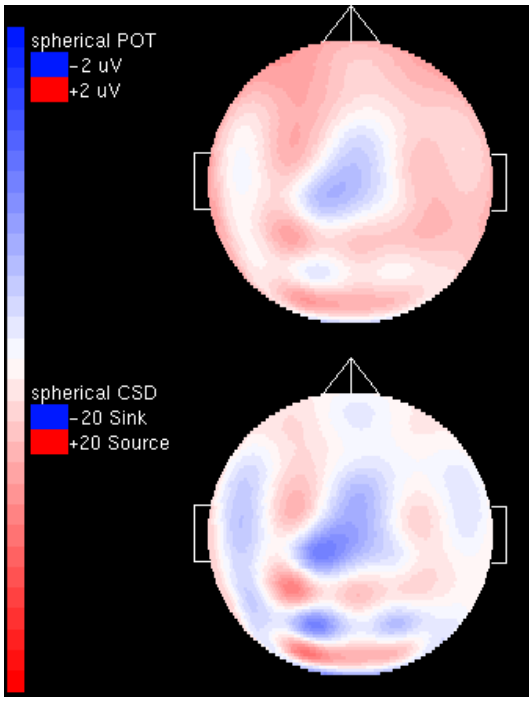


Fig. 4-4: Potential and CSD-topography for parameter PS. Although amplitudes were generally rather low, a similar pattern of amplitudes as during task processing could be observed (cf. chapters 6 & 7)

As for the interaction of coordinates and head model with the electrode location, the results are more difficult to interpret based on the current analysis alone. The higher density in the occipital and parietal scalp region did not result in lower overall interpolation errors, as might have been expected. Unfortunately for this analysis (but very fortunately for the analysis of the brain regions involved in task processing), the regions of higher sampling vastly over-

lapped with the regions with higher task-related activity. This presumably resulted in an increase in interpolation error, since higher inter-electrode differences in amplitude were observed over such regions. Thus, when one electrode was excluded from interpolation, this led to a considerable loss of information concerning the scalp potential field. The opposite seemed to apply to regions of less or now activity. Since amplitudes of neighboring electrodes were almost identical, the exclusion of one electrode did only have a small effect.

On the other hand, parameter PS showed a similar pattern of results as the parameters related to task-processing. This would speak against the interpretation that higher errors are associated with more active regions, since the amplitudes of the pre-stimulus baseline should be near to zero. Although this is certainly correct, a close inspection of the topographic pattern of PS shows higher amplitudes amplitudes in those areas which were more active during task processing (see Fig. 4-4). This might either be due to SCP activity which did not completely resolve during the inter-stimulus interval (which is very likely, since this interval was rather short compared to the median processing time of about 12 seconds; see chapters 6 and 7), or due to a mobilization of task-specific areas preceding task presentation. An analysis of different task paradigms in which the regions of higher activity do not overlap with the regions of higher sampling, and in which activity during complete rest is recorded, might help to resolve the issue whether the method of interpolation has larger effects in regions with more task-specific activity. For the moment, however, one can tentatively conclude that the increase of accuracy related to the usage of individual coordinates and a realistic head model is higher in electrodes placed over task-relevant brain regions.

Another rather unexpected result was that the highest errors were observed for parameter SCP5, although this parameter showed the highest signal amplitude. Initially, it was expected that errors should be lower for parameters with more signal and less "noise." Again, an argument similar as the one for the higher error in task-specific areas might explain this result: When higher amplitudes are observed, removing one electrode might have a larger effect on the interpolation error, particularly in those regions that show higher task-specific amplitudes. On the other hand, there was no clear pattern as to which parameter shows the highest differences between interpolation methods. While the increase in accuracy attributable to the usage of individual coordinates was highest for parameter SCP1, PS showed the highest increase in accuracy related to the usage of a realistic vs. a spherical head model.

Based on the present study, it can be concluded that a higher accuracy in topographic mapping is achieved when individual instead of standard electrode coordinates are used for interpolation. Thus, digitization of individual electrode coordinates is highly recommended in ERP mapping. In addition, usage of realistic head models will result in an even higher increase in the spatial accuracy of ERP maps. Making this a new standard in ERP research should not be to difficult, since 3D-digitizers are now made available by several commercial providers (at a price of about 13.000 €), and since the ever increasing gain in computing power will remove the main obstacle for the usage of realistic head models.

## *5. Consistency of inter-trial activity using single-trial fMRI: assessment of regional differences*

**Abstract**

*Most functional neuroimaging methods use averaging across trials in order to increase the signal-to-noise ratio of their measurements. This requires a sufficiently constant and time-locked signal time-course of the trials which are averaged. Recently, the technique of single-trial fMRI was introduced which allows the assessment of hemodynamic responses to single (sensory, motor, or cognitive) task executions. In this study, regional differences in the inter-trial consistency (ITC) of brain activity related to the processing of a dynamic visuo-spatial imagery task were assessed using single-trial fMRI analysis. For every single trial, a t statistic assessing task-related activity was calculated and thresholded at a p-value of $p \leq .05$ (uncorrected). The percentage of trials with t-values above threshold was used to assess differences in the consistency of brain activity in occipital, parietal, premotor and prefrontal regions of interest. While most of these regions showed activity which was highly consistent across trials, activity was significantly less consistent in the dorsolateral prefrontal cortex. It is suggested that the amount of consistency across trials may be interpreted as an indicator of the functional relevance of a brain region for the processing and solving of a cognitive task. Thus, the analysis concept presented here might provide new insights into the neurocognitive mechanisms of human information processing. In addition, the results of this study confirm that averaging across trials might result in a significant loss of information about functional neuroanatomy. Regions which are active in some trials only, which show only weak activity increases, or whose activity is not time-locked might not show up in averaged neuroimages, and might thus erroneously be considered as irrelevant for task processing.*

### *5.1 Background*

Most neuroimaging techniques (both hemodynamic and electrophysiological) rely on averaging across trials, time and/or subjects to increase the signal-to-noise ratio of their measurements. The best example for this strategy are event-related potentials (ERPs), which are obtained by calculating the arithmetic mean across a number of trials in which the ongoing EEG was recorded. The basic and decisive assumption of this procedure is that those electrophysiologic changes which are contained in a similar way in all trials will be enhanced, while random

fluctuations or noise will be eliminated. This, however, requires signal changes with a consistent time-course across trials. Whenever there is considerable variance in the on- and the offset of neural activity, its electrophysiological signature will hardly be reflected in the average. Another well-known problem associated with this technique is that signal which occurs only in some of the whole set of trials might not be detected appropriately, unless it shows a very high amplitude. Also, the amplitude of the event-related average is rather ambiguous with respect to whether it reflects the amount of neural processing in a certain area, or the consistency of activity across trials. For example, a high-amplitude signal occurring in only 50% of the averaged trials can result in a similar average amplitude as a signal with lower amplitude which is present in all trials (although a calculation of the inter-trial variance in amplitude might help to differentiate between the two cases).

About three to four years ago, the first studies were published in which fMRI data were collected in an event-related manner. This represented a significant advantage over the strategy of acquiring data in blocks of several stimulus or task repetitions, since the latter did not allow the assessment of the task-related time-course of activity. In order to analyze fMRI data acquired in an event-related acquisition mode, most groups incorporated the technique of averaging across trials from event-related potential research. In ERPs, the low signal-to-noise ratio might not be sufficient to detect neural activity with sufficient reliability and precision in single trials (but see also Flexer, 1999). This is in contrast to fMRI, in which the BOLD-response offers a much better signal-to-noise ratio. Hence - provided several requirements are met, such as high field strengths and ultra-fast gradients (see Ugurbil et al., 1999; Thulborn, 1999) - the extraction of functional information evoked by single task executions is feasible. This is reflected in a new concept called single-trial or single-event fMRI (Zarahn et al., 1997; Kim et al., 1997; Menon et al., 1998), in which neural responses related to single sensory, motor or cognitive events are measured.

Single-trial fMRI not only avoids problems associated with averaging, but may also be used to assess several aspects of the neural response which were not accessible to the cognitive neuroscientist before. Intra-subject variation of cortical activity across several trials of the same task type and their (psychological and/or physiological) bases may be investigated. Moreover, inter-subject variation in the consistency of brain activity may be assessed, providing potential clues for the assessment of strategy- or abilityrelated individual differences in cognitive processing. Thus, using single-trial fMRI, it is possible to investigate whether the same brain structures are involved in a similar manner across repeated executions

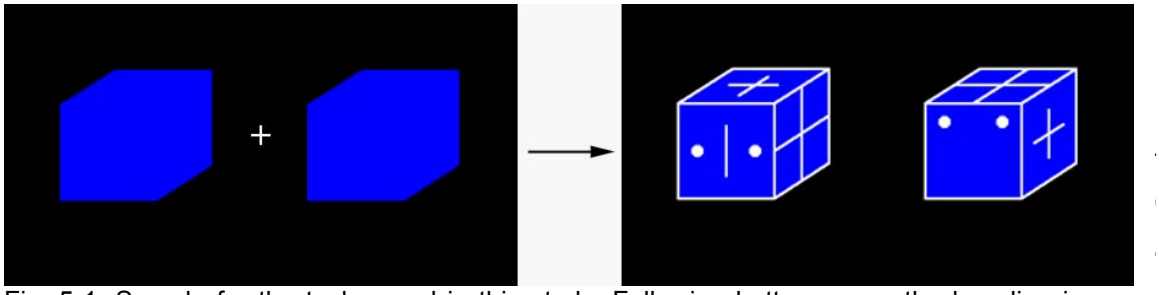

Fig. 5-1: Sample for the tasks used in this study. Following button press, the baseline image (two empty blue cubes on black background) was replaced by a task stimulus consisting of two cubes with white patterns on their faces. Subjects had to decide whether these cubes could be identical (which is the case for the chosen sample).

sumptions commonly have to be based on block-design and/or event-related studies using temporal averaging, potentially useful information might be missed.

In the present study, brain responses to several trials of a dynamic visuo-spatial imagery task were acquired using whole-cortex single-trial fMRI. The main aim was to assess regional differences in the consistency of brain activity across trials. In particular, it should be investigated if brain regions exist which are activated in all trials and if there are regions which are activated in some trials only. This was assessed by computing inter-trial consistency (ITC) maps which reflected the percentage of trials in which a certain brain region was activated or not. The present study was rather exploratory since no comparable analysis has been performed yet. However, it was hypothesized that the parietal cortex - which was repeatedly reported to be involved in dynamic visuo-spatial imagery (see chapters 6 and 7) - would be consistently activated. Concerning the question whether there are brain regions which are less consistently activated, no specific a-priori hypotheses could be formulated.

## *5.2 Material and methods*

### 5.2.1 Subjects

Eight young healthy volunteers with no history of neurological or psychiatric disorders and normal or corrected to normal vision participated in the experiments. Written informed consent was obtained prior to measurements. All subjects were right-handed according to the Marian Annett handedness inventory (Annett, 1985).

Ability-dependent differences in cortical activity during cognitive processing have been repeatedly reported, with poor performers showing increased cortical activity during task solving (Haier et al., 1988; Lamm et al., 1999). In order to ex-

clude the confounding effects of such individual differences, potential participants were pre-tested using a standardized three-dimensional cube comparison test (3DC; Gittler, 1990). Only subjects with high task-specific ability who solved at least 15 out of the 17 test items (corresponding to the 4$^{th}$ performance quartile of the age-, sex- and education-specific calibration sample of the test) of the 3DC were selected for this study. As a result of this pre-testing procedure, all subjects had the same prior experience in performing the tasks used in the experiments.

The homogeneity of the sample was further increased by investigating only male subjects (since gender differences in visuo-spatial processing are well-documented; see, e.g., Voyer, Voyer & Bryden, 1995), by restricting the subjects' age range (mean 22.6 years, range: 19-26), and by keeping the sample homogenous with respect to verbal and general intelligence (IQ 101-129, determined by using a brief word power test; Schmidt & Metzler, 1992).

### 5.2.2 Task material

The task items were an adaptation of the 3DC test used for subject selection. The decision to use 3DC-derived tasks in the investigation of dynamic visuo-spatial imagery was based on several favorable attributes of the 3DC test. Psychometric properties, such as reliability and validity, are well-known and high and have been determined using large calibration samples (Gittler, 1990). This is in contrast to most task material used in functional neuroimaging of cognition where face validity is sometimes the only known psychometric quality. In addition, 3DC tasks allow the assessment of visuo-spatial imagery with increased intra- and interindividual homogeneity since they fulfill the criteria of the Rasch model (Rasch, 1980). Tasks which conform to this probabilistic model allow unidimensional measurements of cognitive abilities, which implies that identical cognitive processes are active in all tasks as well as in different groups of subjects. This is an advantage compared to, e.g., two-dimensional letter or object comparison tests where some tasks do not require mental rotation of stimuli (Corballis et al., 1978; Cohen & Kubovy, 1993), and where some subjects might use predominantly verbalization rather than visuo-spatial strategies. Thus, by using 3DC-derived tasks, neuro-cognitive 'noise' by both intra- and interindividual differences in task processing strategies, or other factors not attributable to spatial imagery per se, were reduced to a minimum. This was of particular importance for the present study since differences in activity across trials should result from a difference in neural processing of the same task type, and not from a change in strategy or from the

usage of different cognitive functions in different trials. Also, 3DC-tasks require rather long processing times (ranging from 5 seconds up to 2 minutes, with a median of approximately 14 seconds) in comparison to the "classical" Shepard-Metzler figures (Shepard & Metzler, 1971), allowing a more extended sampling of fMR images during single trials.

The tasks were presented to the subjects via MRI-compatible video goggles (Resonance Technologies, Northridge/USA), which were connected to the video output of a PC which was controlling task presentation. A small box with three response buttons (Yes/No/Next) was fixed to the subjects right thigh.

### 5.2.3 Task design

Each trial consisted of a baseline image (white crosshair placed between two blue cubes without any graphic elements or white edges) and a task stimulus (see Fig. 5-1). Subjects initiated each trial by pressing a button, following which the baseline image was replaced by a task stimulus. The stimuli consisted of two blue cubes with white graphic elements (triangles, dots, squares, arrows etc.) on each of their three visible faces presented simultaneously on a black background. Subjects had to decide whether or not the two cubes could picture one and the same cube, and responded by pressing one of two response buttons with their dominant right hand (answers "yes" and "no"). Subjects were explicitly instructed that they had to decide only whether the two cubes *could* be identical, keeping in mind that each graphic element was allowed to occur only once on each cube. Without this instruction, the fact that three sides of each cube were not visible would allow any two cube configurations to be showing the same cube. A correct understanding of the instruction and the task content was ascertained by several sample tasks.

The widely used instruction to answer as quickly and accurately as possible affects unidimensionality (Rasch, 1980) and evokes processes not specifically attributable to the particular cognitive task, such as increased effort and working memory demand (Gulliksen, 1965). Since it has been shown that this results in increased cortical activity (Lamm et al., 2001), task presentation time was not restricted in the present study. Subjects were told they would have ample time to solve each task, but that they should enter their answer as soon as they finished working on a task item in order to ensure cognitive processing during the whole item presentation period. After answering, the subjects had ample time to prepare for the next item, which they had to indicate by pressing the "Next"-button. Each

item was presented in an identical manner, with a twenty seconds baseline period being followed by item presentation. Therefore, the minimum inter-trial interval was twenty seconds, allowing the hemodynamic response to return to baseline. As task presentation time was not limited, the number of processed trials answered varied between subjects in the range from 27 to 64 trials.

### 5.2.4 Data acquisition

MR experiments were performed on a 3 Tesla Medspec S300 whole-body system (Bruker Medical, Ettlingen, Germany) equipped with a whole-body gradient system and the standard birdcage coil for excitation/reception. An anatomically formed cushion and a strap around the forehead were used to reduce motion artifacts. A single-shot, gradient-recalled echo-planar imaging sequence with a matrix size of 64 by 64 pixels, echo time of 23 ms and a readout bandwidth of 100 kHz was used. 15 axial slices with a field-of-view of 190 x 190 mm (i.e. in-plane pixel size 2.97 x 2.97 mm), a slice thickness of 5 mm and an interslice gap of 1 mm, covering nearly the whole cerebrum, were acquired. Repetition time for the whole image slab was 1.5 sec. Two runs of 15 min were measured, each starting with 30 seconds of dummy scans to allow for steady-state conditions. The imaging sequence was designed to ensure continuous data acquisition and constant intervals between images.

### 5.2.5 Data analysis

All data sets were 2D motion-corrected using sinc-interpolation as implemented in AIR v3.08 (Woods et al., 1998). These data were smoothed with an isotropic Gaussian kernel of 9 mm FWHM to account for interindividual differences in brain anatomy and were normalized to the MNI template using the SPM99 software package (The Wellcome Department of Cognitive Neurology, London/UK; Friston et al., 1995b).

Each trial was analyzed separately using the information about the timing of task presentation and task response recorded with the controlling PC. A t-statistic was calculated for each trial which contrasted the signal during baseline (pre- and post-stimulus) with the signal during task processing. Only three time points (i.e. an interval of 4.5 s) after task presentation, shifted by 4 TRs or 6 s to account for the delay in hemodynamic response, were used to calculate the t-statistics. The signal intensity at these three time points was tested against the signal intensity

during the baseline before and after the stimulus presentation. The calculation of the t values was confined to the 4.5 s interval since response times, and thus the number of acquired data samples were not constant across trials. Therefore, a computation of t statistics based on all acquired samples would have resulted in different error variances across trials, which might have affected the estimation of inter-trial consistency. In addition, changes in task solving strategy, attention and effort might have emerged in trials with very long processing times. However, it seems plausible that such changes do not occur within the first five seconds of task processing. Thus, differences in brain activity associated with longer trials were excluded by confining the analysis to the initial data points after task presentation.

The t value maps of each single trial were used to calculate inter-trial consistency (ITC) maps. These maps indicated the percentage of trials in which a certain pixel was activated, i.e. its t-value was above the chosen threshold of $t \geq 1.734$ (corresponding to a $p \leq .05$, uncorrected for multiple comparisons). These maps were used to assess the consistency of activity across trials for each subject. A grand mean ITC map was calculated by averaging the eight subject-specific ITC maps. In order to allow for a quantitative analysis of the consistency of activity, the maximum ITC values within a certain activity cluster were determined for the following 11 regions: pre-supplementary motor area (pre-SMA), left and right dorsolateral prefrontal cortex (DLPFC), left and right parietal cortex (PAR), left and right dorsal premotor area (PMd), left and right ventral premotor area (PMv), and left and right occipital cortex (OCC).

## *5.3 Results*

### 5.3.1 Behavioral data

On average, subjects processed 43 tasks (range: 27-64) in the two runs. 91.5 % of the tasks were answered correctly (range: 86-95 %) and median reaction time was 12.88 seconds (range: 5.65-30.75 seconds). The two runs neither differed in reaction times nor in the number of tasks answered correctly (as assessed by Mann Whitney U-tests).

### 5.3.2 Functional activity

All subjects showed bilateral activity in occipital, parietal, and premotor cortex, as well as in the dorsolateral prefrontal cortex (DLPFC; BA9/BA 46) and the supplementary motor area (SMA). Fig. 5-2 shows the grand mean ITC map. Pixels activated in more than 30% of all trials are overlaid on the MNI single-subject template image and color-coded from red (30%) to yellow (100% ITC). Maximum ITC values of all subjects for SMA, DLPFC, PAR, PMd, PMv and OCC are shown in Fig. 5-3. Since ITC values of the eight subjects were not normally distributed, they were z-normalized, and five paired-samples t-tests were computed in order to assess interhemispheric differences in ITC values. Since none of these tests was statistically significant at the Bonferroni corrected p-value of 0.05, ITC values from the left and right hemisphere were averaged for each ROI. Differences between these averaged values were assessed using a repeated measure analysis of variance (corrected for violations of the sphericity assumption using

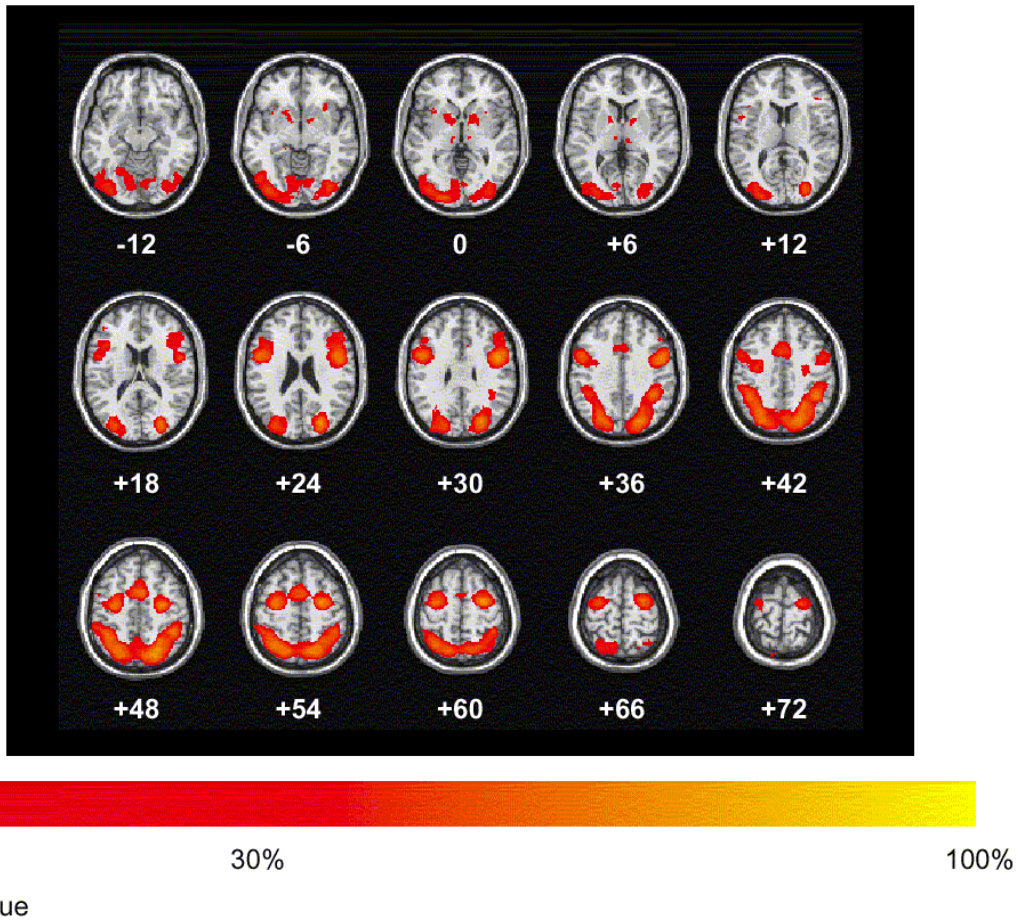


Fig. 5-2: Grand mean inter-trial consistency (ITC) map (n=8) overlaid on the T1 single-subject template brain from SPM99/MNI. The color corresponds to the relative number of trials in which a pixel was activated. Only pixels which were activated in more than 30% of all trials are displayed. Note that the grand mean peak ITC values are highest in the parietal and premotor regions (slices 48-60), while being somewhat lower in the DLPFC (slices 18 and 24).

Greenhouse-Geisser df-adjustment; Greenhouse & Geisser, 1959), which yielded a significant result ($F(5,35)=10.85$, $p_{adjusted}=0.003$, $\eta^2= 0.61$). Linear contrasts (corrected for violations of the sphericity assumption using specific error variances; Boik, 1981) were computed in order to assess which of the six ROIs caused this significant difference. It was revealed that the ITC values of DLPFC significantly differed from the other five ROIs ($F(1,7)=120.22$, $p<.001$, $\eta^2= 0.94$). The rank order of ITC values was DLPFC < SMA < OCC < PMV < PMD < PAR. Importantly (see the discussion section), a significant result was also obtained when DLPFC and PMv were contrasted ($F(1,7)=17.34$, $p=.004$, $\eta^2= 0.60$).

The lower ITC in the DLPFC seemed to indicate that activity in this region reflects a specific aspect of the 3DC-task which is variable across items. It was hypothesized that this aspect might be the difficulty (both subjectively and objec-

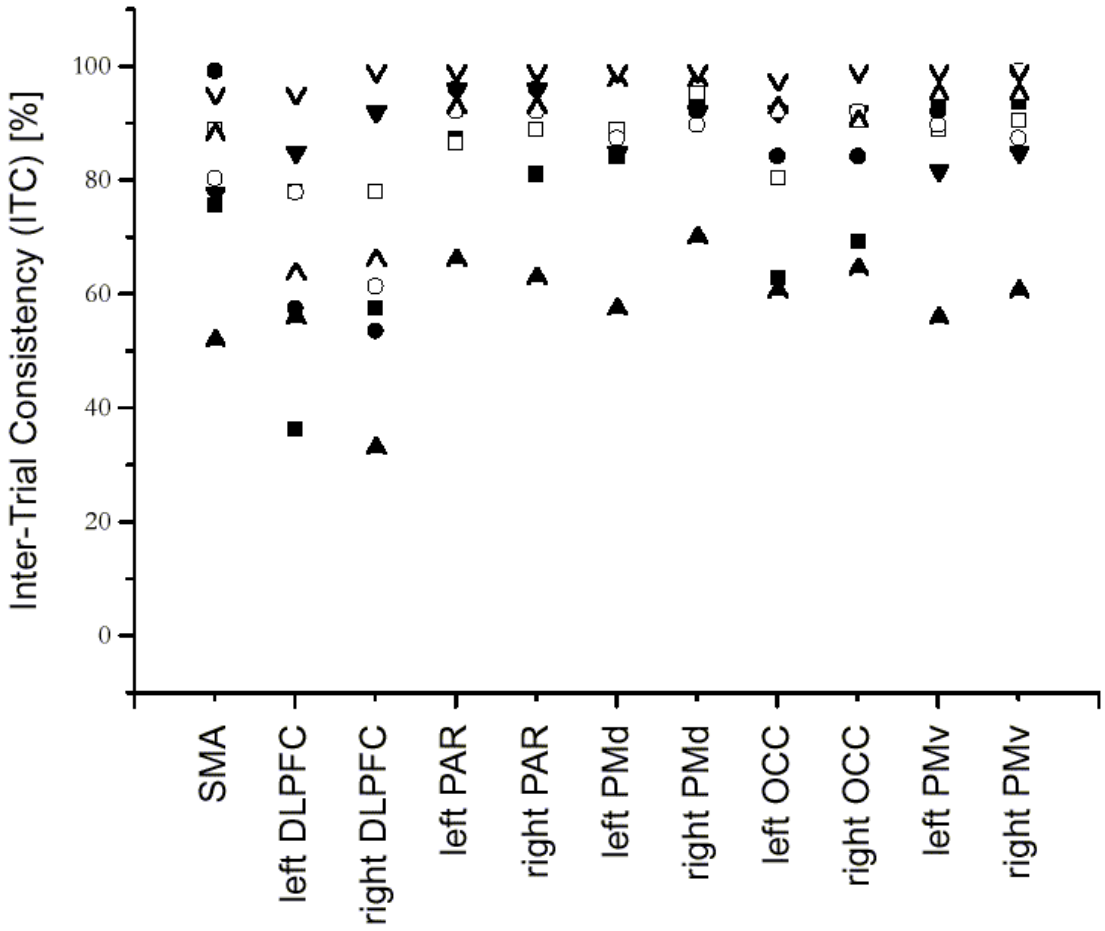


Fig. 5-3: Maximum ITC values in eight subjects determined for the following ROIs: Supplementary motor area (SMA), left/right dorso-lateral prefrontal cortex (DLPFC), left/right parietal cortex (PAR), left/right dorsal premotor area (PMd), left/right occipital cortex (OCC), left/right ventral premotor area (PMv), respectively. Note that ITC-values in DLPFC were significantly lower compared to all other ROIs.

tively) of an item. Consequently, several post-hoc analyses were performed in which it was investigated whether DLPFC activity was modulated by the difficulty of an item. Two behavioral variables existed that could be used to define the difficulty of an item: processing time and success rate (i.e. the percentage of correct answers for a certain task). The first parameter can be seen as a rather subjective indicator of the difficulty of an item, since it can be assessed individually for each subject and each item and shows only moderate correlation with success rate (about 0.45 in the earlier studies of Vitouch et al., 1997 and Lamm et al., 1999). Thus, it might indicate the amount of effort a subject invests into the solving of an item. In contrast, success rate is a subject-independent statistic which estimates the difficulty of a certain item via the percentage of subjects of a calibration sample who solved the item correctly. For this study, these data were available from two earlier brain imaging studies in which the same task material had been used (Vitouch et al., 1997; Lamm et al., 1999, 2001). Two different types of post-hoc analyses were performed using the two indicators of task difficulty.

Post-hoc analysis I tested whether trials which showed DLPFC activity showed longer processing times or higher success rates than trials which were not activated. This was assessed by computing paired t-tests which contrasted response times and success rates of items which did and did not activate DLPFC. A certain item was considered to activate the DLPFC if the pixel with the highest ITC value in the DLPFC ROI had a $t \geq 1.734$.

Post-hoc analysis II categorized the difficulty of items based on their individual response times or success rates in order to assess whether activity was different across these categories (irrespective of whether or not a trial was activated as defined by the $t \geq 1.734$ threshold criterion). For this kind of analysis, all trials which had been processed by a subject were rank-ordered either by processing time (descending rank order) or by success rate (ascending rank order). The lower 33% of the rank-ordered items were considered to contain more difficult items, while the upper 33% of them were thought to consist of easier items. Trials from the two categories were compared using two separate t-contrasts which either assessed whether more difficult or more easier items showed higher ITC values than the respective other category. Significance was defined via a p-value threshold of $p \leq .01$ (uncorrected for multiple comparisons).

#### 5.3.2.1 Post-hoc Analysis I

Fig. 5-4 shows mean task processing times (a) and success rates (b) per

subject for trials that did and did not activate the left or right DLPFC. Statistical analysis determined no significant differences in processing times or success rates.

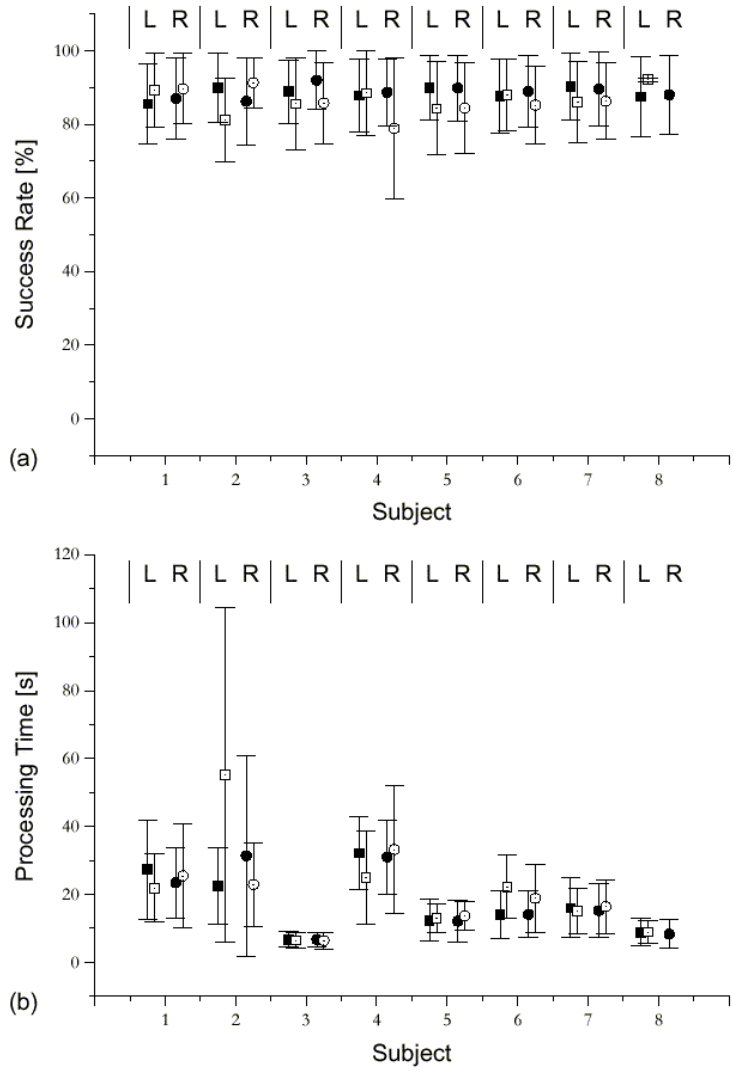


Fig. 5-4: Mean ± standard deviation of (a) success rates and (b) processing times of items that did or did not evoke activity in the left (squares) and right (circles) DLPFC. Closed symbols: values derived from items that activated DLPFC. Open symbols: values derived from items that did not activate DLPFC. There was neither a significant difference in success rate nor in processing time. Note that the right DLPFC was active in all trials in subject 8. Therefore, no symbol for non-active trials is shown.

### *5.3.2.2 Post-hoc Analysis II*

Both contrasts did not reveal a difference in DLPFC activity. However, the contrast assessing whether ITC values for the items with lower response times

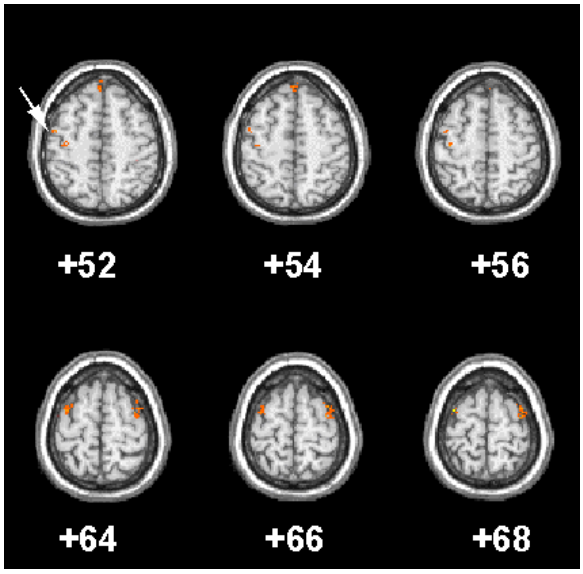


Fig. 5-5: Pixels in primary and pre-motor cortex which showed significantly higher activity in trials with shorter response times compared to trials with longer response times. Note that only the *left* primary motor cortex is active, which is in agreement with the subjects' response with their right hand (arrow: left central sulcus).

were higher than those with longer response times revealed bilateral clusters in premotor areas and in the left primary motor cortex (Fig. 5-5; the corresponding MNI stereotactic coordinates of the peak values were: -34/0/68; 38/-2/72; -38/-18/56). When item difficulty was determined via success rates, both t-contrasts did not reveal any distinct activity clusters.

### *5.4 Discussion*

In this study single-trial fMRI analysis of whole brain data was used to assess brain activity during dynamic visuo-spatial imagery. The results confirmed the well-known finding that the parietal cortex plays a dominant role in the processing of dynamic imagery tasks. The results also show that a number of extra-parietal areas are active, indicating that it is rather the cooperation and coordination of a functional network of brain areas than single brain regions that are responsible for task accomplishment. It should be noted that this kind of information would not have been available when only parts of the cortex had been scanned.

As homogeneous task items and a homogeneous subject group have been used, it may be assumed that brain activity recorded in this study is directly attrib-

utable to task-specific processing. For instance, prefrontal activity may be interpreted as reflecting attentional or working memory processes related to the processing of each individual trial. If a block design had been used, prefrontal involvement might also have been due to the necessity to maintain a constant level of unspecific attention/arousal during the task block. A similar argument applies to SMA activity (see, e.g., Petit et al., 1998).

The main aim of this study was to assess the consistency of activity across repeated executions of the same cognitive task in order to determine if differences in inter-trial consistency across different brain regions exist and whether they provide potentially useful information about the role of certain brain areas in cognitive processing. The ITC maps created from single-trial analysis enabled the differentiation of areas which were activated in every task, and brain regions which were involved in the processing of a limited number of trials only. In this way, additional information about the specificity of cortical regions could be gained which would not have been available when an event-related or blocked design had been used.

The results revealed that the dorsolateral prefrontal cortex was the only region which showed a significantly lower consistency of activity. This might indicate that activity in DLPFC was related to aspects of the imagery task which are variable across trials, while occipital, parietal and premotor cortex were essential to accomplish the spatio-temporal information processing demands required by the 3DC-tasks. However, it might also be argued that there are technical rather than functional accounts for the lower ITC value in DLPFC, e.g. shimming, susceptibility-related artifacts or motion. Although it can not be excluded that part of the variability across trials in this study was attributable to technical noise, it does not seem very likely that the lower ITC values in DLPFC are exclusively related to a higher amount of artifacts in this region. The observation that there were no interhemispheric differences in DLPFC activity speaks against the argument that a difference in shim quality caused the lower ITC values. Also, the lower ITC values can not be explained by susceptibility- or motion-related signal losses or signal distortions since the PMv ROI, which was located only slightly more posterior than the DLPFC ROI, did also show higher ITC values than the DLPFC. Thus, it seems justified to assume that the lower ITC values in DLPFC mainly resulted from differences in cognitive task processing across trials.

From the lower ITC-values in DLPFC it was hypothesized that activity in the DLPFC might be related to the difficulty of an item or the amount of effort it requires. Therefore, it was expected that the processing of more difficult items or of items which subjectively required more effort should lead to activity in the DLPFC,

while easier items should not. For post-hoc analysis I the average processing times for items which did and did not activate the DLPFC were compared and showed no statistically significant difference. The same applied to the success rate values.

Splitting tasks into two categories based on the processing times and testing the resulting ITC maps for higher ITC values in items with longer response times did not reveal significant clusters. On the other hand, significantly higher ITC-values for items with shorter compared to items with longer response times were found bilaterally in the premotor region and in left primary motor cortex (see Fig. 5-5). These regions are known to be involved in movement preparation. Therefore, these differences in activity are interpreted as a correlate of the earlier onset of motor activity required by the trials which shorter processing times.

Consequently, neither task difficulty nor the effort required by an item did explain the lower ITC values in DLPFC. Thus, it seems that there are variables other than task difficulty or effort (as defined by processing time or success rate) which affected the activity in DLPFC. One of them might be the amount of working memory demand required by an item, since it has been repeatedly shown that DLPFC activity is modulated by the amount of visuo-spatial information which has to be kept in working memory (Diwadkar et al., 2000; Carpenter et al., 2000). Whether this also explains the observed variability in DLPFC activity remains to be shown by further investigations since working memory demand could not be systematically varied with the task material used in the present study.

The results of the present study also confirm the repeatedly made objection that averaging across trials might result in a significant loss of information about functional activity. Brain regions which are active in some trials only, which show only weak activity increases, or whose activity is not time-locked might not show up in averaged neuroimages. This might be one reason to explain the considerable number of inconsistencies between different functional neuroimaging studies. Depending on the number and type(s) of items used, and depending on the subjects investigated, activity in brain regions which is only evoked by certain aspects of a task might or might not be obtained in the analyses.

In this study, single-trial analysis was applied to whole-cortex fMRI data of a 3D cube comparison paradigm. It should be noted that - due to current hardware restrictions - this analysis approach is limited to paradigms requiring extended stimulus processing times, i.e. several times TR. The additional information accessible via the single-trial results was used to examine intra-subject inter-trial activity consistency. Distinct cortical areas were revealed which were not involved in all

items, and which might reflect specific, variant aspects of task processing (as increased difficulty or complexity). However, the analyses performed did not reveal which aspect of task processing caused the regional differences in ITC values. Nevertheless, it can be concluded that the single-trial analysis approach presented here is a valuable tool for the cognitive neurocientist, which might help to gain new insights into cognitive processing barely accessible via other brain imaging techniques.

## *6. Functional neuroanatomy of dynamic visuo-spatial imagery revealed by single-trial fMRI and SCPs*

**Abstract:**

*A strong correspondence has been repeatedly observedbetween actually performed vs. mentally imagined object rotation. This suggests an overlap in the brain regions involved in these processes. Functional neuroimaging studies have consistently revealed parietal and occipital cortex activity during dynamic visuo-spatial imagery. However, results concerning the involvement of higher-order cortical motor areas have been less consistent. It was investigated if and when premotor structures are active during processing of a three-dimensional cube comparison task that requires dynamic visuo-spatial imagery. In order to achieve a good temporal and spatial resolution, single-trial functional magnetic resonance imaging (fMRI) and scalp-recorded event-related slow cortical potentials (SCPs) were recorded from the same subjects in two separate measurement sessions. In order to reduce inter-subject variability in brain activity due to individual differences, only male subjects with high task-specific ability were investigated. Functional MRI revealed consistent bilateral activity in the occipital (Brodmann area BA18/19) and parietal cortex (BA7), in lateral and medial premotor areas (BA6), the dorsolateral prefrontal cortex (BA9) and the anterior insular cortex. The time-course of SCPs indicated that task-related activity in these areas commenced around 550-650 msec after stimulus presentation and persisted until task completion. These results provide strong and consistent evidence that human premotor cortex is involved in dynamic visuo-spatial imagery.*

### *6.1 Background*

A strong correspondence between overt object manipulation and mental object transformation via dynamic visuo-spatial imagery has been repeatedly observed (e.g., Shepard and Metzler, 1971; Shepard & Cooper, 1982; Wohlschläger & Wohlschläger, 1998; Wexler et al., 1998), with the most well-known example being originally presented by Shepard & Metzler (1971). Asking subjects to decide about the identity of two differently oriented three-dimensional objects, they observed an almost perfect positive linear increase in reaction times with increasing angular disparity between the two objects. Introspective reports of participants describing task processing as an analog-like rotation of objects into congruence along continuous trajectories led to the designation of this effect as mental rota-

tion. Since then, mental rotation-like effects have been replicated using a variety of other task stimuli, including alphanumeric characters, pictures of body parts and maps, as well as under various more or less exotic experimental conditions such as head tilt or microgravity in the soviet space station MIR (see Wohlschläger & Wohlschläger, 1998; Shepard & Cooper, 1982; Cooper & Shepard, 1984; Kosslyn, 1994, for extensive reviews).

Since reaction times would also increase when objects were actually (e.g., manually) rotated through larger angles, this raised the question whether the physical constraints of the real world affect the rules of how objects are or can be mentally imagined and manipulated. It has been postulated for a long time that motor action and visual perception share common functions and representations (Bain, 1855; James, 1890; Weimer, 1977; Scheerer, 1984; Prinz, 1997). Recently, it has been proposed that this might also apply to visuo-spatial imagery, and that the common functional processing constraints observed for object manipulation by motor actions and by dynamic visuo-spatial imagery indicate functional equivalence of these two processes (Pellizzer & Georgopoulos, 1993; Wohlschläger & Wohlschläger, 1998; Wexler et al., 1998).

One explanation for the correspondence between overt and covert object manipulation is that both processes are supported by similar to identical brain structures. A considerable number of functional neuroimaging studies has already been performed to investigate brain activity during dynamic visuo-spatial imagery. These studies identified the parietal cortex as the brain region which was most consistently and strongly activated. Since it is well-known that parietal areas are involved in spatial information processing (e.g. Mishkin & Ungerleider, 1982; Haxby et al., 1991), this would be consistent with the "visuo-spatial" part of the functional equivalence hypothesis.

However, results concerning activity in cortical areas involved in motor execution and motor planning have been somewhat inconclusive and much less consistent (see, e.g., Carpenter et al., 1999; Cohen et al., 1996). In fact, three recent studies did not report any activity in cortical motor areas during mental rotation of both two- and three-dimensional objects (Kosslyn et al., 1998; Harris et al., 2000; Jordan et al., 2000). While the absence of activity in primary motor areas must not be contradictory to the assumption of functional equivalence since no constant motor output is required in mental rotation tasks, the failure to detect activity in non-primary motor areas such as lateral premotor areas and supplementary motor area (lateral and medial Brodmann areas BA 6) is not compatible with this hypothesis. Premotor areas are known to be of central importance in the planning,

preparation and control of complex movements, functions which are definitely required in overt object manipulation.

One reason for the discrepancies between previous studies might be - apart from the slightly different task and task control paradigms - the difference in the spatial and especially the temporal resolution achieved by the utilized imaging techniques. Thus, the aim of the present study was to assess cortical activity during dynamic visuo-spatial imagery with combined good temporal and spatial resolution.

Multi-slice single-trial fMRI was used to acquire images of task-related hemodynamic changes with high spatial resolution and good temporal resolution. Event-related slow cortical potentials (SCPs) were additionally recorded from the scalp of the same subjects in a separate measurement session. SCPs allowed the examination of cortical activity in the sub-seconds range. Since SCPs are related to sustained excitatory input to apical dendrites of cortical pyramidal cells, they also provide a more direct assessment of neural activity than fMRI-derived measures. Hence SCPs might help to resolve the ambiguity that increased blood flow or oxygenation may equally be related to increased activity of either excitatory or inhibitory neurons. In order to overcome some of the potentially confounding variables of other studies several behavioral parameters were controlled, including the type and consistency of task-processing strategies used, the homogeneity of the sample investigated, and the task presentation mode.

## *6.2 Material and methods*

### 6.2.1 Subjects

Thirteen young healthy volunteers with no history of neurological or psychiatric disorders and normal or corrected to normal vision participated in one SCP and one MRI/fMRI measurement session. The order of the sessions was balanced and the time separating the two session orders was kept constant across subjects. Written informed consent was obtained prior to measurements and subjects were paid ~7.50 € per hour for their participation. All subjects were right-handed according to the Marian Annett handedness inventory (Annett, 1985). Ability-dependent differences in cortical activity during cognitive and especially visuo-spatial task processing have been repeatedly reported, with poor performers showing increased cortical activity during task solving (Haier et al., 1988; Vitouch

et al., 1997; Lamm et al., 1999; see also chapter 7). In order to exclude the confounding effects of such individual differences, potential participants were pre-tested using a standardized three-dimensional cube comparison test (3DC; Gittler, 1990). Only subjects with high task-specific ability who solved at least 15 out of the 17 test items (corresponding to the 4$^{th}$ performance quartile of the age-, sex- and education-specific calibration sample of the test) of the 3DC were selected for this study. As a result of this pre-testing procedure, all subjects had the same prior experience in performing the tasks used in the experiments.

The homogeneity of the sample was further increased by investigating only male subjects (since gender differences in visuo-spatial processing are well-documented; see e.g. Voyer, Voyer & Bryden, 1995), by restricting the subjects' age range (mean 24,5 years, range: 19-28), and by keeping the sample homogenous with respect to verbal and general intelligence (IQ 101-129; determined by using a brief word power test; Schmidt & Metzler, 1992).

### 6.2.2 Task material

Task stimuli consisted of two blue-colored cubes with white elements (triangle, dots, squares, arrows etc.) on each of their three visible faces presented simultaneously on black background (see Fig. 6-1). All tasks were adapted from the standardized three-dimensional cube comparison test (3DC; Gittler, 1990) used for pre-testing, the only difference being that only two instead of six cubes had to be compared. This test is routinely used in the assessment of visuo-spatial imagery abilities in educational and vocational counseling, and in the selection of civil and military aircraft pilots. The decision to use this type of task material in the investigation of dynamic visuo-spatial imagery was based on several favorable attributes

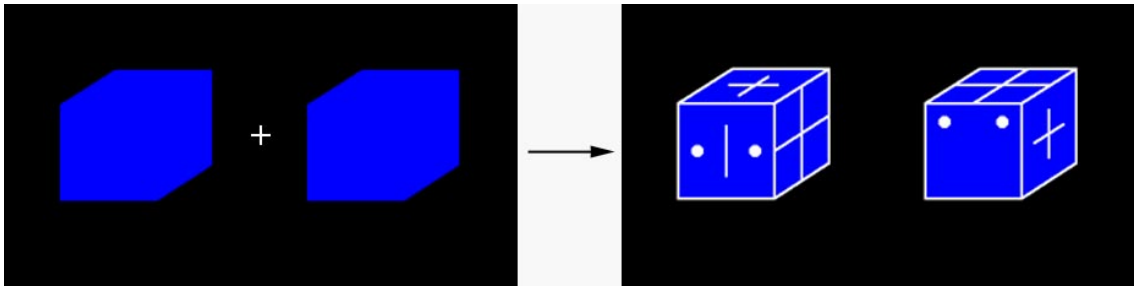

Fig. 6-1: Sample for the tasks used in this study. Following button press, the baseline image (two empty blue cubes on black background) was replaced by a task stimulus consisting of two cubes with white patterns on their faces. Subjects had to decide whether these cubes could be identical (which is the case for the chosen sample). Both image-types were presented centered in the middle of a computer screen (SCP) or of the display of the screens of the video goggles (MR).

of the test. Psychometric properties such as reliability and validity are well-known and high and have been determined using large calibration samples (Gittler, 1990). This is in contrast to most task material used in functional neuroimaging of cognition where face validity sometimes is the only known psychometric quality.

Most important was, however, that 3DC-tasks allow the assessment of visuo-spatial imagery with increased intra- and interindividual homogeneity since they fulfill the criteria of the Rasch model (Rasch, 1980). Tests which conform to this probabilistic test model yield unidimensional measurements of cognitive ability, which implies that identical cognitive operations are used in all tasks as well as in different subjects. This is an advantage compared to, e.g., 2-dimensional letter or object comparison tests in which some tasks do not require mental rotation of stimuli (Corballis et al., 1978; Cohen & Kubovy, 1993), and where some subjects might predominantly use verbalization rather than visuo-spatial strategies. Although such intra- and interindividual differences in task processing strategies are still possible with Rasch-homogeneous task material, they are known to be considerably reduced.

For this study (where subjects processed up to 170 tasks), it was also of particular importance that 3DC-tasks do hardly show practice-related changes in processing strategy. Such changes have been observed when using the classical Shepard & Metzler mental rotation paradigm (Tarr & Pinker, 1989), where subjects with sufficient practice may use stored representations of the 3D objects to decide about their identity and thus do not actually rotate the objects any more. Such a change in strategy had to be avoided in this study since subjects should not use different processing strategies and associated brain regions in the two consecutive measurement sessions.

Another important feature of tasks used in this study is their long processing times, ranging from five seconds up to two minutes with a median around fourteen seconds. These rather long response times are in contrast to those obtained with Shepard & Metzler figures (1971) in which tasks with low angular difference can be answered within one or two seconds. Such short response times make it more difficult to separate cognitive processes related to visuo-spatial imagery from processes related to response preparation and execution.

### 6.2.3 Task design

The stimuli consisted of two blue cubes with white graphic elements (triangles, dots, squares, arrows etc.) on each of their three visible faces presented si-

multaneously on a black background. Subjects had to decide whether or not the two cubes could picture one and the same cube and to respond by pressing one of two response buttons with their dominant right hand (answers "yes" or "no"). Subjects were explicitly instructed that they had to decide only whether the two cubes *could* be identical, keeping in mind that each graphic element was allowed to occur only once on each cube. Without this instruction, the fact that three sides of each cube were not visible would allow any two cube configurations to be showing the same cube. A correct understanding of the instruction and the task content was ascertained by several sample tasks.

The widely used instruction to answer as quickly and accurately as possible affects unidimensionality (Rasch, 1980) and evokes processes not specifically attributable to the particular cognitive task, such as increased effort and working memory demand (Gulliksen, 1965). Since it has been shown that this results in increased cortical activity (Lamm et al., 2001), task presentation time was not restricted in the present study and subjects were told they would have ample time to solve each task. The task presentation and data acquisition mode for SCP and fMRI-measurements were completely identical (except for the minimum inter-trial interval and the display device) in order to enhance the comparability of the behavioral and neuroimaging results obtained by the two different methods. The tasks used in the SCP and fMRI sessions were partially identical, since only a limited number of standardized and calibrated 3DC items exist. However, since their presentation order was randomized across subjects and since all tasks look very similar, distinguishable only by the type and orientation of the graphic elements on the cube faces, it is unlikely that subjects remembered tasks presented in the first measurement session.

### 6.2.4 MRI and fMRI scanning

MRI experiments were performed in a 3 Tesla Medspec S300 tomograph (Bruker Medical, Ettlingen, Germany) equipped with a whole-body gradient system and a standard birdcage coil for RF excitation/reception. An anatomically formed cushion and a strap around the forehead were used to reduce gross head motion. Structural images of the brain were acquired using a 64 slice gradient-echo sequence with 1mm x 1mm in-plane resolution and a slice thickness of 3 mm. A T2*-weighted single-shot, blipped gradient-recalled EPI sequence (flip angle=Ernst angle) with a matrix size of 64 by 64 pixels, an echo time (TE) of 23 ms and a readout bandwidth of 100 kHz was used for functional imaging. 15 axial slices with

a FOV of 190 by 190 mm, a thickness of 5 mm and an interslice gap of 1 mm, covering nearly the whole cerebrum, were acquired. Repetition time (TR) for the whole image slab was 1.5 s. The single-trial sequence was designed to ensure continuous data acquisition and constant intervals between images. Two runs of fifteen minutes each (600 images/slab) were acquired, each starting with thirty seconds of dummy scans to allow for steady state conditions. Although the task content and task difficulty were the same in the two runs, their sequence was balanced across subjects.

Stimuli were presented via MRI-compatible video goggles (Resonance Technologies, Northridge/CA, USA) connected to the video output of a controlling PC running in-house software for stimulus presentation. The visual angle subtended by the two cubes (~ 1.64° vertical, ~ 8° horizontal) was kept as low as feasible in order to reduce the requirement of making large saccadic eye movements. The buttons for responses and task initiation were mounted on a board attached to the subject's right thigh. The minimum inter-trial interval was twenty seconds in order to allow cerebral blood flow changes to return to baseline between trials.

### 6.2.5 fMRI analysis

The structural MR images were normalized to the average brain template of the Montreal Institute of Neurology (MNI) using the software package SPM99 (Friston et al., 1995b; The Wellcome Department of Cognitive Neurology, London/UK). Functional images were corrected for head motion in 2D using sinc-interpolation (AIR v3.08; Woods et al., 1998) and co-registered to the normalized structural images via linear translation and stretching of the functional images using IDL routines (Interactive Data Language; Research Systems, Inc., Boulder/CO, USA) written in-house. The accuracy of normalization and co-registration was carefully checked for each subject based on several brain landmarks and the shape of the slices.

The functional images were spatially smoothed with a Gaussian kernel of 9 mm full-width-at-half-maximum. The main reason for applying spatial smoothing was to reduce the effect of interindividual differences in both structural and functional neuroanatomy. Since a Gaussian kernel was used, the assumption that data were normally distributed also seems to be more valid than without smoothing (see Friston et al., 1995b). This was decisive for the validity of the subsequent statistical tests.

Task-related changes in single trials were assessed by computing t-tests contrasting the signal intensity during task processing with the signal intensity during baseline. A t-test was preferred to a computation of the mean signal change between baseline and task processing since it takes account of the variance across pixels. For each pixel of each single trial of each subject a t-value was obtained and then a t-test (one-sided) of these single trial t-values was performed. The reason for performing such a t-test was to get a summary statistic of the activity of all single trials. The resulting t-values were color-coded and mapped on to the structural images. A thresholding procedure had to be applied in order to identify regions of significant activity (see also the discussion below). Maps were thresholded at a t-value corresponding to a p-value of .00001 (for each single voxel, i.e. uncorrected for multiple comparisons), and significant activity clusters and their peak voxels were identified for each subject. In order to assess activity in the whole sample, the thirteen single-subject t-maps were averaged in stereotactic space. The resulting grand mean fMRI activity map was thresholded at a t-value corresponding to p=.00001 (for each single voxel).

Both the fMRI grand mean activity and the consistency of activity determined on the basis of single-subject activity maps are reported. While the former allows inferences about "average" characteristics, the latter allows inferences about "typical" characteristics of brain activity in the sample investigated (Friston et al., 1999). Anatomical locations and Brodmann areas (BA) of significant activity clusters were determined using the brain atlas published by Talairach & Tournoux (1988) and a digitized Talairach atlas (http://biad73.uthscsa.edu; Lancaster et al., 2000).

### 6.2.6 EEG recording

The EEG was recorded using a 24-channel DC amplifier with high baseline stability and an input impedance ≥100 GΩ. Signals were sampled at 125 Hz and recorded within a frequency range from DC to 30 Hz. Variable signal epochs covering two seconds of pre-presentation baseline to two seconds after response were stored trial by trial. The EEG was recorded using 40 Ag/AgCl EEG electrodes attached to small plastic adapters that were fixed to the subject's scalp with collodion. Recording sites were skin-scratched with sterile single-use needles (Picton & Hillyard, 1974) to minimize skin potential artifacts and to keep electrode impedance homogeneous, stable and below 1 kΩ (which was confirmed for each electrode separately). Degassed electrode gel (Electro-Gel, Electrode-Cap Interna-

tional, Inc., Eaton/OH, USA) was used, and electrodes were filled with the gel at least half an hour before application to allow for stabilization of the electrode potential. A non-cephalic sterno-vertebral reference (Stephenson & Gibbs, 1951) was used for all EEG channels. It consisted of two electrodes, one placed at the 7$^{th}$ cervical vertebra and the other at the right sterno-clavicular junction. A 5 kΩ potentiometer connecting these two electrodes was individually adjusted to minimize electrocardiographic components in the EEG. Vertical (electrodes above and below the right eye) and horizontal (electrodes on outer canthi) electrooculograms (VEOG, HEOG) were recorded bipolarly to check for eye movement artifacts.

Since the DC amplifier had only 24 channels, the EEG was alternately recorded from two interleaved electrode sets, with each set consisting of 20 EEG electrodes and of two electrodes placed on the mastoids. The electrodes of both sets were distributed equally across the scalp surface. With each electrode set at least two blocks of 30 trials were recorded. The sequence of blocks was randomly permuted across subjects. 3D coordinates of all EEG electrodes, and of nasion, inion and the two preauricular points were measured using a photogrammetric head digitizer (Bauer et al., 2000). The tasks were presented in the center of a computer screen located approximately 70 cm in front of the subject, and a response board was positioned to the right of the subject. The visual angle subtended by the stimuli was approximately identical to that used for the fMRI goggles. The minimum inter-trial interval was four seconds.

### 6.2.7 EEG analysis

Eye movement artifacts were eliminated offline using a linear regression algorithm (see Vitouch et al., 1997, for a detailed description). All trials were visually screened to exclude those containing artifacts. Stimulus-onset linked averages were computed for each subject. The mean amplitude in the 200 millisecond epoch preceding task presentation served as the pre-stimulus baseline. Since response times were variable within and across subjects, an analysis epoch of five seconds was selected based on the median reaction times. This epoch length was chosen because it was long enough to reliably induce cognition-related SCPs and because only a few trials had to be rejected due to response times shorter than five seconds (see also Lamm et al., 2001). In order to exclude activity related to motor preparation and execution of the button press, only trials with response times ≥ 5500 ms were included in the averages. In addition, response-linked averages (with the same 200 ms pre-stimulus baseline as for the stimulus-linked aver-

ages) were computed to evaluate activity related to task completion and response execution.

SCP averages and their current source density (CSD) transforms were topographically mapped using the analytical interpolation algorithm proposed by Babiloni et al. (1996). CSD transformation was carried out in order to yield reference-free maps and to attenuate low spatial frequencies ('smearing') introduced into the scalp potential distribution due to volume conduction (Nunez, 1989; Nunez et al., 1994; Srinivasan et al., 1996). In order to map the activity distribution on the scalp surface with increased spatial sampling (Nunez et al., 1994; Srinivasan et al., 1998), the data of the two electrode sets were used simultaneously for the interpolation. SCP and CSD maps were visualized on individual head shapes reconstructed by using spline interpolation of the 3D electrode and landmark coordinates acquired by the photogrammetric head digitizer. The accuracy of this approach was guaranteed by coregistration with MRI-reconstructed head shapes which yielded a mean deviation between EEG- and MRI-derived surface points of only 2.3 mm (Lamm et al., 2000). Coregistration was also used to determine the position of electrodes in relation to individual cortical anatomy. Grand mean SCP and CSD maps (Fig. 5) were computed using the mean electrode coordinates of the whole sample for interpolation. The consistency of activity across subjects was assessed by comparing individual-subject averages with the grand mean. SCP and CSD maps and SCP waveforms were used to assign surface activity to cortical areas that were detected to be active by means of fMRI.

### 6.2.8 Behavioral data and questionnaire

Median processing time and percentage of correctly answered tasks were calculated separately for the SCP and MRI sessions. In addition, two questionnaires that had been specifically designed for this study were completed by each subject. These were used to gain information about the subjects' task solving strategies. Questionnaire A included questions about the task difficulty, the effort and concentration invested by the subjects, the percentage of items they were convinced to have answered correctly, and how motivated they felt during the experiment. Questionnaire A was presented twice, i.e. after the SCP as well as after the MRI session.

As discussed above, 3DC tasks are known to show relatively fewer intra- and interindividual differences in processing strategies than tasks which do not conform to the Rasch model. However, since such differences cannot be pre-

cluded in any type of cognitive task processing, questionnaire B assessed two possible task solving strategies. The most commonly used strategy consists almost exclusively of dynamic visuo-spatial imagery and mental rotation. The second strategy is a more analytical one and includes verbal-analytical descriptions of the relations of the cubes and their graphic elements. Nevertheless, it also relies on visuo-spatial cognition because the cubes and the mutual relations of their graphic elements are coded and compared using spatial descriptors (such as "the arrow on the *upper* face of the left cube points to the *left anterior* corner of this cube"; see also Gittler, 1990). By using the standardized written task instruction of the 3DC test special care was taken not to bias subjects in favor of either of the two strategies (Intions-Peterson, 1983). Since a presentation after the first session might have influenced the subjects' processing strategies in the second session, questionnaire B was presented only once and always after the second measurement session.

## *6.3 Results*

### *6.3.1 Behavioral data*

*Performance:*

On average, 94.14% (range 88.99-97.28) of tasks were answered correctly Average processing time was 14.16 seconds (range of median processing times: 5.25-25.42 seconds). Paired samples t-tests revealed that subjects answered tasks significantly faster ($t_{12}$=2.78, p=.017, two-tailed) and more accurately ($t_{12}$=3.51, p=.004, two-tailed) in the SCP session (see Table 6-1). In the second measurement session, subjects did not recognize those task items which had already been presented during the first measurement session.

Table 6-1: Processing time (in seconds) and response accuracy in the SCP and fMRI measurement session (mean ± standard deviation)

| | Processing Time | Percentage of correctly answered tasks |
|---|---|---|
| SCP | 11.91 ± 4.99 | 96.71 ± 2.59 |
| fMRI | 16.42 ± 7.24 | 91.58 ± 4.87 |

*Questionnaires:*

Questionnaire A: Tasks were generally judged to be easy and to require rather little effort, which was not surprising considering the high task-specific ability of the subjects. None of the subjects had any difficulty to concentrate and most were highly motivated and convinced to have solved most of the tasks correctly. No significant differences ($p > .3$ for all statistical tests) concerning these variables were observed when the answers after the SCP and the MRI sessions were compared using Wilcoxon signed rank tests.

Questionnaire B: Tasks were mainly solved by using one predominant strategy. In all subjects but one this was the dynamic visuo-spatial imagery strategy. Since this particular subject did not show any obvious difference in brain activity in comparison to the other subjects, its results will not be treated separately.

All subjects occasionally also used the verbal-analytic strategy occasionally. When using the visuo-spatial imagery strategy subjects imagined movements of cubes into a new orientation. However, they neither imagined themselves actively executing these movements, nor did they imagine themselves changing their perspective by moving around the cubes. Imagined movements proceeded rather autonomously or "on their own", with cubes moving mostly as a whole. The visual mental images experienced during task processing were reported to be vivid and comparable to actual vision. When using the analytic strategy, subjects coded the spatial relations of the elements on the two cubes and then compared these relations. These comparisons were executed sequentially for each single face of the cubes. In coding the spatial relations, subjects did not refer to their own position, but used an independent frame of reference.

No significant differences were observed - neither for the imagery nor for the analytic strategy - when questions presented after the SCP-and the MRI-session were compared using Mann-Whitney U-tests ($p > .09$ for all statistical tests).

Additional informal reports of subjects during experimental debriefing indicated that task solving consisted of several steps including perceptual analysis of the cubes and the elements on their faces, the construction of a visual mental image of one of the cubes (in most trials, this was the cube presented on the left side), mental rotation (tilting) into supposed congruence with the other cube, and subsequent matching of the two cubes via a comparison of the orientation and location of the elements on their faces (see also Just & Carpenter, 1985).

### 6.3.2 fMRI

The fMRI grand mean revealed significant bilateral activity clusters in occipital and parietal cortex, precentral gyrus, medial superior frontal gyrus, dorsolateral prefrontal cortex and anterior insular cortex (see Fig. 6-2[10]). Table 6-2 lists the neuroanatomical localization and the consistency of these activity clusters across subjects. As Fig. 6-2 shows, activity was most prominent and widespread in the parietal cortex, including the superior parietal lobe and intraparietal sulcus, and partially extending into inferior parietal lobe. The left- and right-hemispheric activity clusters in the precentral gyrus rostrally extended into precentral sulcus, but their maximum and the majority of voxels were clearly located in the precentral gyrus and lateral BA 6. The maximum and the majority of voxels of the activity

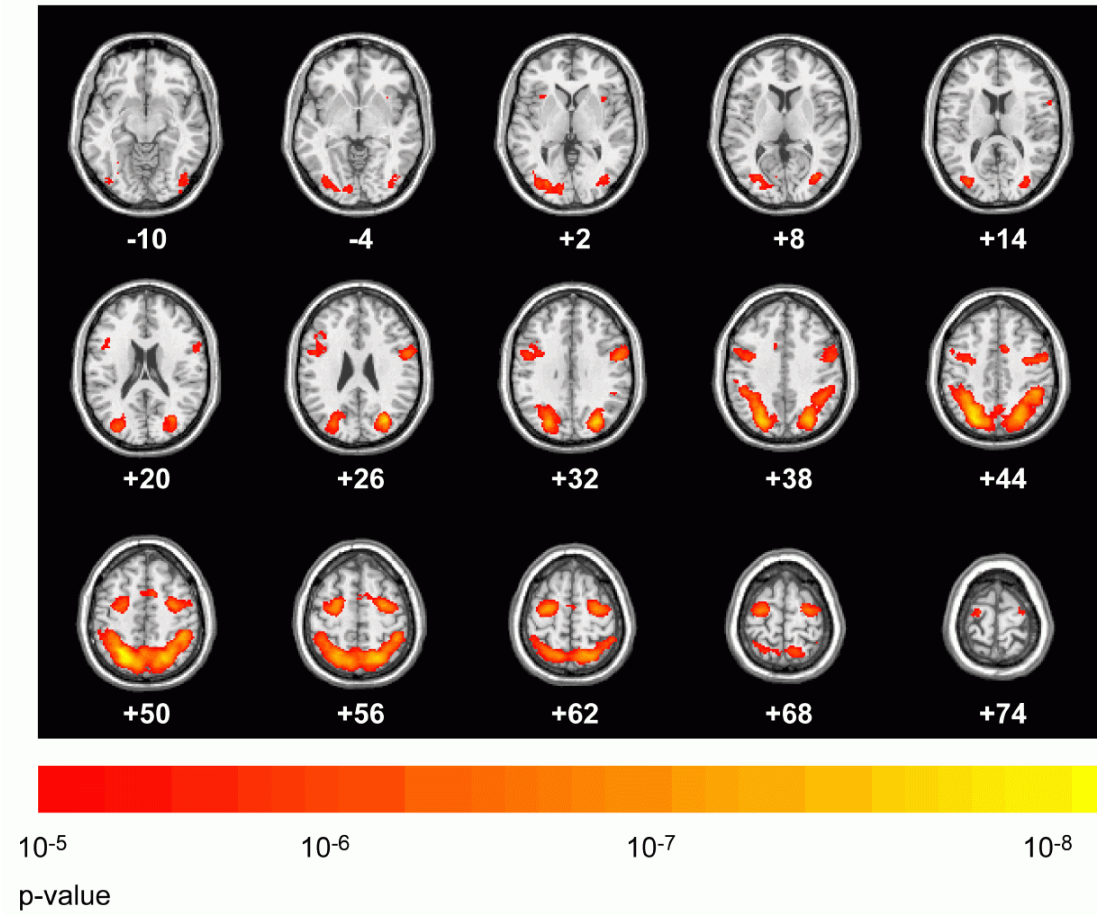


Fig. 6-2a: Grand mean fMRI activity during task processing. Color-coded p-values (thresholded at a value of p=.00001, uncorrected) are overlaid to high-resolution structural MR images in stereotactic space (Montreal Institute of Neurology). Hotter color (yellow) indicates higher p-values (see color-scale). Values below slices indicate z-coordinates in stereotactic space.

[10] Fig. 6.2b was produced using the MRI3dx software, which was kindly provided by K. Singh (see http://www.liv.ac.uk/mariarc/mri3dX/index.html).

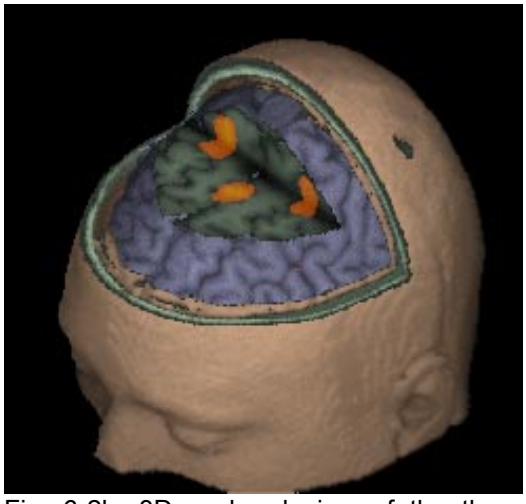

Fig. 6-2b: 3D-rendered view of the three premotor/precentral gyrus activity clusters. A slightly lower threshold was used in order to achieve a better visualization of the spatial extent of the activity clusters.

cluster in medial superior frontal gyrus were located in an area classifiable as rostral supplementary motor area or pre-SMA as opposed to SMA-proper (Roland & Zilles, 1996; Matsuzaka et al., 1992). Activity also partially extended into the anterior cingulate. In addition, a number of anatomical regions were above threshold in either a single or a few maps only. These included gyrus lingualis, gyrus orbitofrontalis, posterior parts of gyrus temporalis inferioris, thalamus, and primary motor cortex.

Table 6-2: Neuroanatomical localization, stereotactic coordinates (local maximum voxel), Brodmann area (BA) and consistency of significant fMRI activity clusters during task processing.

| | | *Coordinates* | | | |
|---|---|---|---|---|---|
| **Anatomical Brain Region** | **BA** | **x** | **y** | **z** | **Consistency** |
| L Occipital | 18/19 | -26 | -82 | 2 | 13/13 |
| R Occipital | 18/19 | 38 | -78 | 6 | 13/13 |
| L Superior Parietal | 7 | -24 | -58 | 52 | 13/13 |
| R Superior Parietal | 7 | 22 | -64 | 54 | 13/13 |
| Medial superior frontal gyrus | 6 | 10 | 8 | 52 | 13/13 |
| L Precentral Gyrus | 6 | -28 | -10 | 64 | 13/13 |
| R Precentral Gyrus | 6 | 30 | -6 | 56 | 13/13 |
| L Dorsolateral Prefrontal Cortex | 9 | -48 | 4 | 28 | 13/13 |
| R Dorsolateral Prefrontal Cortex | 9 | 56 | 4 | 28 | 13/13 |
| L Insular Cortex | | 36 | 14 | 2 | 11/13 |
| R Insular Cortex | | -32 | 18 | 2 | 11/13 |

In order to assess the onset and time course of the hemodynamic response function, signal time courses of selected active pixels were plotted. After stimulus onset, the hemodynamic response showed a delayed, but fairly constant increase with processing time and a peak around one to five seconds after task completion. Most importantly, the onset and the time-course of the signal increase in lateral and medial premotor regions were very similar to those in parietal regions (see Fig. 6-3).

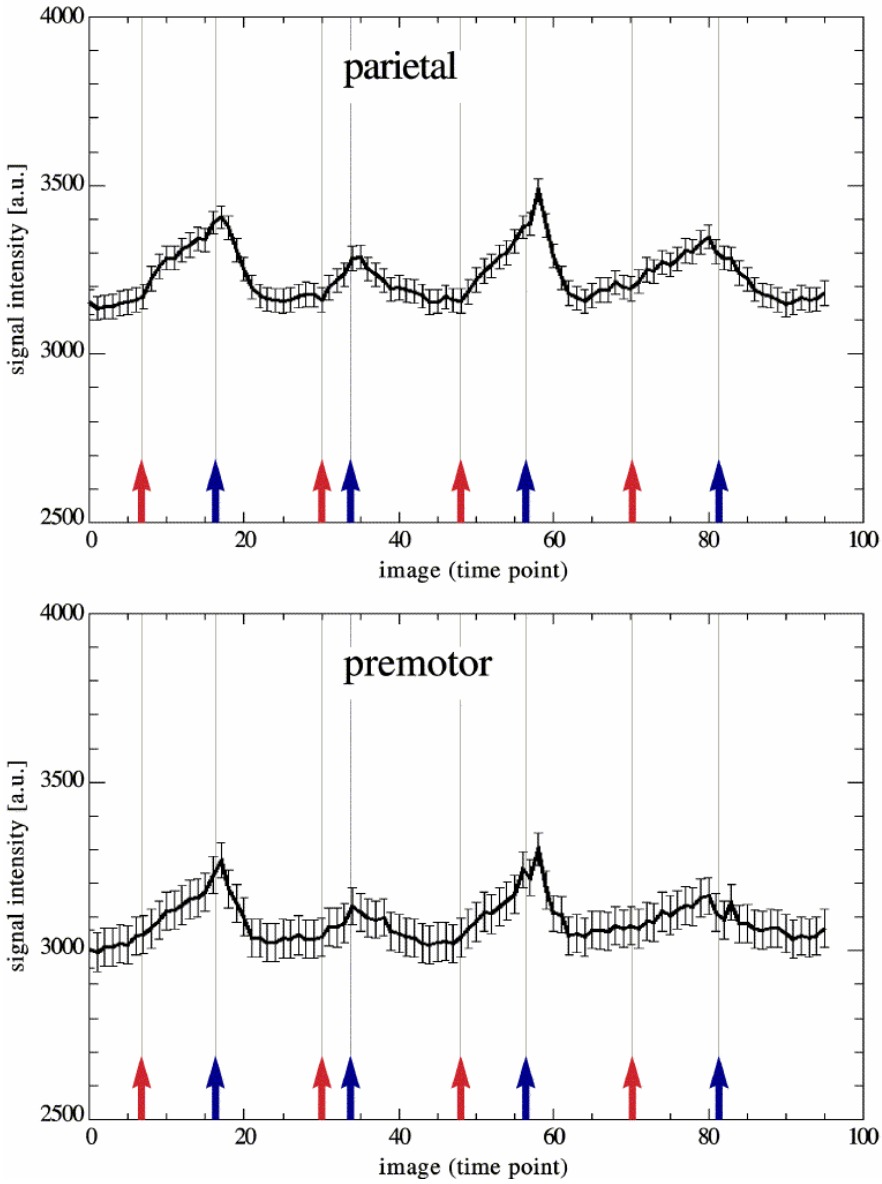


Fig. 6-3: Changes in signal intensity (arbitrary units, mean ± S.E.) of one subject for selected parietal and premotor pixels contingent to task processing and task completion. Task presentation and task completion are marked by red and blue arrows, respectively. Note the almost identical onset and peak time of signal increase for the two brain regions.

### 6.3.3 SCPs

The presentation of the task stimulus evoked a N100-like negative phasic ERP peaking around 120 ms which was focally localized over the occipito-parietal scalp. This component was followed by a phasic positive, P300-like deflection peaking at around 350 ms with a broadly distributed topography and a maximum

Table 6-3: Areas and consistency of significant SCP activity during task processing. *: instead of a clear medial fronto-central current sink, three of the subjects showed two medial bilateral current sinks over the fronto-central region.

| **Scalp region** | **Consistency** |
|---|---|
| L occipital | 12/13 |
| R occipital | 12/13 |
| L parietal | 13/13 |
| R parietal | 12/13 |
| L fronto-central | 13/13 |
| R fronto-central | 13/13 |
| Medial fronto-central | 10(13*)/13 |
| L fronto-lateral | 11/13 |
| R fronto-lateral | 11/13 |

at medio-central recording sites. Following these transient potentials, sustained negative SCPs consistently developed over occipital, parietal, lateral central and medial fronto-central regions, as well as less consistently over fronto-lateral regions. Visual inspection of waveforms suggested that negative SCPs started immediately following the P300-like component, i.e. around 550 ms for occipital and parietal and around 650 ms for central and fronto-central recording locations (see Fig. 6-4a). While the early phasic ERP components were not similar to fMRI results, SCPs indicated activity in similar regions as fMRI. The CSD maps (Fig. 6-5) showed focal current sinks over the parietal, the lateral central, the medial fronto-central and the lateral frontal region. Less focal activity was observed over the occipital scalp.

In order to assess task-related changes in slow potential amplitude independently of the early phasic potentials associated with task presentation and stimulus classification, the difference between SCP amplitude at latencies of five vs. one second after stimulus presentation was computed. This revealed that the highest increase in negativity occurred at the parietal leads (-15.97 μV for electrode Pz'), and that lateral central and fronto-central electrodes showed a smaller, but still considerable increase in slow potential amplitude (-10.79 μV for electrode Cz'; see also Fig. 6-4a). A number of electrodes showed negligible or positive amplitude changes (see electrodes M1 or Fp1, Fp2, respectively, in Fig. 6-4a).

Response-linked averages yielded an almost identical pattern of activity as stimulus-linked averages up to about 200-300 ms prior to the response. During this interval, a Bereitschaftspotential-like component was observed over the central region, and the current sink over the right lateral central region almost disappeared, while the current sink over the left hemisphere remained largely unchanged (see Figs. 6-4b and 6-5).

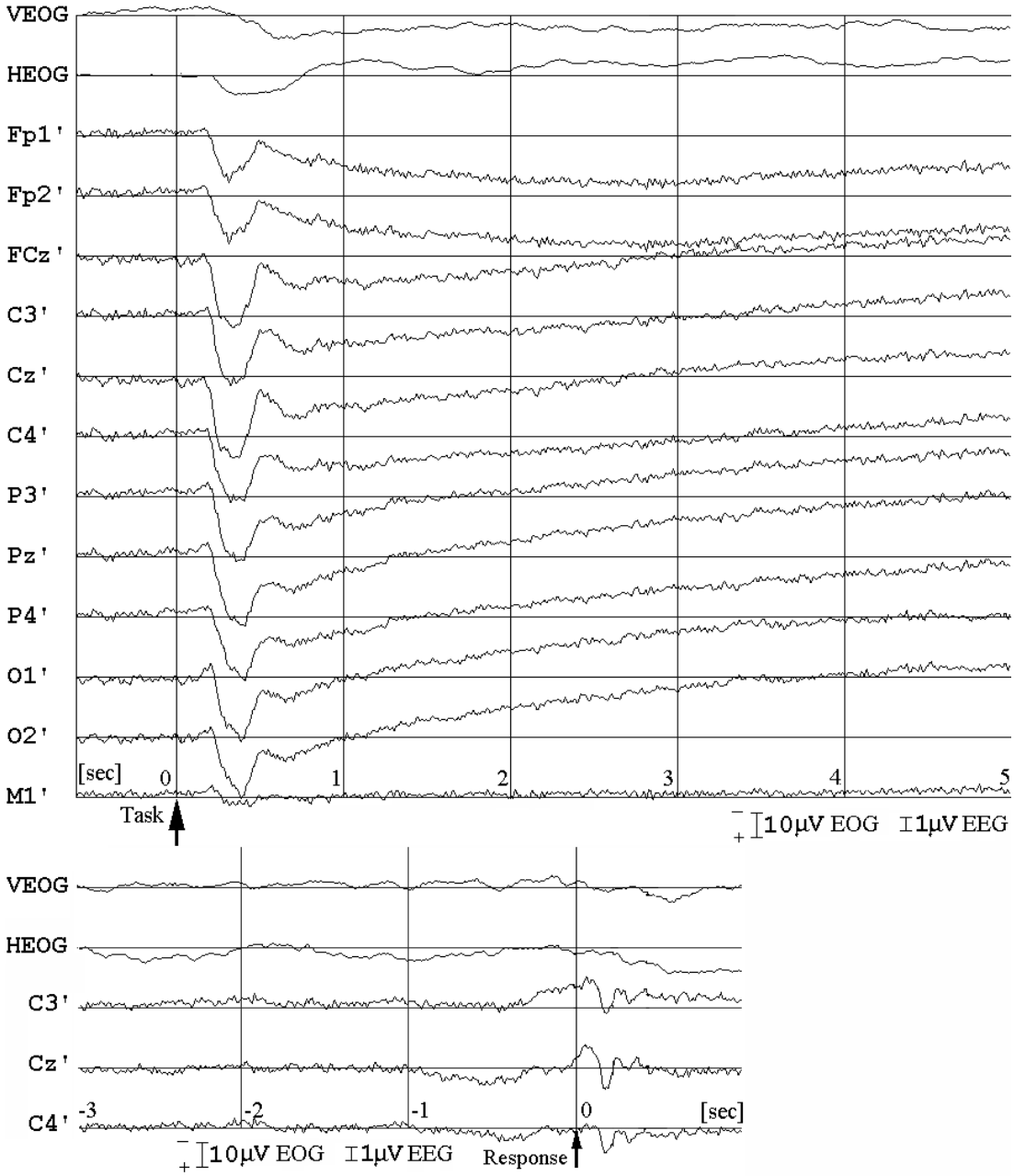


Fig. 6-4a: Stimulus-linked grand mean averaged SCP waveforms of selected channels showing task-related activity changes. Task presentation is marked by an arrow. Cartesian coordinates (x/y/z) of channels (standard 10-20 coordinates in brackets; Jaspers, 1958) were: Fp1': .76/.45/.47 (Fp1: .91/.29/.31), Fp2': .76/-.44/.48 (Fp1: .91/-.29/.31), FCz': .35/-.03/.94 (Fz: .59/0/.81), C3': .09/.43/.9 (C3: 0/.59/.81), Cz': .09/-.02/1 (Cz: 0/0/1), C4': .07/-.48/.88 (C4: 0/-.59/.81), P3': -.47/.43/.77 (P3: -.58/.46/.67), Pz': -.51/-.01/.86 (Pz: -.59/0/.81), P4': -.48/-.45/.75 (P4: -.58/-.46/.67), O1': -.71/.3/.63 (O1: -0.91/.29/.31), O2': -0.71/-.32/.63 (O2: -0.91/-.29/.31); electrode M1 was placed on the left mastoid.
Fig. 6-4b: Response-linked grand mean averaged SCP waveforms of electrodes C3', Cz' and C4' reflecting SCP lateralization immediately before task completion via button pressing (arrow).

Coregistration of SCP electrodes and structural brain images showed that on the average electrodes C3' and C4' were positioned 4.4 and 4.2 cm anterior to

the lateral central sulcus and the electrode Cz' and FCz' were located 5.4 cm and 8.6 cm anterior to the medial central sulcus.

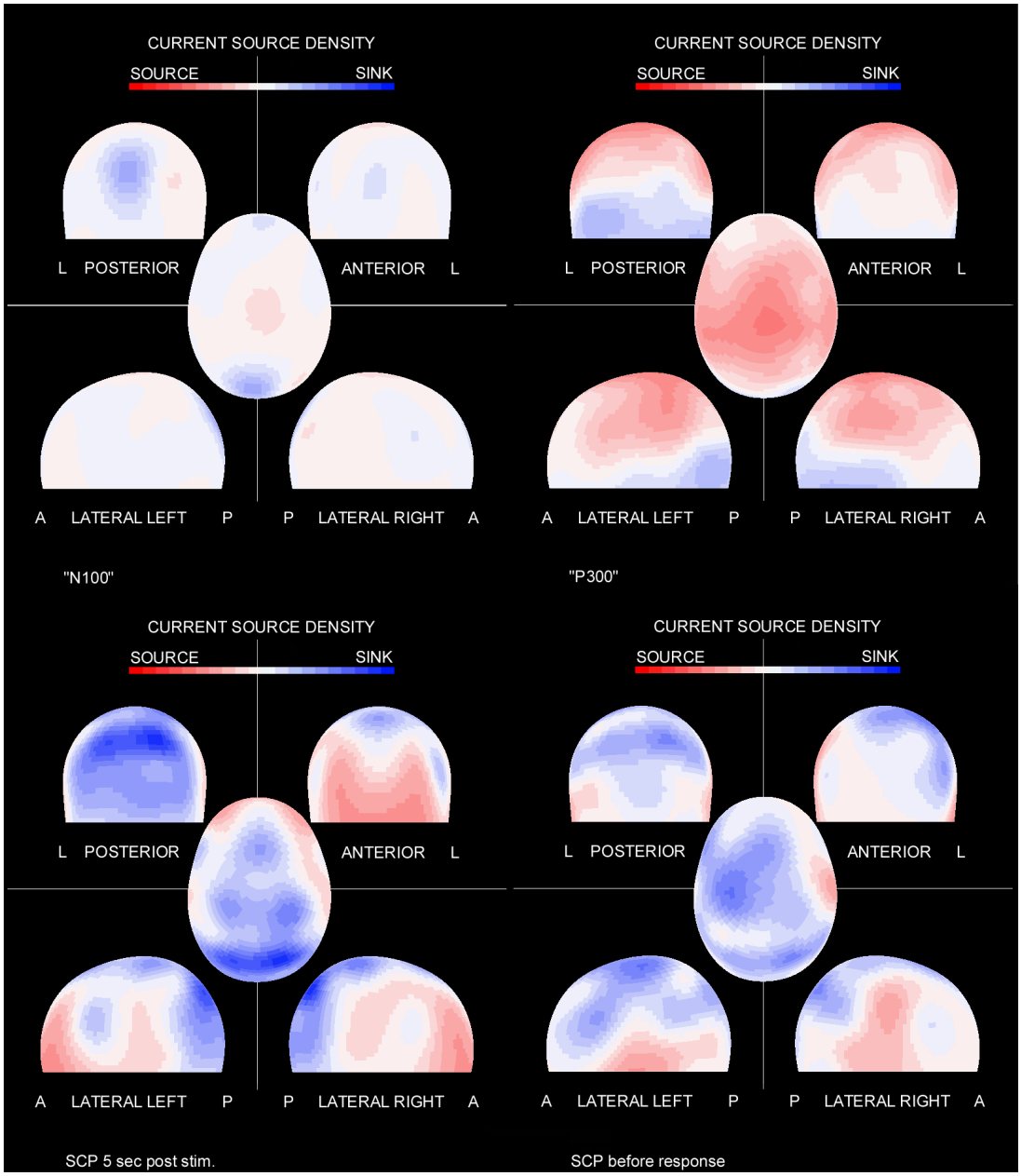


Fig. 6-5: Color-coded grand mean CSD-maps 120 ms after task presentation, 350 ms after task presentation, five seconds after task presentation, and before response execution. Current sources are coded in red and current sinks are coded in blue. Note the similarity of the SCP and of the fMRI map (Fig. 6-2). Activity in parietal cortex is clearly indicated, and the three distinct focal current sinks over the central region are most likely related to activity in premotor structures.

## *6.4 Discussion*

### 6.4.1 Validity of results

Prior to a detailed evaluation of the observed spatio-temporal activity patterns, a few methodological issues regarding the validity of the results should be discussed.

*fMRI*

It was decided to analyze fMRI data using parametric statistics. The application of non-parametric statistics in the analysis of brain images has been repeatedly suggested as a more valid alternative (see, e.g., Holmes et al., 1996) with the main intention to avoid the approximations and assumptions with respect to probability distributions of parametric statistics. Violations of these assumptions might lead to noisy and only approximately valid statistic maps. However, several observations make us believe that the statistical analysis employed in this study yielded valid results.

First, it has been argued that the main reason for violations of the distributional assumptions of parametric statistics are a low number of scans and subjects. In the present study, a comparably high number of subjects (see, e.g., Vitouch & Glück, 1997, for a comparison of the sample sizes of neuroimaging studies) was investigated. Also, single-trial analysis and a calculation of a statistical map for every trial in every subject was performed, leading to a total number of about 550 single-trial results in thirteen subjects that were used for analysis. Second, a re-analysis of the data with an exploratory data analysis technique (fuzzy cluster analysis; Windischberger et al., 2000) indicated activity in very similar regions as the parametric analysis performed here. Third, the combination of SCPs and fMRI yielded a mutual corroboration of results (wich was, however, restricted to cortical activity).

Another topic which is heavily discussed in the statistical analysis of brain imaging data is related to the thresholding of statistical maps. However, the decision how this thresholding should be performed in order to separate „true“ from „false“ activity is not trivial. In addition, conversion of statistics to probability values that are corrected for multiple comparisons is not straightforward. Several approaches have been conceived to solve this problem. On the one hand, it would be feasible to use no inference statistics at all (i.e., no reference to p-values), but to infer „significance“ from a thorough descriptive analysis of images only. How-

ever, this does not circumvent the problem that images have to be thresholded in a certain way – either implicitly by the researcher who decides which descriptive statistic is indicative of activity and which is not, or by the rather arbitrary selection of a threshold. More frequently, p-values are corrected for multiple comparisons (either using Bonferroni-correction or the framework of random Gaussian fields, as implemented in SPM). In this study, a rather high threshold level (p=.00001) was chosen, and no correction for multiple comparisons was performed. Strong hypotheses existed that there is task-related activity in several regions of the brain (with evidence coming both from previously published fMRI studies, previous SCP experiments - e.g., Lamm et al., 1999 - and the SCP data acquired in this study). In the case of such a-priori hypotheses, Bonferroni-correction is known to be overly conservative and was therefore not applied. In addition, it has to be noted that the spatial extent of the activity clusters (especially in parietal and lateral premotor cortex) observed in this study was rather large. Although it is possible that single voxels were falsely indicated as being active, it is highly unlikely that all voxels in these large active areas are false positives. Hence, although single "significant" voxels might not reflect true activity, the main inference that there is activity in parietal and premotor regions during task-processing seems to be well-justified.

*SCPs*

It has been shown repeatedly that SCP topographies are modality- and task-specific (see Rösler et al., 1997; Bauer, 1998, for recent reviews), and both time course and surface location showed a close correlation with simultaneously recorded single cell activity in the mammalian cortex (Caspers et al., 1980). Good correspondence with SPECT-measures of regional cerebral blood flow (rCBF) was also observed, with the scalp maximum of SCPs being located over those areas where maximal increase in rCBF was observed (Lang et al., 1988). SCPs thus reveal information about cognition-related cortical activity with the moderate spatial resolution typical for surface recordings.

In this study, the gross neuroanatomical regions generating surface SCPs were inferred from inspection of event-related SCP waveforms as well as SCP and CSD maps. Information provided by fMRI was then used to relate surface activity to distinct cortical activity spots, which was performed for individual activity maps and for the grand mean. This might be compared to the approach of Scherg & Goebel (1998) who used fMRI activity clusters as seeding points in dipole modeling, with the aim to assess the time-course of activity in cortical structures identi-

fied by fMRI. Nevertheless, it might be questioned whether the assignment of topographically recorded activity to cortical structures was valid in the present study. An answer to this question is especially important for the lateral central and the medial central activity. One might, for instance, hypothesize that SCPs over these regions were due to volume conducted activity originating in parietal cortex.

There are several arguments which make it plausible that the observed SCPs were indeed generated in motor structures and that their time-course can thus also be assigned to these structures. The similarity in the grand mean and in the individual subject fMRI and CSD maps is intriguing. Maps of both methods are dominated by widespread parietal activity, and by three rather focal activity clusters rostral to the central sulcus (see Figs. 6-2 and 6-5). Thus, if the SCP activity pattern were interpreted as an artifact, this argument had to apply to the parietal and to the lateral and medial fronto-central activity. However, the fact that dynamic visuo-spatial imagery is accompanied by parieto-occipital SCPs is well established (Rösler et al., 1995; Bajric et al., 1999; Lamm et al., 1999; Ruchkin et al., 1991; Wijers et al., 1989). Also, fronto-central current sinks distinct from the parietal current sinks in the grand mean map as well as in almost all single subjects were observed (see Table 6-2). This observation is somewhat incompatible with the explanation that parietal activity extended into central and frontal leads since it is well documented empirically and theoretically that Laplacian transformation of surface potentials greatly reduces or eliminates such effects (Nunez et al., 1989; Nunez et al., 1994; Babiloni et al., 1996; Srinivasan et al., 1996). Another important argument comes from the comparison of stimulus- and response-linked averages. It seems very plausible that the left-lateralized activity immediately before response reflects activity of motor areas related to button pressing with the right hand. Activity patterns similar to the one observed in this study were repeatedly observed in studies of finger movements using ERPs/SCPs (Cui et al., 1999; Gerloff et al., 1996; Ball et al., 1999). Since the position of the left lateral current sink and of the medial fronto-central sink did not considerably change in position compared to the stimulus-linked map (see Fig. 6-5), it seems plausible that the lateral and medial SCPs of fronto-central leads reflect cortical activity generated in cortical motor areas. Due to interindividual variability in functional and structural anatomy as well as the rather complicated gyrification and associated surface projection of activity of the human motor cortex, it is, however, more difficult to ascertain whether these SCPs were generated in premotor or in primary motor cortex. Yet, several observations suggest that the SCP generators were located in premotor rather than in primary motor cortex.

The main argument is based on the coregistration of SCP electrodes and structural brain images which showed that the central electrodes C3' and C4' were positioned about 4 cm anterior to lateral central sulcus. Although the two distinct current sinks over the lateral central region were located about 1-1.5 cm behind these coordinates, this would still correspond (if radial projection of the activity to the surface is assumed) to a generator structure located clearly anterior to the central sulcus. Another argument is based on the observation that no significant task-related activity in primary motor cortex was identified using fMRI. Although the generators of SCP and fMRI activity might be quite different in principle, the high correspondence of activity in other brain regions doesn't render it very plausible that there should be an isolated mismatch in activity only for the motor region. Nevertheless, additional studies employing a higher sampling of scalp potentials over the central to pre-central region might be required to obtain a definite answer to this question.

Another issue sometimes discussed with SCPs are slow linear or non-linear signal drifts. Although, of course, one might never exclude the possibility that parts of the signal might contain residual drift, the topographies observed in this study cannot be explained by drift artifacts. A general amplifier drift affecting all electrodes is highly unlikely because of the high baseline stability of the amplifier. General or uniform drift can also be excluded because then, different electrodes would not show different amplitude changes. This was, however, the case, with several electrodes not showing any amplitude change at all (see Fig. 6-4a). It is also unlikely that only parts of the channels were specifically affected by drift artifacts, because similar topographies were observed in all subjects. Since assignment of electrodes to recording locations was randomly permuted across subjects, this fact could only be explained by assuming that some amplifier channels drifted during the whole study which was, however, not the case. Also, topographies such as those observed in this study were repeatedly observed in previous experiments in using the same task material (Lamm et al., 1999, 2000; Vitouch et al., 1997). Thus, the argument that SCP topographies were due to drift can be rejected.

### 6.4.2 Functional neuroanatomy of dynamic visuo-spatial imagery

In the recent literature on functional neuoroimaging some controversy has arisen as to whether or not dynamic visuo-spatial imagery is associated with activity in higher-order human motor areas. Although behavioral studies and theoretical accounts of the phenomenon of mental rotation suggest premotor cortex involve-

ment, two recent PET studies (Kosslyn et al., 1998; Harris et al., 2000) and the latest fMRI study (Jordan et al., 2001) did not detect any such activity. On the other hand, premotor activity has repeatedly been shown using fMRI (e.g., Richter et al., 2000; Cohen et al., 1996; Tagaris et al., 1998), although not always in all of the subjects investigated. A major aim of the present study has been to assess premotor activity during processing of a visuo-spatial imagery task using two complementary brain imaging methods.

The results clearly support the hypothesis that premotor cortex is active during task processing. fMRI provided a precise three-dimensional localization of task-related activities in a distributed network consisting of occipital, parietal, dorso-lateral prefrontal, anterior insular cortex, and lateral and medial premotor cortex. As Table 6-2 shows, these activities were highly consistent between subjects. The SCP results were very comparable to the fMRI results. Despite the lower spatial resolution of SCPs, activity was also indicated in occipital, parietal and lateral frontal regions. Over the central region, CSD maps revealed three clearly separable current sinks, showing a similar activity pattern as fMRI. Although for a number of reasons the ability to localize focal brain activity with surface recordings is inherently limited, the position of the central and pre-central electrodes clearly suggests that this activity originated in the premotor rather than the primary motor cortex. This is also corroborated by the response-linked average showing a Bereitschaftspotential-like component which is known to reflect activity in premotor structures (see, e.g., Cui et al., 1999; Gerloff et al., 1996; Ball et al., 1999).

A very early onset of processing around 650 ms was revealed by the steady increase in relative SCP negativity starting around this time. This onset was similar to that for the occipito-parietal leads. However, it must be noted that the *measured* potentials became negative only around two to three seconds after task presentation. As demonstrated by Heil et al. (1996; see also Bajric et al., 1999), this seems to be due to a superposition of potentials associated with character recognition and classification, which evoke a slow positive deflection of considerable amplitude, and of a slow negative potential with lower amplitude related to mental rotation/object transformation. As a result of this superposition and the lower relative amplitude of the negative potential component, the measured potential became negative only after a delay of about one to two seconds.

Similar to the parietal cortex, the premotor cortex was active during the entire interval of task processing. This was indicated by the time-course of SCPs and of fMRI signal changes. Thus it seems likely that premotor activity is directly re-

lated to task processing and not only to peripheral aspects of the task, an interpretation that is also suggested by the time-resolved analysis of Richter et al. (2000). Although exact response times were rarely reported in earlier studies investigating mental rotation, they were rather low, ranging from approximately 1.5 s (Tagaris et al., 1998) to 4 s (Carpenter et al., 1999) or 6 s (Richter et al., 2000). Even in the latter two studies, tasks with a low angular disparity between objects could be answered within one to two seconds. Several studies investigating single finger movements (Cunnington et al., 1999; Richter et al., 1997; Humberstone et al., 1997) revealed signal increases in premotor and primary motor cortex around three second before to one second after movement onset. Hence, premotor activity in earlier studies might have been interpreted as reflecting the anticipation, preparation and execution of finger movements for task answering. This interpretation can be excluded by the present study in which response times of approximately sixteen and twelve seconds were obtained.

Based on earlier PET and fMRI studies, it may be argued that premotor blood flow or oxygenation increases during metal rotation are due to increased activity of inhibitory rather than excitatory neurons. This explanation can now be ruled out, since SCPs provide a more direct assessment of neural activity than hemodynamic indicators of activity (with negative SCPs indicating an increase and positive SCPs indicating a decrease in neural activity in almost all cases). In particular, there is general agreement that - with some rare exceptions- surface negative changes in SCP amplitude relative to a pre-stimulus baseline indicate an increase in excitatory postsynaptic potentials (EPSPs) of apical cortical dendrites, while positive SCPs are related to decreased input to these dendrites and/or an increase in inhibitory PSPs (Bauer, 1998; Rösler *et al.*, 1997; Birbaumer *et al.*, 1990).

As in all tasks requiring dynamic visuo-spatial imagery, the subjects had to visually scan spatial objects via movements of their eyes. As demonstrated by a considerable number of PET and fMRI studies, saccade execution and preparation as well as foveal fixation lead to activity in brain areas very similar to those active in this study (see, e.g., Anderson et al., 1994; Perry & Zeki, 2000; Petit et al., 1999; Petit & Haxby, 1999). The same applies to visuo-spatial attention, which is also required in visuo-spatial imagery where attention has to be shifted towards specific salient features of the visuo-spatial stimuli (see, e.g., Corbetta et al., 1998; Corbetta, 1998; Nobre et al., 1997, 2000). Recent intracortical recordings of activity in human frontal eye fields (FEFs) have also shown responses to extrafoveally and foveally presented stimuli in the FEF even though saccadic eye movements had to be suppressed (Blanke et al., 1999). While foveal fixation can vastly be

ruled out as an explanation for parietal and premotor activity in the present study since subjects had to fixate a crosshair during the pre-stimulus epoch, part of the activity observed might be related to oculomotor scanning and visuo-spatial attention.

However, several arguments suggest that this activity cannot be exclusively related to such processes. Although the lateral premotor activity clusters in the present study partially extended into the regions known as the frontal eye fields (FEF), stereotactic coordinates of the FEFs, as well as of the overlapping regions active during covert attention, are different from the activity maxima observed in the present study (see, e.g., Paus, 1996, and the recent review by Petit et al*.,* 1999a, which reports mean coordinates of 36/-9/45 for the left FEF and of -35/-11/46 for the right FEF, respectively). In addition, the spatial extent of activity clusters related to eye movements usually is much smaller than that observed in this study in which a rather large part of the lateral precentral gyrus was active. A similar argument applies to the parietal areas where activity related to eye-movements is mainly confined to intraparietal sulcus. Furthermore, a recent fMRI study by Carpenter et al. (1999) specifically addressed the issue of how much of the activity during visuo-spatial imagery can be attributed to saccadic eye movements. The authors contrasted a mental rotation task with a task requiring continuous saccadic scanning of a two-dimensional grid. Although the latter also evoked significant activity in similar parietal and premotor regions as mental rotation, both the amplitude and the spatial extent of this activity were considerably smaller than during mental rotation. Thus, even though there may be overlap between activity related to oculomotor processing and visuo-spatial attention on the one hand and dynamic visuo-spatial imagery on the other, it may be concluded that the latter evokes additional neural processing in both parietal and lateral premotor areas.

A more complicated picture, however, arises for the medial premotor activity. The SMA coordinates related to eye movements and visuo-spatial attention reported by, e.g., Perry & Zeki (2000) or Corbetta et al. (1998), were located much more anterior. On the other hand, several studies (Nobre et al. (2000), Anderson et al*.,* 1990, Petit et al., 1999b; O'Driscoll et al., 2000) report more posterior coordinates. SMA activity in this study might also be related to working memory demands, as Petit et al. (1998) have shown activity in a similar region during memorization of spatial patterns. As for the activity in insular cortex, no study has reported activity in this area during mental rotation of 3D-geometrical objects so far. However, it seems well established that the insular cortex is involved in the control

of eye movements. Thus, whether insular activity is related to task-relevant processing or only to eye-movement control remains to be investigated.

### 6.4.3 Functional equivalence of overt and covert object manipulation

The observation that overt and mental object manipulation share common processing constraints implies that similar or identical brain structures should be active in both processes (Pellizzer & Georgopoulos, 1993; Georgopoulos & Pellizzer, 1995; Wohlschläger & Wohlschläger, 1998; Wexler et al., 1998). Regarding the present results and earlier findings, one might speculate as to the reasons for premotor involvement in a task which does not require continuous motor execution. Activity might be related to motor imagery and associated kinesthetic feelings of limb or body movements (Jeannerod, 1994; Lotze et al., 1999; Porro et al., 1996; Pfurtscheller & Neuper, 1997). However, this would imply that subjects solved the tasks from an internal perspective. This is in contrast to introspective reports of the investigated subjects who neither reported imagining themselves moving the cubes nor moving themselves around the cubes. Likewise in informal discussions with subjects during experimental debriefing, no subject reported imagining their hand(s) or other body parts tilting or rotating the cubes.

Wexler et al. (1998) suggested that the specific interactions of manual and mental rotation showed that mental rotation involves covert simulation of motor rotation. This would imply mechanisms of visuo-motor anticipation, i.e. mechanisms which allow the observer to anticipate the visual consequences of a motor action. A large reciprocally connected neo-cortical network involving parietal (BA 7) and premotor areas (BA 6) is thought to be essential for planning and control of movements and anticipation of their consequences. This might explain the very similar time-courses of activity in these structures in the present study (Jeannerod, 1994; Johnson et al., 1996; Andersen et al., 1997).

Another explanation of parietal and premotor activity might be that it is related to the observation of the rotational movement of the cubes. Several behavioral studies demonstrated interference between perception of rotary motion and mental rotation (the so-called rotation aftereffect; Corballis & Corballis, 1993; Corballis & McLaren, 1982). In fact, there is some evidence that the observation of human movements and gestures is accompanied by activity in premotor areas (see Decety & Grèces, 1999, for a recent review). Also, mirror neurons of primary-motor neurons have been detected in the rostral part of ventral premotor cortex (area F5) of the macaque monkey which are active during the observation of ex-

traneous movements (Rizzolatti & Arbib, 1998). However, it remains to be shown whether these findings are transferable to the merely imagined observation of movements of a non-living object, since a recent fMRI study (Barnes et al., 2000) did not find activity in premotor regions when subjects passively observed the rotation of Shepard-Metzler figures.

The "simulation" and the "observation" approach might partially explain the occurrence of premotor activity during dynamic visuo-spatial imagery. However, neither approach considers the fact that mental rotation is not the only process required when two visuo-spatial objects are compared. Several other processes (object encoding, mental image generation, stimulus matching) are equally important. These processes do neither include anticipation nor observation of movements. A separation of these different task aspects is difficult both with the task paradigm used in this study as well as with Shepard-Metzler figures. Nevertheless, the early onset of premotor SCPs, their continuous increase until task response, as well as the early onset of the hemodynamic response in premotor cortex observed in the present study, and in the time-resolved fMRI study by Richter et al. (2000), suggest that premotor cortex is also active during visuo-perceptual analysis, mental image generation and object matching.

Thus another feasible, but rather speculative account for the involvement of premotor cortex in dynamic visuo-spatial imagery is that motor structures are activated whenever extended visuo-spatial information processing is required. Just as perception and imagery are tightly coupled and show a vast overlap in the brain regions supporting their functions (see Kosslyn, 1994, for extensive review and evidence), this might also apply to motor actions and spatial processing. The tight relationship between motion and space becomes specifically evident in the ontogenetical development of mammals. There, action and spatial perception are coupled inseparably since there is no perception of space without movements and no movement without feedback about the spatial aspects of the movement. The hypothesis that spatial perception and imagery per se activate premotor structures is supported by two recent fMRI studies of visuo-spatial processing and the recognition of 3D-objects. Shen et al. (1999) asked subjects to compare the spatial location of sequentially presented simple geometrical objects. They found activity in premotor structures although the task required no concurrent motor output. Sugio et al. (1999) detected activity in medial and lateral BA 6 when asking subjects to identify objects presented in non-canonical orientations.

However, these results like those of all of the mental-rotation experiments so far only indicate that there is a *correlation* between visuo-spatial processing and

activity in higher-order motor areas. They do not provide a direct explanation or assessment of the specific role or function of these areas in visuo-spatial imagery and perception. For example, one cannot be certain that these regions are functionally relevant for the visuo-spatial transformations initiated by the tasks. It could well be that they do not have a specific functional role in task processing and are only co-activated by default (e.g., because objects that can be grabbed are presented, which, in the monkey, activates ventral premotor cortex even if no subsequent grasping movement is required; Murata et al., 1997; Rizzolatti et al., 1988).

For now, however, it can be concluded that visuo-spatial imagery consistently recruits a distributed network of cortical structures including the premotor cortex. Further experiments that separate visuo-perceptual analysis of objects, visual mental image generation and buffering, mental rotation and object matching, and that vary the amount of dynamic and static visuo-spatial information processing required are necessary to assess the functional role of premotor activity more specifically.

## *7. Individual differences in brain activity during dynamic visuo-spatial imagery*

**Abstract**

*A considerable number of PET and EEG studies has revealed ability- and intelligence-related individual differences in brain activity. For example, Vitouch et al. (1997) and Lamm et al. (1999) demonstrated that processing of a dynamic visuo-spatial imagery task evoked higher negative SCP amplitudes over the posterior and medial fronto-central scalp in subjects with low than in subjects with high visuo-spatial ability. This has been interpreted in the sense of a "neural efficiency" hypothesis which supposes that more intelligent or proficient subjects process information more efficiently than less intelligent or proficient subjects. In order to test two alternative hypotheses concerning the neuro-functional bases of this more efficient neural processing, a replication study was performed in which brain activity of subjects with good and poor visuo-spatial ability was investigated using SCPs and fMRI. In order to achieve a higher spatial resolution than in the former studies, SCPs were recorded from 40 EEG channels, and topographic maps were calculated using individual electrode coordinates and realistic head models. fMRI scanning was used to get more detailed and more direct information about the location of neural activity. The group-independent results of both imaging techniques were highly consistent with those of other studies. Activity in occipital, parietal, lateral premotor, medial premotor and dorso-lateral prefrontal cortex was revealed. However, both methods failed to reveal differences in activity between groups. Thus, the hypothesis that subjects with higher task-specific show more efficient neural processing was not supported by this study.*

### *7.1 Background*

The investigation of the neural bases of individual differences does not only promise a better understanding of the brain mechanisms which allow us to master tasks of enormous complexity. It might also provide important insights into how and why individual differences arise, and how they are embodied in our brains. This information can be useful in the training of individuals with lower abilities (for example by designing training programs which are tailored to an individual's neural processing strategy), but also in making already competent individuals even more competent.

However, revealing individual differences in functional neuroanatomy which are related to individual differences on the behavioral level is not an easy task. The probably best example for the difficulties encountered in this area of research are gender-related differences in brain processing. Despite the more than obvious (biological and behavioral) differences between genders, evidence relating these differences to neural processing is still rather sparse and far from consistent. This might have several reasons. The currently available neuroimaging techniques might not be sensitive enough to detect the relevant neural differences (e.g. because they take place at a neural scale that is not (yet) accessible via the still dominant "localizationist" approach of most techniques). Also, the large amount of general interindividual variability in behavioral measures might obscure individual differences related to the membership to a certain group of individuals (gender, ability etc.). This is again exemplified in gender-related differences in visuo-spatial and verbal ability. Although it seems well-established that females generally perform better in verbal and worse in visuo-spatial tasks, interindividual differences within genders are still much higher (about 1-2 standard deviations) than between genders (about 0.5 standard deviations for spatial ability; see, e.g., Voyer et al., 1993).

Nevertheless, a number of studies has demonstrated differences in neural processing related to differences in task performance, ability or IQ score[11]. One of the first studies was published by Ertl & Schafer (1969), who correlated psychometric scores of intelligence with event-related potential measures and found less "neural activity" in subjects with high IQ scores. This has been interpreted in the sense of a "neural efficiency hypothesis", claiming that high-IQ subjects show more efficient neural processing. Although this study and the activity indices calculated by Ertl & Schafer have been harshly criticized (see, e.g., Verleger, 1999), and although a number of subsequent studies did not find any consistent or only a negligible correlation between EEG-derived measures and psychometric intelligence (e.g., Vogel et al., 1987), some PET, EEG and slow-cortical potential (SCP) studies have led to revitalized speculations about the concept of neural efficiency.

In the PET studies, regional glucose metabolism rate (rGMR) measured via 18-fluor-deoxyglucose (18-FDG) PET was correlated with psychometric intelli-

[11] However, when taking into account the phenomenon of publication bias, it might be that a much higher number of studies failed to reveal such differences. Publication bias describes the phenomenon that significant results have a higher chance of being published than studies which did not confirm their initial hypotheses. It is assumed that this results from the higher skepticism of scientific referees and journal editors towards insignificant results, as well as from their tendency to assign less appeal to such studies. It also seems that "null results" are rarely written up by the researchers, which partly follows from the higher probability of getting such reports rejected.

gence. The main finding was that rGMR during task performance negatively correlated with intelligence, i.e. that subjects with a higher IQ score showed less glucose consumption during task solving (Haier et al., 1988; Haier, 1993; Parks et al., 1988). This finding, however, could not be replicated in another PET study by the Haier group. Surprisingly, no correlation at all was observed in females, while males displayed a positive correlation between rGMR during task solving and IQ (Haier & Benbow, 1995). On the other hand, a similar pattern of results as in the first studies was observed when subjects were PET scanned before and after a training period. It was observed that the amount of improvement in task performance negatively correlated with rGMR (Haier et al., 1992). Unfortunately, the validity of these results is somehow restricted since no control group was investigated, and since subjects who showed a higher increase in performance might have changed their task-solving strategy (see also Lamm et al., 1996, 1997).

The neural efficiency hypothesis also received partial support by several EEG studies. In a recent study, generally lower brain activation (defined in terms of spectral power) during target shooting was observed in skilled marksmen compared to novice shooters (Haufler et al., 2000). Using the method of event-related desynchronization (ERD), Neubauer et al. (1995) showed that solving of the sentence verification task (a so-called elementary cognitive task; Carpenter & Just, 1975) was accompanied by a lower amount of ERD in subjects who had higher scores in an abstract reasoning test (used to assess psychometric intelligence). In a replication study with another elementary cognitive task (Posner's letter matching task; Posner & Mitchell, 1967), Neubauer et al. (1999) observed that this difference was modulated by the complexity of the tasks. While no significant difference in ERD was observed for less complex letter comparisons, the results of the initial study were basically replicated when ERD during the more complex task variant was compared between subjects. This difference between task types was mainly attributable to a higher increase in ERD from the less complex to the more complex task in subjects with a lower reasoning score, while subjects with a higher score did display only small differences in ERD between task types.

Three recent reports using slow cortical potentials (SCPs) also support the neural efficiency hypothesis. Rösler et al. (1995) observed an ability-related difference in the amplitude of negative SCPs. Subjects who achieved higher scores in a 2-dimensional mental rotation task but were matched with respect to their IQ showed a lower SCP amplitude over the left parieto-temporo-occipital region. Two studies in the Brain Research Lab Vienna revealed similar results. Vitouch et al. (1997) and Lamm et al. (1999) compared SCPs of subjects with high vs. low

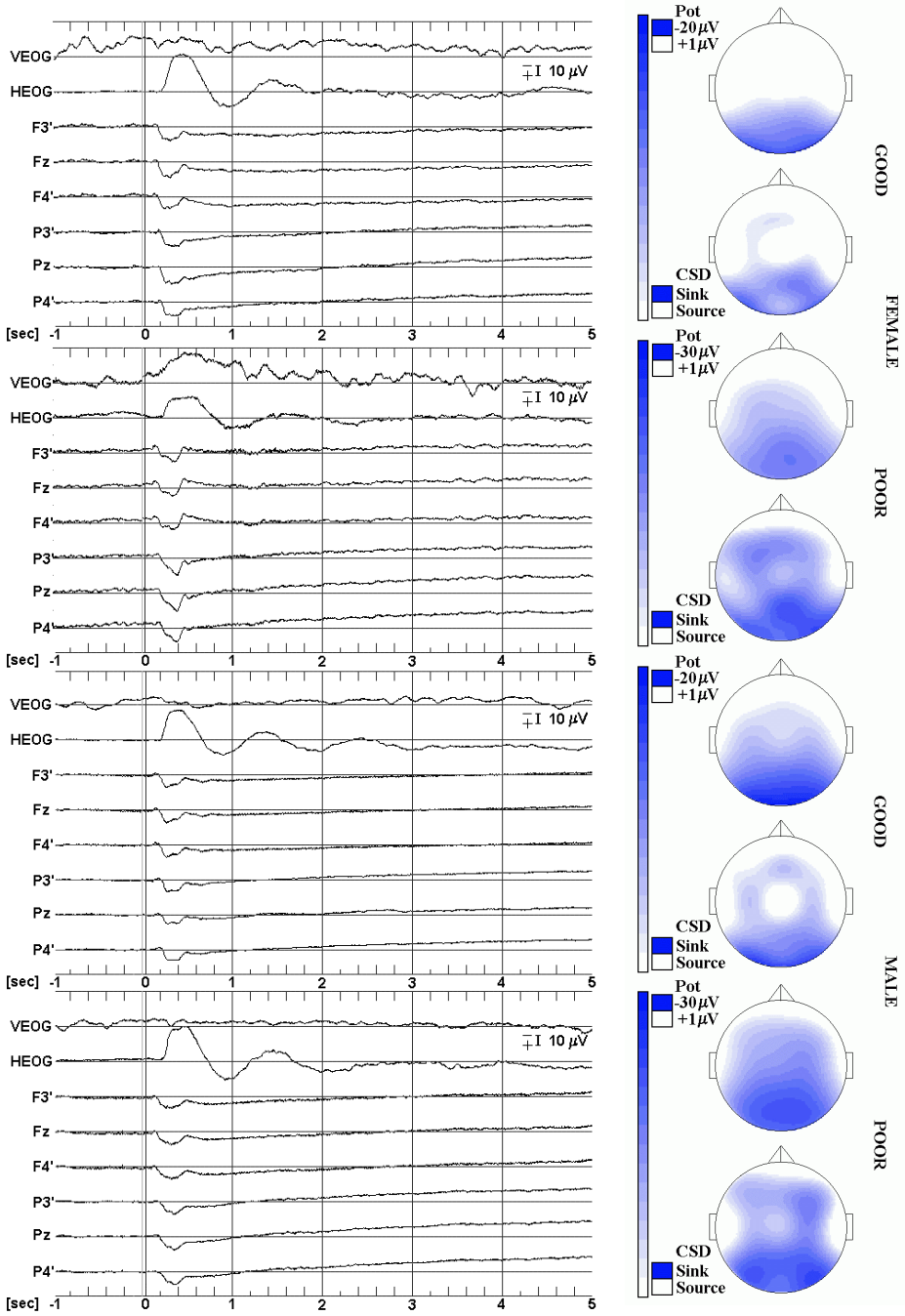


Fig. 7-1: Results of the study by Lamm et al. (1999). The figure shows SCP waveforms and SCP and CSD maps for good and poor male and female spatial test performers. Note the higher activity over the parieto-occipital and fronto-central scalp of poor performers (adapted from Lamm et al., 1999).

scores in a three-dimensional cube comparison test (3DC; Gittler, 1990). Negative SCPs of subjects with high visuo-spatial ability were considerably smaller than those of subjects with lower task-specific ability. This difference was topographically specific, since the highest difference in amplitude was observed over the parietal and medial fronto-central scalp region (see Fig. 7-1). In a control task re-

quiring verbal-analytic reasoning, no differences between groups (neither with respect to brain activity nor to performance scores) were observed. As in the study by Rösler, the differences in brain activity could not be explained by a difference in psychometric intelligence since the two groups were matched for their IQ. In addition, the observed differences between ability-groups completely disappeared when tasks were presented under time pressure (Lamm et al., 2001). Even though this result is contradictory to Neubauer et al. (1999) who observed higher between-subject differences in the more complex task condition, both results demonstrate a modulation of individual differences in brain activity by the amount of task demand or task complexity.

Although between-group differences in the brain regions recruited for task processing were also found in the studies cited above, their most striking result seems to be that the amount of brain activity in similar to identical areas was higher in subjects with lower ability or intelligence. This is somewhat in contrast to two results of a study of Gevins & Smith (2000) who investigated the relationship between several electrophysiological parameters (such as frontal midline theta and the amplitude and latency of the late positive component LPC) and the performance in a working memory task (spatial 'n-back' task). They observed that subjects with a higher general IQ (assessed by the revised Wechsler Adult Intelligence Scale, WAIS-R) showed a higher amplitude of the LPC and an enhanced amplitude in frontal midline theta (which might be interpreted as being contradictory to the neural efficiency hypothesis if assuming that both components are modulated by working memory demands). Interestingly, it was also observed that subjects with higher "verbal intelligence" showed greater use of the left parietal region, while subjects with higher scores in the "performance" subscale of the WAIS-R showed a right-hemispheric parietal asymmetry.

In sum, there exists some (partly inconsistent) evidence that higher IQ scores and better task performance are accompanied by a reduced amount of neural activity during task processing. Several hypotheses have been formulated to explain this correlation. Two of them are based on a consideration of developmental aspects. Haier (1993) has speculated that differences in synaptic pruning (i.e., the termination of abundant synapses and neurons; Huttenlocher, 1979) may cause the individual differences in brain activity. He hypothesized that brains of individuals with lower IQ show a failure in pruning, resulting in an insufficient reduction of redundant neural connections and, consequently, a less efficient brain organization. Miller (1995) assumed that differences in myelination constitute interindividual differences in intelligence, since brains with a higher degree of myeli-

nation should process and transmit information more rapidly. However, it should be noted that a higher speed of information transmission does not necessarily result in a higher quality or efficiency of information processing (since, to mention only one argument, the main computational load rather takes place at the synapses, with the action potential being only a messenger of the output of the synaptic area). Also, both Haier's and Miller's accounts can not explain the task-specific individual differences in SCPs when groups are matched for their general intelligence. Such an effect could only be explained if it was assumed that synaptic pruning or axonal myelination differ across brain regions.

Thus, alternative explanations are required to explain the higher cortical activity of subjects with low task-specific ability in the SCP studies. Two alternative but not mutually exclusive hypotheses shall be presented here. One of them explains the individual differences as a consequence of improved bottom-up processing and might be called the "perceptual analysis/sensory gating" hypothesis. The second main hypothesis relates the activity differences to differences in top-down processing and could be termed the "algorithmic efficiency" hypothesis.

The "perceptual analysis/sensory gating" hypothesis tries to explain the difference in parietal brain activity as a consequence of a better perceptual analysis and extraction of relevant spatial cues from the visuo-spatial stimuli in the more proficient subjects. This should lead to a smaller amount of spatial information that has to be computed by the parietal brain "modules" (which seem to be responsible for the main amount of spatial information processing), and should consequently be reflected in a lower amount of cortical activity in these areas. There are two candidate structures which might be responsible for this supposedly better visuo-perceptual analysis. One is the primary and secondary visual cortex (areas V1 and V2; see, e.g., Zeki, 1993), and one is the thalamus. Since the pioneering experiments of Hubel & Wiesel (1959), it is well-documented that cells in areas V1 and V2 react orientation- and shape-specific and thus extract spatial information from visually presented objects. As for the thalamus, it is well-established that this midbrain structure acts as a gate or filter for sensory information. It could be hypothesized that this gate works more selectively in good performers, yielding a better suppression of irrelevant sensory information (e.g., information from other modalities, but perhaps also the color or the general size of the visual objects) and gating the relevant visuo-spatial information to primary and secondary visual cortex.

The "algorithmic efficiency" hypothesis explains the group-differences in a different way. Its main assumption is that the lower brain activity is the consequence of a more efficient "spatial processing algorithm" in good performers. This

algorithm processes spatial information in a fast and highly effective way, which is supposed to be in contrast to poor performers who have a less efficient "processing algorithm." Since their algorithm does not accomplish the required spatial processing steps quickly enough, more information has to be buffered in working memory. This not only augments the computational demands imposed on the neural system, but also increases the chance that information gets "lost" and has to be recomputed. Even a total "re-start" of spatial information processing might be required. Indeed, such effects are well-known to subjects with lower ability, since many of them report that they repeatedly could not proceed with task solving since they had lost track of the information needed for the next processing step. On a neural level, the more efficient algorithm should be implemented in a small, highly trained cell assembly in the sense of Hebb (1949). Due to the high training this network received and receives, its synapses are very strongly coupled (according to the Hebbian rule that "cells that fire together wire together") and only few redundant connections exist. This results in more reliable inter-neuronal communication and in fewer neural computations and, hence, lower macroscopically visible activity. The opposite applies to the less efficient algorithm. Here, a less well trained cell assembly is "recruited" to solve the task, containing more weakly coupled synaptic connections and an information processing path which is less well defined. This results in a higher frequency of erroneous neural transmission and in a more widely distributed neural network. Hence, macroscopic activity is higher due to the more extended amount of functional tissue activated by this network and due to the larger amount of active inter-neuronal connections.

Evidence in favor of the two hypotheses is, however, rather sparse. As for the thalamic gating effects, SCPs cannot provide direct information on thalamic activities. As for activity in V1 and V2, good subjects showed a more occipitally dominated topography, with their highest amplitude being located rather over the occipital than the parietal scalp (see Fig. 7-1). Also, the difference in activity between groups was lower for occipital compared to parietal leads (~4.5 μV vs. ~8.5 μV for electrodes Oz and Pz, respectively). Nonetheless, negative SCPs recorded over the occipital scalp were still lower in subjects with higher task-specific ability. However, this might have been partly due to volume conduction. Also, since only 22 recordings channels were used in the former studies, the spatial resolution of the topographies was rather poor, making it difficult to decide how much of the scalp-recorded activity was related to parietal and/or occipital generators. Based on surface recordings only, it is also difficult to decide whether the higher amount of parietal activity is related to a cell assembly which involves more neurons, to

similar neuronal generators with different source strength, or to a combination of both.

Thus, the main aim of the present study was to test which of the hypotheses outlined above is most likely. To this end, the same experimental design as in the former studies of Vitouch and Lamm was implemented. However, spatial sampling of neural activity with SCPs was improved by using 40 EEG channels and individual electrode coordinates for SCP mapping. In addition, brain activity was also assessed via fMRI. fMRI was mainly used to circumvent the inverse problem intrinsic to surface recordings: direct assessment of thalamic activity could be achieved, and the extent of activity in parietal, occipital and fronto-central cortex could be measured more directly.

## *7.2 Material and methods*

### 7.2.1 Subjects

The subject selection criteria were identical to those of Vitouch et al. (1997) and Lamm et al. (1999, 2001). Subjects were selected out of a large pre-testing sample in which about 300 subjects had been tested for their visuo-spatial imagery ability using the 3DC (Gittler, 1990). Only healthy young volunteers whose test performance fell either into the first (poor performers) or into the fourth quartile (good performers) of the age-, education and sex-specific calibration sample of the 3DC were included in this study. All subjects were right-handed according to the Marian Annett handedness inventory (Annett, 1992).

As in the previous studies, the sample was kept homogeneous with respect to age (with age range being restricted to 19-28 years), gender (only male subjects) and general and verbal intelligence (tested using a brief word-power test; Schmidt & Metzler, 1992) in order to exclude potentially confounding effects of these variables. In sum, fourteen good and fifteen poor performers with no history of neurological or psychiatric disorders and normal or corrected to normal vision participated in one SCP and one MRI/fMRI measurement session. The order of measurement sessions was balanced and the time separating the two session orders was kept constant across subjects. Written informed consent was obtained prior to measurements and subjects were paid ~7.50 € per hour for their participation.

### 7.2.2 Task material

The task material was adapted from the 3DC-test used for subject selection. Apart from the reason that the studies of Vitouch and Lamm had used the same tasks, 3DC-derived tasks were used in this study for several reasons (see also chapter 6). First, they allow the assessment of visuo-spatial imagery with increased intra- and interindividual homogeneity. This follows from the fulfillment of the criteria of the Rasch model (Rasch, 1980). Tasks which conform to this probabilistic item response model yield unidimensional measurements of cognitive abilities, implying that identical cognitive processes are active in all tasks and in different groups of subjects. The latter property was essential for this study since it had to be ensured that behavioral differences between groups and sexes were based on 'true' differences in spatial processing, and not on differences in processing strategies or other factors not attributable to spatial cognition. Second, it was of particular importance that 3DC-tasks show minimal practice-related changes in processing strategy. Such changes have been observed when using Shepard-Metzler figures (Shepard & Metzler, 1971), in which subjects with sufficient practice may use stored representations of the 3D objects to decide about their identity rather than rotating objects (Tarr & Pinker, 1989). Such a change in strategy had to be avoided since subjects should not display different processing strategies and associated brain activity in the two consecutive measurement sessions.

### 7.2.3 Task design

Each trial consisted of a baseline image (white crosshair placed between two blue cubes with no graphic elements and no white edges) and a task stimulus (see Fig. 7-2). Subjects initiated each trial by pressing a button, which led to the replacement of the baseline image by a task stimulus. Task presentation time was not restricted, and subjects were told they had ample time to solve each task (see also chapter 6 and Lamm et al., 2001). Stimuli consisted of two blue cubes with white graphic elements (triangle, dots, squares, arrows etc.) on each of their three visible faces presented simultaneously on black background. Subjects had to decide whether or not the two cubes could be a picture of the same cube, and responded by pressing one of two response buttons with the dominant right hand

(answers "yes" and "no"). Thus, the task design was - except for one difference[12] - identical to the one of the former studies. This difference was that a fixation cross was presented during the pre-stimulus baseline in the former studies, while two empty blue cubes were additionally presented in this study (see Fig. 7-2). Thus, the amount of change in visual input related to the presentation of the tasks was considerably lower in the present study (see also the discussion below).

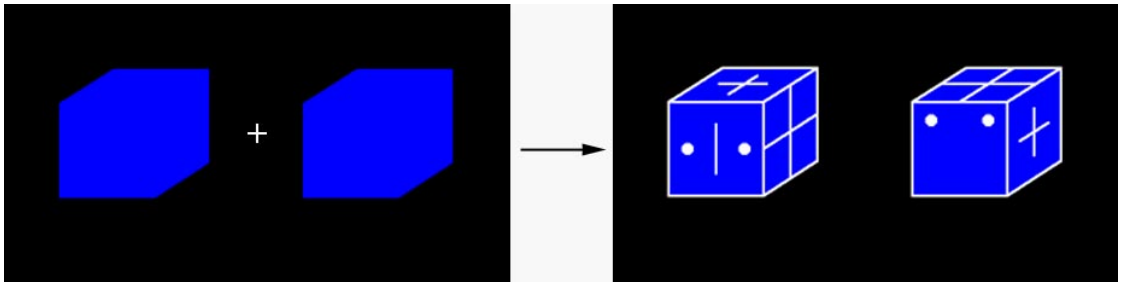

Fig. 7-2: Sample for the tasks used in this study. Following button press, the baseline image (white fixation cross between two blue cubes on black background) was replaced by a task stimulus consisting of two cubes with white graphic elements on their faces. Subjects had to decide whether these cubes could be identical (which is the case for the sample shown). Images were displayed centered in the middle of a computer screen (SCP) or of video goggles (MRI).

### 7.2.4 EEG recording

EEG was recorded using a 24-channel DC amplifier with high baseline stability and an input impedance ≥ 100 GΩ. Signals were sampled at 125 Hz and recorded within a frequency range from DC to 30 Hz. Variable signal epochs covering two seconds of pre-presentation baseline to two seconds after response were stored trial by trial. EEG was recorded from 40 Ag/AgCl scalp electrodes and 2 electrodes placed on the mastoids. All electrodes were attached to small plastic adapters that had been fixed on the subject's skin using collodion. Recording sites were skin-scratched using sterile single-use needles (Picton & Hillyard, 1974) to minimize skin potential artifacts and to keep electrode impedance homogeneous, stable and below 1 kΩ (which was confirmed for each electrode separately). Degassed electrode gel (Electro-Gel, Electrode-Cap International, Inc., Eaton/OH, USA) was used, and electrodes were filled with the gel at least half an hour before application to allow for stabilization of the electrode potential. A non-cephalic sterno-vertebral reference (Stephenson & Gibbs, 1951) was used for all EEG

[12] A presumably negligible difference was the higher inter-stimulus interval which had to be used for the fMRI measurements. Furthermore, no additional verbal task condition was used. However, it does not seem very likely that the exclusion of this condition affected the results of the dynamic visuo-spatial imagery condition.

channels. It consisted of two electrodes, one placed at the 7$^{th}$ cervical vertebra and the other at the right sterno-clavicular junction. A 5 kΩ potentiometer connecting these two electrodes was individually adjusted to minimize electrocardiographic components in the EEG. Vertical (electrodes above and below right eye) and horizontal (electrodes on outer canthi) electrooculograms (VEOG, HEOG) were recorded bipolarly to control for eye movement artifacts.

Since the DC-amplifier had only 24 channels, EEG was alternately recorded from two interleaved electrode sets, each one containing 20 EEG electrodes plus the two mastoid electrodes. Electrodes of both sets were equally distributed across the scalp surface. With each electrode set, at least two blocks of 30 trials were recorded. The sequence of blocks was randomly permuted across subjects. 3D coordinates of all EEG electrodes, and of nasion, inion and the two preauricular points were measured using a photogrammetric head digitizer (Bauer et al., 2000). Tasks were presented in the center of a computer screen located approximately 70 cm in front of the subject, and a response board was positioned to the right of the subject. The visual angle subtended by the stimuli was approximately identical to that used for the fMRI goggles (~ 1.64° vertical, ~ 8° horizontal). The minimum intertrial interval was four seconds.

### 7.2.5 EEG analysis

Eye movement artifacts were eliminated offline using a linear regression algorithm (see Vitouch et al., 1997, for a detailed description). All trials were visually screened to exclude those containing artifacts. Stimulus-onset linked averages were computed for each subject. The mean amplitude in the 200 ms epoch preceding task presentation served as the pre-stimulus baseline. Since response times were variable within and across subjects, an analysis epoch of a length of five seconds was selected based on the median reaction times. This epoch length was chosen because it was long enough to reliably induce cognition-related SCPs, and because only a few trials had to be rejected due to response times shorter than five seconds. In order to exclude activity related to motor preparation and execution of the button press, only trials with response times ≥ 5500 ms were included in the averages. In addition, response-linked averages (with the same 200 ms pre-stimulus baseline as for the stimulus-linked averages) were computed to evaluate activity related to task completion and response execution.

SCP averages and their current source density (CSD) transforms were topographically mapped using the analytical interpolation algorithm proposed by

Babiloni et al. (1996). CSD transformation was applied to yield reference free maps and to attenuate low spatial frequencies ('smearing') introduced into the scalp potential distribution due to volume conduction (Nunez, 1989; Nunez et al., 1994; Srinivasan et al., 1996). In order to map the activity distribution on the scalp surface with increased spatial sampling (Nunez et al., 1994; Srinivasan et al., 1998), the data of the two electrode sets were simultaneously used for interpolation. SCP and CSD maps were visualized on individual head shapes reconstructed using spline interpolation of the 3D electrode and landmark coordinates acquired by the photogrammetric head digitizer (see chapter 3). Group-specific grand mean SCP- and CSD-maps were computed using the mean electrode coordinates of the whole sample for interpolation.

In order to statistically analyze differences in neural activity between the two groups, univariate repeated-measures analyses of variance (ANOVAs) were performed. These included the factors GROUP (2 levels, good and poor performers) and LOCATION (40 EEG electrodes). A priori linear contrasts were computed to specifically compare activity over the parietal, occipital and fronto-central scalp. Bonferroni-corrected linear contrasts were used to assess post-hoc hypotheses. All statistical analyses were performed using amplitude and z-scaled data. Violations of the sphericity assumption were corrected using Greenhouse-Geisser correction and linear contrasts were calculated using individual error variances (Boik, 1981; see also chapter 2). The following parameters were used as the dependent variables:

AN1: Amplitude of the N100-like component, being defined as the most negative peak in the time interval ranging from 50 to 200 ms post stimulus.
TN1: Latency of the N100-like component
AP300: Amplitude of the P300-like component, being defined as the most positive peak in the time interval ranging from 200 to 300 ms post stimulus.
TP300: Latency of the P300-like component
SCP1: Mean amplitude in the interval ranging from 1 to 2 sec post stimulus
SCP5: Mean amplitude in the interval ranging from 4 to 5 sec post stimulus
SCPALL: Mean amplitude in the interval ranging from 1 to 5 sec post stimulus
SCP-R: Mean amplitude in the interval ranging from 5 to 2 sec before response

### 7.2.6 MRI and fMRI scanning

MRI experiments were performed using a 3 Tesla Medspec S300 tomograph (Bruker Medical, Ettlingen, Germany) equipped with a whole-body gradient system and a standard birdcage coil for RF excitation/reception. An anatomically formed cushion and a strap around the forehead were used to reduce gross head motion. Structural images of the brain were acquired using a 64 slice gradient-echo sequence with 1 x 1 mm in-plane resolution and a slice thickness of 3 mm. A T2*-weighted single-shot, blipped gradient-recalled EPI sequence (flip angle=Ernst angle) with matrix size 64 by 64 pixels, echo time (TE) of 23 ms and readout bandwidth of 100 kHz was used for functional imaging. 15 axial slices with a FOV of 190 x 190 mm, a thickness of 5 mm and an interslice gap of 1 mm, covering nearly the whole cerebrum, were acquired. Repetition time (TR) for the whole image slab was 1.5 sec. The single-trial sequence was designed to ensure continuous data acquisition and constant intervals between images. Two runs of fifteen minutes each (600 images/slab) were acquired, each starting with thirty seconds of dummy scans to allow for steady state conditions. Although task content and task difficulty in the two runs were not different, their sequence was balanced across subjects.

Stimuli were presented via MRI-compatible video goggles (Resonance Technologies, Northridge/CA, USA) connected to the video output of a controlling PC running in-house software for stimulus presentation. The visual angle subtended by the two cubes (~ 1.64° vertical, ~ 8° horizontal) was kept as low as feasible in order to reduce the requirement of making large saccadic eye movements. The buttons for responses and task initiation were mounted on a board attached to the subject's right thigh. The minimum inter-trial interval was twenty seconds in order to allow cerebral blood flow changes to return to baseline between trials.

### 7.2.7 fMRI analysis

Since a statistical comparison of groups was required in this study, data were analyzed within the framework of the general linear model as implemented in SPM99 (Friston et al., 1995; The Wellcome Department of Cognitive Neurology, London/UK). After correction for head motion in 2D using sinc-interpolation (AIR v3.08; Woods et al., 1998), functional images were co-registered to the normalized structural images via linear translation and stretching of the functional images using IDL routines (Interactive Data Language; Research Systems, Inc., Boulder/CO,

USA) written in-house. Accuracy of normalization and co-registration were carefully checked for each subject based on several brain landmarks and the shape of the slices. Functional images were then spatially smoothed with a Gaussian kernel of 9 mm full-width-at-half-maximum.

The signal at each voxel was modeled with a canonical hemodynamic response function (hrf; see also chapter 2) and its temporal derivative and filtered with a high-pass filter (with the upper cutoff frequency being derived from twice the maximum time interval between the most frequently occurring events) and a low-pass filter (hemodynamic response function) to eliminate slow drift and high frequency artifacts. Temporal auto-correlation was considered using a first order auto-regressive model, which is mandatory since consecutive measurements are highly correlated in fMRI. Incorporation of the temporal derivative of the hrf into the model was chosen to accommodate for potential differences in hemodynamic response onset between groups. For each subject, a t-contrast contrasting the task-related activity with the baseline activity in the two runs was computed separately for the hrf and the temporal derivative of the hrf. The resulting contrast images were entered into a random effects (Holmes & Friston, 1998) analysis in order to investigate between-group differences (good>poor, poor>good). A random effects analysis was preferred to a fixed-effects analysis since it explicitly considers between-subjects error variance and thus allows a generalization of results to the underlying population. The random effects approach was also chosen since it represents the same analysis concept as the one used for the analysis of the SCP data.

Since precise a-priori hypotheses existed, between-group comparisons restricted to bilateral parietal cortex, bilateral occipital cortex, bilateral lateral premotor cortex, bilateral medial premotor cortex (pre-SMA) and bilateral thalamus were performed to specifically assess activity differences in these regions. Regions of interest (ROI) were manually drawn using a combination of the software MRIcro (http://www.psychology.nottingham.ac.uk/staff/cr1/mricro.html, courtesy of Chris Rorden) and statistically thresholded images of active clusters derived from the earlier analysis of good subjects (chapter 6). The occipital ROI, however, only included the primary and secondary visual cortex and thus did only partially cover the active cluster from the prior analysis. The resulting statistical images were thresholded at a corrected p-value of .05 (with correction being based on random field theory; see chapter 2.1). Corrected thresholds for the ROI volumes were calculated using matlab code (http://www.mrc-cbu.cam.ac.uk/Imaging/vol_corr.html;

provided by Mathew Brett, MRC CBU Cambridge) implementing the suggestions by Worsley et al. (1996b) regarding small volume correction.

### 7.2.8 Behavioral data and questionnaire

Median processing time and percentage of correctly answered tasks were calculated separately for the two groups and the SCP- and the MRI-session. In addition, the two questionnaires which had already been used in the former study (chapter 6) were also used in the present study in order to gain information about task solving strategies of subjects. Questionnaire A included questions about the task difficulty, the effort and concentration subjects invested, the percentage of items they were convinced to have answered correctly, and how motivated they felt during the experiment. Questionnaire A was presented after the SCP- and after the MRI-session. Questionnaire B assessed two possible task solving strategies. The most commonly used strategy consists almost exclusively of dynamic visuo-spatial imagery and mental rotation. The second strategy is a more analytic one and includes verbal-analytic descriptions of the relations of the cubes and their elements. Nevertheless, it also relies on visuo-spatial cognition because cubes and the mutual relations of their elements are coded and compared using spatial descriptors (such as "the arrow on the *upper* face of the left cube points to the *left anterior* corner of this cube"; see also Gittler, 1990).

By using the standardized written task instruction of the 3DC-test, care was taken not to bias subjects in favor of one of the two strategies (Intions-Peterson, 1983). Since presentation after the first session might have influenced the subjects' processing strategies in the second session, questionnaire B was presented only once and always after the second measurement session.

## *7.3 Results*

### 7.3.1 Exclusion of subjects

Unfortunately, several of the 29 investigated subjects had to be excluded from the anaylses. Three subjects had to be excluded from the EEG analyses (in one subject, a slightly different electrode montage had been used; the other two had to be excluded due to excessive artifacts resulting in an insufficient number of trials available for event-related averaging). Thus, a final sample of fourteen good

and twelve poor performers was available for the analyses. As for the fMRI data, functional measurements could not be performed in one subject who could not remain in the scanner because of claustrophobia (of which he had not been aware before entering the scanner). Two subjects had to be excluded since a slightly different fMRI protocol (20 instead of 15 slices, TR=2 sec) had been used, and five subjects had to be excluded due to excessive movements, excessive ghosting artifacts or due to the lack of a reliable hemodynamic response (for unknown reasons). The final fMRI sample consisted of thirteen good and eight poor performers. Fortunately, the excluded subjects partially overlapped: Two of the subjects in whom the EEG could not be analyzed were also excluded from the fMRI analyses.

### 7.3.2 Behavioral data

#### 7.3.2.1 Response times and hit rates

Table 7-1 shows the percentage of correctly answered tasks and the median reaction times of the two groups during the EEG experiments. Mann-Whitney U-Tests revealed that the percentage of correctly answered tasks, reaction times for all tasks, and reaction times for correctly answered items were significantly different between groups ($p<.001$ in all cases).

Table 7-1: Group-specific behavioral data of the SCP experiment. Percentage: percentage of correctly answered tasks (mean and range), RTall: Group-specific response time calculated for all tasks (median ($1^{st}$-$4^{th}$ quartile)), RTcorrect: Group-specific response time calculated for correctly answered tasks (median ($1^{st}$-$4^{th}$ quartile)).

| *GROUP* | *Percentage* | *RTall (seconds)* | *RTcorrect (seconds)* |
|---|---|---|---|
| GOOD (N=14) | 96.41 (90.8-100) | 10.68 (6.43-17.84) | 10.66 (6.42-17.68) |
| POOR (N=12) | 77.43 (61.4-92.5) | 13.22 (8.77-19.90) | 12.73 (8.38-19.21) |

In Vitouch et al.'s (1997) study (in which only male subjects had been investigated, too), basically the same results had been obtained. Median response times for the correctly answered tasks were 10.2 seconds in the good and 13.4 seconds in the poor group. The percentage of correctly answered tasks was 93% and 77%, respectively.

Table 7-2 displays the same behavioral data for the fMRI experiments. Mann-Whitney U-Tests revealed that the percentage of correctly answered tasks, reaction times for all tasks, and reaction times for correctly answered tasks were significantly different between groups ($p<.001$ in all cases).

Table 7-2: Group-specific behavioral data of the fMRI experiment. Percentage: group-specific percentage of correctly answered tasks (mean and range), RTall: group-specific response time calculated for all tasks (median ($1^{st}$-$4^{th}$ quartile)), RTcorrect: group-specific response time calculated for correctly answered tasks (median ($1^{st}$-$4^{th}$ quartile))

| *GROUP* | *Percentage* | *RTall (seconds)* | *RTcorrect (seconds)* |
|---|---|---|---|
| GOOD (N=13) | 90.85 (79.49-97.06) | 12.00 (7.40-20.7) | 11.85 (7.50-20.38) |
| POOR (N=8) | 73.38 (65.91-83.33) | 19.00 (12.10-27.55) | 18.20 (11.88-27.50) |

### 7.3.2.2 Questionnaires

The appendix to this chapter contains a complete description of the questions and answers given in the two questionnaires (in German). In the following paragraphs, I will focus on the differences between groups. Statistical comparisons were performed for the 26 subjects who were available for the SCP analyses.

*Questionnaire A:*

Mann-Whitney U-tests were used to assess whether groups differed in their answers to questionnaire A. Bonferroni-correction was used to keep the family-wise error of these five comparisons per measurement session to a type I error of $\alpha$=.05.

Comparison of the questionnaires completed after the EEG session revealed that groups differed in their answers to the question how difficult the tasks appeared to them (p=.001), and to the question how many tasks they were convinced to have answered correctly (p=.003). Tasks appeared less difficult to good subjects who were also convinced that they had solved more task correctly. A trend-like effect was also observed for the question as to how much effort subjects felt they had to invest in task solving (p=.023, $\alpha_{corrected}$=.01), with poor subjects showing a higher amount of invested effort.

As for the fMRI session, the only significant result after Bonferroni-correction was obtained for the task difficulty question (p=0.01). No significance was obtained for the question how many tasks subjects were convinced to have answered correctly (p=.135). A trend-like effect was observed for the question how motivated subjects felt (with poor subjects feeling less motivated than good ones; p=.02, $\alpha_{corrected}$=.01).

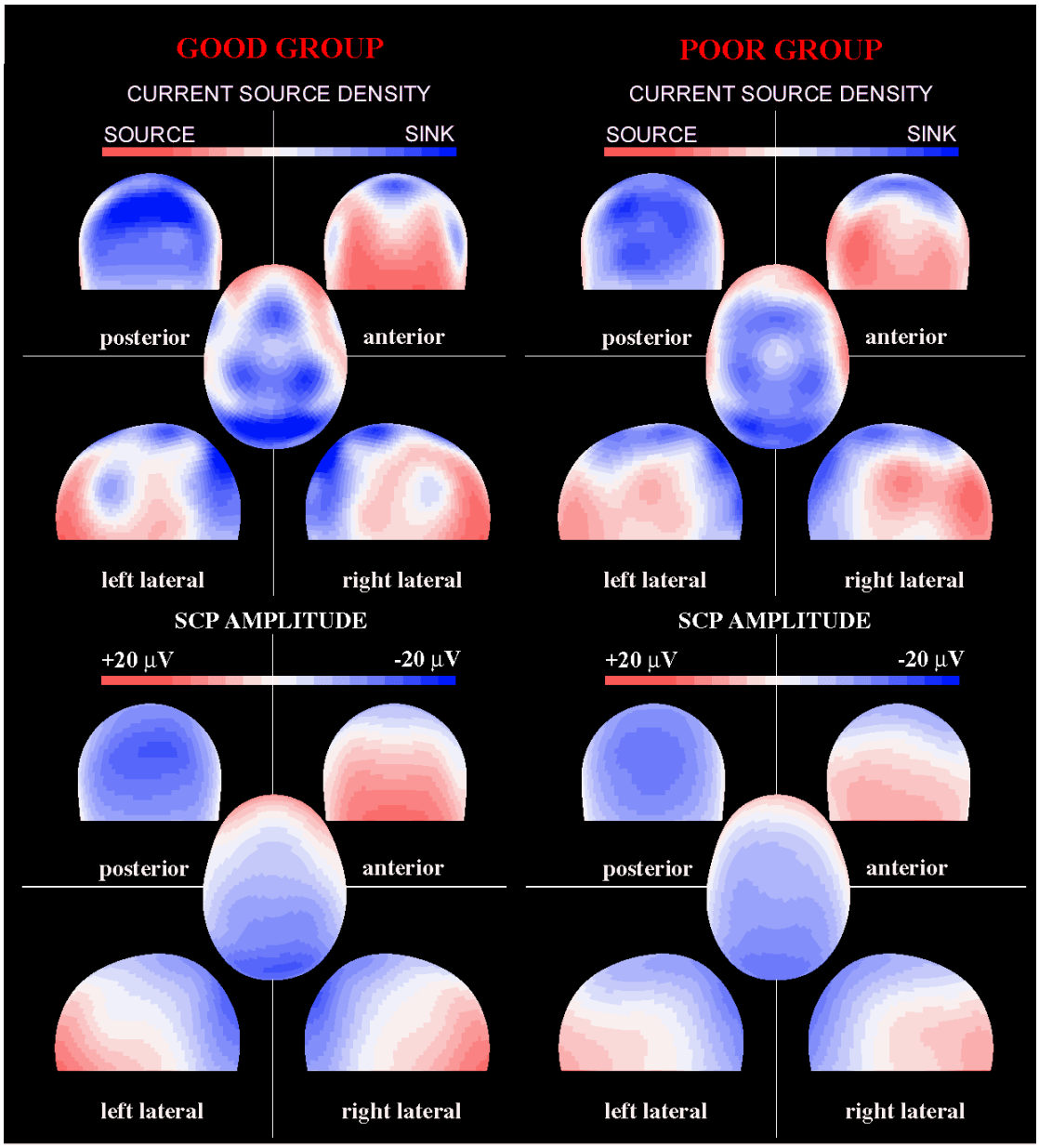


Fig. 7-3: CSD- and SCP-maps 5 seconds after task presentation in subjects with high and low task-specific ability. Note that maps are largely identical except for a slight mismatch in CSD over the lateral frontal scalp.

*Questionnaire B:*

Mann-Whitney U-tests were used to assess whether groups differed in their answers to questionnaire B. Since answers of this questionnaire were highly inter-dependent, a Bonferroni-correction could have led to overly conservative results. However, a higher threshold of $\alpha$=.01 was used to reduce the type I error of the multiple univariate comparisons. The only difference between groups was related to the question whether movements of the cubes rather proceeded on their own or

whether they had to be constructed actively (p=.004). Good subjects had the impression that cubes moved rather "automatically." A Bonferroni-corrected trend-like effect (p=.035) was observed for the question how vivid the mental images appeared to subjects, with good subjects reporting that mental images were more vivid or "close-to-vision."

### 7.3.3 SCPs

Similar activity as in the former studies and in the study presented in chapter 6 was revealed. However, SCP- and CSD-maps of the two groups were almost identical (except for a slight difference in the current sinks over the left fronto-lateral region, see Fig. 7-3). Maps of the early phasic components were also vastly identical and are therefore not shown. Also, waveforms of the two groups were hardly distinguishable (see Fig. 7-4).

ANOVAs neither revealed a significant main effect of the GROUP factor, nor a significant interaction with the LOCATION factor in any of the analyses (p> .10 in all cases). Fig. 7-5 shows the group-specific grand mean amplitudes of the 40 EEG electrodes for parameter SCP5. It reveals that parietal and fronto-central amplitudes of the groups were basically identical, and that good performers showed a slightly higher amplitude over the occipital cortex. However, none of the a-priori linear contrasts were significant. The same applied to a post-hoc contrast calculated with the electrodes showing the highest difference between groups (electrodes O3, Oz and O4, see Fig. 7-5). The only trend-like significance was observed for a post-hoc group contrast of the fronto-medial amplitudes of parameter AP3 (electrodes F5, F3, Fz, F4, F8; F=1.57, p=.031, $\alpha_{corrected}$=.025).

Summing up, with respect to individual differences, the results of the former studies could not be replicated. To the contrary, it rather seemed that good subjects showed more activity over the parietal and occipital cortex than poor ones (see Fig. 7-3 to 7-5). However, this difference was not statistically significant. In addition, the CSD maps indicated a difference in activity over the fronto-lateral cortex which had not been detected in the earlier studies (presumably due to their lower spatial sampling and the improved mapping method used in the present study).

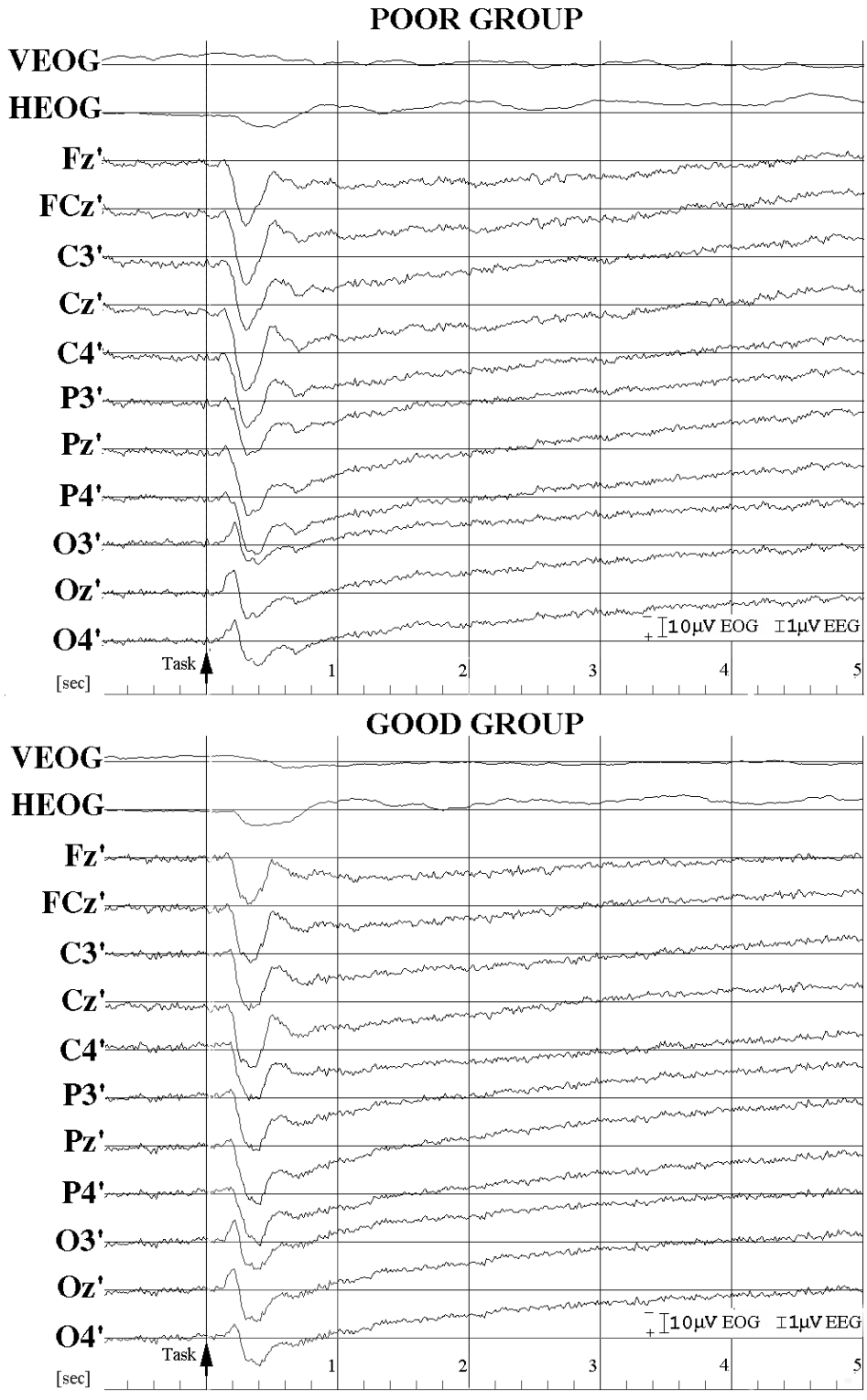


Fig. 7-4: Group-specific stimulus-linked grand mean SCPs of selected EEG channels (task presentation is indicated by an arrow).

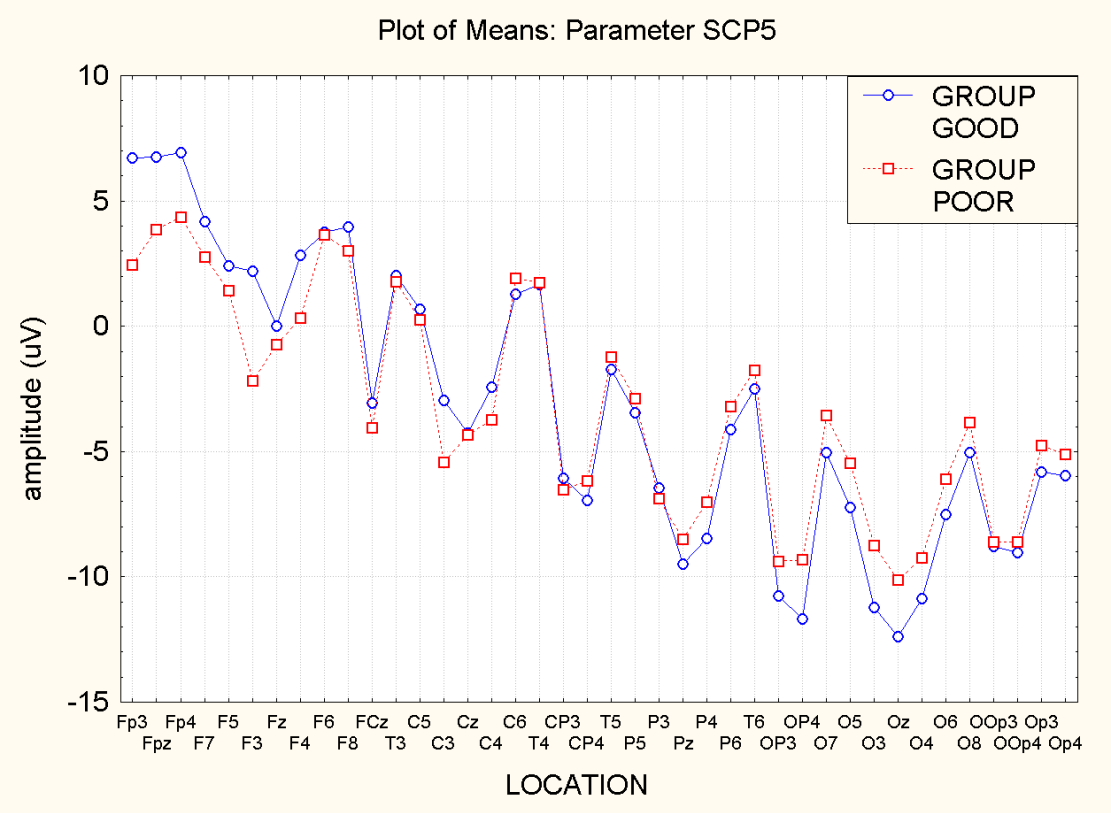


Fig. 7-5: Grand mean amplitude of parameter SCP5 in good and poor test performers.

### 7.3.4 fMRI

As with SCPs, similar activity as detected in the study presented in chapter 6 was revealed (see Fig. 7-6). The small-volume corrected random-effect analyses of the ROIs revealed no significant differences between groups for any of the ROIs (neither for the data modeled with the hrf nor for those modeled with its temporal derivative). Even when the corrected threshold was set to a more liberal value of $p \leq .10$, no significant difference between groups could be observed. Based on the CSD difference over the fronto-lateral region, a post-hoc ROI was drawn over the dorso-lateral prefrontal cortex to assess potential differences between groups in this cortical area. No significant difference was observed for this statistical comparison either.

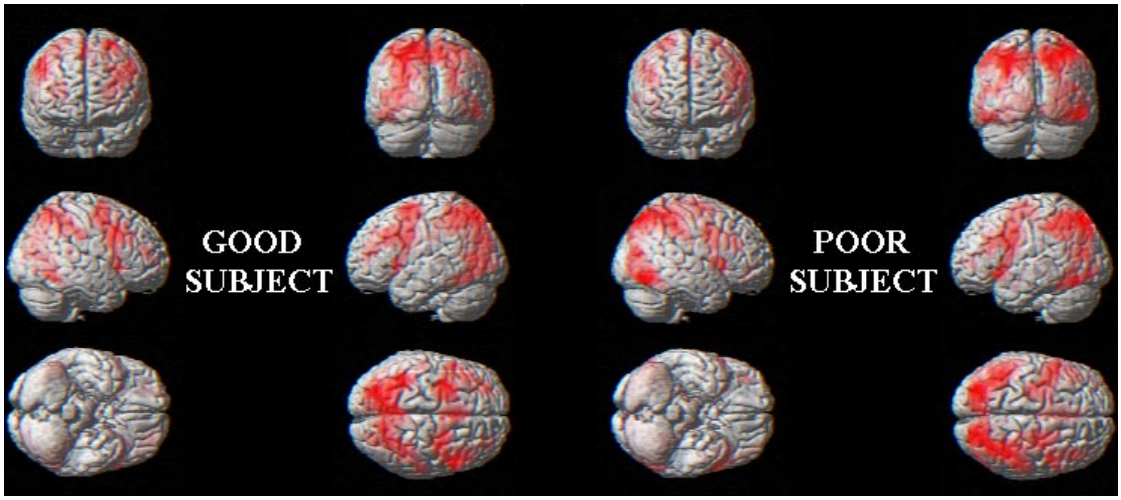


Fig. 7-6: Brain activity as revealed by fMRI in two subjects representative for the two groups with good and poor performance. Shown are maximum intensity projections of significant voxels (hrf modelled, $p \leq .05$ corrected) overlaid on six rendered views of the high-resolution MNI single-subject brain. Similar to the results of the study presented in chapter 6, parietal, lateral and medial premotor, occipital, and prefrontal activities were detected. However, no obvious between-groups difference in brain activity could be observed.

## 7.4 Discussion

In this study, ability-related differences in brain activity during processing of a visuo-spatial imagery task were investigated. Two alternative hypotheses concerning these differences should be tested using a multi-modality imaging approach. In order to achieve maximum comparability with earlier results, the identical experimental design as in the former studies of Vitouch et al. (1997) and Lamm et al. (1999) was used. Since identical subject selection criteria were used, subjects were virtually identical to those of the former studies with respect to age, 3DC-scores, handedness, and general intelligence. On the behavioral level, results of the former studies were replicated. Subjects falling into the $4^{th}$ quartile of the calibration sample of the 3DC-test showed significantly and considerably shorter task processing times and a higher percentage of correctly answered tasks. Surprisingly, however, no concomitant differences in brain activity could be observed in the present study. Therefore, no information concerning the validity of the two mentioned hypotheses could be obtained. Thus, in the remainder of this chapter, I will focus on a discussion of some potential explanations for the lack of between-group differences in neural activity in this study.

It might be argued that the failure to replicate the former SCP results is due to artifacts (e.g. more drift in the present study, non-cooperative subjects etc.). However, several arguments speak against this interpretation. First, brain activity

was also assessed via fMRI, which indicated activity in similar brain regions as SCPs and whose results were consistent with those of a former study (chapter 6). Second, subjects were sufficiently cooperative and most of them were highly motivated, which was clearly revealed by the behavioral data and the answers given in questionnaire A. Third, the same electrode application, data screening and data analysis procedures were used in this study as in the former studies. Data analysis was even improved by using individual electrode coordinates and a more appropriate head model for topographic mapping. In addition, one can certainly say that EEG recordings were performed by a highly experienced EEG experimenter[13]. Consequently, the hypothesis that the data of this study were heavily contaminated by artifacts can be rejected. What cannot be excluded, however, is the interpretation that either the sample investigated in this or in the former studies was not representative for the respective population. This represents a general problem in brain imaging research, since sample sizes are usually rather small due to the amount of effort, time and money related to data acquisition. This partly results from the limited amount of available measurement time, which particularly applies to fMRI, in which a very expensive scanner is used by many different research groups. On the other hand, it should be noted that the sample size of the present study was comparably large (see, e.g., Vitouch & Glück, 1997 for a comparison of sample sizes in brain imaging), and the same subject screening procedure as in the former studies was used. This is, however, neither a guarantee for a representative sampling of the underlying population, nor for a sample which is identical as the one in the former studies.

The lack of group-specific differences in brain activity might also be explained by the higher task-specific training received by the subjects since they processed considerably more tasks than in the former studies. However, as already discussed in the methods section, 3DC-tasks do hardly show practice-related effects. In addition, a re-analysis of the SCP data restricted to those subjects who performed the EEG measurements first did not reveal any relevant or reliably higher effect size of the group factor than the analyses performed for the whole sample. For example, the percentage of explained variance (as assessed by parameter $\eta^2$; see Bortz, 1993) for the GROUP x LOCATION interaction of parameter SCP5 was exactly identical for the two analyses, while $\eta^2$ for the main effect of GROUP was slightly higher ($\eta^2$=.014), but still far from indicating a relevant effect size.

[13] Before this study, I had performed about 100 SCP experiments.

Another explanation might be that the two groups were not as different with respect to their level of ability as in the former studies. However, as already discussed above, the behavioral results of the present study and of the one of Vitouch et al. (1997) were almost identical. The present study even revealed a slightly higher difference in the percentage of correct answers (even though a slightly lower difference in reaction times was observed). Concerning subject selection, the mean 3DC scores of the two groups also were slightly more different than in the study of Vitouch et al. (Good group$_{\text{mean } \pm \text{ standard deviation}}$: 16.5 $\pm$ .76 vs. 16.2 $\pm$ .8 in Vitouch et al.'s study; poor group: 3.25 $\pm$ 3.05 vs. 5.4 $\pm$ 2.4). Nevertheless, Table 7-1 shows a partial overlap of groups in the percentage of correctly answered tasks. Thus, another re-analysis of SCP data was performed in which those subjects were excluded who showed overlapping behavioral scores. Again, $\eta^2$ did not considerably change compared to the analysis with all subjects, and it was even slightly lower for the interaction term. Thus, it seems well-justified to assume that the lack of differences in brain activity cannot be explained by a lack in behavioral differences.

Finally, a rather speculative explanation of the results of this study shall be presented. As repeatedly mentioned, the experimental design was identical to the one of the former studies. However, there was a slight mismatch with respect to the task presentation mode. In the present study, tasks were preceded by two empty blue cubes and a fixation cross, and task presentation itself consisted of an overlay of the graphic elements of the cubes on these empty cubes. Thus, the amount of additional visual input which had to be processed upon task presentation was rather small. This is in clear contrast to the former studies, where only a fixation cross was presented during the baseline. This resulted in a rather massive change in visual input that had to be processed upon presentation of the task stimuli. Thus, one might speculate that the difference between good and poor spatial test performers in the earlier studies was observed because the neural system of poor performers reacts more intensely to visuo-spatial input.

Although this hypothesis might appear rather bold, it receives some support from a recent study conducted in the Brain Research Lab Vienna (Adelbauer, 2001). In this study, it was investigated whether the monoscopic and stereoscopic presentation of pictures of a complex natural scene (containing several 3D objects, as a house, tree, arcade) evokes different neural activity in subjects with good vs. poor visuo-spatial ability (which was determined using the 3DC). Monoscopic and stereoscopic stimulus presentation was achieved via pictures which had been taken using three digital cameras adjusted to have parallel optical axes but hori-

zontal inter-lens distances of 45 mm. Using liquid crystal shutter lenses, pictures taken from the left and right cameras were separately presented to the left and right eyes, while the picture taken by the middle camera was used for monoscopic stimulation. This study was motivated by the hypothesis that group-specific differences at this early and rather basic visuo-spatial processing stage might explain the differences in brain activity during 3DC processing observed in the studies of Vitouch and Lamm. It was hypothesized that subjects with high test scores would perform better because they extract the spatial information contained in a visual scene better than poor subjects. One main assumption was that the highest difference between groups should be observed when SCPs related to the viewing of monoscopic vs. stereoscopic stimuli were compared. However, initial results did not reveal any difference between SCPs recorded during monoscopic and stereoscopic stimulus presentation. Topographies and SCP amplitudes of subjects were virtually identical. A significant between-group difference could nevertheless be observed. The switching from scrambled pictures ("pictures" which had no information content, but identical physical input as the true stimuli) of a scene to the scene itself evoked significantly higher activity in poor subjects than in good ones - irrespective of whether the visual scene was presented in monoscopic or stereoscopic mode. Statistical analysis revealed that this difference was not topographically specific. Rather, poor performers showed a generally higher amplitude in all recording leads. Interestingly, this difference was largely independent of the amount of spatial depth cues contained in the scenes[14]. Thus, the results of this study have tentatively been interpreted in the sense that the neural system of poor performers shows a more intensive reaction to the presentation of visual stimuli *per se*.

On the other hand, initial results of an even more recent study which was also performed in the Brain Research Lab in Vienna show an opposite pattern of results. In this study, good and poor 3DC-performers had to learn to navigate through mazes of different complexity. In contrast to the latter study, poor performers showed a tendency towards lower SCP amplitudes than good performers. Even more interesting, the same result was observed in a control task where subjects only passively viewed the maze. Thus, the group-specific difference seems not to be related to the learning of the spatial trajectory of the maze, but to the requirement to process visuo-spatial information. Nevertheless, it should be noted

[14] Three different pictures had been used in this study: a picture of a tree, of an arcade, and of a house with numerous windows. While the tree represented a rather "two-dimensional" stimulus with a smaller amount of depth cues, the arcade contained lots of 3-dimensional depth information, and the picture of the house contained much spatial orientation information in the picture plane.

that these effects are not (yet) statistically significant, since only about 15 subjects have been tested so far. Also, in contrast to the former studies, stimuli were not static, but consisted of short movies of the trajectories of the mazes. This is likely to recruit different brain areas than the presentation of a static object.

Summing up, a definite explanation for the lack of individual differences can not yet be presented. The present study clearly confirms the discussion in the introduction to this chapter concerning the difficulty to investigate and to establish individual differences in neural processing: Although individual differences were clearly revealed by several former studies, and although the two groups of this study clearly differed on the behavioral level, no concomitant differences in brain activity could be observed. It has to be concluded that the concept of neural efficiency was neither supported by the SCP nor by the fMRI results. As a direction for future work, it would be interesting to know whether poor subjects in fact react more intensively to visual input. This could, for example, be investigated by employing the same experimental design as in this and in the former studies, but using two conditions in which subjects solve tasks which are either preceded by blue cubes or by a fixation cross only.

**APPENDIX**

# Fragebogen A

Bitte beantworten Sie die Fragen auf den folgenden vier Seiten!
Dabei gibt es keine richtigen oder falschen Antworten.
Bitte **kreuzen Sie** daher jeweils auf der Skala unter der Frage
**jene Antwort an,** die für Sie **am ehesten zutrifft!**

A1 Wie viele Aufgaben haben Sie Ihrer Meinung nach **richtig** bzw. **falsch** gelöst?

| **RICHTIG** | | | | | | | **FALSCH** |
|---|---|---|---|---|---|---|---|
| alle | fast alle | die meisten | mehr als die Hälfte | mehr als die Hälfte | die meisten | fast alle | alle |

A2 Wie **schwer** bzw. **leicht** waren die Würfelaufgaben für Sie?

| **SCHWER** | | | | | | | **LEICHT** |
|---|---|---|---|---|---|---|---|
| extrem schwer | sehr schwer | schwer | eher schwer | eher leicht | leicht | sehr leicht | extrem leicht |

A3 Wie **schwer** bzw. **leicht** ist es Ihnen gefallen, sich zu konzentrieren?

| **SCHWER** | | | | | | | **LEICHT** |
|---|---|---|---|---|---|---|---|
| extrem schwer | sehr schwer | schwer | eher schwer | eher leicht | leicht | sehr leicht | extrem leicht |

A4 Wie **schwer** bzw. **leicht** haben Sie sich anstrengen müssen, um die Aufgaben zu lösen?

| **SCHWER** | | | | | | | **LEICHT** |
|---|---|---|---|---|---|---|---|
| extrem schwer | sehr schwer | schwer | eher schwer | eher leicht | leicht | sehr leicht | extrem leicht |

A5 Wie **gern** bzw. **ungern** würden Sie noch weitere Würfelaufgaben bearbeiten?

| **GERN** | | | | | | | **UNGERN** |
|---|---|---|---|---|---|---|---|
| extrem gern | sehr gern | gern | eher gern | eher ungern | ungern | sehr ungern | extrem ungern |

Coding: 1...8

Responses to the questions of questionnaire A [Median(Range)]; EEG/MR: responses for subjects included in the EEG/MR analyses;

| | | **GOOD** | **POOR** | | **GOOD** | **POOR** |
|---|---|---|---|---|---|---|
| | A1 | 2 (2-3) | 3.5 (3-5) | | 2 (2-6) | 4 (2-7) |
| | A2 | 5.5 (4-8) | 4 (3-5) | | 6 (5-7) | 4 (3-6) |
| **EEG** | A3 | 6 (4-8) | 5 (3-6) | **MR** | 6 (4-8) | 4 (1-7) |
| | A4 | 5 (4-7) | 4 (2-6) | | 5 (3-7) | 4 (2-5) |
| | A5 | 3 (2-6) | 5 (3-6) | | 3 (2-7) | 5 (3-8) |

## Fragebogen B

Geben Sie bitte nun an, was Sie getan haben, um bei den Würfelaufgaben zu Lösungen zu kommen. Sie erhalten meist **zwei Alternativen** beschrieben und sollen sich selbst dahingehend einschätzen, in welchem Verhältnis die beiden Möglichkeiten auf Sie zutreffen.

B1 Haben Sie die Aufgaben **alle in gleicher Weise** bearbeitet?

| **GLEICH bearbeitet:** Sie haben die Aufgaben **alle in gleicher Art und Weise** bearbeitet. | | | | | **UNTERSCHIEDLICH bearbeitet:** Sie haben die Aufgaben **unterschiedlich** bearbeitet. | | |
|---|---|---|---|---|---|---|---|
| aus-schließlich | fast nur | mehr-heitlich | ein wenig mehr | ein wenig mehr | mehr-heitlich | fast nur | aus-schließlich |

B2 Sie haben zwar die Instruktion erhalten, zur Bearbeitung Ihre **Vorstellung einzusetzen** und sich sicherlich bemüht, dies zu tun. Doch haben Sie möglicherweise bemerkt, daß Sie zusätzlich auch **nachgedacht** haben. **Wie sind Sie nun tatsächlich vorgegangen? Geben Sie bitte an, in welchem Verhältnis Sie die beiden Möglichkeiten eingesetzt haben!**

| **VORSTELLEN:** | | | | | | | **NACHDENKEN:** |
|---|---|---|---|---|---|---|---|
| Sie könnten in unterschiedlichster Weise vorgegangen sein - Sie haben vielleicht versucht, die linken Würfel oder die rechten Würfel vor Ihrem „inneren Auge“ so zu sehen, wie sie von anderen Seiten aus betrachtet aussehen. Sie haben möglicherweise die ganzen Würfel oder auch nur einzelne ihrer Deckflächen (Muster) in der Vorstellung gedreht bzw. gekippt oder sind in der Vorstellung um die Würfel „herumgegangen“. Vielleicht haben Sie auch ganz anders vorgestellt. **Wichtig ist**, Sie haben versucht, die Würfel ganz oder teilweise in veränderter Ausrichtung zu sehen, also **VORSTELLUNGEN** gebildet und so Ihre Entscheidungen gefällt. | | | | | | | Auch hier könnten Sie in unterschiedlichster Weise vorgegangen sein. Sie haben vielleicht die linken oder die rechten Würfel in ihrem Aufbau, also der Lage, der Beziehung Ihrer Deckflächen (Mus-ter) zueinander innerlich zu beschreiben versucht und überlegt, ob der Würfel auf der rechten Seite genauso aufgebaut ist. Sie haben möglicherweise auch auf bestimmte Deckflächen (Muster) geachtet, diese jeweils zwischen den Würfeln hinsichtlich ihrer Lage verglichen und überlegt, wie sich andere Deckflächen (Mus-ter) davon abhängig in ihrer Lage verändern müssen. Vielleicht haben Sie auch ganz anders überlegt. **Wichtig ist**, Sie haben über die Würfel oder ihre Deckflächen (Muster) **NACHGEDACHT** und so Ihre Entscheidungen gefällt. |
| aus-schließlich | fast nur | mehr-heitlich | ein wenig mehr | ein wenig mehr | mehr-heitlich | fast nur | aus-schließlich |

**Wie war Ihr Bearbeiten durch VORSTELLEN im Detail?**

B3 Wenn Sie vorgestellt haben, haben Sie **Bewegungen oder bereits gedrehte bzw. gekippte Lagen** der Würfel oder ihrer Deckflächen (Muster) **vorgestellt**?

| **BEWEGUNGEN VORGESTELLT:** Sie haben die Würfel oder ihre Deckflächen (Muster) **gedreht bzw. gekippt** oder sich selbst in der Vorstellung **bewegt**, d.h. Sie haben einen **Bewegungsablauf** gesehen. | | | | | | | **NEUE LAGEN VORGESTELLT:** Sie haben die Würfel oder ihre Deckflächen (Muster) in **gedrehten bzw. gekippten Lagen** vorgestellt, Sie haben dabei **keinen Bewegungsablauf** gesehen. |
|---|---|---|---|---|---|---|---|
| aus-schließlich | fast nur | mehr-heitlich | ein wenig mehr | ein wenig mehr | mehr-heitlich | fast nur | aus-schließlich |

B4 Wenn Sie vorgestellt haben, haben Sie dabei die Würfel **als Ganzes** oder nur **einzelne Deckflächen (Muster)** vorgestellt oder in der Vorstellung bewegt?

| **GANZ VORGESTELLT:** Sie haben die Würfel immer **als ganzes** vorgestellt. | | | | | | | **MUSTER VORGESTELLT:** Sie haben nur **einzelne Deckflächen (Muster)** der Würfel vorgestellt. |
|---|---|---|---|---|---|---|---|
| aus-schließlich | fast nur | mehr-heitlich | ein wenig mehr | ein wenig mehr | mehr-heitlich | fast nur | aus-schließlich |

B5 Wenn Sie vorgestellt haben, haben Sie die **Würfel bzw. ihre Deckflächen (Muster)** oder **sich selbst** in der Vorstellung **bewegt bzw. in anderen Lagen vorgestellt**?

| **WÜRFEL:** Sie haben die Bewegungen oder neuen Lagen der **Würfel oder ihrer Deckflächen (Muster)** vorgestellt. | | | | | | | **SELBST:** Sie haben **sich selbst** in der Vorstellung um die Würfel bewegt bzw. neue Positionen eingenommen, die Würfel blieben fest. |
|---|---|---|---|---|---|---|---|
| aus-schließlich | fast nur | mehr-heitlich | ein wenig mehr | ein wenig mehr | mehr-heitlich | fast nur | aus-schließlich |

B6 Wie **klar und deutlich** waren Ihre Vorstellungen?

| **DEUTLICH:** Ihre Vorstellungen waren vollkommen deutlich und klar **wie bei wirklichem Sehen.** | | | | | | | **SELBST:** Ihre Vorstellungen waren fast nicht erkennbar, eher **nur ein Wissen, wo sich die einzelnen Teile befinden**. |
|---|---|---|---|---|---|---|---|
| voll-kommen | fast voll-kommen | weit-gehend | ein wenig mehr | ein wenig mehr | weit-gehend | fast voll-kommen | voll-kommen |

B7 Wie **selbständig** liefen die Bewegungen in der Vorstellung ab bzw. tauchten die neuen Ansichten auf?

| **VON SELBST:** Die Bewegungen, **Veränderungen liefen von selbst ab** bzw. die neuen Ansichten **tauchten von selbst auf**. | | | | | | | **AKTIV DURCHGEFÜHRT:** Die Bewegungen, die neuen Ansichten mußten von Ihnen im Geiste **aktiv konstruiert** werden. |
|---|---|---|---|---|---|---|---|
| ausschließlich | fast nur | mehrheitlich | ein wenig mehr | ein wenig mehr | mehrheitlich | fast nur | ausschließlich |

B8 Glauben Sie, daß die Beschreibungen, die Sie soeben zum **VORSTELLEN** machen konnten, dem entsprechen, was bei der Bearbeitung der Würfelaufgaben „in Ihrem Kopf" vorgegangen ist?

| **ENTSPRICHT:** Die Beschreibung entspricht vollkommen dem, was „in Ihrem Kopf" vorgegangen ist. | | | | | | | **ENTSPRICHT NICHT:** Die Beschreibung entspricht nicht dem, was „in Ihrem Kopf" vorgegangen ist. |
|---|---|---|---|---|---|---|---|
| vollkommen | fast vollkommen | weitgehend | ein wenig mehr | ein wenig mehr | weitgehend | fast vollkommen | vollkommen |

---

**Wie war Ihr Bearbeiten durch NACHDENKEN im Detail?**

(bitte lassen Sie die folgenden 5 Fragen aus, falls Sie niemals "nachgedacht" haben)

B9 Wenn Sie nachgedacht haben, wie sind Sie vorgegangen?

| **AUFBAU ÜBERLEGT:** Sie haben jeweils den **Aufbau der Würfel, also die Lagen, die Beziehungen der Deckflächen (Muster) zueinander analysiert** und dann überlegt, ob diese Beziehungen bei den zu vergleichenden Würfeln gelten. | | | | | | | **VERÄNDERUNGEN ÜBERLEGT:** Sie haben sich jeweils die **Veränderungen zwischen den zu vergleichenden Würfeln überlegt**, d.h. Sie haben darauf geachtet, wie sich die Lage einzelner Deckflächen (Mus-ter) in Abhängigkeit vom Kippen oder Drehen anderer Deckflächen (Muster) verändert. |
|---|---|---|---|---|---|---|---|
| ausschließlich | fast nur | mehrheitlich | ein wenig mehr | ein wenig mehr | mehrheitlich | fast nur | ausschließlich |

B10 Wenn Sie nachgedacht haben, haben Sie den **ganzen Würfel** oder nur **einzelne Deckflächen (Muster)** in Ihre Überlegungen einbezogen?

| **GANZ BERÜCKSICHTIGT:** Sie haben die Würfel **als ganzes** berücksichtigt. | | | | | | **MUSTER BERÜCKSICHTIGT:** Sie haben nur **einzelne Deckflächen (Muster)** der Würfel vorgestellt. | |
|---|---|---|---|---|---|---|---|
| ausschließlich | fast nur | mehrheitlich | ein wenig mehr | ein wenig mehr | mehrheitlich | fast nur | ausschließlich |

B11 Wenn Sie nachgedacht haben, haben Sie Ihre **eigene Position berücksichtigt**?

| **EIGENE POSITION:** Sie haben die Würfel oder die Veränderungen **aus Ihrer eigenen Person** überlegt (z.B. „zeigt von **mir** weg“). | | | | | | **KEINE EIGENE POSITION:** Sie haben die Würfel oder die Veränderungen **unabhängig von Ihrer eigenen Position** überlegt. | |
|---|---|---|---|---|---|---|---|
| ausschließlich | fast nur | mehrheitlich | ein wenig mehr | ein wenig mehr | mehrheitlich | fast nur | ausschließlich |

B12 Wenn Sie nachgedacht haben, wie bewußt waren Ihnen während der Bearbeitung Ihre Gedanken?

| **BEWUSST:** Ihre Überlegungen waren Ihnen vollkommen bewußt, Sie haben mit sich **„innerlich gesprochen“.** | | | | | | **UNBEWUSST:** Ihre Überlegungen waren Ihnen vollkommen unbewußt, Sie liefen **ganz automatisch** ab**.** | |
|---|---|---|---|---|---|---|---|
| vollkommen | fast vollkommen | weitgehend | ein wenig mehr | ein wenig mehr | weitgehend | fast vollkommen | vollkommen |

B13 Glauben Sie, daß die **Beschreibung**, die Sie soeben zum **NACHDENKEN** machen konnten, dem **entspricht**, was bei der Bearbeitung der Würfelaufgaben „in Ihrem Kopf“ vorgegangen ist?

| **ENTSPRICHT:** Die Beschreibung entspricht vollkommen dem, was „in Ihrem Kopf“ vorgegangen ist. | | | | | | **ENTSPRICHT NICHT:** Die Beschreibung entspricht nicht dem, was „in Ihrem Kopf“ vorgegangen ist. | |
|---|---|---|---|---|---|---|---|
| vollkommen | fast vollkommen | weitgehend | ein wenig mehr | ein wenig mehr | weitgehend | fast vollkommen | vollkommen |

Coding: 1...8

Responses to the questions of questionnaire B [Median(Range)]; EEG/MR: responses for subjects included in the EEG (Ngood=14, Npoor=12)/MR (Ngood=13, Npoor=8) analyses

| | | **GOOD** | **POOR** | | **GOOD** | **POOR** |
|---|---|---|---|---|---|---|
| | B1 | 3 (1-6) | 3 (1-6) | | 3 (1-6) | 3 (2-6) |
| | B2 | 3 (1-6) | 3 (1-4) | | 3 (1-6) | 3 (1-4) |
| | B3 | 3.5 (2-7) | 3 (1-7) | | 3.5 (2-7) | 4 (1-7) |
| | B4 | 3.5 (1-7) | 5 (1-8) | | 3.5 (1-7) | 5 (1-8) |
| | B5 | 2 (1-4) | 2 (1-3) | | 2 (1-4) | 2 (1-3) |
| **EEG** | B6 | 3 (1-6) | 3 (3-7) | **MR** | 3 (2-6) | 3 (3-7) |
| | B7 | 4 (1-6) | 6 (3-7) | | 4 (1-6) | 6.5 (4-7) |
| | B8 | 3 (2-4) | 3 (1-3) | | 3 (2-4) | 3 (3-3) |
| | B9 | 3.5 (2-7) | 6 (3-7) | | 3.5 (2-7) | 6 (5-7) |
| | B10 | 5 (1-7) | 6 (3-7) | | 5 (2-7) | 6.5 (3-7) |
| | B11 | 7 (3-8) | 6 (2-8) | | 7 (3-8) | 7 (3-8) |
| | B12 | 3 (2-6) | 3 (2-5) | | 3 (2-6) | 3 (2-5) |
| | B13 | 3 (2-4) | 3 (1-7) | | 3 (2-4) | 3 (2-7) |

## 8. Wrap up and conclusions

The primary intention of this thesis was to achieve a more detailed account of the functional neuroanatomy of dynamic visuo-spatial imagery. This was attained via an investigation of brain activity during solving of a three-dimensional cube comparison task using a combination of functional magnetic resonance imaging (fMRI) and event-related slow cortical potentials (SCPs; chapters 6 and 7). In addition, several methodological issues have been investigated (chapters 3 to 5). The structure of the empirical part of this thesis is shown in Table 8-1.

Table 8-1: Overview of the empirical chapters of this thesis.

| Main Focus On: | Chapter | Contents |
|---|---|---|
| *Methods* | *3* | *Co-registration using spline-interpolated head shape reconstruction* |
| *Methods* | *4* | *Spatial accuracy of SCPs using different interpolation algorithms* |
| *Methods/Neuro-anatomy* | *5* | *Assessment of inter-trial consistency in neural activity using single-trial fMRI* |
| *Neuroanatomy* | *6* | *Brain activity during dynamic visuo-spatial imagery - assessment of parietal and premotor activity* |
| *Neuroanatomy* | *7* | *Individual differences in brain activity during dynamic visuo-spatial imagery - neural efficiency* |

In *chapter 3*, a new method for the co-registration of EEG and MRI data has been presented. This method relies on an iterative matching of the MRI-segmented head surface with the head surface reconstructed using spline-interpolation of individually digitized electrode coordinates. The results revealed a high co-registration accuracy and a high practicability of the method. Thus, it seems justified to recommend this new co-registration approach for future multi-modality imaging studies. In addition, the high accuracy of the surface matching also suggests to utilize spline-interpolated surface reconstructions for the display of 3D-rendered EEG and ERP maps. Importantly, it was shown that this approach is not limited to high-resolution EEG studies, but can also be used when only 22 channels and electrode coordinates are available for EEG measurements.

In *chapter 4*, it was investigated whether the spatial accuracy of SCP maps can be increased using individual electrode coordinates and realistic head models. Spatial accuracy was assessed via comparing the interpolation error of SCP maps computed with individual or standard electrode coordinates and realistic or spherical

head models. The results revealed that interpolation errors were lowest when interpolation was performed using individual electrode coordinates and realistic head models. This was in agreement with the hypothesis that mapping accuracy is increased when electrode coordinates are precisely known and when the surface from which EEG is recorded is modeled more accurately. Thus, it seems mandatory to invest the additional time and effort required by the digitization of electrode coordinates, since this will result in an increase in the accuracy of scalp potential maps. Although the analyses have been restricted to SCP components, it seems plausible to assume that this conclusion is also valid for other EEG-derived indices of neural activity. In addition, an even higher increase in spatial accuracy might be obtained for dipole solutions or other source localization algorithms.

The aim of the study presented in *chapter 5* was to assess the consistency of brain activity across repeated executions of the same type of tasks. To this end, fMRI data were analyzed using a new analysis concept. This concept was based on an identification of the activity evoked by single task executions. Most brain regions which are known to be involved in visuo-spatial processing showed highly consistent activity across trials. On the other hand, a region in the prefrontal cortex, the so-called dorso-lateral prefrontal cortex (DLPFC), was active only in some trials. This suggests that averaging across trials might result in a loss of information in cognitive neuroimaging. However, no definite answer could be obtained concerning the aspects of task processing which were modulating activity in the DLPFC. Thus, further studies are necessary in order to identify the cognitive processes which were additionally required by the active trials - with one plausible explanation for the lower consistency of activity being the amount of information which had to be kept in working memory. Nevertheless, the analysis concept presented in chapter 5 has revealed new information concerning the neural bases of cognitive processing and might thus be useful in further studies. One might even anticipate an application of single-trial analysis in the development of psychological tests - since task items which are recruiting different brain regions than other task items might affect the unidimensionality (Rasch, 1980) of a test. However, at least two requisites have to be met before such an application will be feasible: First, it needs to be shown that the recruitment of different brain regions also implies a recruitment of different cognitive functions. Second, it will be necessary to separate inter-trial variability which results from "true" variations in cognitive processing from inter-trial variability which results from artifacts and technical noise. This might be achieved via improved statistical models, but also via improvements in MR scanner hardware (e.g., higher field strengths, more homogeneous magnetic fields, faster gradients).

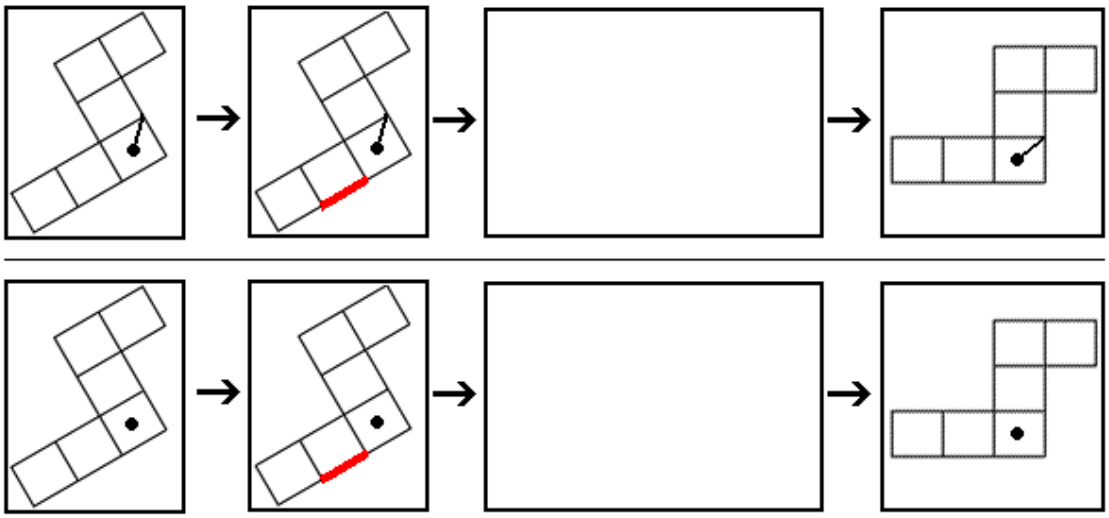

Fig. 8-1: Samples for the tasks which are used in a follow-up study to this thesis. In this study, it is investigated whether premotor cortex activity is functionally relevant for dynamic visuo-spatial imagery, or rather results from unspecific co-activation of premotor neurons. To this end, the main phases involved in the solving of a dynamic imagery task are separated, and the amount of spatial information which has to be processes is modulated. Subjects are presented with a two-dimensional object containing either a visual or a spatial geometrical symbol. After 2 seconds of inspection time, an orange bar indicates how the object has to be rotated. During rotation, no visual input is provided (indicated by the blank screen). After about four seconds, the object with which the mentally rotated object has to be compared is presented, and subjects have to decide whether the real and the imagined object match.

The main intention of the study presented in *chapter 6* was to identify the brain regions which are active during dynamic visuo-spatial imagery. In particular, the question was addressed whether premotor cortex is active during task processing. Using a combination of single-trial fMRI and SCPs, brain activity evoked by the processing of a three-dimensional cube comparison test was assessed with increased spatial and temporal resolution. The results revealed that a number of areas was involved in task processing, including lateral and medial premotor cortex. This provides some support for the hypothesis that mental and manual object manipulation are functionally equivalent. On a conceptual level, the results seem to indicate a tight coupling of spatial perception and imagery on the one and motor acts or motor behavior on the other hand. However, before this conclusion can be drawn, it needs to be shown whether premotor cortex activity truly reflects functionally relevant processing, or rather results from unspecific coactivation of premotor neurons. This is currently investigated in a follow-up study to this thesis. In this study, it is investigated whether premotor cortex activity is evoked by mental rotation only, or whether the numerous other processing steps which are involved in the solving of dynamic imagery tasks (e.g. perceptual analysis, image generation, stimulus matching) also activate premotor cortex. This question is addressed by a newly developed task paradigm which allows for an explicit separation of these different processes (see Fig. 8-1). In addition, it is investigated whether the amount of spatial information which has to be processed modulates premotor cortex activity. If this is the case, and if the

premotor cortex is active during all task processing steps, this would indicate that motor regions are functionally relevant for spatial processing and spatial imagery.

In the last empirical chapter (*chapter 7*), two alternative hypotheses concerning the results of two former SCP studies were investigated. These studies had revealed a lower amount of neural activity in subjects who were more proficient in the processing of the task used in chapters 5 and 6. The lower amount of neural activity might be explained either in the sense of an algorithmic efficiency hypothesis, which states that more proficient subjects dispose of a more efficient neural network for task solving, or in the sense of a perceptual analysis/sensory gating hypothesis, which postulates that subjects with higher ability show a better sensory-perceptual analysis of the visuo-spatial stimuli. In order to test these hypotheses, brain activity in a group of subjects with good and poor ability was compared using fMRI and SCPs. Although the same experimental design as in the former studies was used, and although the two groups were clearly different on the behavioral level, no difference in brain activity between groups could be observed. Thus, no definite answer concerning the two hypotheses which should be tested could be presented. The rather unexpected result of a lack of individual differences might be interpreted in several ways. On the one hand, it might be that the sample investigated in this thesis was different from the samples investigated in the former studies. However, it can be excluded that such differences occurred in variables as task-specific ability, general intelligence, gender, age and handedness, since all these variables were controlled and vastly identical in both the former studies and in this thesis. Second, a slight difference in the way tasks were presented in the study performed for this thesis might explain the lack of individual differences. This difference was the amount of visual input which had to be processed upon task presentation. The validity of this explanation could be easily tested in a further replication study in which the amount of visual input is systematically varied. To conclude, the study presented in chapter 7 indicates that even small differences in experimental design, or in the subjects investigated, might affect the results of brain imaging studies. One problem which should be particularly considered in the investigation of individual differences is sample size. Even though the samples investigated were comparably large, it seems that a perfect control or balancing out of the confounding effects of uncontrolled or uncontrollable variables might not have been achieved.

## *Acknowledgments*

This thesis would not have been possible without the financial and personal support from several institutions and person.

Thus, I would like to acknowledge the financial support from the following institutions:

The *Jubiläumsfonds der Oesterreichischen Nationalbank*, who partially funded the studies described in chapters 3 to 7 (projects # 7174, 8184).

The *University of Vienna*, *faculty for Human- and Social Sciences*, who supported me with a research grant ("Förderstipendium") and with travel grants which allowed me to present the results of this thesis on several international conferences.

The *Austrian Research Association*, who supported me with a short-term scholarship (program "International Communication"). This scholarship gave me the chance to present the results of chapters 4 and 7 at the 6th Annual Meeting of the Organization for Human Brain Mapping in San Antonio/USA.

In addition, I would like to express my gratitude to the following persons:

The head of the BRL (Brain Research Laboratory, Department of Psychology, University of Vienna), *Herbert Bauer*, and the head of the AG NMR (Institute for Medical Physics, University of Vienna), *Ewald Moser*. They not only gave me access to state-of-the art bneuroimaging methods, but also allowed me to perform my thesis in a highly stimulating and efficient academic environment.

*Christian Windischberger* - for his expertise in performing and analyzing fMRI data, and for many stimulating and fruitful discussions (not only about fMRI, physics and neuroscience). It has been fun to work with you, and I also thank you for numerous coffees and cigarettes (although we both wanted to stop smoking) at the MR institute.

*Ulrich Leodolter* - for his excellent technical support, and for accepting the lots of programming work and advice he had to provide for many of the analyses performed in this thesis.

*Oliver Vitobuch* - for his interest in Music Psychology, which gave me the chance to become his successor as a research assistant in the BRL, and for his feedback on some of the chapters of this thesis.

*Nadia Taylor* - for proof reading some of the chapters of this thesis.

**Last, but not least, the greatest thank goes to my mother *Milly Lamm* - for being a wonderful and supportive mother who always accepted me the way I am.**

## *References*

Adelbauer, J. 2001. *DC-Topographie ereigniskorrelierter langsamer corticaler Potentiale induziert durch monoskope und stereoskope Reize - eine Evaluation der neuronalen Effizienzhypothese,* Unpublished Master's Thesis, University of Vienna, Faculty of Human and Social Sciences, Vienna.

Aine, C.J. 1995. A conceptual overview and critique of functional neuroimaging techniques in humans: I. MRI/fMRI and PET. *Critical Reviews in Neurobiology* **9:** 229-309.

Alivisatos, B., and Petrides, M. 1997. Functional activation of the human brain during mental rotation. *Neuropsychologia* **35:** 111-118.

Anderson, T.J., Jenkins, I.H., Brooks, D.J., Hawken, M.B., Frackowiak, R.S.J., and Kennard, C. 1994. Cortical control of saccades and fixation in man. A PET study. *Brain* **117:** 1073-1084.

Annett, M. 1985. *Left, right, hand, and brain: the right shift theory*, Erlbaum, London.

Babiloni, F., Babiloni, C., Carducci, F., Fattorini, L., Anello, C., Onorati, P., and Urbano, A. 1997. High resolution EEG: a new model-dependent spatial deblurring method using a realistically-shaped MR-constructed subject's head model. *Electroencephalography and Clinical Neurophysiology* **102:** 69-80.

Babiloni, F., Babiloni, C., Carducci, F., Fattorini, L., Onorati, P., and Urbao, A. 1996. Spline laplacian estimate of EEG potentials over a realistic magnetic resonance-constructed head surface model. *Electroencephalography and Clinical Neurophysiology* **98:** 363-373.

Bain, A. 1855. *The senses and the intellect*, Parker, London.

Bajric, J., Rösler, F., Heil, M., and Hennighausen, E. 1999. On separating processes of event categorization, task preparation, and mental rotation proper in a handedness recognition task. *Psychophysiology* **36:** 399-408.

Ball, T., Schreiber, A., Feige, B., Wagner, M., Lücking, C.H., and Kristeva-Feige, R. 1999. The role of higher-order motor areas in voluntary movement as revealed by high-resolution EEG and fMRI. *Neuroimage* **10:** 682-694.

Bandettini, P.A., Jesmanowicz, A., Wong, E.C., and Hyde, J.S. 1993. Processing strategies for time-course data sets in functional MRI of the human brain. *Magnetic Resonance in Medicine* **30:** 161-173.

Barnes, J., Howard, R.J., Senior, C., Brammer, M., Bullmore, E.T., Simmons, A., Woodruff, P., and David, A.S. 2000. Cortical activity during rotational and linear transformations. *Neuropsychologia* **38:** 1148-1156.

Barnett, G.H., Kormos, D.W., Steiner, C.P., and Morris, H. 1993. Registration of EEG electrodes with three-dimensional neuroimaging using a frameless, armless stereotactic wand. *Stereotactic and Functional Neurosurgery* **61:** 32-38.

Bauer, H. 1998. Slow potential topography. *Behavioral Research Methods, Instruments, and Computers* **30:** 20-33.

Bauer, H., Birbaumer, N., and Rösler, F. 1998. Slow scalp recorded brain potentials, sensory processing and cognition. In *Glial cells: their role in behaviour* (P.R. Laming, E. Sykova, A. Reichenbach, G.I. Hatton, and H. Bauer, Eds.), pp. 267-290. Cambridge University Press, Cambridge.

Bauer, H., Korunka, C., and Leodolter, M. 1989. Technical requirements for high-quality scalp DC recordings. *Electroencephalography and Clinical Neurophysiology* **72:** 545-547.

Bauer, H., Korunka, C., and Leodolter, M. 1993. Possible glial contribution in the electrogenesis of SPs. In *Slow potential changes in the human brain* (W.C. McCallum, and S.H. Curry, Eds.), pp. 23-34. Plenum Press, New York.

Bauer, H., Lamm, C., Holzreiter, S., Holländer, I., Leodolter, U., and Leodolter, M. 2000. Measurement of 3D electrode coordinates by means of a 3D photogrammetric head digitizer. *Neuroimage* **11:** S461.

Bauer, H., Steinringer, H., and Schock, P. 1980. A new highly sensitive DC-amplifier for steady biopotential recording. *Archiv für Psychologie* **133:** 333-337.

Baumgartner, R., Scarth, G., Teichtmeister, C., Somorjai, R., and Moser, E. 1997. Fuzzy clustering of gradient-echo functional MRI in the human visual cortex. Part I: reproducibility. J*ournal of Magnetic Resonance Imaging* **7:** 1094-1101.

Belliveau, J.W., Kennedy, D.N.J., McKinstry, R.C., Buchbinder, B.R., Weisskoff, R.M., Cohen, M.S., Vevea, J.M., Brady, T.J., and Rosen, B.R. 1991. Functional mapping of the human visual cortex by magnetic resonance imaging. *Science* **254:** 716-719.

Birbaumer, N., Elbert, T., Canavan, A.G.M., and Rockstroh, B. 1990. Slow potentials of the cerebral cortex and behavior. *Physiological Reviews* **70:** 1-41.

Birbaumer, N., and Schmidt, R.F. 1999. *Biologische Psychologie*, Springer-verlag, Berlin.

Blüml, S., Schad, L.R., Stepanow, B., and Lorenz, W.J. 1993. Spin-lattice relaxation time measurement by means of a TurboFLASH technique. *Magnetic Resonance in Medicine* **30:** 289-295.

Böcker, K.B.E., van Avermaete, J.A.G., and van den Berg-Lennsen, M.M.C. 1994. The international 10-20 system revisited: cartesian and spherical co-ordinates. *Brain Topography* **6:** 231-235.

Boik, R.J. 1981. A priori tests in repeated measures designs: effects of nonsphericity. *Psychometrika* **46:** 241-255.

Bortz, J. 1993. *Statistik für Sozialwissenschafter*, Springer-Verlag, Berlin.

Brett, M. The MNI brain and the Talairach atlas, 1999. http://www.mrc-cbu.cam.ac.uk/Imaging/mnispace.html

Brinkmann, B.H., O'Brien, T.J., Dresner, M.A., Lagerlund, T.D., Sharbrough, F.W., and Robb, R.A. 1998. Scalp-recorded EEG localization in MRI volume data. *Brain Topography* **10:** 245-253.

Buckner, R.L., Bandettini, P.A., O'Craven, K.M., Savoy, R.L., Petersen, S.E., Raichle, M.E., and Rosen, B.R. 1996. Detection of cortical activation during averaged single trials of a cognitive task using functional magnetic resonance imaging. *Proceedings of the National Academy of Sciences USA* **93:** 14878-14883.

Buckner, R.L., Koutstaal, W., Schacter, D.L., Dale, A.M., Rotte, M., and Rosen, B.R. 1998. Functional-anatomic study of episodic retrieval. II. Selective averaging of event-related fMRI trials to test the retrieval success hypothesis. *Neuroimage* **7:** 163-175.

Bullmore, E.T., Brammer, M.J., Rabe-Hesketh, S., Curtis, V.A., Morris, R.G., Williams, S.C., Sharma, T., and McGuire, P.K. 1999. Methods for diagnosis and treatment of stimulus-correlated motion in generic brain activation studies using fMRI. *Human Brain Mapping* **7:** 38-48.

Carpenter, P.A., and Just, M. 1975. Sentence comprehension: a psycholinguistic processing model of verification. *Psychological Review* **82:** 45-73.

Carpenter, P.A., Just, M.A., Keller, T.A., and Eddy, W. 1999. Graded functional activation in the visuospatial system with the amount of task demand. *Journal of Cognitive Neuroscience* **11:** 9-21.

Carpenter, P.A., Just, M.A., and Reichle, E.D. 2000. Working memory and executive function: evidence from neuroimaging. *Current Opinion in Neurobiology* **10:** 195-199.

Caspers, H. 1993. DC potentials of the brain. In *Slow potential changes in the brain* (W. Haschke, E.-J. Speckmann, and A.I. Roitbak, Eds.), pp. 9-20. Birkhäuser, Boston.

Caspers, H., Speckmann, E.J., and Lehmenkühler, A. 1980. Electrogenesis of cortical DC potentials. In *Motivation, motor and sensory processes of the brain. Electrical potentials, behavior and clinical use (Progress in brain research 54)* (H.H. Kornhuber, and L. Deecke, Eds.), pp. 3-16. Elsevier, Amsterdam.

Cohen, D., and Kubovy, M. 1993. Mental rotation, mental representation, and flat slopes. *Cognitive Psychology* **25:** 351-382.

Cohen, M.S. 1996. Rapid MRI and functional applications. In *Brain mapping: the methods* (A.W. Toga, and J.C. Mazziotta, Eds.), pp. 223-255. Academic Press, San Diego.

Cohen, M.S. 1999. Echo-planar imaging and functional MRI. In *Functional MRI* (C.T.W. Moonen, and P.A. Bandettini, Eds.), pp. 137-148. Springer-Verlag, Berlin.

Cohen, M.S., Kosslyn, S.M., Breiter, H.C., DiGirolamo, G.J., Thompson, W.L., Anderson, A.K., Bookheimer, S.Y., Rosen, B.R., and Belliveau, J.W. 1996. Changes in cortical activity during mental rotation: a mapping study using functional MRI. *Brain* **119:** 89-100.

Cooper, L.A., and Shepard, R.N. 1984. Turning something over in the mind. *Scientific American* **251:** 106-114.

Corballis, M.C., and McLaren, R. 1982. Interaction between perceived and imagined rotation. *Journal of Experimental Psychology: Human Perception and Performance* **8:** 215-224.

Corballis, M.C., Zebrodoff, N.J., Shetzer, L.I., and Butler, B.B. 1978. Decisions about identity and orientation of rotated letters and digits. *Memory & Cognition* **6:** 98-107.

Corballis, P.M., and Corballis, M.C. 1993. How apparent motion affects mental rotation: Push or pull? *Memory and Cognition* **21:** 458-466.

Corbetta, M. 1998. Frontoparietal cortical networks for directing attention and the eye to visual locations: identical, independent, or overlapping neural systems? *Proceedings of the National Academy of Sciences USA* **95:** 831-838.

Corbetta, M., Akbudak, E., Conturo, T.E., Snyder, A.Z., Ollinger, J.M., Drury, H.A., Linenweber, M.R., Petersen, S.E., Raichle, M.E., Van Essen, D.C., and Shulman, G.L. 1998. A common network of functional areas for attention and eye movements. *Neuron* **21:** 761-773.

Crease, R.P. 1991. Images of conflict: MEG vs. EEG. *Science* **253:** 374-375.

Cui, R.Q., Hutter, D., Lang, W., and Deecke, L. 1999. Neuroimage of voluntary movement: Topography of the Bereitschaftspotential, a 64-channel DC current source density study. *Neuroimage* **9:** 124-134.

Cunnington, R., Windischberger, C., Barth, M., Beisteiner, R., Edward, V., Erdler, M., Kaindl, T., and Moser, E. 1999. Single-event functional MRI of supplementary and primary motor cortical areas. *Neuroimage* **9:** S465.

Decety, J., and Grèzes, J. 1999. Neural mechanisms subserving the perception of human actions. *Trends in Cognitive Sciences* **3:** 172-178.

DeMunck, J.C., Vijn, P.C.M., and Spekreijse, H. 1991. A practical method for determining electrode positions on the head. *Electroenecephalography and Clinical Neurophysiology* **78:** 85-87.

D'Esposito, M., Zarahn, E., and Aguirre, G.K. 1999. Event-related functional MRI: implications for cognitive psychology. *Psychological Bulletin* **125:** 155-164.

Diwadkar, V.A., Carpenter, P.A., and Just, M.A. 2000. Collaborative activity between parietal and dorso-lateral prefrontal cortex in dynamic spatial working memory revealed by fMRI. *Neuroimage* **12:** 85-99.

Elbert, T. 1993. Slow cortical potentials reflect the regulation of cortical excitability. In *Slow potential changes in the human brain* (W.C. McCallum, and S.H. Curry, Eds.), pp. 235-254. Plenum Press, New York.

Ertl, J., and Schafer, E. 1969. Brain response correlates of psychometric intelligence. *Nature* **223:** 421-422.

Evans, A.C., Collins, D.L., Mills, S.R., Brown, E.D., Kelly, R.L., and Peters, T.M. 1993. 3D statistical neuroanatomical models from 305 MRI volumes. *Proceedings IEEE-Nuclear Science Symposium and Medical Imaging Conference***:** 1813-1817.

Fabiani, M., Gratton, G., Corballis, P.M., Cheng, J., and Friedman, D. 1998. Bootstrap assessment of the reliability of maxima in surface maps of brain activity of individual subjects derived with electrophysiological and optical methods. *Behavior Research Methods, Instruments, & Computers* **30:** 78-86.

Fitzgerald, R., Lamm, C., Oczenski, W., Stimpfl, T., Vycudilik, W., and H., B. 2001. Direct current auditory evoked potentials during wakefulness, anesthesia, and emergence of anesthesia. *Anesthesia and Analgesia* **92:** 154-160.

Flexer, A. 1999. *Spatio-temporal clustering of cognitive evoked potentials*, Unpublished Ph.D. thesis/University of Vienna, Vienna.

Fox, P.T., Raichle, M.E., Mintun, M.A., and Dence, C. 1988. Nonoxidative glucose consumption during focal physiological neural activity. *Science* **241:** 462-464.

Fretska, E., Bauer, H., Leodolter, M., and Leodolter, U. 1999. Loss of control and negative emotions: a cortical slow potential topography study. *International Journal of Psychophysiology* **33:** 127-141.

Friston, K.J., Holmes, A., Poline, J.-B., Price, C.J., and Frith, C.D. 1995a. Detecting activations in PET and fMRI: levels of inference and power. *Neuroimage* **40:** 223-235.

Friston, K.J., Holmes, A.P., and Worsley, K.J. 1999. How many subjects constitute a study? *Neuroimage* **10:** 1-5.

Friston, K.J., Holmes, A.P., Worsley, K.J., Poline, J.P., Frith, C.D., and Frackowiak, R.S.J. 1995b. Statistical parametric maps in functional imaging: A general linear approach. *Human Brain Mapping* **2:** 189-210.

Gaillard, A.W.K., and Näätänen, R. 1980. Some baseline effects on the CNV. *Biological Psychology* **10:** 31-39.

Gazzaniga, M.S., Ivry, R.B., and Mangun, G.R. 1998. *Cognitive Neuroscience - the biology of the mind*, W.W. Norton & Company, New York.

Georgopoulos, A.P. 2000. Neural aspects of cognitive motor control. *Current Opinion in Neurobiology* **10:** 238-241.

Georgopoulos, A.P., and Pellizzer, G. 1995. The mental and the neural: psychological and neural studies of mental rotation and memory scanning. *Neuropsychologia* **33:** 1531-1547.

Gerloff, C., Grodd, W., Altenmüller, E., Kolb, R., Naegele, T., Klose, U., Voigt, K., and Dichgans, J. 1996. Coregistration of EEG and fMRI in a simple motor task. *Human Brain Mapping* **4:** 199-209.

Gevins, A., Le, J., Brickett, P., Reutter, B., and Desmond, J.E. 1991. Seeing through the skull: advanced EEGs use MRIs to accurately measure cortical activity from the scalp. *Brain Topography* **4:** 125-131.

Gevins, A., Le, J., Martin, N.K., Brickett, P., Desmond, J., and Reutter, B. 1994. High resolution EEG: 124-channel recording, spatial deblurring and MRI integration methods. *Electroencephalography and Clinical Neurophysiology* **90:** 337-358.

Gevins, A., and Smith, M.E. 2000. Neurophysiological measures of working memory and individual differences in cognitive ability and cognitive style. *Cerebral Cortex* **10:** 829-839.

Gevins, A., Smith, M.E., McEvoy, L.K., Leong, H., and Le, J. 1999. Electroencephalographic imaging of higher brain function. *Philosophical Transactions of the Royal Society of London. Series B: Biological Sciences* **354:** 1125-1133.

Gittler, G. 1990. *Dreidimensionaler Würfeltest (3DW): Ein Rasch-skalierter Test zur Messung des räumlichen Vorstellungsvermögens, Theoretische Grundlagen und Manual*, Beltz Test, Weinheim.

Glaser, E.M., and Ruchkin, D.S. 1976. *Principles of neurobiological signal analysis*, Academic Press, New York.

Goldman, R.I., Stern, J.M., Engel, J., and Cohen, M.S. 2000. Acquiring simultaneous EEG and functional MRI. *Clinical Neurophysiology* **111:** 1974-1980.

Grafton, S.T., Fadiga, L., Arbib, M.A., and Rizzolatti, G. 1997. Premotor cortex activation during observation and naming of familiar tools. *Neuroimage* **6:** 231-236.

Greenhouse, S.W., and Geisser, S. 1959. On methods in the analysis of profile data. *Psychometrika* **24:** 95–112.

Gulliksen, H. 1965. *Theory of mental tests*, Wiley, New York.

Haier, R.J. 1993. Cerebral glucose metabolism and intelligence. In *Biological approaches to the study of human intelligence* (P.A. Vernon, Ed.), pp. 317-332. Ablex, Norwood (NJ).

Haier, R.J., and Benbow, C.P. 1995. Sex differences and lateralization in temporal lobe glucose metabolism during mathematical reasoning. *Developmental Neuropsychology* **11:** 405-414.

Haier, R.J., Siegel, B., MacLachlan, A., Soderling, E., Lottenberg, S., and Buchsbaum, M.S. 1992. Regional glucose metabolic changes after learning a com-

plex visuospatial/motor task: a positron emission tomographic study. *Brain Research* **570:** 134-143.

Haier, R.J., Siegel, B., Nuechterlein, K.H., Hazlett, E., Wu, J.C., Paek, J., Browning, H.L., and Buchsbaum, M.S. 1988. Cortical glucose metabolic rate correlates of abstract reasoning and attention studied with positron emission tomography. *Intelligence* **12:** 199-217.

Haig, A.R., Gordon, E., and Hook, S. 1997. To scale or not to scale: McCarthy and Wood revisited. *Electroencephalography and Clinical Neurophysiology* **103:** 323-325.

Hajnal, J.V., Myers, R., Oatridge, A., Schwieso, J.E., Young, I.R., and Bydder, G.M. 1994. Artifacts due to stimulus correlated motion in functional imaging of the brain. *Magnetic Resonance in Medicine* **31:** 283-291.

Harris, I.M., Egan, G.F., Sonkkila, C., Tochon-Danguy, H.J., Paxinos, G., and Watson, J.D. 2000. Selective right parietal lobe activation during mental rotation: a parametric PET study. *Brain* **123:** 65-73.

Haufler, A.J., Spalding, T.W., Santa Maria, D.L., and Hatfield, B.D. 2000. Neurocognitive activity during a self-paced visuospatial task: comparative EEG profiles in marksmen and novice shooters. *Biological Psychology* **53:** 131-160.

Haxby, J.V., Grady, C.L., Horitz, B., Ungerleider, L.G., Mishkin, M., Carson, R.E., Herscovitch, P., Shapiro, M.B., and Rapoport, S.I. 1991. Dissociation of object and spatial visual processing pathways in human extrastriate cortex. *Proceedings of the National Academy of Sciences USA* **88:** 1621-1625.

Heil, M., Bajric, J., Rösler, F., and Hennighausen, E. 1996. Event-related potentials during mental rotation: dissentangling the contributions of character classification and image transformation. *Journal of Psychophysiology* **10:** 326-335.

Heinemann, U., and Walz, W. 1998. Contribution of potassium currents and glia to slow potential shifts (SPSs). In *Glial cells: their role in behaviour* (P.R. Laming, E. Sykova, A. Reichenbach, G.I. Hatton, and H. Bauer, Eds.), pp. 197-209. Cambridge University Press, Cambridge.

Holmes, A.P., Blair, R.C., Watson, J.D., and Ford, I. 1996. Nonparametric analysis of statistic images from functional mapping experiments. *Journal of Cerebral Blood Flow and Metabolism* **16:** 7-22.

Holmes, A.P., and Friston, K.J. 1998. Generalisability, random effects and population inference. *Neuroimage* **5:** S480.

Hubel, D.H., and Wiesel, T.N. 1959. Receptive fields of single neurons in the cat's striate cortex. *Journal of Physiology* **148:** 574-591.

Humberstone, M., Sawle, G.V., Clare, S., Hykin, J., Coxon, R., Bowtell, R., MacDonald, I., and Morris, P.G. 1997. Functional magnetic resonance imaging of

single motor events reveals human presupplementary motor area. *Annals of Neurology* **42:** 632-637.

Huppertz, H.-J., Otte, M., Grimm, C., Kristeva-Feige, R., Mergner, T., and Lücking, C.H. 1998. Estimation of the accuracy of a surface matching technique for registration of EEG and MRI data. *Electroencephalography and Clinical Neurophysiology* **106:** 409-415.

Intions-Peterson, M.J. 1983. Imagery paradigms: How vulnerable are they to experimenter's expectations? *Journal of Experimental Psychology: Human Perception and Performance* **9:** 394-412.

Ives, J.R., Warach, S., Schmitt, F., Edelman, R.R., and Schomer, D.L. 1993. Monitoring the patient's EEG during echo planar MRI. *Electroencephalography and Clinical Neurophysiology* **87:** 417-420.

James, W. 1890. *The principles of psychology*, MacMillan & Co., London.

Jasper, H.H. 1958. The ten twenty electrode system of the International Federation. *Electroencephalography and Clinical Neurophysiology* **10:** 371-375.

Jausovec, N., and Jausovec, K. 2000. Differences in resting EEG related to ability. *Brain Topography* **12:** 229-240.

Jeannerod, M. 1994. The representing brain: Neural correlates of motor intention and imagery. *Behavioral and Brain Sciences* **17:** 187-202.

Johnson, P.B., Ferraina, S., Bianchi, L., and Caminiti, R. 1996. Cortical networks for visual reaching-physiological and anatomical organization of frontal and parietal lobe arm regions. *Cerebral Cortex* **6:** 102-119.

Jueptner, M., and Weiler, C. 1995. Does measurement of regional cerebral blood flow reflect synaptic activity? Implications for PET and fMRI. *Neuroimage* **2:** 148-156.

Just, M.A., and Carpenter, P.A. 1985. Cognitive coordinate systems: accounts of mental rotation and individual differences in spatial ability. *Psychological Review* **92:** 137-172.

Karniski, W., Blair, R.C., and Snider, A.D. 1994. An exact statistical method for comparing topgraphic maps, with any number of subjects and electrodes. *Brain Topography* **6:** 203-210.

Kavanagh, R.H., Darcey, T.M., Lehmann, D., and Fender, D.H. 1978. Evaluation of methods for three-dimensional localization of electrical sources in the human brain. *IEEE-Biomedical Engineering* **25**.

Keselman, H.J. 1982. Multiple comparisons for repeated measures means. *Multivariate Behavioral Research* **17:** 87-92.

Keselman, H.J. 1998. Testing treatment effects in repeated measures designs: an update for psychophysiological researchers. *Psychophysiology* **35:** 470-478.

Kim, S.G., Richter, W., and Ugurbil, K. 1997. Limitations of temporal resolution in functional MRI. *Magnetic Resonance in Medicine* **37:** 631-636.

Kischka, U., Wallesch, C.-W., and Wolf, G. 1997. Methoden der Hirnforschung: eine Einführung, Spektrum Akademischer Verlag, Heidelberg.

Klose, U., Lotze, M., and Grodd, W. 1999. Vergleich von Auswertungsverfahren für die funktionelle Kernspintomographie. *Zeitschrift für Medizinische Physik* **9:** 157-168.

Kornhuber, H.H., and Deecke, L. 1964. Hirnpotentialänderungen beim Menschen vor und nach Willkürbewegungen, dargestellt mit Magnetbandspeicherung und Rückwärtsanalyse. *Pflügers Archiv* **281:** 52.

Kosslyn, S.M. 1994. *Image and Brain. The resolution of the imagery debate*, The MIT Press/A Bradford Book, Cambridge (MA).

Kosslyn, S.M., Digirolamo, G.J., Thompson, W.L., and Alpert, N.M. 1998. Mental rotation of objects versus hands: Neural mechanisms revealed by positron emission tomography. *Psychophysiology* **35:** 151-161.

Kruggel, F., and von Cramon, D.Y. 1999. Modeling the hemodynamic response in single-trial functional MRI experiments. *Magnetic Resonance in Medicine* **42:** 787-797.

Kwong, K.K., Belliveau, J.W., Chesler, D.A., Goldberg, I.E., Weisskoff, R.M., Poncelet, B.P., Kennedy, D.N., Hoppel, B.E., Cohen, M.S., Turner, R., and al, e. 1992. Dynamic magnetic resonance imaging of human brain activity during primary sensory stimulation. *Proceedings of the National Academy of Sciences USA* **89:** 5675-5679.

Lagerlund, T.D., Sharbrough, F.W., Jack, C.R., Bradley, J.E., Strelow, D.C., Cicora, K.M., and Busacker, N.E. 1993. Determination of 10-20 system electrode locations using magnetic resonance imaging scanning with markers. *Electro-encephalography and Clinical Neurophysiology* **86:** 7-14.

Laming, P. 1998. Changing concepts on the role of glia. In *Glial cells: their role in behaviour* (P.R. Laming, E. Sykova, A. Reichenbach, G.I. Hatton, and H. Bauer, Eds.), pp. 1-21. Cambridge University Press, Cambridge.

Laming, P.R., Sykova, E., Reichenbach, A., Hatton, G.I., and Bauer, H. 1998. Glial cells: their role in behaviour, Cambridge University Press, Cambridge.

Lamm, C. 1996. *Raumvorstellungstraining und langsame ereigniskorrelierte Potentiale. Eine Untersuchung von Trainingseffekten auf DC-EEG derivierte corticale Aktivitätsmaße unter Verwendung Rasch-homogenen Stimulusmaterials*, University of Vienna/Unpublished Master Thesis, Vienna.

Lamm, C., Bauer, H., Vitouch, O., Durec, S., Gronister, R., and Gstättner, R. 2001. Restriction of task processing time affects cortical activity during processing of

a cognitive task: an event-related slow cortical potential study. *Brain Research: Cognitive Brain Research* **10:** 275-282.

Lamm, C., Bauer, H., Vitouch, O., and Gstättner, R. 1999. Differences in the ability to process a visuo-spatial task are reflected in event-related slow cortical potentials of human subjects. *Neuroscience Letters* **269:** 137-140.

Lamm, C., Bauer, H., Vitouch, O., Leodolter, M., and Leodolter, U. 1997. Changes of slow potential topography following training of spatial cognition. *Brain Topography* **9:** 72-73.

Lamm, C., Windischberger, C., Leodolter, U., Moser, E., and Bauer, H.H.a.o.m.s.-i.E.-w.M.-d.h.s.P.o.t.I.S.o.M.R.i.M., 8, 859. 2000. High accuracy of matching spline-interpolated EEG- with MRI-derived head surfaces. *Proceedings of the International Society of Magnetic Resonance in Medicine* **8:** 859.

Lancaster, J., Kochunov, P., Woldorff, M., Liotti, M., Parsons, L., Rainey, L., Nickerson, D., and Fox, P. 2000. Automatic talairach labels for functional activation sites. *Neuroimage* **11:** S483.

Lang, W., Lang, M., Podreka, M., Steiner, M., Uhl, F., Suess, E., Müller, C., and Deecke, L. 1988. DC-potential shifts and regional cerebral blood flow reveal frontal cortex involvement in human visuomotor learning. *Experimental Brain Research* **71:** 353-364.

Lange, N. 1996. Statistical approaches to human brain mapping by functional magnetic resonance imaging. *Statistics in Medicine* **15**: 389-428.

Lange, N., Strother, S.C., Anderson, J.R., Nielsen, F.A., Holmes, A.P., Kolenda, T., Savoy, R., and Hansen, L.K. 1999. Plurality and resemblance in fMRI data analysis. *Neuroimage* **10:** 282-303.

Law, S.K., and Nunez, P. 1991. Quantitative representation of the upper surface of the human head. *Brain Topography* **3:** 365-371.

Le, J., Lu, M., Pellouchoud, E., and Gevins, A. 1998. A rapid method for determining standard 10/10 electrode positions for high resolution EEG studies. *Electroencephalography and Clinical Neurophysiology* **106:** 554-558.

Leahy, R.M., Mosher, J.C., Spencer, M.E., Huang, M.X., and Lewine, J.D. 1998. A study of dipole localization accuracy for MEG and EEG using a human skull phantom. *Electroencephalography and Clinical Neurophysiology* **107:** 159-173.

Lee, A.C., Harris, J.P., and Calvert, J.E. 1998. Impairments of mental rotation in Parkinson's disease. *Neuropsychologia* **36:** 109-114.

Libet, B. 1979. Slow postsynaptic actions in ganglionic funtions. In *Integrative functions of the autonomic nervous system* (C. McBrooks, K. Koizumi, and A. Sato, Eds.), pp. 197-222. Elsevier, Amsterdam.

Lutzenberger, W., Birbaumer, N., Flor, H., Rockstroh, B., and Elbert, T. 1992. Dimensional analysis of the human EEG and intelligence. *Neuroscience Letters* **143:** 10-14.

Lutzenberger, W., Elbert, T., and Rockstroh, B. 1987. A brief tutorial on the implications of volume conduction for the interpretation of the EEG. *Journal of Psychophysiology* **1:** 81-89.

Magistretti, P.J., and Pellerin, L. 1999. Cellular mechanisms of brain energy metabolism and their relevance to functional brain imaging. *Philosophical Transactions of the Royal Society of London. Series B: Biological Sciences* **354:** 1155-1163.

Mangun, G.R., Buonocore, M.H., Girelli, M., and Jha, A.P. 1998. ERP and fMRI measures of visual spatial selective attention. *Human Brain Mapping* **6:** 383-389.

Mansfield, H. 1977. Multi-planar image formation using NMR spin echoes. *Journal of Physics* **C10:** L55--L58.

Matsuzaka, Y., Aizawa, H., and Tanji, J. 1992. A motor area rostral to the supplementary motor area (presupplementary motor area) in the monkey: neuronal activity during a learned motor task. *Journal of Neurophysiology* **68:** 653-662.

Maurer, C.R., Fitzpatrick, J.M., Wang, M.Y., Galloway, R.L., Maciunas, R.J., and Allen, G.S. 1997. Registration of head volume images using implantable fiducial markers. *IEEE Transactions on Medical Imaging* **16:** 447-462.

McCarthy, G. 1999. Event-related potentials and functional MRI: a comparison of localization in sensory, perceptual and cognitive tasks. *Electroencephalography and Clinical Neurophysiology* **49 (Suppl.):** 3-12.

McCarthy, G., and Wood, C.C. 1985. Scalp distribution of event-related potentials: an ambiguity associated with analysis of variance mode. *Electroencephalography and Clinical Neurophysiology* **62:** 203-208.

Mellet, E., Petit, L., Mazoyer, B., Denis, M., and Tzourio, N. 1998. Reopening the mental imagery debate: lessons from functional anatomy. *Neuroimage* **8:** 129-139.

Menon, R., Luknowsky, D.C., and Gati, J.C. 1998. Mental chronometry using latency-resoved functional MRI. *Proceedings of the National Academy of Sciences USA* **95:** 10902-10907.

Menon, R.S., and Kim, S.-G. 1999. Spatial and temporal limits in cognitive neuroimaging with fMRI. *Trends in Cognitive Sciences* **3:** 207-216.

Miezin, F.M., Maccotta, L., Ollinger, J.M., Petersen, S.E., and Buckner, R.L. 2000. Characterizing the hemodynamic response: effects of presentation rate, sampling procedure, and the possibility of ordering brain activity based on relative timing. *Neuroimage* **11:** 735-759.

Mishkin, M., Ungerleider, L.G., and Macko, K.A. 1983. Object vision and spatial vision: Two cortical pathways. *Trends in Neuroscience* **6:** 414-417.

Morris, P.G. 1987. *Nuclear Magnetic Resonance in Medicine and Biology*, Clarendon Press, Oxford.

Moser, E., Baumgartner, R., Barth, M., and Windischberger, C. 1999. Explorative signal processing in functional MR imaging. *International Journal of Imaging Systems and Technology* **10:** 166-176.

Moser, E., Diemling, M., and Baumgartner, R. 1997. Fuzzy clustering of gradient-echo functional MRI in the human visual cortex. Part II: quantification. *Journal of Magnetic Resonance Imaging* **7:** 1102-1108.

Mosso, A. 1881. *Über den Kreislauf des Blutes im menschlichen Gehirn*, von Veit & Companie, Leipzig.

Murata, A., Fadiga, L., Fogassi, L., Gallese, V., Raos, V., and Rizzolatti, G. 1997. Object representation in the ventral premotor cortex (area F5) of the monkey. *Journal of Neurophysiology* **78:** 2226-2230.

Neubauer, A., Freudenthaler, H.H., and Pfurtscheller, G. 1995. Intelligence and spatiotemporal patterns of event related desynchronisation. *Intelligence* **20:** 249-266.

Neubauer, A., Sange, G., and Pfurtscheller, G. 1999. Psychometric intelligence and event-related desynchronization uring performance of a letter matching task. In *Event-related desynchronization* (G. Pfurtscheller, and F.H. Lopes da Silva, Eds.), pp. 219-232. Elsevier, Amsterdam.

Nobre, A.C., Gitelman, D.R., Dias, E.C., and Mesulam, M.M. 2000. Covert visual spatial orienting and saccades: overlapping neural systems. *Neuroimage* **11:** 210-216.

Nobre, A.C., Sebestyen, G.N., Gitelman, D.R., Mesulam, M.M., Frackowiak, R.S.J., and Frith, C.D. 1997. Functional localization of the system for visuospatial attention using positron emission tomography. *Brain* **120:** 515-533.

Nunez, P. 1989. Estimation of large scale neocortical source activity with EEG surface Laplacians. *Brain Topography* **2:** 141-154.

Nunez, P.L., and Silberstein, R.B. 2000. On the relationship of synaptic activity to macroscopic measurements: does co-registration of EEG with fMRI makes sense? *Brain Topography* **13:** 79-96.

Nunez, P.L., Silberstein, R.B., Cadusch, P.J., Wijesinghe, R.S., Westdorp, A.F., and Srinivasan, R. 1994. A theoretical and experimental study of high resolution EEG based on surface Laplacians and cortical imaging. *Electroencephalography and Clinical Neurophysiology* **90:** 40-57.

O'Brien, R.G., and Kaiser, M.K. 1985. MANOVA method for analyzing repeated measures designs: an extensive primer. *Psychological Bulletin* **97:** 316-333.

O'Driscoll, G.A., Wolff, A.-L.V., Benkelfat, C., Florencio, P.S., Lal, S., and Evans, A.C. 2000. Functional neuroanatomy of smooth pursuit and predictive saccades. *NeuroReport* **11:** 1335-1340.

Ogawa, S., Lee, T., Nayak, A.S., and Glynn, P. 1990a. Oxygenation-sensitive contrast in magnetic resonance image of rodent brain at high magnetic fields. *Magnetic Resonance in Medicine* **14:** 68-78.

Ogawa, S., Lee, T.M., Kay, A.R., and Tank, D.W. 1990b. Brain magnetic resonance imaging with contrast dependent on blood oxygenation. *Proceedings of the National Academy of Sciences USA* **87:** 9868-9872.

Ogawa, S., Tank, D.W., Menon, R., Ellermann, J.M., Kim, S.G., Merkle, H., and Ugurbil, K. 1992. Intrinsic signal changes accompanying sensory stimulation: functional brain mapping with magnetic resonance imaging. *Proceedings of the National Academy of Sciences USA* **89:** 5951-5955.

Opitz, B., Mecklinger, A., Friederici, A.D., and von Cramon, D.Y. 1999. The functional neuroanatomy of novelty processing: integrating ERP and fMRI results. *Cerebral Cortex* **9:** 379-391.

Owen, A.M., Stern, C.E., Look, R.B., Tracey, I., Rosen, B.R., and Petrides, M. 1998. Functional organization of spatial and nonspatial working memory processing within the human lateral frontal cortex. *Proceedings of the National Academy of Sciences USA* **95:** 7721-7726.

Parks, R.W., Loewenstein, D.A., Dodrill, K.L., Barker, W.W., Joshii, F., Chang, J., Emran, A., Apicella, A., Sheramata, W.A., and Duara, R. 1988. Cerebral metabolic effects of a verbal fluency test: a PET scan study. *Journal of Clinical and Experimental Neuropsychology* **10:** 565-575.

Pascual-Leone, A., Bartres-Faz, D., and Keenan, J.P. 1999. Transcranial magnetic stimulation: studying the brain-behaviour relationship by induction of 'virtual lesions'. *Philosophical Transactions of the Royal Society of London. Series B: Biological Sciences* **354:** 1229-1238.

Pascual-Marqui, R.D. 1999. Review of methods for solving the EEG inverse problem. *International Journal of Bioelectromagnetism* **1:** 75-86.

Pascual-Marqui, R.D., Michel, C.M., and Lehmann, D. 1994. Low resolution electromagnetic tomography: a new method for localizing electrical activity in the brain. *International Journal of Psychophysiology* **18:** 49-65.

Paus, T. 1996. Location and function of the human frontal eye-field: a selective review. *Neuropsychologia* **34:** 475-483.

Pelizzari, C.A., Chen, G.T.Y., Spelbring, D.R., Weichselbaum, R.R., and Chen, C.T. 1989. Accurate three-dimensional registration of CT, PET and/or MR images of the brain. *Journal of Computer Assisted Tomography* **13:** 20-26.

Pellouchoud, E., Leong, H., and Gevins, A. 1997. Implications of electrolyte dispersion for high resolution EEG methods. *Electroencephalography and Clinical Neurophysiology* **102:** 261-263.

Peronnet, F., and Farah, M.J. 1989. Mental rotation: An event-related potential study with a validated mental rotation task. *Brain & Cognition* **9:** 279-288.

Perrin, F., Pernier, J., Bertrand, O., and Echallier, J.F. 1989. Spherical splines for scalp potential and current density mapping. *Electroencephalography and Clinical Neurophysiology* **72:** 184-187.

Perrin, F., Pernier, J., Bertrand, O., Giard, M.H., and Echallier, J.F. 1987. Mapping of scalp potentials by surface spline interpolation. *Electroencephalography and Clinical Neurophysiology* **66:** 75-81.

Perry, R.J., and Zeki, S. 2000. The neurology of saccades and covert shifts in spatial attention. An event-related fMRI study. *Brain* **123:** 2273-2288.

Petit, L., Courtney, S.M., Ungerleider, L.G., and Haxby, J.V. 1998. Sustained activity in the medial wall during working memory delays. *Journal of Neuroscience* **18:** 9429-9437.

Petit, L., Dubois, S., Tzourio, N., Dejardin, S., Crivello, F., Michel, C., Etard, O., Denise, P., Roucoux, A., and Mazoyer, B. 1999. PET study of the human foveal fixation system. *Human Brain Mapping* **8:** 21-43.

Petit, L., and Haxby, J.V. 1999. Functional anatomy of pursuit eye movements in humans as revealed by fMRI. *Journal of Neurophysiology* **81:** 463-471.

Pfurtscheller, G., and Neuper, C. 1997. Motor imagery activates primary sensorimotor area in humans. *Neuroscience Letters* **239:** 65-68.

Picton, C., and Hillyard. 1974. Cephalic skin potentials in electroencephalography. *Electroencephalography and Clinical Neurophysiology* **33:** 419-424.

Pihan, H., Altenmüller, E., and Ackermann, H. 1997. The cortical processing of perceived emotion: a DC-potential study on affective speech prosody. *NeuroReport* **8:** 623-627.

Pihan, H., Altenmüller, E., Hertrich, I., and Ackermann, H. 2000. Cortical activation patterns of affective speech processing depend on concurrent demands on the subvocal rehearsal system-a DC-potential study. *Brain* **123:** 2338-2349.

Poline, J.-B., Holmes, A., Worsley, K., and Friston, K. 1997. Making statistical inferences. In *Human brain function* (R. Frackowiak, K.J. Friston, C.D. Frith, R. Dolan, and J.C. Mazziotta, Eds.), pp. 55-78. Academic Press, New York.

Porro, C.A., Francescato, M.P., Cettolo, V., Diamond, M.E., Baraldi, P., Zuiani, C., Bazzocchi, M., and di Prampero, P.E. 1996. Primary motor and sensory cortex activation during motor performance and motor imagery: a functional magnetic resonance imaging study. *Journal of Neuroscience* **16:** 7688-7698.

Posner, M.I., and Mitchell, R.F. 1967. Chronometric analysis of classification. *Psychological Review* **74:** 392-409.

Prinz, W. 1997. Perception and action planning. *European Journal of Cognitive Psychology* **9:** 129-154.

Raichle, M.E. 2000. A brief history of human functional brain mapping. In *Brain mapping: the systems* (A.W. Toga, and J.C. Mazziotta, Eds.), pp. 33-77. Academic Press, San Diego.

Rasch, G. 1980. *Probabilistic models for some intelligence and attainment tests*, The University of Chicago Press, Chicago.

Richter, W., Samorjai, R., Summers, R., Menon, R.S., Gati, J.S., Georgopoulos, A.P., Tegeler, C., Ugurbil, K., and Kim, S.-G. 2000. Motor area activity during mental rotation studied by time-resolved single-trial fMRI. *Journal of Cognitive Neuroscience* **12:** 310-320.

Richter, W., Ugurbil, K., Georgopoulos, A., and Kim, S.G. 1997. Time-resolved fMRI of mental rotation. *NeuroReport* **8:** 3697-3702.

Rizzolatti, G., and Arbib, M.A. 1998. Language within our grasp. *Trends in Neuroscience* **21:** 188-194.

Rizzolatti, G., Camarda, R., Fogassi, L., Gentilucci, M., Luppino, G., and Matelli, M. 1988. Functional organization of inferior area 6 in the macaque monkey. II. Area F5 and the control of distal movements. *Experimental Brain Research* **71:** 491-507.

Rockstroh, B., Elbert, T., Canavan, A.G.M., Lutzenberger, W., and Birbaumer, N. 1989. Slow cortical potentials and behavior, Urban & Schwarzenberg, Baltimore.

Roitbak, A.I. 1983. *Neuroglia. Eigenschaften - Funktionen - Bedeutung*, Gustav Fischer Verlag (VEB), Jena.

Roland, P.E., and Gulyas, B. 1994. Visual imagery and visual representation. *Trends in Neuroscience* **17:** 281-287.

Roland, P.E., and Zilles, K. 1996. Functions and structures of the motor cortices in humans. *Current Opinion in Neurobiology* **6:** 773-781.

Rolke, B., Heil, M., Hennighausen, E., Haussler, C., and Rosler, F. 2000. Topography of brain electrical activity dissociates the sequential order transformation of verbal versus spatial information in humans. *Neuroscience Letters* **282:** 81-84.

Rösler, F., Heil, M., Bajric, J., Pauls, A.C., and Hennighausen, E. 1995. Patterns of cerebral activation while mental images are rotated and changed in size. *Psychophysiology* **32:** 135-149.

Rösler, F., Heil, M., and Röder, B. 1997. Slow negative brain potentials as reflections of specific modular resources of cognition. *Biological Psychology* **45:** 109-141.

Ruchkin, D.S., Johnson, R., Jr., Canoune, H., and Ritter, W. 1991. Event-related potentials during arithmetic and mental rotation. *Electroencephalography and Clinical Neurophysiology* **79:** 473-487.

Ruchkin, D.S., Johnson, R.J., and Friedman, D. 1999. Scaling is necessary when making comparisons between shapes of event-related potential topographies: a reply to Haig et al. *Psychophysiology* **36:** 832-834.

Rugg, M.D. 1998. Convergent approaches to electrophysiological and hemodynamic investigations of memory. *Human Brain Mapping* **6:** 394-398.

Sarter, M., Berntson, G.G., and Cacioppo, J.T. 1996. Brain imaging and Cognitive Neuroscience: toward strong inference in attributing function to structure. *American Psychologist* **51:** 13-21.

Scheerer, E. 1984. Motor theories of cognitive structure: A historical review. In *Cognition and motor processes* (W. Prinz, and A.F. Sanders, Eds.), pp. 77-98. Springer-Verlag, Berlin.

Scherg, M., and Ebersole, J.S. 1993. Models of brain sources. *Brain Topography* **5:** 419-423.

Scherg, M., and Goebel, R. 1998. Spatio-temporal source imaging of the human visual cortex: a comparison of MEG and fMRI. *International Journal of Psychophysiology* **30:** 78-79.

Scherg, M., and Von Cramon, D. 1986. Evoked dipole source potentials of the human auditory cortex. *Electroencephalography and Clinical Neurophysiology* **65:** 344-360.

Schmidt, K.H., and Metzler, P. 1992. *Wortschatztest (WST)*, Beltz Test, Weinheim.

Schmitt, B., Molle, M., Marshall, L., and Born, J. 2000. Scalp recorded direct current potential shifts associated with quenching thirst in humans. *Psychophysiology* **7:** 766-776.

Shen, L., Xiaoping, H., Yacoub, E., and Ugurbil, K. 1999. Neural crrelates of visual form and visual spatial processing. *Human Brain Mapping* **8:** 60-71.

Shepard, R.N., and Cooper, L.R. 1982. *Mental images and their transformations*, The MIT Press, Cambridge (MA).

Shepard, R.N., and Metzler, J. 1971. Mental rotation of three-dimensional objects. *Science* **171:** 701-703.

Sidtis, J.J., Strother, S.C., Anderson, J.R., and Rottenberg, D.A. 1999. Are brain functions really additive? *Neuroimage* **9:** 490-496.

Simpson, G.V., Pflieger, M.E., Foxe, J.J., Ahlfors, S.P., Vaughan, H.G.J., Hrabe, J., Ilmoniemi, R.J., and Lantos, G. 1995. Dynamic neuroimaging of brain function. *Journal of Clinical Neurophysiology* **12:** 432-449.

Singh, K.D., Holliday, I.E., Furlong, P.L., and Harding, G.F. 1997. Evaluation of MRI-MEG/EEG co-registration strategies using Monte Carlo simulation. *Electro-encephalography and clinical Neurophysiology* **102:** 81-85.

Society, A.E. 1991. American Electroencephalographic Society guidelines for standard electrode position nomenclature. *Journal of Clinical Neurophysiology* **8:** 200-202.

American Society for Electroenecephalography, 1994. Guideline thirteen: guideline for standard electrode position nomenclature. *Journal of Clinical Neuro-physiology **11***: 111-113.

Srebro, R. 1996. A bootstrap method to compare the shapes of two scalp fields. *Electroencephalography And Clinical Neurophysiology* **100:** 25-32.

Srinivasan, R., Nunez, P.L., Tucker, D.M., Silberstein, R.B., and Cadusch, P.J. 1996. Spatial sampling and filtering of EEG with spline laplacians to estimate cortical potentials. *Brain Topography* **8:** 355-366.

Srinivasan, R., Tucker, D.M., and Murias, M. 1998. Estimating the spatial nyquist of the human EEG. *Behavioral Research Methods, Instruments, and Computers* **30:** 8-19.

Stephenson, W., and Gibbs, F. 1951. A balanced non-cephalic electrode reference. *Electroencephalography and Clinical Neurophysiology* **3:** 237-240.

Sugio, T., Inui, T., Matsuo, K., Matsuzawa, M., Glover, G.H., and Nakai, T. 1999. The role of the posterior parietal cortex in human object recognition: a functional magnetic resonance imaging study. *Neuroscience Letters* **276:** 45-48.

Tagaris, G.A., Kim, S.-G., Strupp, J.P., Andersen, P., Ugurbil, K., and Georgopoulos, A.P. 1997. Mental rotation studied by funtional magnetic resonance imaging at high field (4 Tesla): Performance and cortical activation. *Journal of Cognitive Neuroscience* **9:** 419-432.

Talairach, J., and Tournoux, P. 1988. *Co-planar stereotaxic atlas of the human brain*, Thieme Medical Publishers, New York.

Tarr, M.J., and Pinker, S. 1989. Mental rotation and orientation-dependence in shape recognition. *Cognitive Psychology* **21:** 233-282.

Thompson, W.L., and Kosslyn, S.M. 2000. Neural systems activated during visual mental imagery - a review and meta-analyses. In *Brain mapping: The systems* (A.W. Toga, and J.C. Mazziotta, Eds.), pp. 535-560. Academic Press, San Diego.

Thulborn, K.R. 1999. Clinical rationale for very-high-field (3.0 Tesla) functional magnetic resonance imaging. *Topics in Magnetic Resonance Imaging* **10:** 37-50.

Towle, V.L., Balanos, J., Suarez, D., Tan, K., Grzeszczuk, R., Levin, D.N., Cakmur, R., Frank, S.A., and Spire, J.P. 1993. The spatial location of EEG electrodes:

locating the best fitting sphere relative to cortical anatomy. *Electroencephalography and Clinical Neurophysiology* **86:** 1-6.

Trimmel, M., Stässler, F., and Knerer, K. 2000. Brain DC potential changes in computerized tasks and paper/pencil tasks. *International Journal of Psychophysiology* **40:** 187-194.

Tucker, D.M. 1993. Spatial sampling of head electrical fields: the geodesic sensor net. *Electroencephalography and Clinical Neurophysiology* **87**.

Tucker, D.M., Liotti, M., Potts, G.F., Russell, G.S., and Posner, M.I. 1994. Spatiotemporal analysis of brain electrical fields. *Human Brain Mapping* **1:** 134-152.

Ugurbil, K., Hu, X., Chen, W., Zhu, X.H., Kim, S.-G., and Georgopoulos, A. 1999. Functional mapping in the human brain using high magnetic fields. *Philosophical Transactions of the Royal Society London B Biological Sciences* **354:** 1195-1213.

Vasey, M.W., and Thayer, J.F. 1987. The continuing problem of false positivities in repeated measures ANOVA in psychophysiology: a multivariate solution. *Psychophysiology* **24:** 479-486.

Verleger, R. 1999. The g factor and event-related EEG potentials. Book review of Jensen on Intelligence-g-Factor.
*PSYCHOLOQUI* **10:** htttp://psycoloquy.99.10.039.intelligence-g-factor.032.verleger.

Villringer, A. 1999. Physiological changes during brain activation. In *Functional MRI* (C.T.W. Moonen, and P.A. Bandettini, Eds.), pp. 3-14. Springer-Verlag, Berlin.

Vitouch, O., Bauer, H., Gittler, G., Leodolter, M., and Leodolter, U. 1997. Cortical activity of good and poor spatial test performers during spatial and verbal processing studied with Slow Potential Topography. *International Journal of Psychophysiology* **27:** 183-199.

Vitouch, O., Bauer, H., Lamm, C., Vanecek, E., and Leodolter, M. 1998. DC-Potentialtopographien musikbezogener Kognitionen: imaginative und motorische Komponenten beim Klavierspiel. In *Perspektiven psychologischer Forschung in Österreich* (J. Glück, O. Vitouch, M. Jirasko, and B. Rollett, Eds.), pp. 113-116. Wiener Universitätsverlag, Wien.

Vogel, F., Kruger, J., Schalt, E., Schnobel, R., and Hassling, L. 1987. No consistent relationships between oscillations and latencies of visually and auditory evoked EEG potentials and measures of mental performance. *Human Neurobiology* **6:** 173-182.

Voyer, D., Voyer, S., and Bryden, M.P. 1995. Magnitude of sex differences in spatial abilities: A meta-analysis and consideration of critical variables. *Psychlogical Bulletin* **117:** 250-270.

Walter, W.G. 1964. The contingent negative variation: an electrical sign of significant association in the human brain. *Science* **146:** 434.

Wang, B., Toro, C., Zeffiro, T.A., and Hallet, M. 1994. Head surface digitization and registration: a method for mapping positions on the head onto magnetic resonance images. *Brain Topography* **6:** 185-192.

Wang, J., Zhou, T., Qiu, M., Du, A., Cai, K., Wang, Z., Zhou, C., Meng, M., Zhuo, Y., Fan, S., and Chen, L. 1999. Relationship between ventral stream for object vision and dorsal stream for spatial vision: an fMRI + ERP study. *Human Brain Mapping* **8:** 170-181.

Wasserman, S., and Bockenholt, U. 1989. Bootstrapping: applications to psychophysiology. *Psychophysiology* **26:** 208-221.

Weimer, W.B. 1977. A conceptual framework for cognitive psychology: Motor theories of the mind. In *Perceiving, acting, and knowing* (R. Shaw, and J. Bransford, Eds.), pp. 267-311. Erlbaum, Hillsdale.

Wexler, M., Kosslyn, S.M., and Berthoz, A. 1998. Motor processes in mental rotation. *Cognition* **68:** 77-94.

# Curriculum Vitae Claus Lamm

## Personal Data

**Name:** Claus LAMM
**Current Address:** Neulerchenfelderstr. 58/9, A-1160 Vienna
**Tel:** +43 (699) 11379077
**Email:** Claus.Lamm@univie.ac.at
**WWW:** http://mailbox.univie.ac.at/claus.lamm
**Place of Birth:** Lustenau, Austria
**Date of Birth:** December 10 1973
**Profession:** University Assistant, University of Vienna
**Nationality:** Austrian
**Sex:** male
**Marital Status:** single

## Academic Education

1980 - 1984 Primary School in Esslingen-Zell (Germany)
1984 - 1992 Gymnasium in Esslingen-Oberesslingen (Germany) and Dornbirn (Austria); graduation in all classes with excellent success (average grade < 1.5)
19-06-1992 School leaving examination (graduation with excellent success; subjects: German, English, French, Mathematics and Psychology & Philosophy)
24-01-1997 Graduation in Psychology as Master of Science with excellent success (average grade incl. master thesis: 1)
22-10-1998 Enrolment for doctoral dissertation (Project: Neuronal Efficiency and Mental Rotation: Investigating Spatial Cognition Using functional Magnetic Resonance Imaging and Slow Potential Topography)
07-2001 Anticipated graduation as Dr. rer.nat.

*SummerSchools*

30.6.-11.7.1997: Graduate School for Behavioral and Cognitive Neurosciences, Groningen, Courses "Cognitive Modeling with ACT-R" and "Methodology for Neuroimaging"
24.6.-30.6.2000: University of Aberdeen, Dept. of Bio-Medical Physics, "Physical Basis of MRI"
25.6.2001-6.7.2001: Fourteenth McDonnell Summer Institute in Cognitive Neuroscience, The James S. McDonnell Foundation & The National Institute of Mental Health & The National Institute on Drug Abuse Summer Institute in Cognitive Neuroscience, Dartmouth College, Hanover (NH), Courses: "Human cognition as determined with human brain imaging" and "Reward as studied from the neural, systems and ecological persepective"

*Courses:*

12.6.2000: Functional MRI basics and beyond: From fundamentals to state of the art. Educational program full-day course at the 6th Annual Meeting of the Organization for Human Brain Mapping; San Antonio/USA. Organization: Organization for Human Brain Mapping, M. Bandettini.

20.10.-21.10.2000: SPM2000: 3. Kurs zur funktionellen Bildgebung. (SPM2000: 3rd course functional imaging); Hamburg/Germany. Organization: Neurologische Klinik Universitäts-Krankenhaus Eppendorf/Hamburg, Ch. Büchel, in cooperation with the Functional Imaging Laboratory London/UK.

3.5-4.5.2001: Seminar: Vom Schreiben wissenschaftlicher Texte (Writing Scientific Papers); Vienna/Austria. Organization: Personalabteilung Universität Wien/Wien.

## Honors and Awards

- 1994-1997: Scholarships ('Leistungsstipendium') by the faculty of Human and Social Sciences, University of Vienna
- 1995-1997: Scholarships by the Academic Senate of the University of Vienna
- 1997: Award ('Förderpreis des Bundesministers für Wissenschaft und Verkehr') by the Austrian Federal Minister of Science and Transportation (designated to appreciate excellence in master's studies and master's thesis)
- 1998: Scholarship (Program International Communication) by the Austrian Science Association
- 1999: Research Scholarship ('Förderstipendium') by the Faculty of Human and Social Sciences of the University of Vienna
- 2000: Theodor-Körner Award for Science and Arts
- 2001: Fellowship for the 2001 Summer Institute in Cognitive Neuroscience, Dartmouth College, Hanover/USA

## Memberships

- Deutsche Gesellschaft für Psychologie (German Psychology Association)
- Österreichische Gesellschaft für Neurowissenschaften (Austrian Neuroscience Association)
- Österreichische Gesellschaft für Cognitive Science (Austrian Society of Cognitive Science)

## Publications

### A) Peer Reviewed (J)ournals, (M)onographs, (B)ook Chapters, (T)echnical Reports

Windischberger, C., Barth, M., Lamm, C., Bauer, H., Schroeder, L., Gur, R.C., Moser, E. (2001). Fuzzy cluster analysis of high-field functional MRI data. Artificial Intelligence in Medicine (accepted for publicaton 06/2001) (J)

Lamm, C., Windischberger, C., Leodolter, U., Moser, E., Bauer, H. (2001). Evidence for premotor cortex activity during dynamic visuo-spatial imagery from single-trial functional magnetic resonance imaging and event-related slow cortical potentials. Neuroimage (accepted for publication 04/2001) (J)

Flexer, A., Bauer, H., Lamm, C., Dorffner, G. (2001). Single trial estimation of evoked potentials using Gaussian mixture models with integrated noise component. Technical Report, Österreichisches Forschungsinstitut für Artificial Intelligence, Wien, TR-2001-05 (T)

Lamm, C., Windischberger, C., Leodolter, U., Moser, E., Bauer, H. (2001). Combination of functional magnetic resonance and slow cortical potential imaging in the assessment of cognitive processing. In K.W. Kallus, N. Posthumus, & P. Jiménez (Eds.), Current psychological research in Austria. Proceedings of the 4th scientific conference of the Austrian Psychological Society (ÖGP). Graz: Akademische Druck- u. Verlagsanstalt (B)

Fitzgerald, R., Lamm, C., Oczenski, W., Stimpfl, T., Vycudilik, W., Bauer. H. (2001). Direct current auditory evoked potentials during wakefulness, anesthesia, and emergence of anesthesia. Anesthesia and Analgesia, 92, 154-160. (J)

Lamm, C., Bauer, H., Vitouch, O., Durec, S., Gronister, R., & Gstättner, R. (2001). Restriction of task processing time affects cortical activity during processing of a cognitive task: an event-related slow cortical potential study. Brain Research: Cognitive Brain Research, 10, 275-282. (J)

Sauter, C., Asenbaum, S., Popovic, R., Bauer, H., Lamm, C., Klösch, G., & Zeilhofer, J. (2000). Excessive daytime sleepiness in patients suffering from different levels of obstructive sleep apnoea syndrome. Journal of Sleep Research, 9, 293-301. (J)

Lamm, C., Bauer, H., Vitouch, O. & Gstättner, R. (1999). Differences in the ability to process a visuo-spatial task are reflected in event related slow cortical potentials of human subjects. Neuroscience Letters, 269, 137-140. (J)

Lamm, C. (1999). Radical explanations, but trivial descriptions (commentary). Behavioral and Brain Sciences, 22(5), 843-844. (J)

Lamm, C. (1999). Bewußtsein: neurale Grundlagen, subjektives Erleben und Grenzen menschlicher Erkenntnis. In T. Slunecko, O. Vitouch, C. Korunka, H. Bauer & B. Flatschacher (Hrsg.), Psychologie des Bewußtseins - Bewußtsein der Psychologie. Wien: Wiener Universitäts Verlag. (B)

Lamm, C. (1998). Does brain activity-oriented modelling solve the problem? Commentary on Green on Connectionist-Explanation. PSYCOLOQUY, 9(19)

ftp://ftp.princeton.edu/pub/harnad/Psycoloquy/1998.volume.9/psycoloquy.98.9.19.connectionist-explanation.16.green. (J)

Lamm, C., Klauda, E., Bauer, H., Vitouch, O. & Leodolter, M. (1998). Kortikale Korrelate unterschiedlicher Bearbeitungspräferenzen bei visuell und akustisch evozierten Vorstellungsprozessen. In J. Glück, O. Vitouch, M. Jirasko & B. Rollett (Hg.), Perspektiven psychologischer Forschung in Österreich. Wien: WUV-Universitätsverlag. (B)

Bauer, H., Lamm, C. & Vitouch, O. (1998). Topographie der Bestandspotentialänderungen bei Bearbeitung räumlicher Aufgaben. In J. Glück, O. Vitouch, M. Jirasko & B. Rollett (Hg.), Perspektiven psychologischer Forschung in Österreich. Wien: WUV-Universitätsverlag. (B)

Vitouch, O., Bauer, H., Lamm, C., Vanecek, E., & Leodolter, M. (1998). DC-Potentialtopographien musikbezogener Kognitionen: Imaginative und motorische Komponenten beim Klavierspiel. In J. Glück, O. Vitouch, M. Jirasko & B. Rollett (Hg.), Perspektiven psychologischer Forschung in Österreich. Wien: WUV-Universitätsverlag. (B)

Bauer, H., Lamm, C. & Vitouch, O. (1998). Slow potential topography and cognitive anatomy. In F. Rattay (Ed.), Proceedings TU-BioMed Symposium 1998 'Brain Modelling' (ARGESIM Report No. 10). Vienna: ARGESIM. (B)

Lamm, C. (1996). Raumvorstellungstraining & langsame ereigniskorrelierte Potentiale. Eine Untersuchung von Trainingseffekten auf DC-EEG derivierte corticale Aktivitätsmaße unter Verwendung Rasch-homogenen Stimulusmaterials. Master's thesis, University of Vienna. (M)

**B) Published abstracts**

Windischberger, W., Lamm, C., Bauer, H. & Moser, E. (2000). Paradigm-free fuzzy cluster analysis of a mental rotation paradigm at 3 T. MAGMA 11 (Suppl. 1), 61.

Bauer, H., Lamm, C., Holzreiter, S., Holländer, I., Leodolter, U. & Leodolter, M. (2000). Measurement of 3D electrode coordinates by means of a 3D photogrammetric head digitizer. Neuroimage, 11(5), S. 461.

Lamm, C., Bauer, H., Leodolter, U., Holländer, I. & Holzreiter, S. (2000). Accuracy of analytical and spherical interpolation algorithms for event related potential mapping. Neuroimage, 11(5), S. 462.

Windischberger, W., Lamm, C., Bauer, H. & Moser, E. (2000). Whole-Cortex fMRI with Single-Trial Analysis of a Mental Rotation Paradigm at 3 Tesla. Neuroimage, 11(5), S. 75.

Lamm, C., Windischberger, C., Moser, E., Leodolter, U. & Bauer, H. (2000). The role of motor and premotor areas in mental rotation: combined evidence from slow cortical potential and fMRI coregistration. Neuroimage, 11(5), S. 60.

Lamm, C., Windischberger, C., Leodolter, U., Moser, E. & Bauer, H. (2000). High accuracy of matching spline-interpolated EEG- with MRI-derived head surfaces. Proceedings of the International Society of Magnetic Resonance in Medicine, 8, 859.

Windischberger, C., Lamm, C., Bauer, H. & Moser, E. (2000). Single-trial analysis and whole-brain coverage in functional MRI of a mental rotation paradigm.

Proceedings of the International Society of Magnetic Resonance in Medicine, 8, 906.

Lamm, C., Windischberger, C., Moser, E., Bauer, H. (1999). Coregistrierung von Slow Potential Topography und funktioneller Magnetresonanztomographie bei der Verarbeitung von Raumvorstellungsaufgaben. Aktuelle Ergebnisse psychologischer Forschung in Österreich. Abstractband der 4. Wissenschaftlichen Tagung der Österreichischen Gesellschaft für Psychologie, Graz 1999, S. 21.

Bauer, H., Lamm, C., Leodolter, M. (1999). Topographie langsamer kortikaler Potentiale bei Emotionen. Aktuelle Ergebnisse psychologischer Forschung in Österreich. Abstractband der 4. Wissenschaftlichen Tagung der Österreichischen Gesellschaft für Psychologie, Graz 1999, S. 16.

Lamm, C., Oczenski, W., Stimpfl, T., Bauer, H., Fitzgerald, R.D. (1999). DC auditory evoked potentials during rest, anesthesia, and emergence from anesthesia. Anesthesiology, 91(34), A596.

Lamm, C. & Vitouch, O. (1999). Bootstrap-Verfahren: Anwendungen in der Analyse von Multikanal EEG-Daten. In E. Sommerfeld, F. Piontek & U. Schuster (Hrsg.), 4. Tagung der Fachgruppe Methoden in der DGPs - Programm & Abstracts (S. 19). Leipzig: Institut für Allgemeine Psychologie der Universität Leipzig.

Vitouch, O., Lamm, C. & Glück, J. (1999). Matrix-strukturelle Probleme bei der inferenzstatistischen Analyse von Brain Imaging-Daten. In E. Sommerfeld, F. Piontek & U. Schuster (Hrsg.), 4. Tagung der Fachgruppe Methoden in der DGPs - Programm & Abstracts (S. 31). Leipzig: Institut für Allgemeine Psychologie der Universität Leipzig.

Lamm, C., Windischberger, C., Leodolter, U., Doleisch, H., Moser, E. & Bauer, H. (1999). Coregistration of MR and EEG coordinate systems: accuracy of matching spline-interpolated with MRI-derived head surfaces. Magnetic Resonance Materials in Physics, Biology and Medicine (MAG*MA), 8 (S1), p. 164.

Windischberger, C., Lamm, C., Bauer, H. & Moser, E. (1999). Mental rotation using 3D-cubes studied by functional MRI. Magnetic Resonance Materials in Physics, Biology and Medicine (MAG*MA), 8 (S1), p. 162-163.

Lamm, C. (1999). Slow waves and spatial cognition. In V. Csepe, I. Czigler, G. Karmos, M. Molnar & I. Winkler (eds.), 7th International Conference on Cognitive Neuroscience - Program and Abstracts, Budapest 1999, p. 81.

Lamm, C., Windischberger, C., Moser, E. & Bauer, H. (1999). Coregistration of slow potential topography and fMRI in a spatial task. In V. Csepe, I. Czigler, G. Karmos, M. Molnar & I. Winkler (eds.), 7th International Conference on Cognitive Neuroscience - Program and Abstracts, Budapest 1999, p. 130.

Vitouch, O., Lamm, C. & Bauer, H. (1999). Slow waves and music performance. In V. Csepe, I. Czigler, G. Karmos, M. Molnar & I. Winkler (eds.), 7th International Conference on Cognitive Neuroscience - Program and Abstracts, Budapest 1999, p. 133.

Herold, Ch.J., Lamm, C., Rémy-Jardin, M., Grenier, P., Rémy, J., Schnyder, P., Verschakelen, J.A., Prokop, M., van Rossum, A., Laurent, F., Carette. M.-F., Hahne, J. (1999). Prospective evaluation of pulmonary embolism: initial

results of the European Multicenter Trial (ESTIPEP). European Radiology, 9(S1), 226.

Herold, Ch.J., Hahne, J., Grenier, P., Rémy-Jardin, M., Rémy, J., Schnyder, P., Verschakelen, J.A., Prokop, M., Pattynama, P.M.T., Laurent, F., Carette. M.-F., Lamm, C. (1999). Interobserver agreement in prospective evaluation of pulmonary embolism: results from the ESTIPEP trial. European Radiology, 9(S1), 227.

Lamm, C., Bauer, H., Vitouch, O., Gstättner, R., Durec, S. & Gronister, R. (1998). Slow potential topographic activities with spatial cognition under speed and power conditions. International Journal of Psychophysiology, 30(1-2), 210-211.

Lamm, C., Bauer, H., Leithner, D., Kastner-Koller, U. & Leodolter, M. (1998). Slow potential topographic activities accompanying reading aloud in adult dyslexic and control subjects. International Journal of Psychophysiology, 30(1-2), 249.

Bauer, H., Lamm, C., Adelbauer, G., Leodolter, M., Leodolter, U. & Guttmann, G. (1998). Slow potential topographic activities with stereoscopic versus monoscopic stimulus presentation. International Journal of Psychophysiology, 30(1-2), 210.

Fitzgerald, R.D., Lamm, C., Leodolter, M., Bauer, H. & Guttmann, G. (1998). Sensory evoked DC-potential changes accompanying anesthesia. International Journal of Psychophysiology, 30(1-2), 270.

Vitouch, O., Lamm, C., Bauer, H. & Vanecek, E.(1998). Functional mapping in time and space: a SPT investigation of piano playing. International Journal of Psychophysiology, 30(1-2), 186.

Lamm, C., Winkler, B., Bauer, H., Vitouch, O. & Leodolter, M. (1998). Slow Potential Topography bei mentaler Transformation und Rotation haptisch dargebotener Stimuli. Abstractband des 41. Kongresses der Deutschen Gesellschaft für Psychologie, Dresden 1998.

Vitouch, O., Bauer, H., Lamm, C., Vanecek, E., & Leodolter, M. (1998). Melodische und motorische Abläufe bei Pianisten. Analyse kognitiver Subprozesse mit non-invasivem Brain Imaging. Abstractband des 41. Kongresses der Deutschen Gesellschaft für Psychologie (Diskettenversion), Dresden 1998.

Bauer, H., Vitouch, O., Lamm, C. & Leodolter, M. (1997). Topographie der Bestandspotentialänderungen bei Bearbeitung räumlicher Aufgaben. Psychologische Forschung in Österreich. Abstractband der 3. Wissenschaftlichen Tagung der Österreichischen Gesellschaft für Psychologie, Salzburg 1997, S. 6.

Lamm, C., Klauda, E., Bauer, H., Vitouch, O. & Leodolter, M. (1997). Kortikale Korrelate unterschiedlicher Lösungsstrategien bei visuell und akustisch dargebotenen Vorstellungsaufgaben. Psychologische Forschung in Österreich. Abstractband der 3. Wissenschaftlichen Tagung der Österreichischen Gesellschaft für Psychologie, Salzburg 1997, S. 40.

Vitouch, O., Bauer, H., Vanecek, E., Lamm, C. & Leodolter, M. (1997). DC-Potentialtopographien musikbezogener Kognitionen: Imaginative und motorische Komponenten beim Klavierspiel. Psychologische Forschung in Österreich. Abstractband der 3. Wissenschaftlichen Tagung der Österreichischen Gesellschaft für Psychologie, Salzburg 1997, S. 81.

Lamm, C., Bauer, H., Vitouch, O., Leodolter, M. & Leodolter, U. (1997). Changes of slow potential topography following training of spatial cognition. Brain Topography, 9(3), 72-73.